SENSING AND SENSITIZER ACTIVATION BY BIOLOGICAL THIOLS AND 1,2-DIOXETANES BASED CHEMILUMINESCENCE PROBES

A DISSERTATION SUBMITTED TO

MATERIALS SCIENCE AND NANOTECHNOLOGY PROGRAM

OF THE GRADUATE SCHOOL OF ENGINEERING AND SCIENCE

OF BILKENT UNIVERSITY

IN PARTIAL FULFILLMENT OF THE REQUIREMENTS

FOR THE DEGREE OF

DOCTOR OF PHILOSOPHY

By

İLKE ŞİMŞEK TURAN

September, 2014

I certify that I have read this thesis and that in my opinion it is fully adequate, in scope and in quality, as a thesis of the degree of Doctor of Philosophy.

…….

Prof. Dr. Engin U. Akkaya (Advisor)

I certify that I have read this thesis and that in my opinion it is fully adequate, in scope and in quality, as a thesis of the degree of Doctor of Philosophy.

…….

Assoc. Prof. Dr. Tamer Uyar

I certify that I have read this thesis and that in my opinion it is fully adequate, in scope and in quality, as a thesis of the degree of Doctor of Philosophy.

…….

Assoc. Prof. Dr. Özgür Altan Bozdemir

I certify that I have read this thesis and that in my opinion it is fully adequate, in scope and in quality, as a thesis of the degree of Doctor of Philosophy.

…….

Assoc. Prof. Dr. Dönüş Tuncel

I certify that I have read this thesis and that in my opinion it is fully adequate, in scope and in quality, as a thesis of the degree of Doctor of Philosophy.

…….

Assist. Prof. Dr. Salih Özçubukçu

Approved for the Graduate School of Engineering and Science

…….

Prof. Dr. Levent Onural

Director of the Graduate School of Engineering and Science

Dedicated to
my husband and my mother,
for their continuous support and encouragement

ABSTRACT

SENSING AND SENSITIZER ACTIVATION BY BIOLOGICAL THIOLS AND 1,2-DIOXETANES BASED CHEMILUMINESCENCE PROBES

İlke Şimşek Turan

PhD in Materials Science and Nanotechnology

Supervisor: Prof. Dr. Engin Umut Akkaya

September, 2014

Biologically important biothiols like Cystein (Cys), Homocystein (Hcy) and Glutathione (GSH) are vital for the maintenance of cellular redox status and alterations in their levels is linked to a number of severe diseases such as AIDS, cancer and Alzheimer's therefore the design and synthesis of nitroolefin functionalized bodipy dyes responding to biological thiols by both absorbance and emission changes have been accomplished. Through the incorporation of hydrophilic groups, bright signaling of biothiols in the longer wavelength region of the visible spectrum is deemed to operate in biological environment. With this knowledge, bioconjugation of the nitroolefin functionalized dyes with thiol groups like those belonging to cysteine residues on proteins has been proved via large spectral changes and targeted to visualize dynamics of proteins, cell-cell interactions, mechanisms of life cycles of proteins. Hence, the result suggests that nitroolefin functionalization of BODIPY dyes is a promising way to sense biological thiols and hence labeling proteins having thiol groups. Since GSH plays vital roles in the oxidative stress exists within the cells and thus, high concentration of it is the indication of cancer development, design and synthesis of cancer related parameter based activation of bodipy based photosensitizers have been achieved to enhance spatiotemporal selectivity in photonic sensitization of dissolved molecular oxygen and thus, improves the potential and practice of photodynamic therapy and their effectiveness are validated by cell culture studies. Chemiluminescence in principle can provide a rapid, qualitative and/or quantitative test for analytes of interest; because of that synthesis of novel probes for the sensing of biologically important (fluoride) anion have been devised to combine the power of chemiluminescence and self immolative amplifiers which offers a chemical avenue for enhancing the signal produced in response to a given analyte. Through the development of chemiluminogenic perspective for sensing of palladium ions, rapid and selective response of probe to

palladium ions with regardless of their charge in aqueous environment have been accomplished. Considering the convenience of the methods and substantial results, we are confident that other probes combining the power of chemiluminescence will emerge.

Keywords: fluorescence, chemosensors, biological thiols, protein labeling, photodynamic therapy, chemiluminescence.

ÖZET

BİYOLOJİK TİYOLLERİN TANISI İLE FOTOSENSİTİZÖR AKTİVASYONU VE 1,2-DİOKSETAN TEMELLİ KEMİLÜMİNESAN PROBLAR

İlke Şimşek Turan

Malzeme Bilimi ve Nanoteknoloji, Doktora

Danışman: Prof. Dr. Engin Umut Akkaya

Eylül, 2014

Biyolojikçe aktif olan tiyollerden sistein (Cys), homosistein (Hcy) ve glutatiyon (GSH), hücresel redoks durumunun düzenlenmesinde hayati önem taşımaktadır ki hücresel değerlerindeki değişiklikler AIDS, kanser, Alzheimer gibi birçok rahatsızlıkla ilişkilendirilmektedir. Bu nedenle, biyolojikçe aktif tiyollere tepki veren nitroolefin grubu ile fonksiyonlandırılmış bodipy boyalarının dizayn ve sentezi hedeflenmektetir ve bu probların tiyollere olan seçiciliği de absorbans ve emisyondaki değişikiklerle kanıtlanmıştır. Hidrofilik gruplar ile modifiye edilen probların, biyolojikçe aktif tiyollere uzun dalga boyundaki tepkileri, bu moleküllerin biyoloik ortamlarda uygulanabilirliğini kanıtlamaktadır. Bu bilgiler ışığında, Nitroolefin ile fonksiyonlandırılmış bodipy boyalarının proteinlerin tiyol grupları ile biyokonjugasyonları, protein dinamiklerini gözlemlemek, hücrelerin birbirleriyle etkileşimleri belirlemek, proteinlerin yaşam döngülerinin mekanizmalarını anlamak amacıyla tasarlanmış olup, bu konjugasyon, boyar maddenin fotofiziksel özelliklerindeki değişikler ile kanıtlanmıştır. Elde edilen sonuçlar, BODIPY boyalarının nitroolefin fonksiyonlandırılmasının, hem biyolojik tiyollerin algılanması hemde tiyol grupları bulunduran proteinlerin etiketlenmesi açısından gelecek vaad eden bir yol olduğunu göstermektedir. Biyolojik öneme sahip tiyol içeren bu bileşiklerden olan GSH, hücre içi oksidatif stresin düzenlemesinde son derece büyük önem taşımaktadır ki hücre içerisinde yüksek konsantrasyonu kanser gelişimi ile ilişkilendirilmektedir. Hedef dışı hassasiyeti ortadan kaldırmak amacıyla (GSH) varlığında sönümlendirici modülün uzaklaştırılması ile aktiflendikten sonra singlet oksijen üretebilen sönümlendirilmiş seçici PDT fotoduyarlaştırıcılarının geliştirilmesi hedeflenmekte olup GSH'ın aktif olmayan kromoforu, terapatik pencerede uyarıldığı zaman singlet oksijen üretebilen son derece etkili bir fotoduyarlaştırıcıya dönüştürebildiği hücre deneyleriyle kanıtlanmıştır. Elde edilen sonuçlar ışığında, PDT'nin pratikte uygulanabilirliğine de yeni bir yön verilmektedir.

Kemiluminesans prensipte analitlerin hızlı, kalitatif ve kantitatif belirlenmesinde kullanılan son derece etkili bir yöntem olduğu için kemilüminesan temelli kendini feda eden moleküler sistemleri florür iyonunu tayin edecek şekilde tetikleyici bir grup ile fonksionlandırmayı başardık. Dizayn ettiğimiz bu molekülün bir birim florür iyonuna karşılık çoklu kemiluminesans özellikte muhabir gruplarının salınımını ve bu molekülün sadece florür iyonuna seçicilik gösterdiğini analitik olarak kanıtladık. Paladyumun aşırı alınımının astım, bulantı, saç dökülmesinde artış ve dermatit gibi birçok önemli rahatsızlığın gelişmesine neden olduğudan kemiluminogenik perspektif kullanılarak hassas ve spesifik olarak paladyum iyonunu tayin edebilecek yeni probların dizayn ve sentezini hedefledik. Pd probu olarak kemilüminesan reaktiflerin geliştirilmesi planlanmış ve tasarlanan sensörlerin kemilüminesans yaparak kendi ışımalarını sağlaması paladyumun algılanmasını daha avantajlı kılmaktadır. Yaptığımız bu çalışmalardaki, kemilüminesansa dayalı metodların uygunluğu ve elde edilen sonuçlara dayanarak, kemilümenesans temelli yeni problar tasarlanacağına inanıyoruz.

Anahtar kelimeler: floresans, sensör, biyolojikçe aktif tiyoller, protein işaretleme, fotodinamik terapi, kemiluminesans

ACKNOWLEDGEMENT

I would like to express my gratitude to my supervisor Prof. Dr. Engin U. Akkaya for giving me chance to be a member of his research group. I would like to express my sincere thanks for his guidance, support, and patience during the course of this research. I am also grateful to him for teaching us how to become a good scientist by looking everything from different point of views. Besides his scientific perspective, I admire his personality, view of life and I believe it is a privilege to know him as a person and as a scientist. I will never forget his support throughout my life.

I am sincerely grateful for my close friend Özlem Seven for her help, encouragement during the studies and especially for her endless support, understanding, caring throughout years that I have known her. It is good to know that there are people like her in this world. I would like to express my sincere thanks to my dear friend Seylan Ayan for her understanding, kind collaboration, joyful friendships and caring. I would like to express my special thanks to Özge Yılmaz, for her valuable help, we have confronted difficulties together. Additionally, I would like to thank to Deniz Yıldız for her valuable joyful friendship and I am very happy to know her. They have made tough events and days bearable. I feel lucky to have such a great friends.

I would like to thank to Ayşegül Gümüş, Fatma Pir Çakmak for their partnership and friendship.

I would like to thank TÜBİTAK (The Scientific and Technological Research Council of Turkey) for financial support in the form of scholarship during PhD programme. Also, our experimental work was supported by TÜBİTAK in the form of a grant 112T480 and 113Z526.

I would like to thank to present and past members of Akkaya Lab. Nisa Yeşilgül, Hale Atılgan, Fazlı Sözmen, Ahmet Atılgan, Bilal Uyar, Ahmet Bekdemir, Elif Ertem, Hatice Turgut, Tuğçe Durgut, Jose Luis Bila, Ceren Çamur, Darika Okeava, Melek Baydar, Dilek Karışan, Ruslan Gluiyev, Onur Büyükçakır, Yusuf Çakmak,

Sündüs Erbaş Çakmak, Safacan Kölemen, Tuğba Özdemir and rest of the SCL (Supramolecular Chemistry Laboratory) members. It was wonderful to work with them.

I would like to thank to Zeynep Aytaç, Aslı Çelebioğlu, Yelda Ertaş, Gözde Uzunallı for their endless help.

I also would like to thank all members of UNAM family for providing a multidisciplinary research atmosphere.

I would like to express my gratitude to my family and my husband, Tufan Turan for their endless love, support, and understanding.

LIST OF ABBREVIATIONS

AcOH	:	Acetic Acid
Bodipy	:	Boradiazaindacene
$CHCl_3$	:	Chloroform
DDQ	:	Dichlorodicyanoquinone
DMF	:	Dimethylformamide
ET	:	Energy Transfer
Et_3N	:	Triethylamine
FRET	:	Förster Resonance Energy Transfer
HOMO	:	Highest Occupied Molecular Orbital
ICT	:	Internal Charge Transfer
IFE	:	Inner Filter Effect
LUMO	:	Lowest Unoccupied Molecular Orbital
MALDI	:	Matrix-Assisted Laser Desorption/Ionization
MS	:	Mass Spectroscopy
NMR	:	Nuclear Magnetic Resonance
PET	:	Photoinduced Electron Transfer
TFA	:	Trifluoroacetic Acid
THF	:	Tetrahydrofuran
TLC	:	Thin Layer Chromotography
TOF	:	Time of Flight

TABLE OF CONTENTS

LIST OF FIGURES

LIST OF TABLES

CHAPTER 1

1. INTRODUCTION

Science is always fascinated by the magnificence of the nature. Mankind discovers notable ideas by observing it with wide open eyes and the questions are clarified by the whispers of the nature. Nature reaches down mankind in several forms and "light" is one of the most indispensable one since one of the prerequisites required for the permanence of life is light. There would be no vegetation and thus, no food chain in the absence of light. We can explain several everyday phenomena like rainbows, growth of garden flowers by thinking about light. There is remarkable harmony between the light and matter or living organisms. When the light is appreciated in the electromagnetic spectrum, the term "Luminescence" takes part in the literature of the science.

In this thesis, "light" will be introduced to you in two parts as "let the light be there" and "let the light glow there". As it is understood from the heading, first part covers the three glorious projects based on fluorescence phenomena that require the presence of the light. The second part however, covers the two wondrous projects at which light are produced (glow) there.

First part of the thesis is composed of three different projects which are based on the significance biological thiols. Biologically important biothiols like Cystein (Cys), Homocystein (Hcy) and Glutathione (GSH) are vital for the maintenance of cellular redox status and alterations in their levels is linked to a number of severe diseases such as AIDS, cancer and Alzheimer's. Judicious design of dyes carrying nitroolefin substituents in conjugation with the BODIPY core, yields dyes which respond to biological thiols by both absorbance and emission changes. The result is bright signaling of biologically relevant thiols in the longer wavelength region of the visible

spectrum and in aqueous solutions (Chapter 3). With this knowledge, nitroolefin functionalized dyes were targeted to result in conjugation of nitroolefin with thiol groups such as those belonging to cysteine residues on proteins in order to visualize dynamics of proteins, cell-cell interactions, mechanisms of life cycles of proteins, etc. To prove bioconjugation of the dyes with proteins, absorbance and emission changes were recorded after reaction with both L-cysteine and Bovine Serum Albumin (BSA) and large spectral changes were obtained (Chapter 4). From these biological thiols, Glutathione is related with the oxidative stress exits in cells. In consideration of high intracellular Glutathione concentrations in the cancer cells, we designed and synthesized a series of Bodipy based sensitizers which can generate cytotoxic singlet oxygen only after a glutathione mediated cleavage of the electron sink module because enhanced spatiotemporal selectivity in photonic sensitization of dissolved molecular oxygen is an important target for improving the potential and practice of photodynamic therapy. Cell culture studies not only validate our design, but also suggest an additional role for the relatively hydrophobic quencher module in the internalization of the photosensitizer (Chapter 5).

The other part of the thesis contains two different projects which are developed based on chemiluminescence. In the case of chemiluminogenic sensing of fluoride ions (Chapter 7), Enhanced chemiluminescence signal is obtained when electronically triggered dioxetane cleavage is initiated by fluoride mediated deprotection of the silyl-protecting group, followed by self-immolation via 1,4-quinone-methide rearrangement. The reaction takes place even when the probe is trapped within a PMMA layer on top of a glass plate. In that arrangement, fluoride in aqueous solutions can be detected selectively at low micromolar concentrations. Rapid assessment of fluoride concentrations in drinking water could be a possible application, and the bright chemiluminescence of the probe or structurally related derivatives could provide a promising alternative. New methodology has been developed for sensing of palladium ions (Chapter 8). We have used the power of chemiluminescence for rapid, qualitative and/or quantitative test for analytes of interest; we have analyzed the palladium ions regardless of their charge and source in

aqueous environment. Considering the convenience of the method and substantial results, we are confident that other chemiluminogenic probes will emerge.

CHAPTER 2

2. BACKGROUND 1:

"LET THE LIGHT BE THERE"

2.1 Photoluminescence

One of the prerequisites required for the permanence of life is "light". There would be no vegetation and thus, no food chain in the absence of light. We can explain several everyday phenomena like rainbows, growth of garden flowers, etc., if we appreciate the visible light in electromagnetic spectrum that bring us to the substantial question: what happens when light hits to matter. This can be explained by considering the harmony between radiation and matter. For example, if there is harmony between radiation and matter, absorption of energy is possible otherwise, reflection or scattering occurs.[1] Light can be characterized by electromagnetic radiation of a definite wavelength (λ). The wavelengths from 400nm to 750nm represent the visible part of the spectrum which corresponds to the region of shorter wavelength range of γ-rays to longer wavelength end of radio waves (figure 1). While the color of a chemical compound depends on which part of electromagnetic spectrum it absorbs, the transmitted spectral mixture of light determines the color that we see. Additionally when we are working with dilute solutions, by considering spectral characteristics of absorbed light, we can get information about the electronic structure and concentration of the sample.[2]

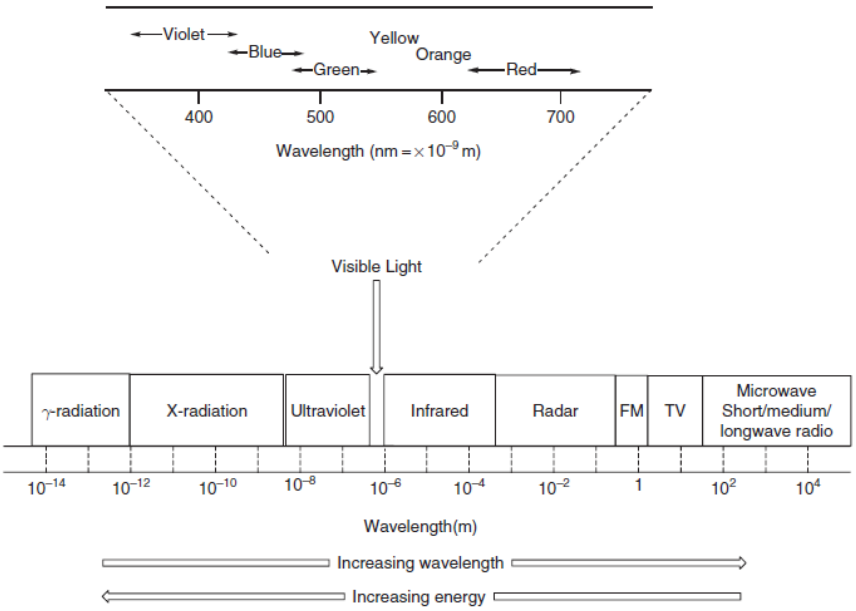

Figure 1: Electromagnetic Spectrum[1]

2.1.1 Principles and Characteristics of Luminescence

The umbrella term for light emission processes is "Luminescence" which can be defined as the emission of light resulted from the excitation of a chemical compound trough high energy radiations or electrons. When a chemical compound is exposed to the light which has energy equal to the energy of possible electronic transition, some of the light absorbed by compound leads to the excitation of an electron to a higher energy orbital which relaxes back to ground state by losing their excess energy through several possible pathways.[3] There are actually two forms of radiation in competition which are radiative and nonradiative transitions. If electronically excited molecule relaxes back to ground state by emitting its excess energy *radiatively* through the emission of photon or *nonradiatively* vibrations which heats the lattice (figure 2). These deactivation processes can be visualized simply via The Perrin-Jablonski diagram (figure 3).

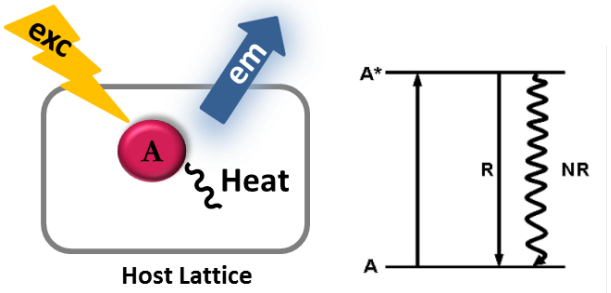

Figure 2: (a) General representation of luminescence mechanism, *exc* represents excitation, *em* represents emission and *heat* represents the nonradiative transition (b) Representative Energy Level Diagram A*: Excited State of Activator, A: Ground State of activator, R: Radiative transition to the ground state or emission, NR: Non-radiative transition or heat.

When light hits to a chemical compound, an electron from ground state (S_0) is jumped to an excited state depending on the energy of absorbed light. Since the excited state of a molecule by absorption occurs through conservation of the electron spin-paring, the excited state is called as singlet state (S_1). According to Kaska's rule, either luminescence emission or chemical reaction by excited molecules originates from v=0 of S_1 or T_1 because relaxations from higher electronically excited states to S_1 (or T_1) occurs swiftly. If the absorbed light has higher energy required for a simple electronic transition, the excess energy is converted into vibrational and rotational energy which leads to excitation of upper vibronic levels of excited state. When absorbed light having excess vibrational energy leads to the excitation of an electron to a higher vibrationally excited state and *vibrational relaxation* occurs within the order of 10^{-12}s between vibrationally excited state v>0 and v=0 of given state as a result of possible collisions with solvent molecules. On the other hand, *internal conversion* occurs from upper excited electronic levels like S_2, S_3, etc. to the lowest electronically excited state S_1 by preserving the same spin multiplicity. Internal conversion occurs within the order of 10^{-14}-10^{-11}s between excited states and the order of 10^{-9} -10^{-7}s between S_1 and S_0.

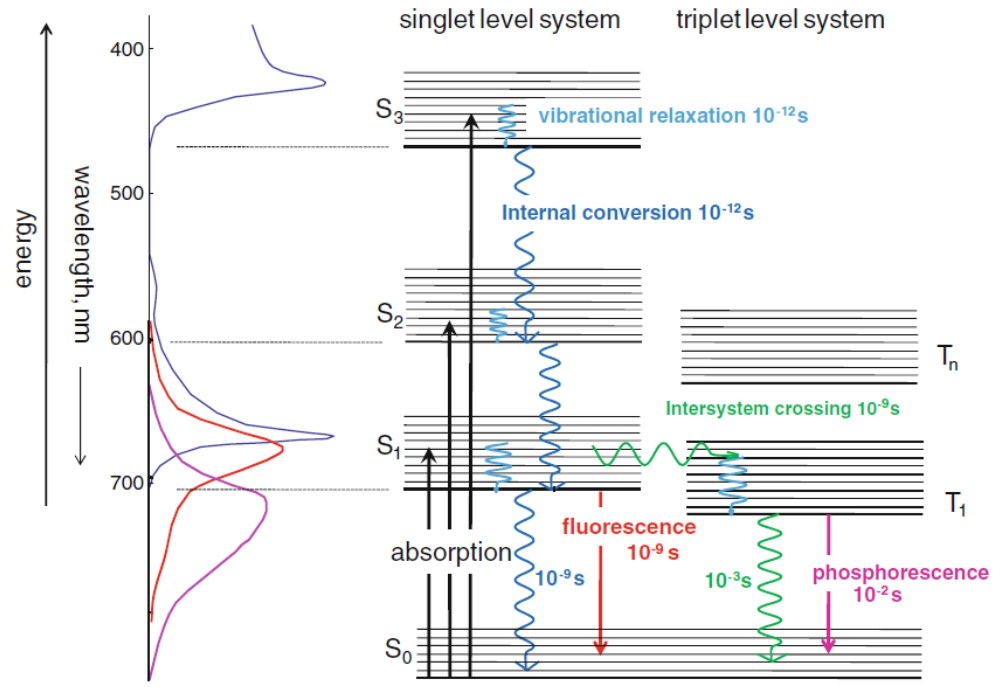

Figure 3: Jablonski diagram representing the typical photophysical processes in molecules [2]

Another nonradiative process is based on intramolecular transitions which occur between isoenergetic states of different multiplicities called *intersystem crossing*. This is a spin forbidden process and it can be obtained as a result of spin-orbit coupling which is the action of an effective magnetic field and it can originate while electrons orbit around the charged nuclei. This causes little mixing of singlet and triplet states thus in turn, electron can move from S_1 to T_1. In a molecule, spin-orbit coupling can be enhanced with the introduction of heavy atoms like bromine and iodine.

After the excited state molecule release its excess energy through vibrational relaxation or interval conversion in order to reach S_1 state, it can relaxes back to ground state via the emission of light. This is called as f*luorescence* and it occurs between the states of same multiplicity and in the order of 10^{-9}s. Although

fluorescence competes with other deactivation processes of same multiplicity when electrons are excited to higher vibrational levels of S_1 state or higher vibrational levels of upper energetic states, it always wins the race from S_1 state.

When an electron is moved to T_1 state, it can also relax back to ground state with emission of light. This spin-forbidden radiative transition is called as *phosphorescence*. Since transitions to S_0 are forbidden, the rate of emission is slow thus in turn, the phosphorescence lasts typically milliseconds to few hours so that emission can continue even after light source has been removed.[4]

2.1.2 Phenomena of Fluorescence

The world of fluorescence is a world of beautiful color.
In the darkness, all the ordinary colors of our daylight would disappear.
Only the intensely glowing hues of fluorescent substances touched by the
Ultraviolet beam shine out with striking clarity.

Sterling Gleason, 1960

Fluorescence can be defined as the radiative transition which can occur between the states of same multiplicity.[5,6] Fluorescence can be used for the quantitative analysis of fluorescence compounds since emission intensity is proportional to the concentration of the compound. Due to the high sensitivity and selectivity of fluorescence, it has diverse spectrum of application areas. Because of that in order to comprehend and interpret the analysis, there are several parameters related with fluorescence which has to be learned deeply.

The energy of fluorescence is less than that of absorption because of that fluorescence occurs at longer wavelengths than absorbance. When a molecule is excited upon exposure to light, there are possibilities of collisions between the

molecule and solvents so that molecule loses some of its energy as heat. Therefore, since energy and wavelength are inversely proportional to each other, lower energy fluorescence emission occurs at longer wavelength which is spectrally red shifted. The difference between band maxima of absorption and emission spectra is called as *Stokes Shift*. There are several causes of Stokes shift such that rapid decay to lowest vibrational level of S_1, solvent effects, excited state reactions, complex formation and energy transfer.[7]

Quantum yield and fluorescence efficiency are one of the most important characteristics of a fluorophore. *Quantum yield* (Φ_f) can be defined as the number of emitted photons by S_1 relative to the number of absorbed photons by S_0. The highest value of quantum yield approaches to unity in molecules relatively rigid which have large and planar conjugated systems. In the case of more flexible molecules, quantum yield will be low due to the possibility of having high vibrational and rotational freedom compared to rigid ones. Quantum yield is specific for each fluorescent compound and it is independent of either excitation or emission wavelength.[8] *Fluorescence lifetime* (τ) can be defined as the average value of time which is spent by molecules in the excited states before relaxing back to ground state. It is related with the decay rate of fluorescence intensity after a short excitation pulse. These two parameters are closely related by

$$\Phi_f = \tau_f / \tau_n \qquad \text{equation 1}$$

where τ_n is the natural lifetime of excited state which represents the lifetime that fluorophore would have if fluorescence is the only way for a molecule deactivates from lowest excited singlet state.[9] Lifetime becomes shorter in the case of quenching processes.

Fluorescence quenching is the decrease or suppression of the fluorescence intensity via different mechanisms. The decrease or suppression in the fluorescence intensity has been observed due to formation of transition complex when excited fluorophore contacts with quencher like molecular oxygen, compounds bearing heavy atoms, halogen ions or another fluorophore. The possible quenching mechanisms are static

and collisional according to the type of contact between fluorophore and quencher. Static quenching occurs when a fluorophore and quencher takes place in ground state thus, forms a nonfluorescent complex whose efficiency depends on both the concentration of quencher and the formation constant of the complex. On the other hand, collisional quenching occurs when excited fluorophore is deactivated upon contact with the quencher. Oxygen, halogens, amines and electron deficient molecules act as quenchers but the quenching mechanism is different and depends on the fluorophore-quencher pair. For example, quenching resulted from halogens or heavy atoms occur via spin orbit coupling and inter system crossing.[10] Another term is *photobleaching* which can be defined as photo-induced chemical destruction of fluorophore upon exposure to excitation that leads to the loss of ability of the fluorophore to fluoresce.[11]

2.1.3 Factors Affecting Fluorescence

There are several factors having considerable effects on fluorescence quantum yield that can be listed as molecular structure, substituent effects, solvent effects, temperature and viscosity. These factors are explained in order.

Molecular Structure: Fluorescence is mostly observed in compounds having rigid structures as a result of aromaticity or extended conjugation. Consequently, the higher the rigidity of the compound, the lesser the vibrational and rotational freedom, the higher the probability of fluorescence since the energy gap between S_1 and S_0 becomes large so that fluorescence predominate over nonradiative processes.[4]

Substituent Effect: The introduction of freely rotating substituents into aromatic compounds decreases both fluorescence quantum yield and intensity due to the enhanced probability of rotational and vibrational freedom. Additionally, modification of aromatic compounds with electron donating substituents increases fluorescence quantum yield due to the increased rate of radiative decay. On the other hand, introduction of electron withdrawing substituents having sp^2 hybridized

nonbonding electrons and heavy atoms reduces the fluorescence quantum yield owing to the mixed spin-orbital electronic motions of aromatic system and enhanced probability of spin-triplet intersystem crossing.[9]

Solvent Effect: Solvent has profound effects on fluorescence emission in different ways. For instance, fluorescence intensity could be decreased in solvents containing heavy atoms due to the increase in probability of spin orbit coupling thus in turn, increase in phosphorescence. Hydrogen bonding between fluorophore and solvent has significant effect on fluorescence whose intensity has been affected by the stabilization or destabilization effect of generated hydrogen bond on the electronic excited state. When excited, organic molecules become more polar and thus, enhances the interaction between the dye and its molecular environment resulting in the energy loss.[12]

Temperature: Temperature and fluorescence is inversely proportional with each other since the increase in temperature leads to increase in either molecular motions or collisions via lowering viscosity of the solvent and thus, fluorescence decreases.

Viscosity: Fluorescence can also be affected by viscosity of the solvents which determines the collisions between solvent molecules and excited state molecules. In viscous solutions, the molecular collisions are reduced which reduces the energy transfer. Consequently, the lesser the molecular collisions, the lower the energy loss and thus in turn, the higher the fluorescence.[7]

2.2 Fluorescent Probes

Methods based on fluorescence like fluorescence spectroscopy, fluorescence imaging and fluorescence indicators become indispensible diagnostic, monitoring and analytical tools in biochemistry, material science, biotechnology, environmental and analytical chemistry since they provide worthless information for investigating the molecular interactions in chemical and biological systems.

Fluorogenic probes can be defined as the reagent which can convey the information upon interaction with the analyte as the changes in its photophysical characteristics and based on these spectroscopic changes, analyte of interests could be detected[8,13]. Fluorescent probes have wide range of application areas due to distinct advantages offered by fluorescence detection in terms of simplicity, sensitivity, selectivity, monitoring of dynamic changes in space and in time, having high spatial and temporal sampling capability and response time.[14] Generally chromogenic and fluorogenic probes are composed of three vital parts which are recognition site, signaling unit and linker.[13] While recognition site is designed in a way as to recognize the analyte of interest, signaling unit is designed in a way as to provide visible, fluorescent readouts as a result of a change in photophysical properties upon reaction of recognition site with the analyte. Linkers are responsible for the connection of recognition and signaling moiety however, they are mostly integrated directly. Although various types of fluorescent probes specific to different analytes exist, there is still growing need for the development of fluorescent probes with improved sensitivity and selectivity, minimum response time and minimum perturbation in biological environment. Because of that for the development of rational fluorescent probes, there are several significant parameters required to be considered extensively.[15] (a) Designed probe should respond only to the analyte of interest and elicit fluorescent response (b) The fluorescence obtained upon interaction with the analyte should be bright which means that it should acquire large extinction coefficient at the excitation wavelength and high quantum yield. (c) Probe should have high stability against the chemicals and light. (d) Fluorescence emission by turn-on or shifts in excitation and /or emission wavelength is more favored than turn off response. Actually, applications of fluorescent probes for the identification of molecular interactions are very important in the sense of chemistry and biology. Therefore, fluorescent probes are designed to work in live cells, too and this brings the consideration of other parameters during the design of fluorogenic probes. (a) The probe should be selective to the analyte and it should not respond to other cellular analytes. (b) Fluorogenic probes should represent high brightness with low dye concentration in order to eliminate photo cytotoxicity to live cells. (c) Probes

designed to operate in near IR range is better for live cell studies since the possibility of photodamage is low and additionally, biological samples have low background emission in NIR region which enhances the signal to noise ratio.

There are several photophysical processes responsible for the changes in fluorescence like quenching via collision, photoinduced electron transfer, exciplex formation, photoinduced charge transfer, energy transfer, etc. In this thesis, analyte detection by fluorogenic probes proceeds over mostly two different photophysical processes which are photoinduced electron transfer (PeT) and photoinduced charge transfer (PCT).

2.2.1 Photoinduced Electron Transfer (PeT)

Probes designed to operate via PeT processes contain acceptor (fluorophore), linker and donor (chelator constructs). The use of linkers is necessary to prevent the full conjugation between acceptor and donor molecule. In case of Bodipy dye, introduction of donor group in the meso position of Bodipy fluorophore enables the disconnection between the acceptor and donor units due to the perpendicular arrangement of donor group. PeT process can be explained better by using simple representative molecular orbital (MO) diagrams.[16] When fluorophore is exposed to the light, an electron from highest occupied molecular orbital (HOMO) is promoted to the lowest molecular orbital (LUMO). Since HOMO level of donor is higher than HOMO level of the acceptor, electron from HOMO of donor is transferred to the HOMO of acceptor which enables the PeT process and thus, fluorescence is quenched (i.e. probe is in fluorescence off state). When the analyte is added to the medium, it interacts with the chelator unit and energy of HOMO level becomes lower than HOMO level of fluorophore; consequently PeT becomes inactive (i.e. probe is fluorescence on state). As a result of this, excited electron relaxes back to ground state and fluorescence emission can be observed (figure 4).[17]

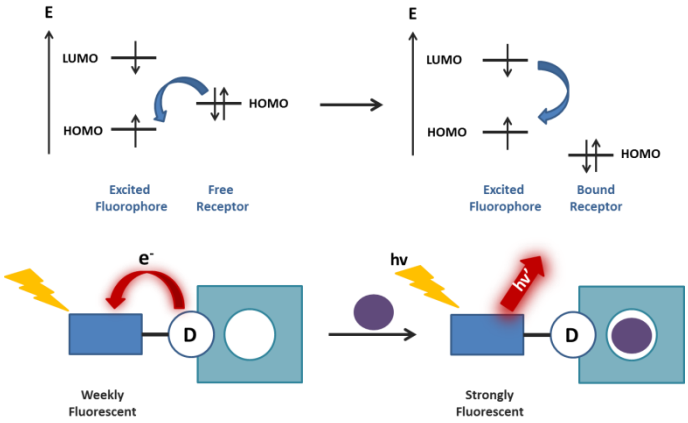

Figure 4: Representative scheme for the photophysical mechanism of reductive PeT

In the case of oxidative PeT which is shown schematically in figure 5, electron donation occurs from fluorophore (donor) to the chelator (acceptor). When fluorophore is exposed to light, an electron from HOMO level of donor is promoted to LUMO level. Since LUMO level of donor is higher in energy than that of acceptor, excited electron is transferred from LUMO of donor to the LUMO of acceptor; consequently fluorescence is in off state. Upon reaction with the analyte, LUMO level is higher than that of donor. Therefore, PeT becomes inactive (i.e. probes is fluorescent on state)[15]. In the literature there are several examples which operate through oxidative PeT mechanism based on Bodipy dyes.[18,19]

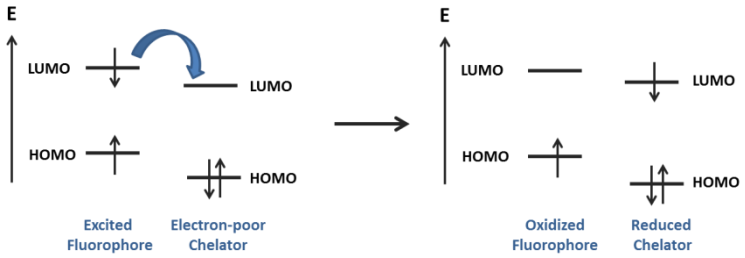

Figure 5: Representative scheme for the photophysical mechanism of oxidative PeT

2.2.2 Photoinduced Charge Transfer (PCT)

PCT operates in probes when electron donating moiety is in full conjugation with electron withdrawing moiety and intramolecular charge transfer from donor to the acceptor occurs upon excitation; consequently, changes in dipole moment leads to the stokes shift which is observed as red or blue shifts in the fluorescence emission spectra. When the analyte like a cation interacts with electron donor moiety of the probe, the ability to donate electrons is reduced. Therefore, due to the presence of full conjugation, a blue shift is observed (figure 6a). On the other hand, when analyte like a cation interacts with acceptor moiety, it enhances electron withdrawing ability of the acceptor group thus in turn, a red shift is observed (figure 6b). Beside these shifts, there will be changes in either quantum yield or lifetimes of the probes.[16]

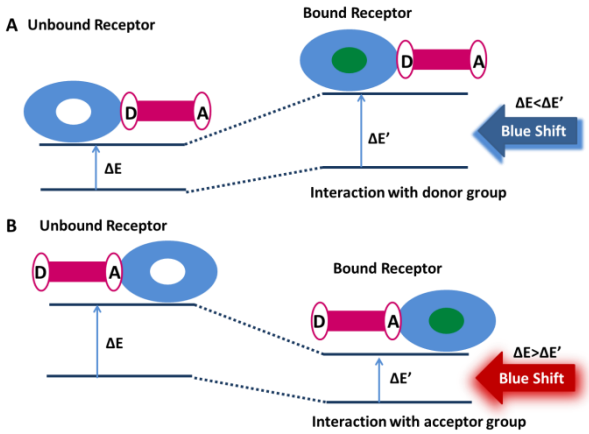

Figure 6: Schematic Representation of PCT Mechanism

2.2.3 Design Strategies for Probe Development

In the literature, there are several classification types for the design strategies required for probe development. Analyte detection can be achieved via three different reaction mechanisms based on (a) protonation-deprotonation (b) complexation (c) carbon-carbon bond forming and breaking reactions.[13] Additionally, analyte recognition mechanisms based on carbon-carbon bond forming

and bond breaking reactions can be diversified by nucleophilic addition/substitution type reactions.[20] Studies presented in the thesis are developed based on the conjugate addition and nucleophilic substitution reactions of analytes so that these reactions are explained deeply in next chapters.

Protonation-deprotonation mechanism has been used to develop pH responsive fluorogenic probes. They are mostly designed to work in neutral pH however modification via OH, COOH and amino groups enable the development of probes with wide pH ranges. In order to enhance the response range, probes should be modified with the introduction of multiple H^+ responsive units in different positions of the molecule.[21] Since pH sensitive groups like OH, COOH and amino have affinity for the metal ions, there is a possibility of complexation reaction which can be eliminated by the arrangement of electronegative groups such that they cannot enable the formation of suitable cavities for metal ions. Large number of pH probes has been reported in the literature based on xanthene[22-24], bodipy[25-28] and cyanine[29-31](figure 7).

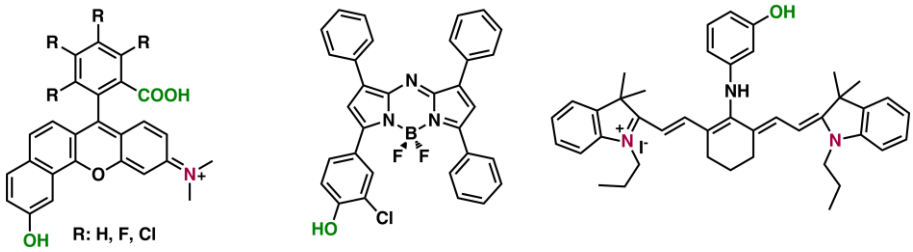

Figure 7: pH responsive fluorogenic probes

Complexation based probes could be developed based on the attachment of receptor and reporter units either covalently or noncovalently. In this type of probes, construction of specific receptor units for the analyte is important because probes respond via the combination of different photophysical processes. Additionally, since several electronegative groups have been introduced for the development of complexation probes, the effect of pH should be examined. Furthermore, the great

challenge in the design and development of this type of fluorogenic probes is the high selectivity for a specific metal ion because most metal ions may interfere with each other due to having similar reactivities (e.g., Mg^{2+} vs Ca^{2+}, Ag^{+} vs Hg^{2+}, and Cd^{2+} vs Zn^{2+}). Complexation based probe in figure 8 works based on the PeT process. Due to electron transfer from donor (receptor) to the acceptor (fluorophore), PeT is on state and consequently, fluorescence of the probe is weak. However, in the presence Zn^{+2} ion, receptor unit makes complexation with the ion and thus, fluorescence emission is enhanced due to the inactivation of PeT.[32]

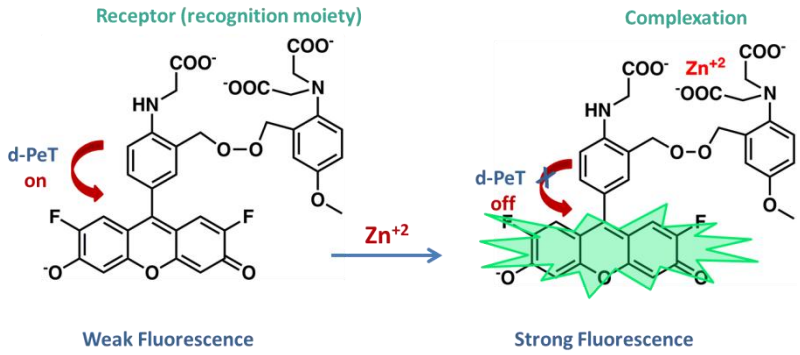

Figure 8: Fluorogenic probes based on complexation with metal ions

Probes based on *carbon-carbon bond forming and breaking reactions* could be accepted as *reaction based probes* which can be classified into different groups based on the reaction types. In general, since these probes recognize the analyte through specific reactions, the spectroscopic changes in the fluorophore will be irreversible which enhances the sensitivity of the probe whereas reduces the applicability of it for dynamic range studies. Probes designed based on the nucleophilic addition to carbonyl group can be applied for the detection of anions, neutral species. When considering the nature of the reaction in terms of chemistry behind it, analytes with high nucleophilicity can be detected by using this type of reaction based probes. For example, cyanide, bisulfite, carboxylates and amines are the common analytes for this type of reaction. Although photophysical changes can be adjusted accordingly, these probes work based on the PeT process. Cyanide ion

can be detected via cyanohydrin formation (figure 9). Probe A is non-fluorescent since PeT operates. When cyanide is added to reaction medium, it attacks to carbonyl carbon of the fluorophore forming cyanohydrin adduct; consequently PeT becomes inactive thus in turn, fluorescent is turned on.[33]

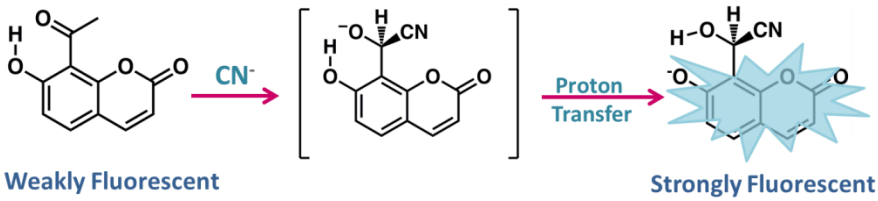

Figure 9: Turn on fluorescent sensing of cyanide

Carbonyl addition based probes can be designed for the sensing of biological thiols which can be detected upon the formation of thiazoline ring through the nucleophilic addition of thiols to aldehyde moiety. In the case of formaldehyde derived fluorescein (figure 10a), selective detection of thiols has been achieved via turn-off fluorescence response.[34] When coumarin has been used for the detection of thiols, turn-on fluorogenic response has been observed.[35]

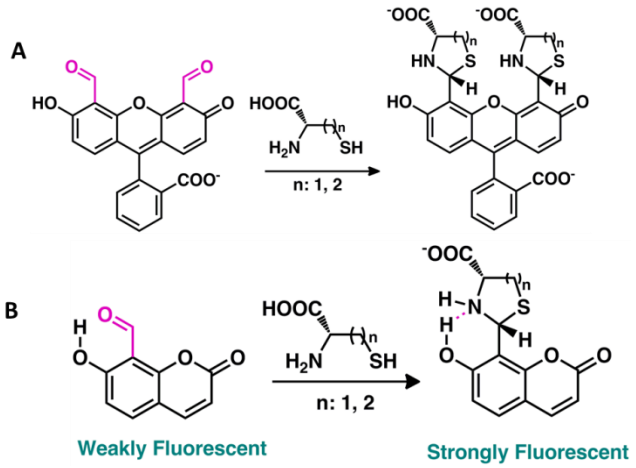

Figure 10: Fluorescence turn-off (A) and turn-on (B) probes for the detection of thiols

Since thiols are soft nucleophiles, they prefer to attack to soft electrophiles. Because of that biological thiol detection operates through the *Michael addition* reaction which can also be named as 1, 4-conjugate addition. Many fluorescent probes have been developed based on the thiol addition to maleimide unit modified fluorophore like bodipy as in figure 11a.[18] Beside maleimide unit, quinone derived fluorophores can be used for the conjugate addition of thiols as in figure 11b.[36]

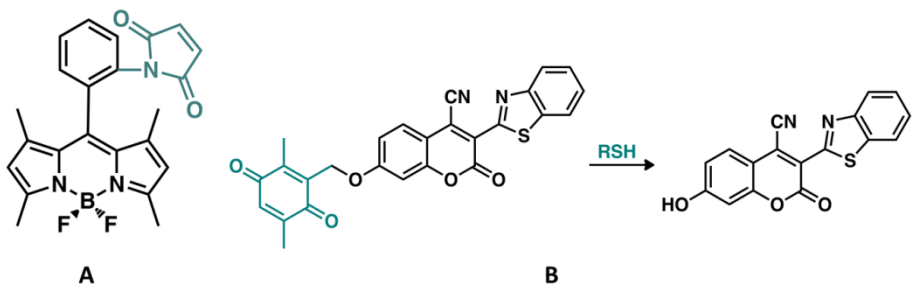

Figure 11: Fluorescence based detection of thiols via conjugate addition.

Thiols can also be detected by *nucleophilic substitution* reaction by use of electron sink 2,4-dinitrobenzenesulfonyl moiety[37] or by the use of disulfide bridges.[38]

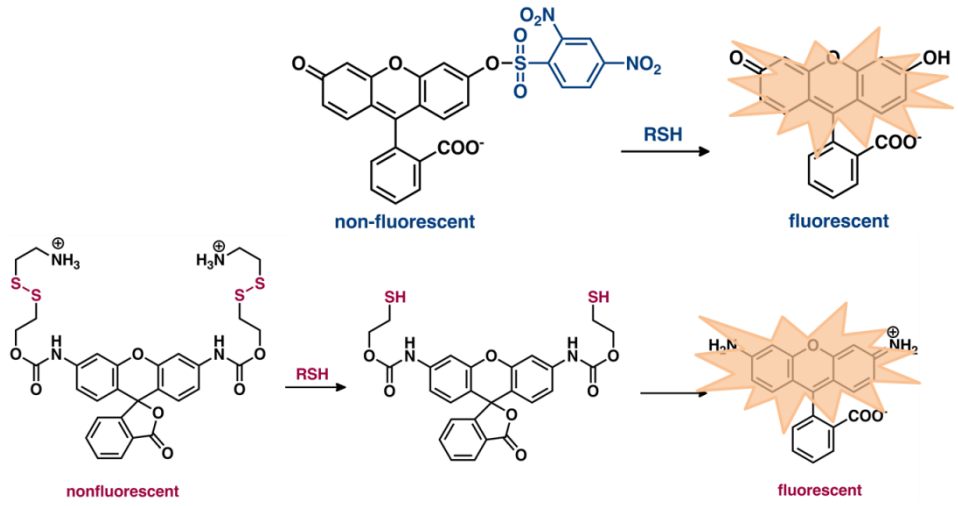

Figure 12: Fluorescence based detection of thiols via nucleophilic substitution

2.3 Protein Labeling

Proteins are one of the major biological macromolecules which are composed of different combinations of amino acids. Proteins can be accepted as worker biological molecules existing in all living organisms whose functions like catalysis of metabolic reactions, DNA replication, molecular recognition, visualization of cell-cell interactions, protein dynamics, mechanisms of life cycles of proteins, etc. affect whole organization of life. Because of that it is important to figure out how they function normally, how they interact with other molecules or how some diseases are caused by the abnormal shapes of them.[39] Protein labeling can be depicted as tagging of proteins in order to figure out their functions, interactions and movements either *in vitro* or *in vivo*. In the literature, there are several approaches which enable the introduction of small probes bearing wide range of photophysical properties to purify target proteins *in vitro*. Labeled purified proteins can be applied to identify protein-protein interactions but they have differences in behavior compared to those in live cells. Proteins have at least two functional groups which can be used for the labeling procedures are amino functionality (N-terminus) and carboxyl functionality (C-terminus). In order to label the proteins, chemical methods like covalent bonding can be used to interact with functional groups on aminoacids specifically. Additionally, nonspecific attachment methods to N or C terminus of amino acids are also possible. Other than these, methods involving enzymes requiring related polymerases, ATP and labeled amino acids or nucleotides can also be used to labels proteins and amino acids. The expression of tagged proteins via *in vitro* translation is difficult since this requires proper protein length, folding and post-translational modifications which cannot be provided by some of the kits.

2.3.1 Fluorescence based labeling of proteins

The need for chemical protein labels has led the researchers to develop new strategies for labeling of proteins. Traditional methods used for labeling studies are not good enough for *in vivo* studies since purification of protein, chemical labeling, repurification and reintroduction into cells by invasive methods like microinjection are hardly necessary.[40] Spectroscopic measurement based methods are more prosperous since they are minimally invasive; allow real time monitoring of cellular events without any perturbation. For this reason, spectroscopic tags must be employed for labeling of the target proteins. Among spectroscopic methods, use of fluorescence based methods is more promising because fluorescent response is obtained swiftly in a short time. Beside *fast signal acquisition*, *sensitivity* of *detection* has been developed which enable single molecule detection due to the development of current technologies.[41] Additionally, dyes can be prepared in multiple colors which can be applied for multiplex assays. Furthermore, since the size of the tag is small, this reduces the possibility of perturbation in the behavior of the tagged protein. Different from enzymatic reactions in which the signals amplify and diffuse, fluorescent signals is localized with high spatial resolution. Moreover, fluorescent labeling reagents are stable and robust in biological environment. Lastly, the labeling process is very straightforward.[41,42]

Characteristics for a good labeling tag and method: First of all, after the determination of labeling strategy, either the nature of suitable tag or the type of conjugation reaction has to be considered extensively. As labeling strategy, choice of tag is very important for effectiveness of the method. Small-sized tags should be preferred in order to eliminate the possibility of perturbation in natural behavior of labeled protein. Preferred tag should show performance equally in cell surface, in cytosol and also in an organelle. Having multiple choices of tags are beneficial in order to introduce multiple probes with wide spectrum ranges. The methods have to be chosen in a way as to ensure specific and selective labeling of the target protein in

a cell which contain other biomolecules. The interaction between label and protein must be stable enough to enable the stable interaction between two molecules so that label remains securely attached to the protein during the assay. Lastly, labeling reaction should be designed to be orthogonal to any reactions.[42]

2.3.1.1 Fluorescent- protein based labeling

Fluorescent labeling of proteins has started with the use of green fluorescent protein (GFP) or one of its variants when their genetic sequence becomes available. After the expression of gene fusion, autofluorescent GFP fusion could be detected microscopically. Due to its small size (ca.27kDa), compactness, its single domain structure enable GFP to be fused to a variety of proteins without causing any interferences in native protein functionality.[40] Modified versions of GFP like cyan fluorescent protein (CFP), yellow fluorescent protein (YFP) and blue variants have been generated to offer various emission wavelengths with improved photo-stability. Availability of multicolored variants of fluorescent proteins (FP) contributes to the development of cell biology studies by consenting the multicolor labeling of multiple proteins in a single cell. FP based labeling of proteins is an extremely sensitive method since FP fused proteins are only fluorescent species in the target cells. Beside, fluorescence intensity can be used for the determination of amount of protein since there is a direct correlation between them. This method can be used for live cell monitoring of either dynamic distributions or localizations of proteins, protein-protein interactions and quantifying the expression levels of proteins in real time.[42] Moreover, since fluorescent proteins are highly stable and it cannot be sheltered by proteins barrel structure, they can be used to track the localization and movement of fusion proteins in cells.

On the other hand, this approach brings several intrinsic limitations. GFP is a large protein consisting of 238 amino acid proteins which can interfere with localization,

structure and activity of the proteins to which they are fused. Additionally, some FP may form dimers, tetramers which cause detrimental effects both on the function and movements of host protein inside the cell. After the expression, FP needs a few hours to become fluorescent which makes it time consuming. Fluorescent proteins are poor against the environmental cues like pH, hydrophobicity and ion concentrations. Modification of fluorescent proteins leads to loss of fluorescence. Furthermore, they are not bright and photostable enough.[43] Because of that alternative approaches for fluorescent labeling of proteins are extremely demanding.

2.3.1.2 Chemical Labeling of Strategies

Chemical labeling of proteins can be accomplished through either covalent labeling or non-covalent labeling strategies. Both of them requires the use of fluorescent dyes like rhodamine, cyanine, fluorescein, bodipy, etc. which offer superior advantages such that fluorescent dyes can be designed and synthesized easily accordingly with desired excitation and emission wavelengths. Since their synthetic modifications are possible, they can be modulated by the introduction of variety of functional groups for different purposes. Through the introduction of dye surface modification groups, charge and solubility of the fluorescent label can be controlled. Conjugation could be very simple. The brightness of the dyes can be altered by attaching multiple low molecular weight dyes. Beside, by extending the conjugation, dyes fluorescence at longer wavelengths can be synthesized in order to reduce background fluorescence resulted from cell debris, buffer components and plastic materials. Excitation of them is easy since they can be excited by red-emitting lasers and laser diodes.[41]

Covalent Labeling: Two systems have been employed for the labeling of proteins on cell surface is ACP-PPTase[44] system (figure 13) and self-alkylation reaction of human O^6-alkylguanine transferase (hAGT) to label hAGT fusion protein (figure 14). [43,45]

ACP-PPTase system has been developed for the labeling of cell surface proteins or other constituents of cell. In this system, acyl carrier protein (ACP) undergoes post-translational modification by phosphopantetheine transferase (PPTase) in order to enable the transfer of 4′-phosphopantetheine from coenzyme A (CoA) to a serine residue of ACP. Unfortunately, this system can be applied for the protein labeling studies inside the cells due to the activity of endogenous enzymes and low cell permeability of the dyes.[44]

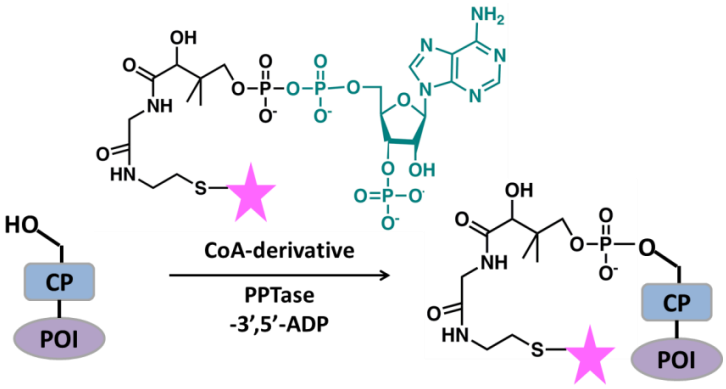

Figure 13: Labeling of ACP proteins on cell surface

Other covalent labeling strategy has been developed for labeling of label hAGT fusion proteins with a type of fluorescent O^6-benzylguanine substrates with the self-alkylation reaction of human O^6-benzylguanine transferase (hAGT). Due to the covalent nature of label, it can be applied for long term studies. The limitation of this method comes from the background labeling of human AGT which can be overcome by using fast AGT mutants and using specific inhibitors.[43-45]

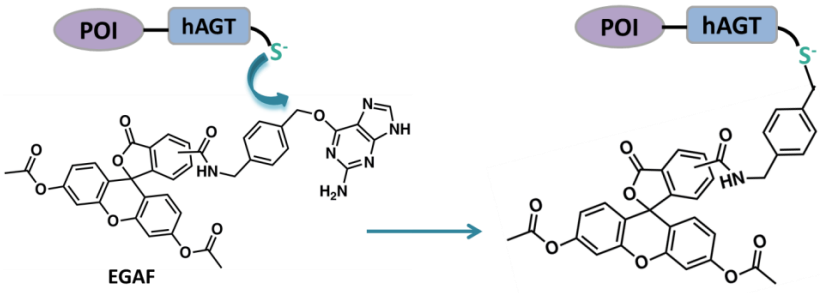

Figure 14: Covalent labeling techniques for the hAGT system

Noncovalent Labeling: Unlike covalent labeling strategies, non-covalent labeling techniques do not represent problems derived from either endogenous enzyme or substrates. One of the oldest methodologies is based on the metal ion interaction which is the tetracysteine/biarsenical method (figure 15). This strategy proceeds based on the specific interaction between membrane-permanent biarsenical dyes and tetracysteine motif of a short peptide tag containing six aminoacids like CCPGCC. TC dye at the beginning is nonfluorescent but as a result of its interaction with TC tag, fluorescence is on and tag-dye adduct fluoresces.[46] The fluorescent labeling works based on the PET process and due to the increase in fluorescence emission as a result of binding to the target, background noise common to labeling experiments could be reduced. Since tetracysteine motif is small enough to be fused with either N terminus or C terminus of the protein. The specific interaction between TC/biarsenical dyes is stable and it offers multi-coloring options. On the other hand, there is a possibility of nonspecific labeling of cysteine rich proteins. Additionally, cysteines in tag should be in reduced form otherwise, labeling of proteins in oxidizing environments becomes difficult.[40] Beside this, there are other techniques such that hexahistidine-tag-Ni^{+2}-nitrilotriacetate-fluorophore complex[46] and TMP-eDHFR labeling system.[47]

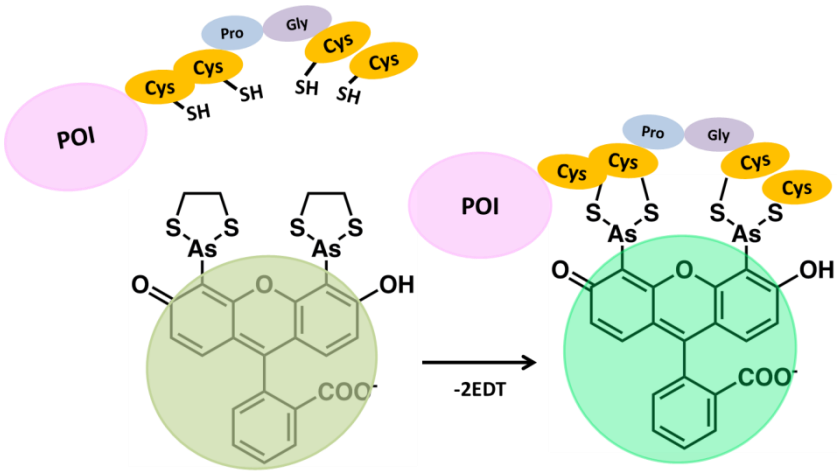

Figure 15: Noncovalent labeling strategies based on tetracysteine/biarsenical system[46]

2.4 Photodynamic Therapy

Photochemotherapy[48] of cancer is often called as photodynamic therapy (PDT) which can be stated as minimally invasive treatment methodology applied for the treatment of both cancer diseases and non-oncological disorders. This approach is multicomponent treatment methodology combining the effects of photosensitizer (PS), light, and molecular oxygen and proceeds with the systematic administration, selective accumulation and retention of a photosensitizer in tumor tissue prior to irradiation with light of specified wavelength (therapeutic window: 600-800nm).[49] Vital biological molecules having chromophores like melanin, nucleotide bases in DNA/RNA, hemoglobin (Hb)/ oxyhemoglobin (OxyHb) absorb at UV region. Due to the presence of endogenous absorbers, long-wavelength light is required for tissue penetration and thus, the photosensitizers applied in PDT should have absorption at 600-800nm which is called as therapeutic window. PDT aims the selective destruction of cancer tissue via direct cellular damage, vascular shutdown and activation of an immune response against the targeted cells by preventing toxicity toward the healthy tissue.[50]

Although PDT is a new treatment methodology, the advantages offered by PDT could not be underestimated. PDT based treatment requires the one time injection of drug (PS) after a definite time interval by single illumination and it proceeds over outpatient basis. On the other hand, radiotherapy requires 6-7 weeks and chemotherapy can last for several months. In the case of surgery which is a single shot procedure requires general anesthesia and hospitalization for several weeks. Considering these, PDT is a cost-effective methodology with increased life expectancy. PDT is local rather than systematic treatment methodology. Since it can be targeted precisely, scarring will be little or none after healing. Limited light penetration offers an advantage of protection of healthy tissue beneath tumor from phototoxicity. Unlike radiation it can be repeated many times even at the same site in case of recurrence or a new primary tumor in the previously treated area.[51,52]

PDT has also its limits. Due to lack of selectivity for tumor, photosensitization may occur in the healthy tissue. There is a possibility of light absorption by endogenous absorbers. The penetration of red light in tissue is generally 5 mm which is limiting factor of PDT since it cannot be used for the treatment of tumors in deeper tissues. PDT action can be effective only in the presence of molecular oxygen because of that in the necrotic tumor core, PS action is reduced. Due to irregular structure of tumor tissue, selective uptake and distribution of PS is not possible and amounts of transmitted light will be different.[1]

2.4.1 Photosensitizer and Singlet Oxygen as Key Elements of PDT

2.4.1.1 Photosensitizer

PS is one of the key components of PDT and characteristics of an ideal photosensitizer can be classified as essential and desirable criteria for the effective application of the methodology. PS should be pure chemical compound not a mixture which has high chemical and photo-stability with intense and long wavelength absorption. The photosensitizer should be selective for the target. Besides, it must be efficient in situ, non-toxic to host and excreted rapidly from the body. Additionally, PS should have aqueous solubility, short drug-light interval, straightforward synthesis, and thus, simplified scale up. Moreover, PS has high extinction coefficients at longer wavelengths for tissue penetration of light, low quantum yields of photobleaching and high quantum yield of singlet oxygen.[53]

Chemical Purity: In order to administer a drug or therapeutic agent into the human body, its exact chemical composition and purity should be known since when they are injected, their structure can be altered which may cause severe side effects. If the chemical composition of the therapeutic agent is known, it will be easy to comprehend the metabolism, pharmacokinetics, etc. and also, the resultant side effects could be explained in rational manner. Additionally, the purity of the drug is

very important since the application of drug as a mixture worsens the scenario by increasing possible side effects. ***Efficiency of a photosensitizer in situ***: PS should be active in the cancerous target area and it should produce singlet oxygen in the desired tissue. ***Chemical Stability****:* PS should be relatively inert. When administered to the body, the immune system and the metabolism start to fight with PS. For a PS to be active in desired area, it should be stable against the hydrolysis or the actions of esterase or protease enzymes. ***Photostability****:* Illumination should be applied when PS has reached their targets. Photodegradation and photosensitization process are acceptable as a result of target illumination, thus in turn, this reduces the post-treatment photoeffects. Additionally, PS should not have any dark toxicity. ***Light absorption****:* in order to eliminate the effect of endogenous absorbers, PS should be designed in way that it should absorb between 600 and 900 nm.[1]

2.4.1.2 Singlet Oxygen

In PDT, singlet oxygen has been accepted for the main cytotoxic agent which demonstrate biological effects and it is generated via photosensitization by using PS whose singlet oxygen quantum yield of 0.2-0.7. Singlet oxygen generated can be determined in several ways. Direct measurement at 1270 nm is possible however; more commonly, it can be measured based on the reaction of it with singlet oxygen quenching agents with spectroscopically by detecting the changes in the absorbance of dyes as a result of oxidation and fading of them. There are three significant aspects of singlet oxygen which must be understood deeply in order to comprehend the biological consequences. First of all, concentration and source of singlet oxygen have great impact on the singlet oxygen generation capacity thus in turn, biological activity. Each tissue has different oxygenation status and solid tumors are known as under hypoxic condition. This means that reduction of oxygen concentration from 5% to 1% leads to decrease in the effect of PDT. Another important criterion of singlet oxygen is its life time in cells which were estimated to be short with a limited

diffusion distance (10-300 nm). Because of that generated singlet oxygen in cells does not damage to the neighboring cells. This gives most important property to the PDT which selectively damage to the target cells over non-targeted normal cells in the irradiated area. The other important criterion is the singlet oxygen quantum yield which is the quantitative expression of the ability of a PS to yield singlet oxygen. This parameter can be used to assess the potential applicability of PS for PDT.[54,55]

2.4.2 Mechanism of Action and Biological Response

After injection of a non-toxic photosensitizer (PS) whose absorption lies in therapeutic window into the target tissues, photoirradiation has been employed in order to excite PS from its low energy ground state (S_0) to a short lived high energy singlet excited state (S_1) which goes to triplet excited state (T_1) via intersystem crossing (ISC). PS in triplet state contributes to the initiation of biological response through two different mechanisms as Type-I and Type-II. In the case of Type-I, ^{3}PS can react with a substrate like cell membrane or molecule to form radicals upon transfer of hydrogen (electron) and initiating an electron transfer leading to formation of radicals which react with molecular oxygen to produce reactive oxygen species (ROS) like hydrogen peroxide (H_2O_2), superoxide anion ($O_2^{\cdot -}$), hydroxyl radical ($OH^{\cdot}$) as shown in figure 16. On the other hand, in the case of Type-II mechanism, triplet state photosensitizer transfers its energy to molecular oxygen which leads to the formation of singlet oxygen. Although both types of reactions can induce cell death, $^1O_2$ generated by via Type-II mechanism is believed to be responsible for cell death through apoptosis and necrosis. When considering the mechanism, PDT action of a PS can't occur in anoxic areas of tissue due to oxygen dependent nature of the drugs.[56]

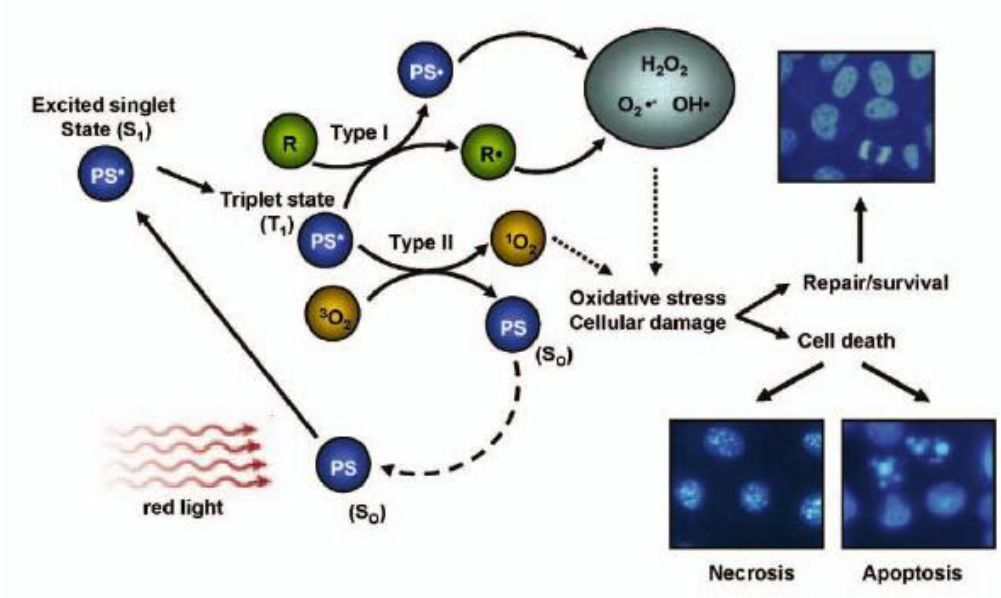

Figure 16: Action Mechanism of photosensitizers in PDT.[57]

After the administration of PS systemically, PS circulate for an appropriate time interval and then it starts to localize preferentially in tumor tissue due to the physiological differences between tumor and healthy tissue prior to light activation. Localization of PS in tumor cells in a way to achieve maximum tumor to normal cell concentration may take 3 to 96 hours which depends on the type of the administered photosensitizer and the nature of the tumor. Fluorescence from PS helps to diagnose and detect tumor. PS accumulation is expected to occur totally in tumor tissue. If it is not the case, light activation represents another chance of selectivity for the generation of cytotoxic effect. When light at a wavelength specific to the photosensitizer is administered, PS produces singlet oxygen which reacts to destroy tumor tissue (figure 17). PS activated singlet oxygen generation causes cell death in two major routes such as apoptosis or necrosis.[58,59]

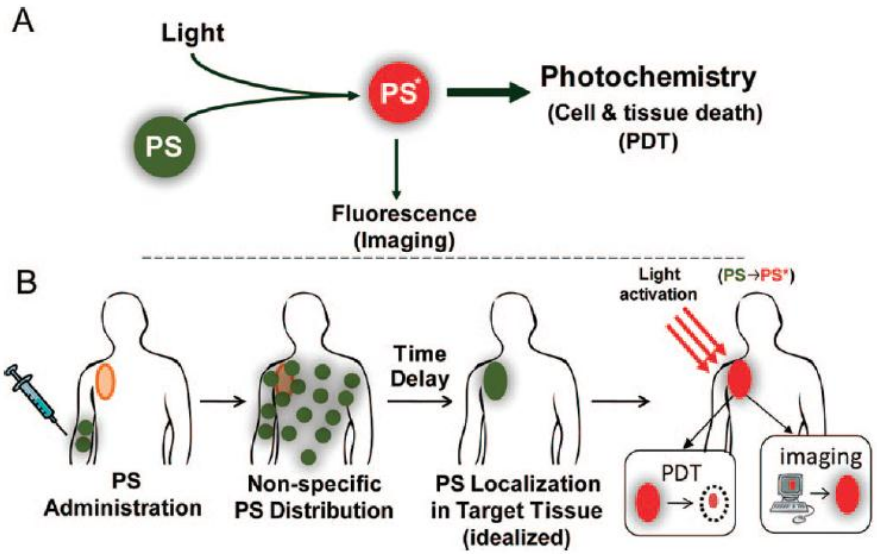

Figure 17: (A) Schematic representation of PDT (B) Schematic representation of sequence of events in PDT[59]

Necrosis represents the gross damage to cellular structure however apoptosis causes subacute damage which leads to cascade mechanism of various aspects of cell machinery and signaling. Cell death by necrosis is the result of generation of high concentration of singlet oxygen which leads to drastic perturbation with immediate morphological changes in tumor tissue. Oxygenation-dependent cell disruption of cell membrane is a type of necrotic damage. In the case of cell death by apoptosis, even small amount of singlet oxygen triggers a cascade of events which leads to the systematic shutdown of cell function. Photodamage to membrane, endoplasmic reticulum, lysosomes, mitochondria or DNA may induce apoptosis. These processes are affected by photosensitizer localization and time of illumination but at the end, cell death is probably is the result of mixture of both processes.[1,60]

2.4.2 Activatable Photosensitizers

Traditional PDT employs the passive photosensitizers which can also localize in the normal cells. Since the use of passive PS increases the possibility of healthy tissue damage, restricted feasibility of method due to the delivery challenge, there is a growing need for the development of activatable photosensitizers which would be active in the presence of specific triggers in diseased cell thus in turn, damage to nearby healthy tissue is going to be reduced. Activatable photosensitizers can be designed to be activated by different triggers specific to diseased tissue. When PS has been administered to the body, firstly it should be inactive prior to molecular activation which unqenches the PS so that singlet oxygen generation efficiency is increased. There are several ways to keep PS in quenched mode. Quenching can be accomplished before either energy transfer between singlet and triplet excited state or self-quenching[61] of PS. Additionally, quenching can be accomplished at the excited state via photoinduced electron transfer. Furthermore, quenching may occur via the use of singlet oxygen quenchers during the singlet oxygen generation as a result of triplet state energy transfer.[52,62]

FRET is a non-radiative energy transfer processes in which chromophores (electron donor) in its excited state transfers its energy to other chromophores (electron acceptor) in the ground state, thus in turn; due to the overlap between absorption and fluorescence, fluorescence is quenched. FRET is only active when PS and quencher are nanometers apart (figure 18). FRET based quenched photosensitizers can be activated through the tumor specific enzymes like proteases. Photodynamic molecular beacons are modified with triggering units according to either cleavable[63] or openable[64] activation mechanism in which the linker is cleaved by the enzyme specific to the targeted tumor followed by the removal of the quencher from the vicinity of PS that enable the cytotoxic singlet oxygen generation (figure 18).

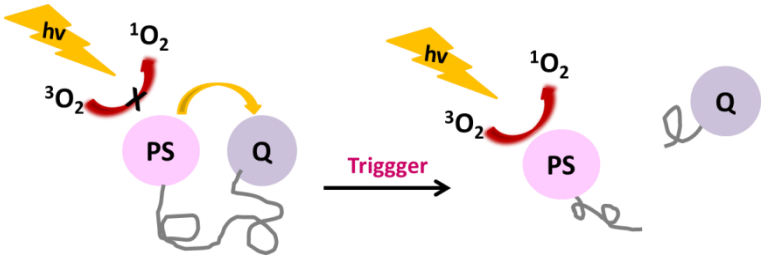

Figure 18: Schematic representation of FRET based quenching

Molecule in figure 19, PS and quencher are connected via the linker of which proline-asparagine bond can be cleaved by fibroblast activation protein (FAP) enzyme via cleavable activation mechanism.[63]

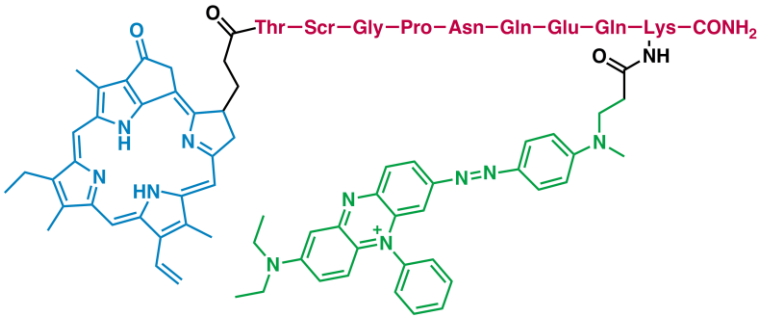

Figure 19: Photosensitizer activation through cleavable activation mechanism.

PET is photophysical process which is based on the switching off and on mechanism to control the fluorescence. When PeT becomes inactive upon reaction with the triggering group specific to a tumor, PS is activated to generate singlet oxygen (figure 20).

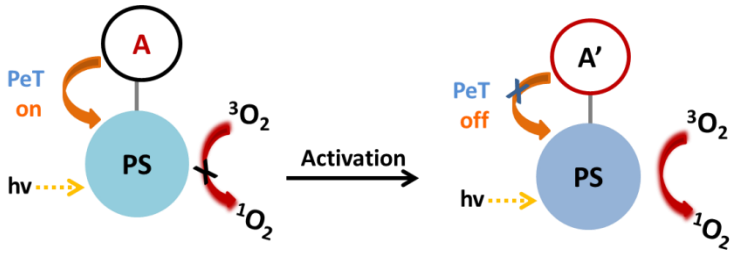

Figure 20: Photoinduced electron transfer based control of PDT action.

Photosensitizer in figure 21 becomes inactive by using PeT approach in combination with environment activation strategy like pH.[65] The differences between intracellular and extracellular pH of targeted cell has played a vital role in drug delivery to specific to target as a result of acidic nature of growing malignant tumors (pH 6.5-6.8) compared to normal tissue (pH 7.4). Photosensitizer at physiological pH is inactivated via PeT process however, in the tumor tissue, PeT is off which leads to the activation of PS to generate singlet oxygen. The introduction of pH activatable PS in tumor cell provides therapeutic selectivity in cancer treatment.

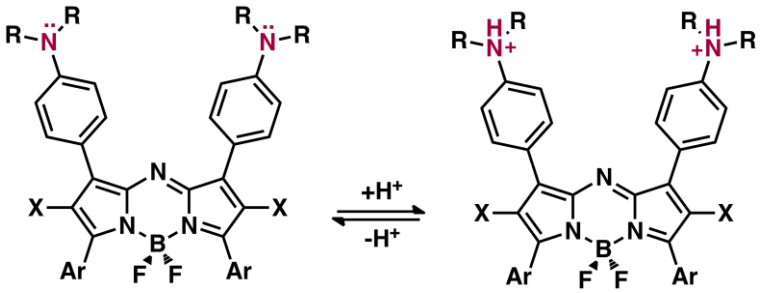

Figure 21: pH activatable photosensitizer

CHAPTER 3

3. Chromogenic and Fluorogenic Sensing of Biological Thiols in Aqueous Solutions using Bodipy Based Reagents

This work is partially described in the following publication

Murat Isik, Tugba Ozdemir, Ilke Simsek Turan, Safacan Kolemen

and Engin U. Akkaya[*,†,‡]

Org. Lett., **2013**, *15* (1), pp 216–219

3.1 Objective

Sensing and signaling of biological thiols is at the focus of recent flurry of work. These reaction based probes take advantage of high nucleophilicity of thiol functions found in biologically relevant species such as Cystein (Cys), Homocystein (Hcy) and Glutathione (GSH). These biothiols are vital for the maintenance of cellular redox status and alterations in their levels is linked to a number of severe diseases such as AIDS, cancer and Alzheimer's. Consequently, probes which respond to these thiols by color change, emission change or both are highly valued. If they are made to function in aqueous solutions, naturally, they are deemed to be more desirable considering potential applications. Because of that in this study, two different nitroolefin-BODIPY conjugates operating at different wavelengths were designed and evaluated in biothiol (Cys, Hcy and GSH) sensing in aqueous solutions. We have decided to evaluate their success in terms of the selective, sensitive and rapid detection of biologically relevant thiols via colorimetric and fluorometric changes.

3.2 Introduction

Sulfhydryl-bearing compounds have sole chemical reactivity and utility in either chemical reactions or biological processes. While thiols and thiophenols are commonly used in synthetic chemistry, thiothreitol and 2-mercaptoethanol are widely used as antioxidants in biological studies. Besides, cysteine (Cys), homocysteine (Hcy) and glutathione (GSH) have very significant metabolic roles in biological systems. The alterations in their levels are associated with number of serious diseases.

From these thiol bearing compounds, Cys which is a precursor of GSH plays vital roles in protein structure and function. Due to its ability to meet reversible redox reactions under physiological conditions, it is an indispensable thiol bearing amino acid for maintenance of the tertiary and quaternary protein structures with disulfide bond formation[66,67]. Abnormal levels are related with severe disorders. For instance, slow

growth in children, hair depigmentation, edema, lethargy, liver damage, loss of muscle and fat, skin lesions and weakness are the severe consequences of Cys deficiency.[68] Abnormal levels of Hcy is the messenger of cardiovascular disorders, Alzheimer's disease, folate and cobalamin deficiency, birth defects and cognitive impairment in elderly.[69] Tripeptide GSH is the most abundant intracellular non-protein thiol which plays vital roles in cellular functions such that maintenance of intracellular redox activities, xenobiotic metabolism, intracellular signals transduction and gene regulation. GSH is present at higher levels (0.1-10mM) compared to other cellular thiols. Additionally, since it is responsible for redox homeostasis between sulfhydryl (reduced form, SH) and disulfide (oxidized form, S-S), GSH plays indispensable role in maintaining the oxidative homeostasis for cell growth and function. Additionally, its levels can be correlated with many diseases like cancer, Alzheimer's disease and cardiovascular diseases. Because of that their sensitive and selective detection in biological environment has attracted growing interest.

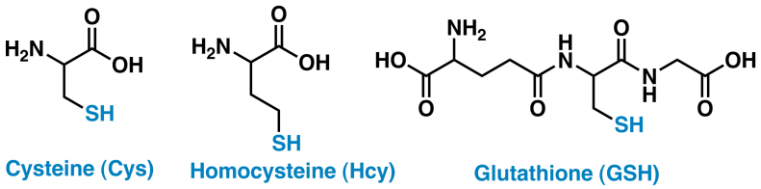

Figure 22: Structure of thiol bearing biological compounds

Thiols have wide range of applications in synthesis and in the literature, there are several examples reported for the selective, sensitive and rapid detection of biological thiols. When considering their synthetic properties (figure 23), their detection can be accomplished via nucleophilic addition, nucleophilic substitution, etc. as explained in chapter 2.2.3.

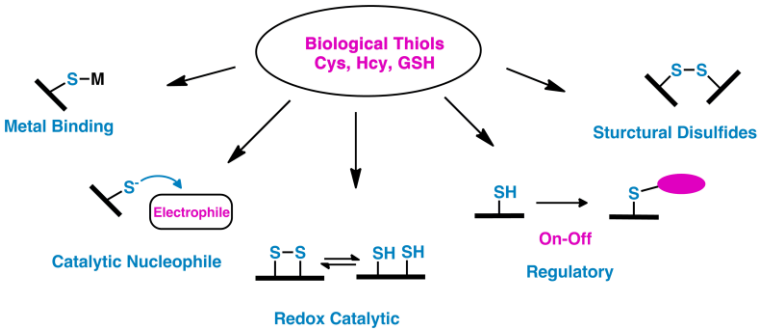

Figure 23: Type of reactions based on Sulfhydryl containing biological thiols[67]

Since thiols are weak nucleophiles, they have tended to react with weak electrophiles and this reaction is specific to thiol containing compounds. Conjugate addition is most appropriate strategy to design thiol sensitive probes. Michael addition reactions can be devised via the incorporation of maleimide (**A**)[70], nitroolefin (**B**)[71], malononitrile (**C**)[72] functionalities to the fluorophores.[73]

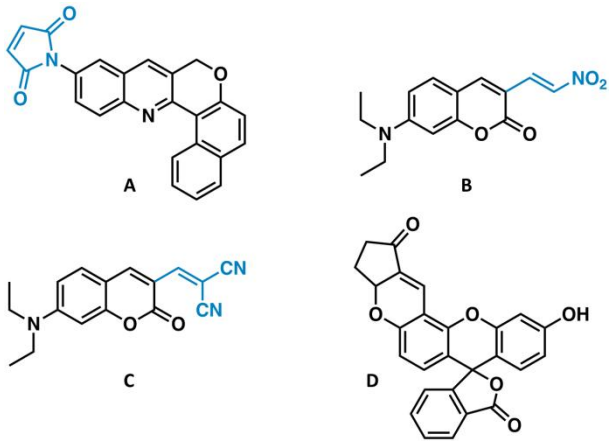

Figure 24: Structures of probes proceeds based on conjugate addition of thiols.

3.3 Design of Probes

Sensing and signaling of biological thiols via color change, emission change or both are very valuable since they are vitally responsible for either the maintenance of cellular redox status or the alterations in their levels are linked to severe diseases.

While considering these, we have started to design our probes by deciding the type of reaction which could be applied for thiol sensing. Since we have wanted to detect thiols irreversibly, it is best to design the probes as reaction based manner. Michael addition or conjugate addition is one of the major reaction types that can be applied for reactions with thiols since thiols are weak nucleophiles; they react readily with the weak electrophilic carbon of the Michael acceptors. In the design of active probes, the reaction used for the sensing applications is vital as its reactivity which means that probe should react with the analyte swiftly. This bring us to a point that we have decided to modify our Michael acceptor by introducing electron withdrawing unit (nitro group) in order to enhance the electrophilicity of the Michael acceptor carbon. We have functionalized bodipy core via Henry Reaction in order to incorporate thiol reactive group.

Additionally, if the designed probes have high water solubility with enhanced functionality in aqueous solutions, they would become potential candidates for the biological applications. Because of that we have wanted to incorporate ethylene glycol moieties in order to enhance water solubility of probes. Furthermore, we have widened the scopes of this reaction by devising another probe which has ability to sense and signal biological thiols in longer wavelength region with increased water solubility (figure 25).

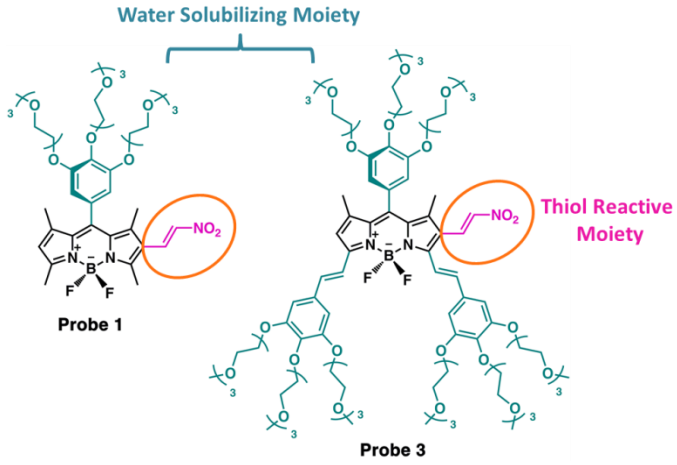

Figure 25: Design elements of Thiol Probes

3.4 Results and Discussion

3.4.1 Synthetic Approach

We have devised our structure with water solubilizing ability and for this, the synthetic journey for this project starts with the synthesis of triethyleneglycol functionalized aromatic aldehyde which is very familiar with our research group. The synthesis of aromatic aldehyde with aqueous solubility (TEG-aldehyde) requires four synthetic steps involving modification of triethyleneglycol monomethylether with good leaving group (*p*-toluenesulfonyl group, **1**), introduction of synthesized compound into methyl-3,4,5-trihydroxybenzoate (**2**), reduction of ester with $LiAlH_4$ (**3**) and PCC oxidation of benzyl alcohol (TEG-aldehyde **4**) to afford the target aldehyde. Later, we have preferred to construct bodipy skeleton through the use of TEG-aldehyde in the presence of acid catalysis (figure 26). Formed air sensitive dipyyromethanes have been oxidized by *p*-chloranil or DDQ to yield dipyrromethene. Abstraction of acidic proton through the use of excess base followed by borontrifluoride on the dipyrrin affords the target bodipy cores (**8**). Nitroolefin functionality can be introduced to the structure through aldehyde functionality via Henry Reaction and because of that, we have continued with the Vilsmeier Haack reaction in order to incorporate the formyl functionality into the core (**9**).

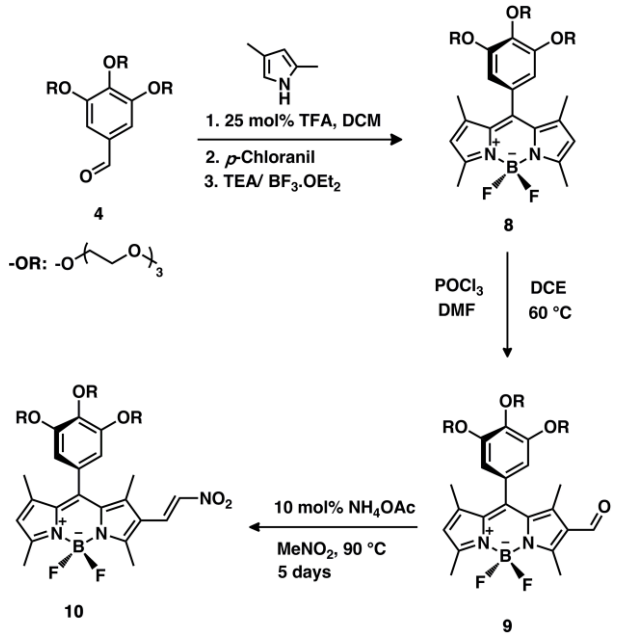

Figure 26: Pursued Synthetic route for thiol probe **1**

NH_4OAc catalyzed nitromethane condensation affords our target compounds (Thiol probe **1**, **10**). Unlike from thiol probe **1**, Thiol probe **3** requires extra step not only for the incorporation of extra aqueous solubility units but also for the extension of conjugation which is indispensable property for a probe to be used in biological applications. After the synthesis of core bodipy (**8**), Knoevenagel condensation has been employed for the introduction of extra water solubility with enhanced conjugation (**11**) prior to Vilsmeier Haack (**12**) and Henry reaction (Thiol probe **3**, **13**).

3.4.2 Working Principle

Michael reaction based thiol sensing protocols emerges to bloom among other strategies. Incoming of thiol to the β-position of nitroolefin is expected to disrupt the π-conjugation and block the Intramolecular Charge Transfer (ICT) process, which is

intrinsically anticipated to induce a blue shift in absorbance. Gallic acid derived (TEG) unit substituted at the *meso*-position of BODIPY core plays two crucial functions: i) efficient Photoinduced-electron-Transfer (PeT) control is brought in such a way that inherently electron rich Gallic acid moiety could quench the emission of the probe to some degree if attached to the electron poor, nitroolefin substituted BODIPY in the exited state and ii) last but not least, ethylene glycolic entities anchored on phenolic hydroxyl functionalities should facilitate water solubility, thus the probe **1 (10)** may find broader interest regarding potential bio-applications. Since they are soft nucleophiles, biological thiols attacks to soft nucleophilic carbon of nitroolefin functionality of BODIPY conjugates and blocks both the PeT and ICT process and thus, fluorescence enhancement is deemed as interruption of PeT mechanism operating in the free probe **1** (**10**) (figure 27).

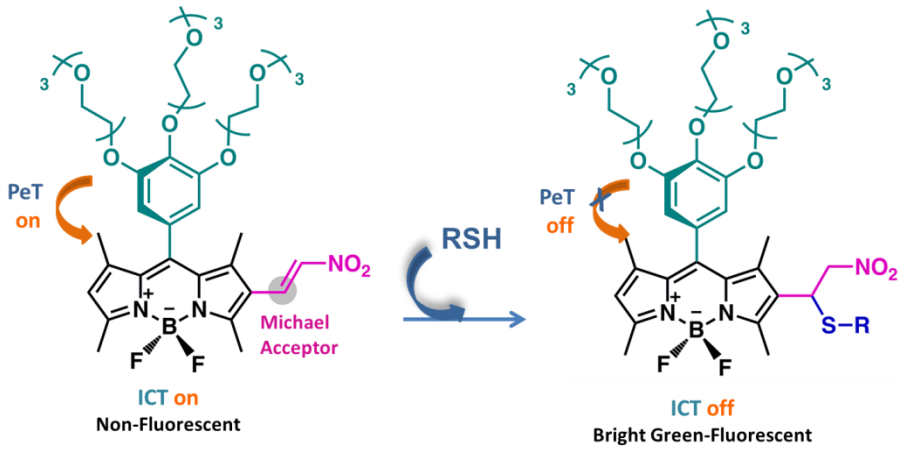

Figure 27: Design elements of the nitroolefin-BODIPY conjugate thiol probe **1**.

3.4.3 Spectral Proofs for Sensing Process

To test aforementioned hypothesis, we have initiated our studies by focusing on the synthesis of a simpler analog of **1**, and revelation of its 1,4-addition reactivity with thiols. *Meso*-H substituted thiol sensor **2 (7)** was prepared from the readily available 2-formylBODIPY precursor via tandem Henry/elimination reaction. Once *β*-

mercaptoethanol (**ME**), chosen as the simple biothiols model compound, reacted with the thiol sensor **2** an apparent color change from red to orange was noticed. This bright green fluorescing 2-ME adduct was presumed to be the 1,4-conjugate addition product (figure 28). Due to poor solubility of probe **2** in common organic solvents, absorption and emission spectra were not recorded. Michael reaction of probe **2** and **ME** was trackable by ^{1}H-NMR spectroscopy and HRMS analysis. Comparison of ^{1}H-NMR spectra of **2** and adduct clearly shows that the addition of **ME** to the sensor **2** perishes the vinylic protons (H_a and H_b) resonating at 8.07 and 7.44 ppm with the concomitant appearance of α-protons of newly formed nitroalkane signaling at 4.80 ppm. About 0.1 ppm high field shift of aromatic hydrogens (*meso*-H and 6-H) of BODIPY core is an indication of electron density restoration of signaling unit upon conjugate addition. Assuring Michael acceptor reactivity of nitroolefin-BODIPY hybrid **2** towards the thiol **ME**, we have turned our attention to the water soluble derivative **1**.

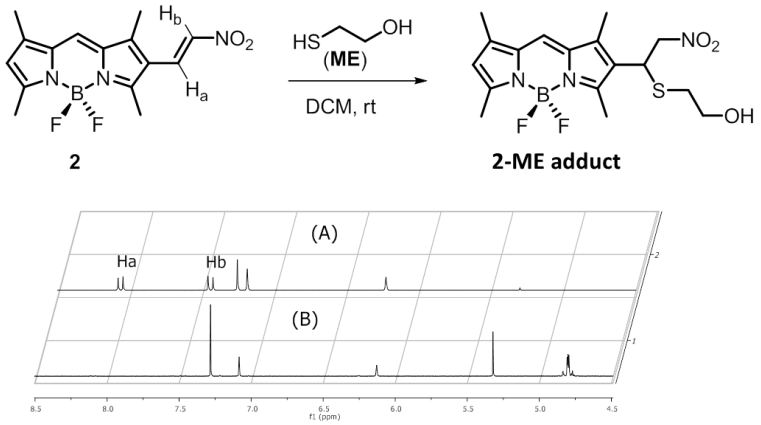

Figure 28: Stacked partial ^{1}H-NMR spectra of thiol probe **2** (A) and conjugate addition product **2**-ME adduct (B) in $CDCl_3$ at 25 °C.

Figure 29 shows the UV-vis absorbance and fluorescence emission response of the thiol probe **1** (5 μM) in 50 mM HEPES: CH_3CN (80:20, v/v, pH=7.20) to increasing Cys concentrations (0-400 equiv.). Upon addition of Cys, absorption band of free dye

1 centered at 525 nm gradually decreased and a new band appeared with a maxima at 510 nm. A 15 nm blue shift with a well-defined isosbestic point localized at 518 nm is apparent from the absorption spectrum (A). This Cys-induced hypsochromic shift reveals the eradication of ICT process that occurs between donor BODIPY core and acceptor nitroalkene unit, as prescribed. Probe **1** is essentially nonfluorescent (Φ_f=0.056) as evidenced by emission spectrum B. As seen from Figure 2, fluorescence intensity ratiomerically increases up to 20-fold upon increasing Cys concentrations (0-400 equiv.) with an emission band centered at 515 nm (λ_{ex} 500 nm). In parallel with our judicious design (*vide supra*), this fluorescence enhancement is deemed as interruption of PeT mechanism operating in the free probe **1** upon attack of Cys nucleophile.

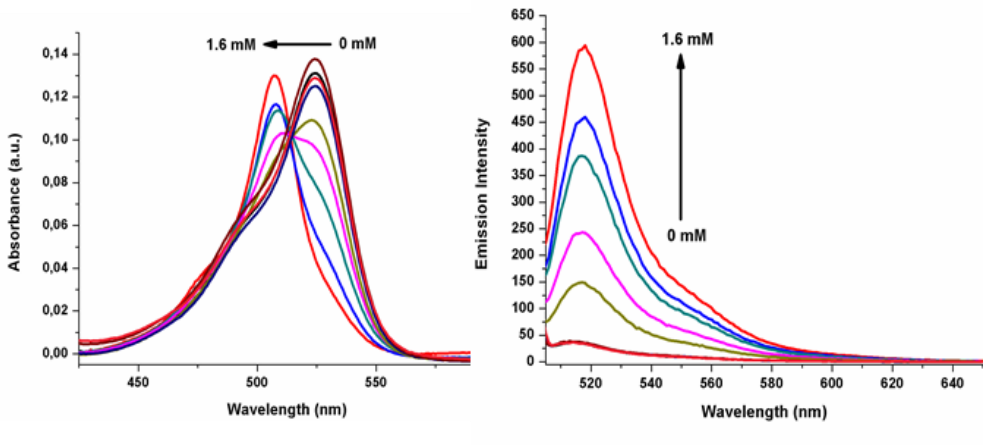

Figure 29: UV-vis absorption spectra (A) and fluorescence spectra (B) of the thiol probe **1** (5 μM) upon increased Cys concentrations (0-400 equiv.) in 50 mM HEPES: CH_3CN (80:20, v/v, pH=7.20, λ_{ex}: 500 nm at 25 °C).

Among biothiols, Cys reacted swiftly with probe **1**, Sensing experiments were also carried out in HEPES: CH_3CN (60:40, v/v) and 100% HEPES buffer solutions. While 40% acetonitrile solution produces essentially the same responses as that of 20%, fluorescence intensity of **1** towards biothiols was halved in case of 100% HEPES solution but still proves to be sensitive and selective enough for the qualitative detection of those thiols (*vide infra*) (figure 30).

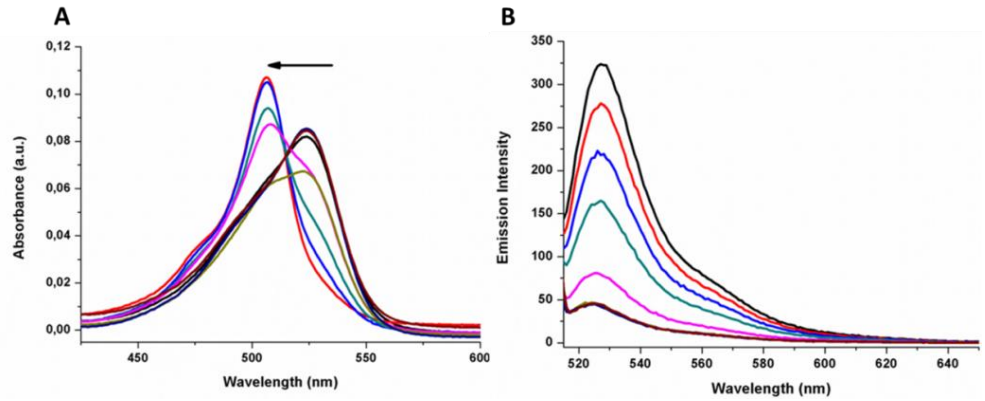

Figure 30: UV-vis absorption spectra (A) and Fluorescence Spectra (B) of the Thiol Probe **1** (4 μM) upon increased Cys concentrations (0-400 equiv.) in 50 mM HEPES (pH=7.2, λ_{ex}:500 nm at 25 °C).

Under identical conditions, other biothiolic molecules, such as Hcy and GSH afforded similar turn on fluorescence responses, as well (figure 31).

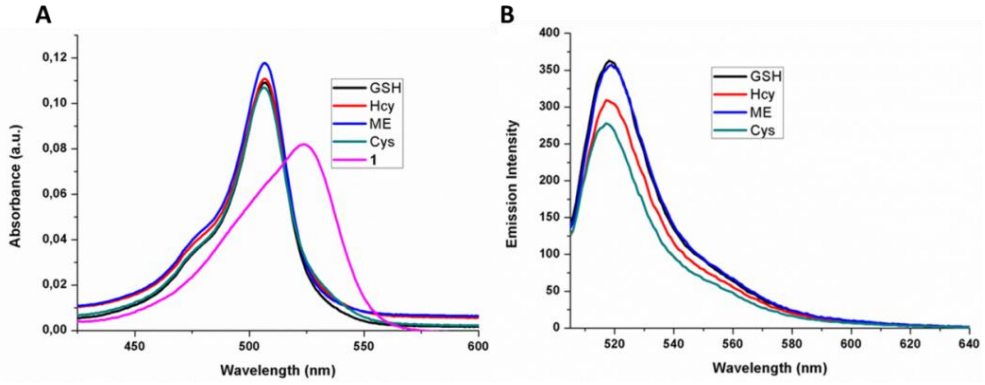

Figure 31: Absorption spectra (A) and Fluorescence spectra (B) of Thiol Probe **1** (4 μM) upon addition of 200 eqv. of Cys, Hcy, ME and GSH in 50 mM HEPES (pH=7.2, λ_{ex}:500 nm at 25 °C).

As a natural extension of this study, we have investigated the selectivity of probe **1** toward Cys, Hys and GSH over potentially competing biologically relevant natural amino acids in 100% HEPES buffer (50 mM) at physiological pH (7.20). Remarkably, no significant change was observed in fluorescence emission (figure 32) spectra when natural amino acids other than biothiols are treated with the probe

1. Unreactivity of non-thiolic amino acids toward dye **1** is validated by this set of experiments. To put in a nutshell, this protocol offers selective and fast sensing of biothiols in the presence of biologically relevant non-thiolic amino acids and akin species.

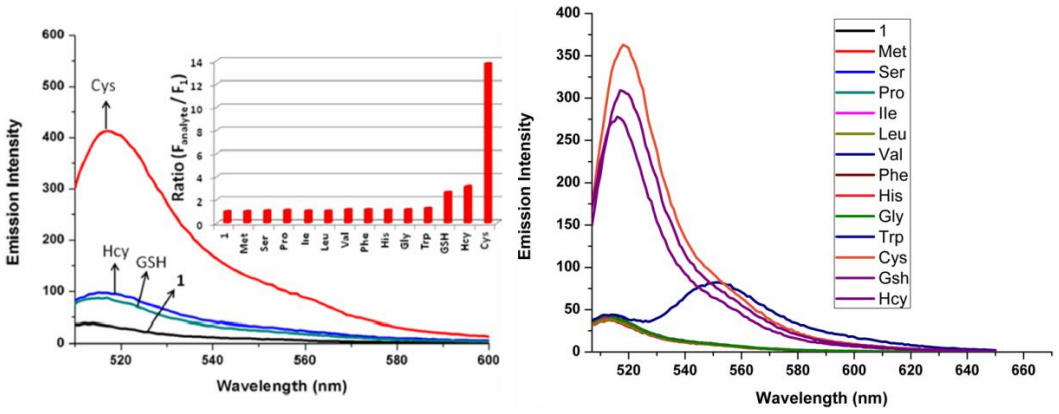

Figure 32: Fluorescence response of the thiol probe **1** (2.4 μM) toward biothiols (Cys, Hcy and GSH; 200 equiv. each) and other natural amino acids (400 equiv.) in 50 mM HEPES: CH_3CN (80:20, v/v, pH = 7.20, λ_{ex}: 500 nm at 25 °C).

Monitoring and imaging of biothiols or the use of a fluorescent label may offer great advantages if they absorb or emit in the longer wavelength regions of electromagnetic radiation (red, near-IR e.g.). To this end, we made use of fruitful Knoevenagel condensation reaction to decorate the probe **1** such that the absorbance and fluorescence maxima went far red (λ_{abs}: 623 nm and λ_{em}: 650 nm) with enhanced water solubility as a bonus. Optical properties of probe **1** and probe **3 (13)** are given below in Table 1. Compared to **1**, probe **3** has extended π-conjugation which in turn causes significant bathochromic shifts (≈100 nm in absorption and ≈125 nm in emission wavelengths). However, this extention of conjugation diminished the fluorescence quantum yield of probe **3** to approx. one-third of probe **1**, that is to say a more pronounced PeT process is allowed then.

Table 1. Optical properties of the probes **1** and **3**.

Compound[a]	λ_{abs} (nm)	λ_{em} (nm)	Φ_f[b]	ε_{max}[c]
1(10)	525	540	0.056[d]	32,000
3(13)	623	655	0.016[e]	26,000

[a] Data acquired in water and methanol in dilute solutions. [b] Relative quantum yields. [c] unit: $cm^{-1}M^{-1}$. [d] Reference dye: Rhodamine 6G in water ($\Phi_f = 0.95$). [e] Reference dye: Cresyl violet in methanol ($\Phi_f = 0.90$).

Sensor **3** displayed impressive water solubility and that was fairly attributable to triply assembled hydrophilic triethyleneglycolic aryl units on single fluorophore. UV-vis and fluorescence response (figure 33) of this red-emitting chromophore **13** were examined as the last. It is remarkable to note that almost equal ratiometric response was observed with the probe **3** and **1** upon incremental Cys additions (0-400 equiv.).

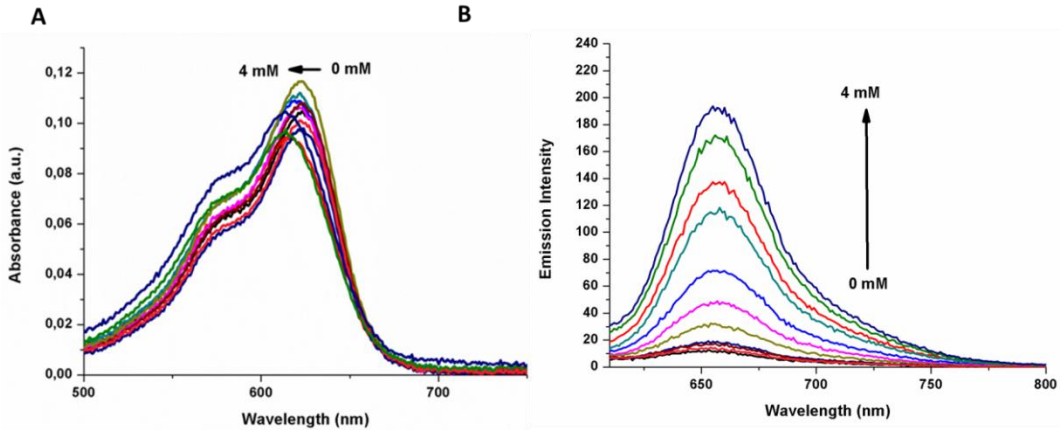

Figure 33: UV-vis absorption spectra (A) of the Thiol Probe **3** (4 μM) upon increased Cys concentrations (0-1000 equiv.) in 50 mM HEPES: CH_3CN (80:20, v/v, pH=7.2, λ_{ex}:600 nm at 25 °C). Fluorescence spectra of the red-emitting thiol probe **3** (5 μM) upon increased Cys concentrations (0-400 equiv.) in 30 mM 100% HEPES solution (pH=7.04, λ_{ex}: 600 nm at 25 °C).

3.5 Experimental Details

3.5.1 Synthesis

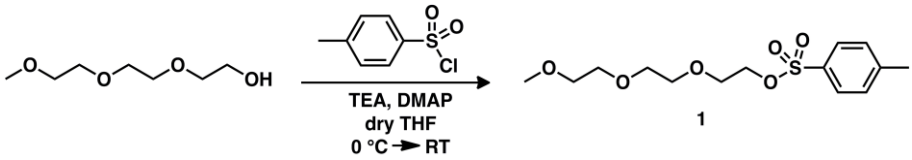

Synthesis of Compound 1: Triethyleneglycol monomethyl ether (20 g, 121 mmol) and TEA (34 mL, 242 mmol) was dissolved in 100 ml dry THF and mixture was stirred at room temperature for 30 min. Then, it was cooled to 0 °C by using ice-bath. 15 min later, catalytic amount of DMAP was added. *p*-toluenesulfonyl chloride (34.6 g, 0.181 mmol) dissolved in dry THF was added dropwise to the reaction mixture at 0 °C. The progress of the reaction was monitored by TLC and when TLC shows no starting material, it was extracted with DCM and washed with water. Combined organic phases were dried over Na_2SO_4 and concentrated under reduced pressure. The crude product was subjected to the F.C.C. using EtOAc as the eluent. Compound **1** was obtained as colorless liquid (36.6 g, 95%).

^{1}H NMR (400 MHz, $CDCl_3$): δ_H 7.78 (d, 2H; *J* = 8.2 Hz), 7.32 (d, 2H, *J* =8.0 Hz) 4.15 (t, 2H; *J* = 4.8 Hz), 3.67 (m, 4H), 3.60 (m, 4H), 3.51 (m, 2H), 3.34 (s, 3H), 2.42 (s, 3H).

^{13}C NMR (100 MHz, $CDCl_3$) δ_C 144.8, 133.0, 129.8, 127.9, 71.9, 70.7, 70.5, 70.5, 69.3, 68.6, 59.0, 21.6.

MS (TOF- ESI): m/z: Calcd for 319.12099 $[M+H]^+$, Found: 319.11472 $[M+H]^+$, Δ= 19.7 ppm.

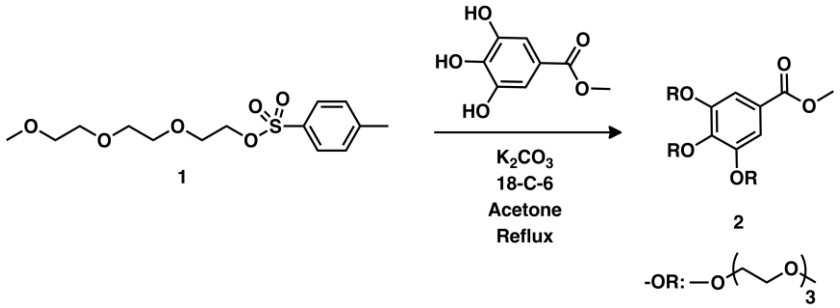

Synthesis of Compound 2: Compound **1** (15 g, 47 mmol) and methyl-3,4,5-trihydroxybenzoate (2.75 g, 15 mmol) were dissolved in 200 mL acetone. K_2CO_3 (8.3 g, 60 mmol) and catalytic amount of benzo-18-crown-6 were added to the reaction mixture and it was refluxed at 60 °C. The progress of the reaction was monitored by TLC and when TLC shows no starting material, reaction mixture was filtered and concentrated under vacuo. The crude product was dissolved in DCM and washed with water. Combined organic phases were dried over Na_2SO_4 and concentrated under reduced pressure. The crude product was subjected to the F.C.C. using EtOAc/ MeOH (90:10, v/v) as the eluent. Compound **2** was obtained as colorless liquid (6 g, 64%).

^{1}H NMR (400 MHz, $CDCl_3$): δ_H 7.30 (s, 2H), 4.22 (m, 2H + 4H), 3.88 (m, 4H + 3H), 3.80 (m, 2H), 3.74 (m, 6H), 3.65 (m, 12H), 3.56 (m, 6H), 3.38 (s, 9H).

^{13}C NMR (100 MHz, $CDCl_3$): δ_C 166.5, 152.3, 142.6, 124.9, 109.0, 72.4, 71.9, 70.8, 70.7, 70.6, 70.5, 69.6, 68.8, 52.1.

MS (TOF- ESI): m/z: Calcd for $[M+H]^+$: 623.32733, Found: $[M+H]^+$: 633.33349, Δ=-9.88 ppm.

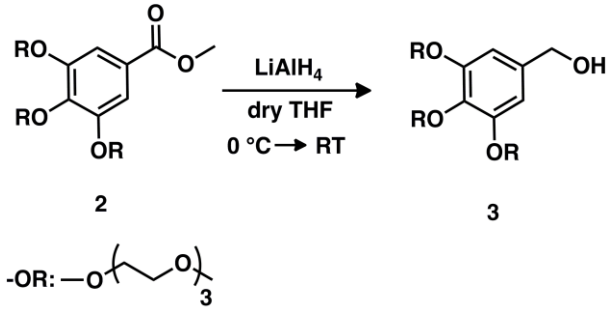

Synthesis of Compound 3: $LiAlH_4$ (0.347 g, 9.6 mmol) was added to the freshly distilled THF which was kept at 0 °C. Compound **2** (3.0 g, 4.8 mmol) dissolved in freshly dissolved THF was added dropwise to the reaction mixture and left to stir at room temperature. The progress of the reaction was monitored by TLC and when TLC shows no starting material, it was cooled to 0 °C in order to quench the excess $LiAlH_4$ by adding ice cold water. It was extracted with EtOAc and washed with brine. Combined organic phases were dried over Na_2SO_4 and concentrated under reduced pressure. The crude product was subjected to F.C.C. by using gel column chromatography using EtOAc/ MeOH (90:10, v/v) as the eluent. Compound **3** was obtained as colorless liquid (2.5 g, 88%)

^{1}H NMR (400 MHz, $CDCl_3$): δ_H 6.63 (s, 2H), 4.58 (s, 2H), 4.15 (m, 2H + 4H), 3.84 (t, 4H, *J* = 5.29 Hz), 3.79 (t, 2H, J = 5.44 Hz), 3.73 (m, 6H), 3.65 (m, 12H), 3.54 (m, 6H), 3.38 (s, 9H).

^{13}C NMR (100 MHz, $CDCl_3$): δ_C 152.7, 137.8, 136.7, 106.6, 72.3, 71.9, 70.8, 70.7, 70.5, 69.8, 68.9, 65.2, 59.0.

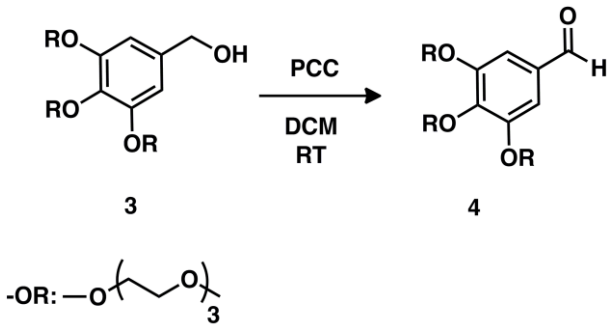

Synthesis of Compound 4: Compound **3** (2.4 g, 4 mmol) was dissolved in DCM and pyridinium chlorochromate (2.15 g, 10 mmol) was added to the reaction mixture. It was stirred at room temperature. The progress of the reaction was monitored by TLC and when TLC shows no starting material, it was filtered through the celite and the crude product was directly subjected to F.C.C. by using EtOAc/TEA (95/5; v/v) as eluent. Compound **4** was obtained as colorless liquid (2.37 g, quantitative).

^{1}H NMR (400 MHz, $CDCl_3$): δ_H 9.82 (s, 1H), 7.14 (s, 2H), 4.21 (m, 6H), 3.89 (m, 4H), 3.82 (m, 2H), 3.80-3.50 (m, 24H), 3.38 (s, 9H).

^{13}C NMR (100 MHz, $CDCl_3$): δ_C 191.0, 153.0, 144.1, 131.6, 109.0, 72.5, 71.9, 70.8, 70.7, 70.6, 70.5, 69.6, 68.9, 59.0.

MS (TOF- ESI): m/z Calcd. for $C_{28}H_{48}NaO_{13}$ 593.31677 $[M+H]^+$, Found: 593.32133 $[M+H]^+$, Δ= -7.69 ppm.

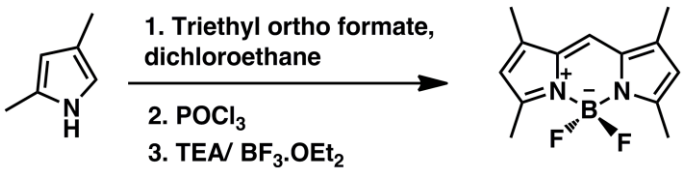

5

Synthesis of Compound 5: 2,4-dimethyl pyrrole (1.0 mL, 11.37 mmol), triethylorthoformate (0.95 mL, 5.69 mmol) and $POCl_3$ (0.58 mL, 6.25 mmol) were dissolved in 250 mL Ar-deaerrated 1,2-dichloroethane. Reaction was left to stir at room temperature for a few hours and the progress of the reaction was monitored via TLC. Triethyl amine (TEA) (5.0 mL) was then added dropwise to this mixture over a period of 15 min, and the resulting dark brown solution was allowed to stir for an additional 15 min. BF_3•OEt_2 (5.0 mL) was then added dropwise over a period of 15 min. and the resulting dark red solution was allowed to stir further for 1h at rt. The slurry reaction mixture was washed with water (3 × 300 mL) and dried over anhydrous Na_2SO_4. The solvent was evaporated and the crude product was purified

via F.C.C. using $CHCl_3$ as the eluent. Compound **4** was obtained as orange crystalline solid (0.4 g, 28% yield).

^{1}H NMR (400 MHz, $CDCl_3$): δ_H 7.09 (s, 1H), 6.10 (s, 2H), 2.60 (s, 6H), 2.29 (s, 6H).

^{13}C NMR (100 MHz, $CDCl_3$): δ_C 156.8, 141.3, 133.5, 120.2, 119.1, 14.8, 11.2.

MS (TOF- ESI): m/z Calcd. for 246.12599 $[M-H]^-$, Found: 246.12394 $[M-H]^-$, Δ= 8.33 ppm.

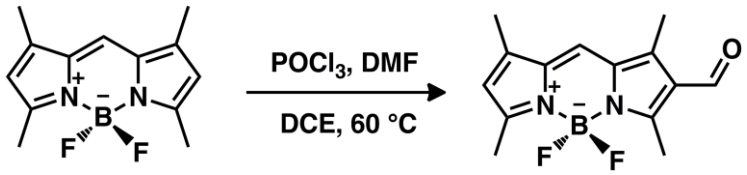

5 **6**

Synthesis of Compound 6: $POCl_3$ (2 mL) was added dropwise to a vigorously stirring anhydrous DMF (2 mL) which was kept in ice bath under N_2. Resulting pale yellow viscous liquid was allowed to stir at room temperature for additional 30 min. To this, 1,2-dichloroethane (DCE) (50 mL) solution of compound **5** (0.10 g, 0.328 mmol) was then slowly introduced and the resultant brown solution was heated at 60 °C for 2 h. (Attention!: 60 °C is critical to get mono-formylated product **6** as the major, side product formation was observed otherwise at higher temperatures.) Reaction was cooled to room temperature, and poured into ice-cold saturated $NaHCO_3$ solution. This mixture was extracted twice with DCM (100 mL portions) and dried over anhydrous Na_2SO_4. Solvent was evaporated in vacuo and compound was purified by silica gel F.C.C. using $CHCl_3$ as the eluent to obtain target compound **6** as reddish crystalline solid (0.106 g, 95% yield).

^{1}H NMR (400 MHz, $CDCl_3$): δ_H 10.02 (s, 1H), 7.20 (s, 1H), 6.20 (s, 1H), 2.77 (s, 3H), 2.58 (s, 3H), 2.48 (s, 3H), 2.28 ppm (s, 3H).

^{13}C NMR (100 MHz, $CDCl_3$): δ_C 185.5, 163.5, 157.2, 145.4, 140.6, 136.4, 131.1, 125.8, 122.0, 121.5, 15.2, 12.9, 11.5, 10.4.

MS (TOF-ESI): m/z: Calcd for $C_{14}H_{15}BF_2N_2O^+$: 275.1246 $[M+H]^+$; found: 275.1212 $[M+H]^+$, Δ = 12.3 ppm.

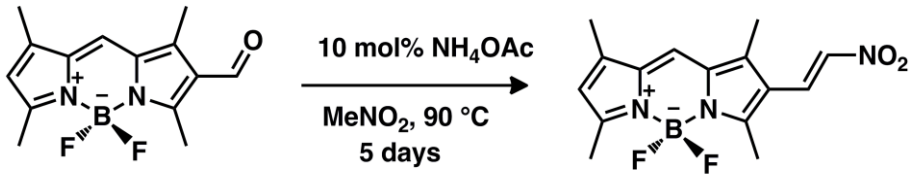

6 7

Synthesis of Compound 7: NH_4OAc (0.0028 g, 0.036 mmol) was added to a nitromethane (3,5 mL) solution of compound **6** (0.10 g, 0.36 mmol) and the solution was left to stir at 90 ^oC for 5 days. Product formation was monitored with TLC using DCM as the eluent. At the end of reaction, nitromethane was removed in vacuo and obtained crude mixture was subjected to silica gel F.C.C. using DCM as the eluent. Compound **7** was obtained as orange crystalline solid (0.036 g, 31.3% yield).

^{1}H NMR (400 MHz, $CDCl_3$): δ_H 8.07 (d, *J* = 13.7 Hz, 1H), 7.44 (d, *J* = 13.7 Hz, 1H), 7.19 (s, 1H), 6.22 (s, 1H), 2.66 (s, 3H), 2.60 (s, 3H), 2.39 (s, 3H), 2.31 (s, 3H). Due to the low solubility of the compound, ^{13}C-NMR spectrum could not be obtained.

MS (TOF-ESI): m/z: Calcd. for 318.1304 $[M-H]^-$, Found: 317.1277 $[M-H]^-$, Δ= -3.09 ppm

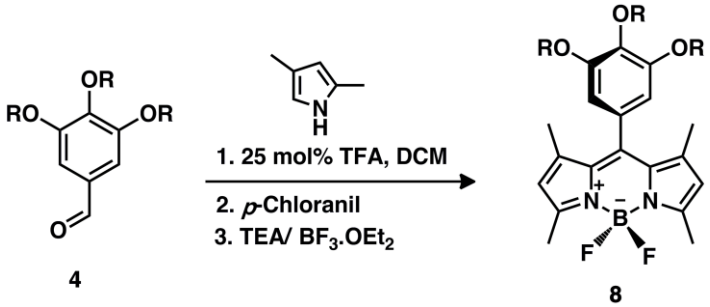

4 8

Synthesis of Compound 8: Trifluoroacetic acid (TFA; 1 drop) was added dropwise to a vigorously stirring solution of 3,4,5-tris(2-(2-(2-methoxyethoxy)ethoxy)benzaldehyde **4** (1.0 g, 1.7 mmol) and 2,4-dimethylpyrrole (0.352 g, 3.7 mmol) in 350 mL Ar-deaerrated dichloromethane (DCM). The resulting red solution was stirred at room temperature in the dark for 1 day. *p*-Chloranil (0.415 g, 1.7 mmol) was then added in one portion and reaction was stirred for an additional hour. Triethyl amine (TEA) (5.0 mL) was then added dropwise to this mixture over a period of 15 min, and the resulting dark brown solution was allowed to stir for an additional 15 min. BF_3•OEt_2 (5.0 mL) was then added dropwise over a period of 15 min. and the resulting dark red solution was allowed to stir further for 2h at rt. The slurry reaction mixture was washed with water (3 × 300 mL) and dried over anhydrous Na_2SO_4. The solvent was evaporated and the residue was purified by silica gel flash column chromatography (F.C.C.) using DCM:MeOH (95:5) as the eluent. Standing on air, compound **8** was solidified as a dark orange solid (0.780 g, 56% yield).

^{1}H NMR (400 MHz, $CDCl_3$): δ_H 6.55 (s, 2H), 5.99 (s, 2H), 4.22 (t, *J*= 5.0 Hz, 2H), 4.12 (t, *J*= 4.7 Hz, 4H), 3.84 (t, *J*= 5.3 Hz, 6H), 3.51-3.76 (m, 25H), 3.38 (s, 2H), 3.36 (s, 6H), 2.54 (s, 6H), 1.52 (s, 6H).

^{13}C NMR (100 MHz, $CDCl_3$): δ_C 155.8, 153.7, 142.9, 141.1, 139.0, 131.1, 129.9, 121.1, 107.7, 2.7, 71.9, 71.9, 70.8, 70.7, 70.6, 70.5, 69.7, 69.2, 58.8, 29.6 14.4, 14.2.

MS (TOF-ESI): m/z: Calcd for $C_{19}H_{16}BF_2N_2O_3$: 809.4286 $[M-H]^-$, Found: 808.4299 $[M-H]^-$, Δ= -6.16 ppm.

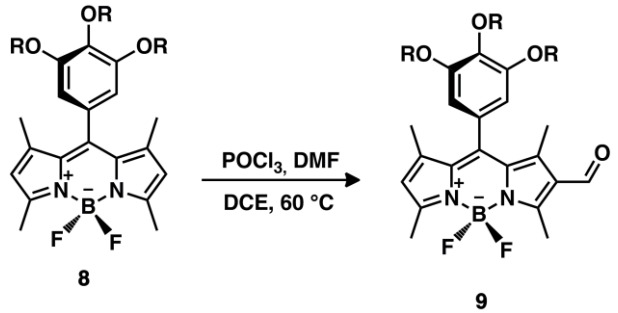

8 **9**

Synthesis of Compound 9: $POCl_3$ (1 mL) was added dropwise to a vigorously stirring anhydrous DMF (1 mL) which was kept in ice bath under N_2. Resulting pale yellow viscous liquid was allowed to stir at room temperature for additional 30 min. To this, 1,2-dichloroethane (DCE) (50 mL) solution of compound **8** (0.810 g, 1.0 mmol) was then slowly introduced and the resultant brown solution was heated at 60 °C for 3 h. (Attention!: 60 °C is critical to get mono-formylated product **9** as the major, side product formation was observed otherwise at higher temperatures.) Reaction was cooled to room temperature, and poured into ice-cold saturated $NaHCO_3$ solution. This mixture was extracted twice with DCM (100 mL portions) and dried over anhydrous Na_2SO_4. Solvent was evaporated in vacuo and compound was purified by silica gel F.C.C. using 98:2 / DCM: MeOH as the eluent to obtain target compound **9** as orange crystalls (0.769 g, 91.7% yield).

^{1}H NMR (400 MHz, $CDCl_3$): δ_H 9.98 (s,1H), 6.53 (s, 2H), 6.15 (s, 1H), 4.23 (d, *J*= 4.3 Hz, 2H), 4.12 (d, *J*= 4.3 Hz, 4H), 3.83 (d, *J*= 4.8 Hz, 6H), 3.75-3.49 (m, 25H), 3.37 (s, 2H), 3.34 (s, 6H), 2.80 (s, 3H), 2.59 (s, 3H), 1.78 (s, 3H), 1.57 (s, 3H).

^{13}C NMR (100 MHz, $CDCl_3$): δ_C 185.8, 161.6, 156.5, 154.0, 147.2, 143.1, 142.7, 139.5, 134.0, 129.7, 128.9, 126.3, 123.9, 107.0, 72.8, 71.9, 71.9, 70.8, 70.7, 70.6, 70.6, 70.5, 69.7, 69.3, 59.0, 14.8, 11.6.

MS (TOF-ESI): m/z: Calcd for $C_{20}H_{16}BF_2N_2O_4$: 837.4235 $[M-H]^-$, Found: 836.4186 $[M-H]^-$, Δ= -1.47 ppm.

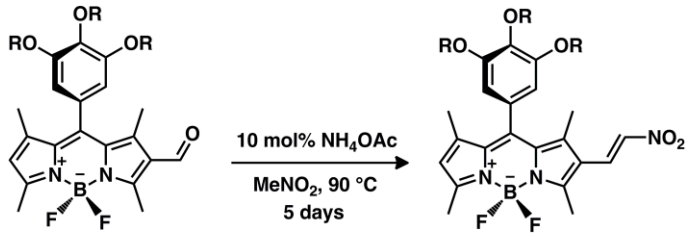

9 10

Synthesis of Compound 10: NH_4OAc (0.0013 g, 0.017 mmol) was added to a nitromethane (2 mL) solution of compound **9** (0.139 g, 0.17 mmol) and the solution was left to stir at 90 ^oC for 5 days. Product formation was monitored with TLC using

DCM: MeOH (98:2) as the eluent. At the end of reaction, nitromethane was removed in vacuo and obtained crude mixture was subjected to silica gel F.C.C. using DCM: MeOH (98:2) as the eluent. Compound **10** was obtained as a wine-red waxy solid (0.040 g, 27% yield).

^{1}H NMR (400 MHz, $CDCl_3$): δ_H 8.05 (d, *J*= 13.8 Hz, 1H), 7.37 (d, *J*= 13.6 Hz, 1H), 6.56 (s, 2H), 6.18 (s, 1H), 4.26 (t, *J*= 4.6 Hz, 2H), 4.14 (t, *J*= 4.5 Hz, 4H), 3.86 (t, *J*=5.2 Hz, 6H), 3.52- 3.76 (m, 25H), 3.40 (s, 2H), 3.37 (s, 6H), 2.72 (s, 3H), 2.63 (s, 3H), 1.64 (s, 3H), 1.59 (s, 3H).

^{13}C NMR (100 MHz, $CDCl_3$): δ_C 161.5, 154.2, 154.0, 147.2, 147.2, 140.2, 139.7, 134.6, 133.7, 130.7, 130.6, 128.9, 123.9, 120.0, 107.4, 72.8, 72.0, 71.9, 70.9, 70.7, 70.7, 70.6, 70.6, 69.8, 69.4, 65.3, 59.0, 29.7, 14.7, 12.9,11.1.

MS (TOF-ESI): m/z: Calcd. for $C_{21}H_{17}BF_2N_3O_5$: 880.7612 $[M-H]^-$, Found: 879.4238 $[M-H]^-$, Δ= -2.09 ppm.

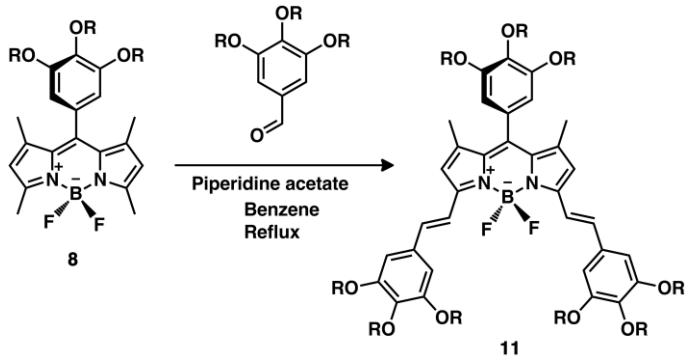

Synthesis of Compound 11: 3,4,5-tris(2-(2-(2-methoxyethoxy)ethoxy)benzaldehyde (0.365 g, 0.62 mmol) was added to a solution of 25 mL of compound **8** (0.20 g, 0.247 mmol) in benzene containing piperidine acetate (179 mg, 1.23 mmol). Mixture was refluxed until all the starting material consumed and the product formation was monitored by TLC using DCM: MeOH (95:5) as the eluent. At the end of the reaction, obtained crude mixture was subjected to silica gel F.C.C. using DCM:

MeOH (95:5) as the eluent. Compound **11** was obtained as a dark-blue waxy solid (0.20 g, 41.4% yield).

^{1}H NMR (400 MHz, $CDCl_3$): δ_H 7.53 (d, *J*=16.0 Hz, 2H), 7.17 (d, *J*=15.9 Hz, 2H), 6.85 (s, 4H), 6.64 (s, 2H), 6.61 (s, 2H), 4.21-4.27 (m, 14H), 4.13-4.17 (m, 5H), 3.86-3.90 (m, 13H), 3.82-3.84 (m, 5H), 3.73-3.78 (m, 19H), 3.63-3.71 (m, 39H), 3.53-3.60 (m, 19H), 3.41 (s, 2H), 3.40 (s, 5H), 3.38 (s, 15H), 1.60 (s, 6H).

^{13}C NMR (100 MHz, $CDCl_3$): δ_C 153.6, 152.8, 152.6, 141.8, 139.9, 139.1, 138.2, 136.3, 133.2, 132.0, 129.9, 118.4, 117.8, 108.1, 107.6, 72.7, 72.4, 71.9, 71.8, 70.84, 70.80, 70.69, 70.66, 70.62, 70.54, 70.50, 69.7, 69.2, 69.1, 58.98, 58.94, 14.50.

MS (TOF-ESI): m/z: Calcd. for $C_{33}H_{18}BF_2N_2O_9$: 1958.0264 $[M-H]^-$, Found: 1956.9858 $[M-H]^-$, Δ= 18.91 ppm.

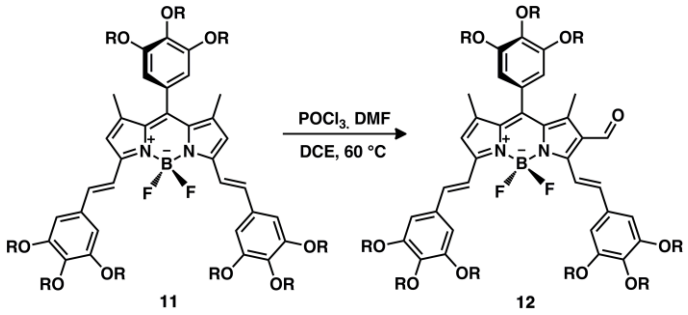

Synthesis of Compound 12: $POCl_3$ (0.1 mL) was added dropwise to a vigorously stirring anhydrous DMF (0.1 mL) which was kept in ice bath under N_2. Resulting pale yellow viscous liquid was allowed to stir at room temperature for additional 30 min. To this, 1,2-dichloroethane (DCE) (50 mL) solution of compound **11** (0.20 g, 0.102 mmol) was then slowly introduced and the resultant brown solution was heated at 60 °C for 3 h. (Attention!: 60 °C is critical to get mono-formylated product **12** as the major, side product formation was observed otherwise at higher temperatures.) Reaction was cooled to room temperature, and poured into ice-cold saturated $NaHCO_3$ solution. This mixture was extracted twice with DCM (100 mL portions) and dried over anhydrous Na_2SO_4. Solvent was evaporated in vacuo and compound

was purified by silica gel F.C.C. using 95:5 / DCM: MeOH as the eluent. Product **12** was obtained as dark blue oily compound (0.178 g, 87.7% yield).

^{1}H NMR (400 MHz, $CDCl_3$): δ_H 10.05 (s, 1H), 7.52 (dd, *J*= 16.3 Hz, 2H), 7.31 (d, *J*=17.9 Hz, 1H), 7.03 (d, *J*=16.2 Hz, 1H), 6.90 (s, 4H), 6.77 (s, 1H), 6.59 (s, 2H), 4.13-4.27 (m, 19H), 3.81-3.89 (m, 18H), 3.70-3.75 (m, 18H), 3.61-3.69 (m, 37H), 3.51-3.57 (m, 19H), 3.35-3.39 (m, 24H), 1.85 (s, 3H), 1.64 (s, 3H).

^{13}C NMR (100 MHz, $CDCl_3$): δ_C 187.1, 157.1, 153.9, 153.4, 152.9, 152.8, 146.1, 141.4, 141.2, 141.0, 140.5, 140.3, 139.9, 139.5, 136.1, 131.7, 131.18, 131.10, 129.1, 126.9, 120.4, 117.5, 116.5, 108.2, 107.8, 107.5, 72.7, 72.5, 72.4, 71.95, 71.90, 70.85, 70.82, 70.80, 70.7, 70.66, 70.64, 70.55, 70.52, 69.7, 69.3, 69.2, 69.05, 59.01, 59.00, 58.9, 15.0, 12.3.

MS (TOF-ESI): m/z: Calcd. for $C_{34}H_{18}BF_2N_2O_{10}$: 1986.0213 $[M-H]^-$, Found: 1984.9894 $[M-H]^-$, Δ= 14.25 ppm.

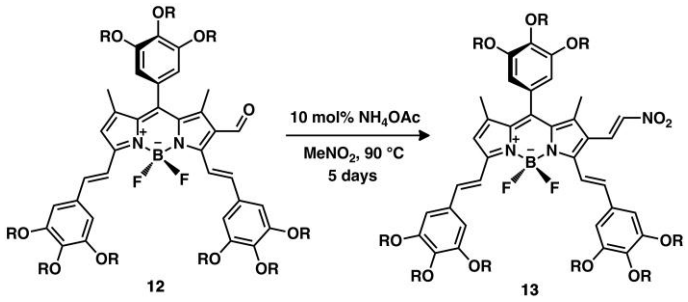

Synthesis of Compound 13: NH_4OAc (0.005 g, 0.0065 mmol) was added to a nitromethane (1 mL) solution of compound **12** (0.130 g, 0.065 mmol) and the solution was left to stir at 90 ^{o}C for 15 days. Product formation was monitored with TLC using DCM: MeOH (95:5) as the eluent. At the end of reaction, nitromethane was removed in vacuo and obtained crude mixture was subjected to silica gel F.C.C. using DCM: MeOH (95:5) as the eluent. Compound **13** was obtained as a dark blue waxy solid (0.025 g, 19% yield).

^{1}H NMR (400 MHz, $CDCl_3$): δ_H 8.16 (d, *J*=13.6 Hz, 1H), 7.51 (d, *J*=16.3 Hz, 2H), 7.38 (d, *J*=13.6 Hz, 1H), 7.32 (d, *J*=16.3 Hz, 2H), 6.87 (s, 2H), 6.85 (s, 2H), 6.78 (s, 1H), 6.61 (s,2H), 3.3-4.29 (m, 135H), 1.69 (s, 3H), 1.65 (s, 3H).

MS (TOF-ESI): m/z: Calcd. for $C_{35}H_{19}BF_2N_3O_{11}$: 2028.0235 $[M-H]^-$, Found: 2028.0288 $[M-H]^-$, Δ=2.63 ppm.

CHAPTER 4

4. Nitroolefin Functionalized Bodipy Dyes for Protein Labeling

Murat Isik, Ilke Simsek Turan, Hatice Turgut and Engin U. Akkaya[*,†,‡]

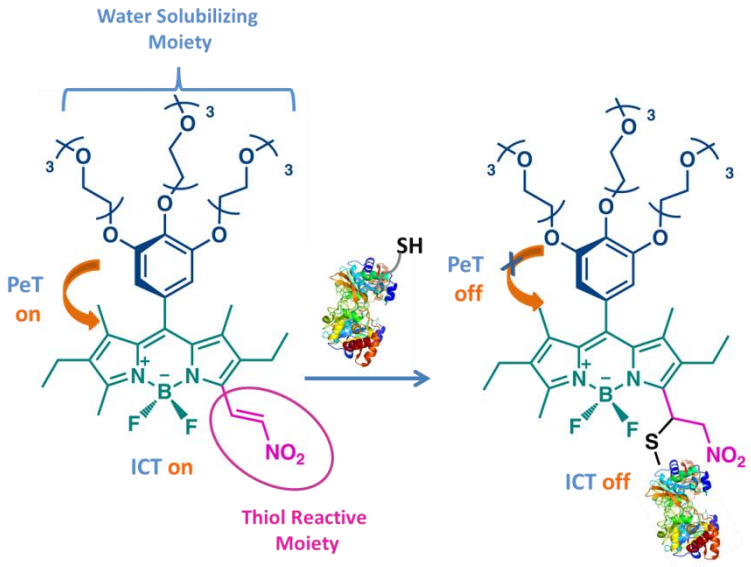

4.1 Objective

Proteins are one of the major biological macromolecules which are composed of different combinations of amino acids and their behaviors, interactions with other biological molecules, their life cycle and their shapes have to be tracked since their functions and interactions affect whole organization of life and the alterations in their structure may even be linked to severe diseases. Sensing and signaling of proteins via color change, emission change or both are very valuable in order to figure out how they function normally, how they interact with other molecules or how some diseases are caused by the abnormal shapes of them. Because of that we have devised three bodipy dyes modified with nitroolefin functionality through different photophysical changes due to the differences in the Michael acceptor connectivity. The enhanced aqueous solubility of the designed dyes makes them good candidates for protein labeling applications. Based on their spectroscopic results which were recorded after reaction with both L-cysteine and Bovine Serum Albumin (BSA), nitroolefin functionalization of BODIPY dyes is a promising alternative to sense biological thiols and hence labeling proteins having thiol groups.

4.2 Introduction

Development of fluorescent labels and probes is a thriving subject which has a diverse spectrum of application in biomedicine, polymer science, sensor chemistry and so on. Besides, extensive efforts have been dedicated for the design and synthesis of fluorescent labels for protein tagging as non-radioactive labels. Fluorescence methodology is favored due to absence of background absorption, autofluorescence from cell components, reduced light scattering and low cost of irradiation and thus, design and synthesis of new fluorogenic probes are highly demanding. Among the most organic dyes like rhodamine, cyanines, etc, 4,4-difluoro-4-bora-3a,4a-diaza-s-indacene (Bodipy) dyes are more promising due to its outstanding photophysical properties. Bodipy dye has relatively high molar

absorption coefficients, fluorescence quantum yields, narrow emission bandwidths with enhanced chemical and photo-stability. Additionally, synthesis and functionalization according to purpose of study are easy and bodipy dyes have high solubility[15]. Bodipy dyes can be modified to label proteins in such a way that they can be modified with water solubilizing units and with aromatic groups to extend the conjugation in order to enhance the biological applications of dye in aqueous solutions. In the literature there are a few dyes (figure 34) designed based on Bodipy core for protein labeling applications and thus, there is growing demand for the design and synthesis of highly specific and selective labeling agents with low response time.[74,75]

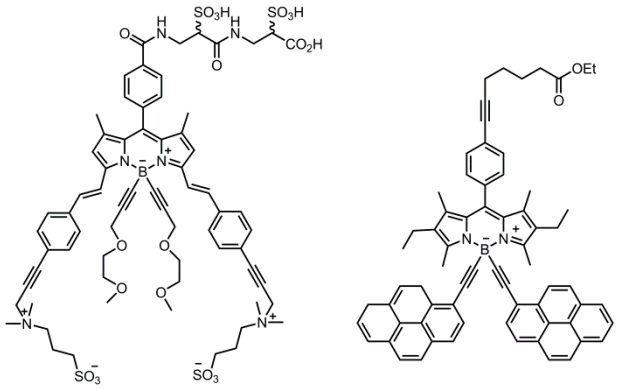

Figure 34: Bodipy based Protein Labeling Agents

4.3 Design of Labeling Agents

Proteins, comprising one of the major classes of biomolecules of life, have to be tracked in order to observe their mechanisms, determination of turnover numbers of enzymes and sometimes even for targeting a tumor tissue because of that their functions and interactions affect the whole organization of the life. Sensing and signaling of proteins via color change, emission change or both are very valuable in order to figure out how they function normally, how they interact with other molecules or how some diseases are caused by the abnormal shapes of them. Since we are familiar with the design and development of thiol based probes, we have

integrated our knowledge for the development of a dye which can be used for bioconjugation of thiol bearing proteins. Since we have wanted to label proteins irreversibly, it is best to design the probes as reaction based manner as in the case of thiol sensing project. In this work, we have modified our protein labeling agents (PL) with nitroolefin functionality due to the high specificity, high selectivity and fast response with biological thiols. The aqueous solubility of the probes (**2** and **3**) is enhanced by the introduction of triethyleneglycol units.

Three dyes with differences in connectivity of nitroolefin functionality have been synthesized (figure 35). Protein labeling agent **1** (PL**1**) is designed to label proteins via enhancement in the fluorescence emission. The labeling agents **2** and **3** have been devised to study the labeling process via both colorimetric and emission changes. Incorporation of the aqueous solubility to labeling agents **2** and **3** makes them potential candidates for biological applications.

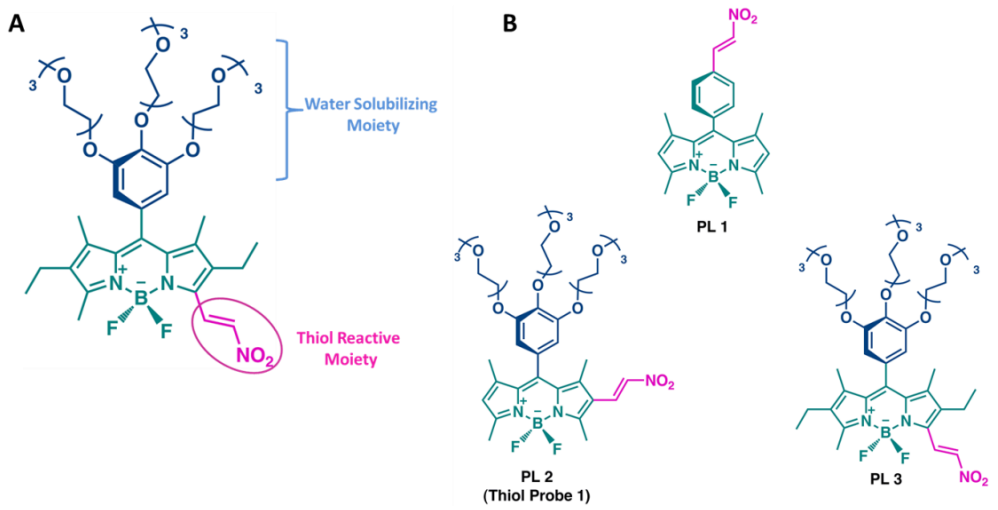

Figure 35: (A) Design elements of the nitroolefin-BODIPY conjugate for protein labelling (B) Chemical Structures of Bodipy based Protein Labeling Agents

4.4 Results and Discussion

4.4.1 Synthetic Approach

The synthesized compound for thiol sensing project, thiol probe **1** is used for thiol bearing protein labeling project and the synthetic pathway for it has been explained in Chapter 3. The synthesis of PL **1** (figure 36) has been started with the synthesis of aldehyde from teraphthaldehyde which could not be employed directly due to the presence of two identical formyl groups leading formation of bilateral bodipy structure. Because of that, mono-reduction of teraphthaldehyde was achieved by using $NaBH_4$ and then, this aldehyde was used for the synthesis of bodipy **14**. Since formyl functionality is required for Henry reaction, oxidation reaction of benzylalcohol functionalized bodipy was done by using Dess Martin periodinane (**15**). Although PCC oxidation is milder, Dess Martin oxidation was preferred since the yields of the reaction is high. Last step is the formation of ethylene nitro functionality which was implemented via NH_4OAc catalyzed nitromethane condensation. PL **3** has been synthesized via three step procedure. The bodipy core was generated from 3-ethyl-2,4-dimethyl pyrrole and TEG-aldehyde. Ethyl functionality at 2 and 6 positions which are reactive compared to 3 and 5 positions is required to prevent side products during formylation reaction. Compound **18** was synthesized via C-H activation by DDQ oxidation in the presence of water as nucleophile prior to nitromethane condensation reaction (PL**3**, **19**).

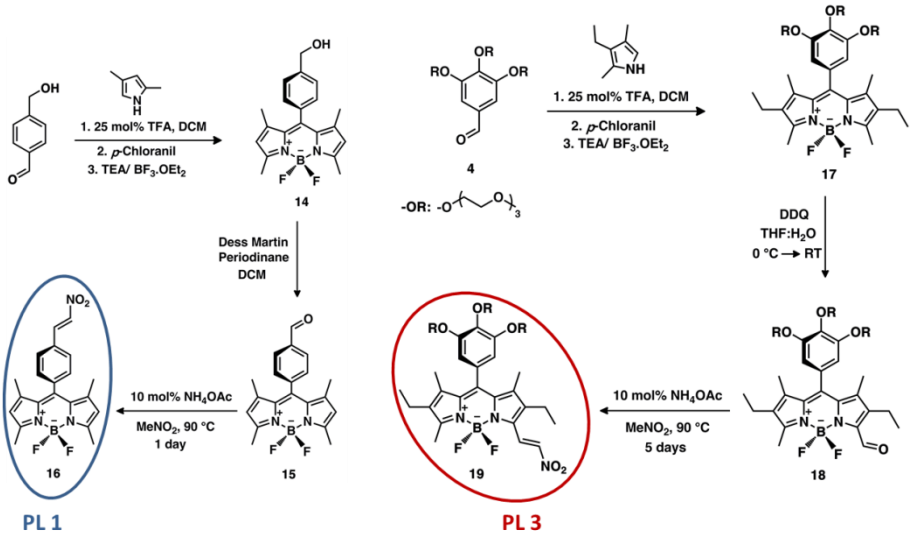

Figure 36: Pursued Route for the synthesis of PL**1** and PL**3**

4.4.2 Working Principle

Protein labeling agent **1** (PL **1**) is designed to label proteins via photoinduced electron transfer and thus, enhancement in the fluorescence emission would occur. Prior to bioconjugation with proteins, dye would be off state since oxidative PeT is active and when dye interacts with thiol bearing protein, PeT becomes inactive and fluorescence would be on. In the case of PL **3** (figure 37), incoming of thiol bearing protein to the β-position of nitroolefin is expected to disrupt the π-conjugation and block the Intramolecular Charge Transfer (ICT) process, which is intrinsically anticipated to induce a blue shift in absorbance. Efficient Photoinduced-electron-Transfer (PeT) control is brought in such a way that inherently electron rich Gallic acid moiety could quench the emission of the probe to some degrees attached to the electron poor, nitroolefin substituted BODIPY in the exited state since they are soft nucleophiles, biological thiols attacks to soft nucleophilic carbon of nitroolefin functionality of BODIPY conjugates and blocks both the PET and ICT process and thus, fluorescence enhancement is deemed as interruption of PET mechanism

operating in PL **3**. The working principle of PL **2** was explained thoroughly in chapter 3 and it is similar to PL **3**.

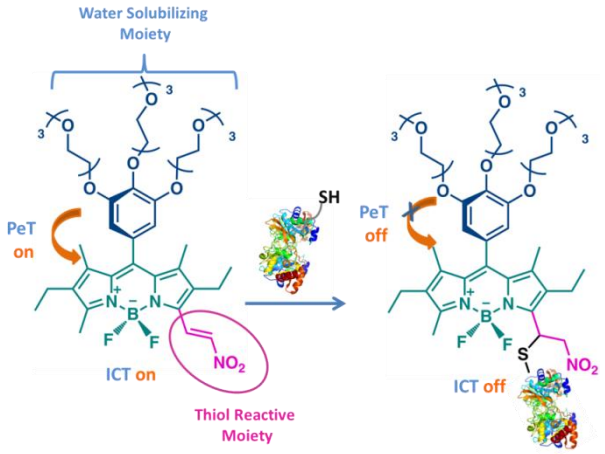

Figure 37: Working Principle of the nitroolefin-BODIPY conjugates PL **3**.

4.4.3 Spectral Proofs for Sensing and Labeling Process

In the case of PL **1** since there is no operating ICT process, we would not expect to observe any change in the absorbance spectrum of the dye upon increasing Cys concentration (figure 38). On the other hand, since the operating process is d-PeT, upon increasing concentrations of Cys, electron transfer from electron donor bodipy core to electron deficient nitroethylene unit has been blocked which leads to the enhancement in the fluorescence emission intensity due to irruption of d-PeT process. In the case of PL **3**, upon addition of Cys, absorption band of PL**3** centered around 570 nm gradually decreased and a new band appeared with maxima around 520 nm. The blue shift is apparent from the absorption spectrum (figure 39 A). This Cys-induced hypsochromic shift reveals the eradication of ICT process that occurs between donor BODIPY core and acceptor nitroalkene unit. There was a total of 43 nm blue shift in the spectra and an isosbestic point at 550 nm was observed. Additionally, due to interruption of PeT process, fluorescence intensity has been increased upon increase in Cys concentrations (0-200 equiv.) Although PL**3** is

essentially nonfluorescent at the beginning, these results are in accordance with our expectations. The optical properties of protein labeling agents were given table 2.

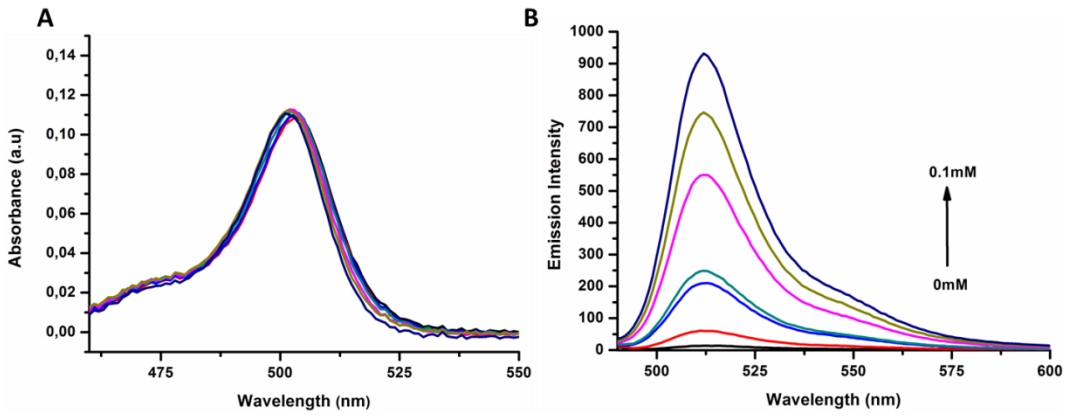

Figure 38: UV-vis absorption spectra (A) and Fluorescence Spectra (B) of the PL **1** (1 μM) upon increased Cys concentrations (0-100 equiv.) in **1X** PBS: DMSO (5:95, v/v, pH=7.40, λ_{ex}: 490 nm at 25 °C).

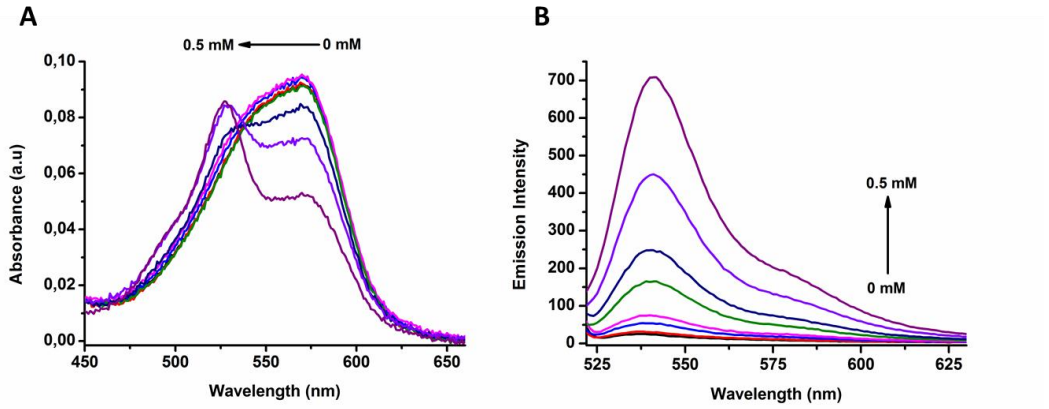

Figure 39: UV-vis absorption spectra (A) and Fluorescence Spectra (B) of the PL **3** (2.5 μM) upon increased Cys concentrations (0-200 equiv.) in **1X** PBS:DMSO (5:95, v/v, pH=7.40, λ_{ex}: 520 nm at 25 °C).

Table 2: Photophysical properties of dyes.* relative quantum yields. Reference dye: Rhodamine 6G in water (Φ_f:0.95)

Compound	λ_{abs} (nm)	λ_{em} (nm)	Φ_f*	ε_{max} ($cm^{-1}M^{-1}$)
PL1	503	515	0.067	105,694
PL2	525	540	0.056	58,500
PL3	570	530	0.019	38,918

We have characterized the reaction between labeling agent and mercaptoethanol via ^{1}H-NMR in order to prove conjugate addition of biological thiols. When figure 40 was examined, it is clear that after reaction with mercaptoethanol, olefinic protons are removed due to the breakage of the double bonds.

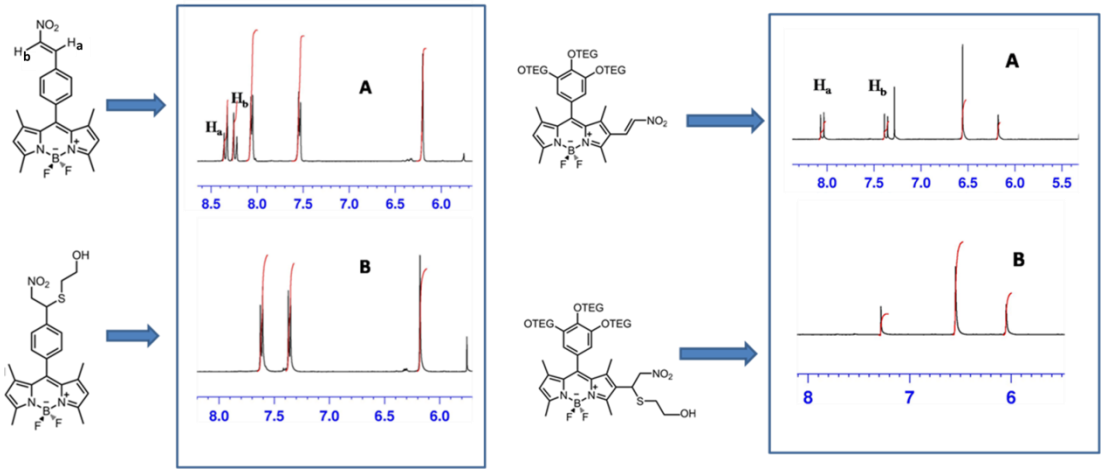

Figure 40: Comparison of aromatic regions of ^{1}H-NMR of PL **1** and PL **2** and that of their adducts with mercaptoethanol

Since our primary objective is to label proteins containing thiol moieties, after proving the effectiveness of our probes for thiol sensing and signaling, we have continued with protein labeling. When spectroscopic results belongs to BSA-label conjugate have been examined (figure 41 and 42), it is clear that the results obtained

from reaction of labeling agents with Cys are consistent with the results obtained from that with BSA. The results suggest that nitroolefin functionalization of BODIPY dyes is a promising way to sense biological thiols and hence label proteins bearing thiol groups.

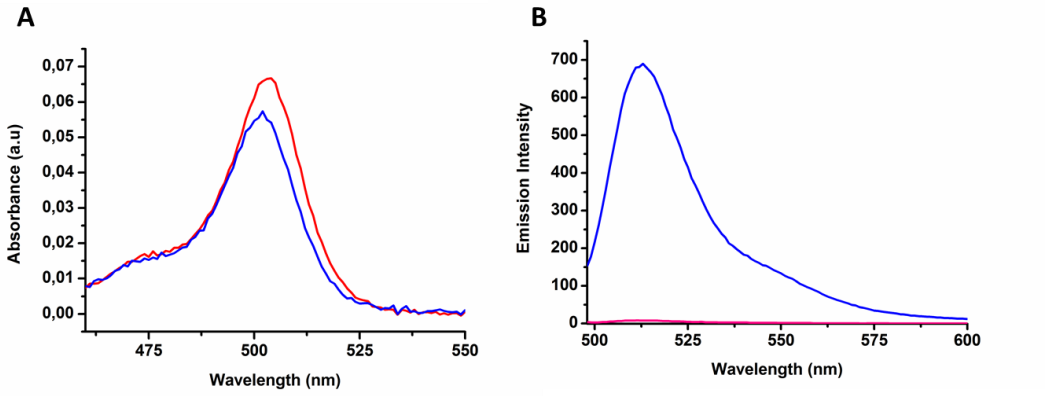

Figure 41: (A) Absorbance spectra (B) Fluorescence spectra of PL **1** and BSA-PL **1** conjugate in 50 mM HEPES:ACN (80/20, v/v, pH:7.4 λ_{ex}: 490 nm at 25 ^{0}C)

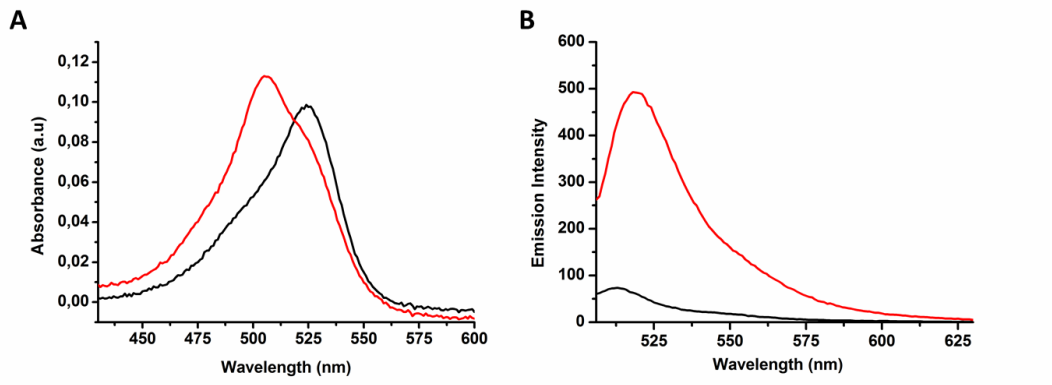

Figure 42: (A) Absorbance spectra (B) Fluorescence spectra of PL **2** and BSA-PL **2** conjugate in 50 mM HEPES:ACN (80/20, v/v, pH:7.4 λ_{ex}: 500 at 25 ^{0}C)

4.5 Experimental Details

4.5.1 Protein Labeling Studies

Bovine Serum Albumin (BSA) was used as the sample protein. BSA was dissolved in buffer (PBS or HEPES) as 1 mg/mL prior to addition of excess Bodipy (50equiv. in the case of PL**1** and 100 equiv in the case of PL**2**) which is dissolved in DMSO. The mixtures are protected from light and incubated in a shaker at room temperature for overnight.

4.5.2 Dialysis

A dialysis membrane with molecular weight cut off (MWCO) between 12-6000 KDa was used to remove excess dye from the reaction medium. Labeled mixture was transferred to the membrane and dialyzed for about 12 hours. Dialysis operates based on the differences between the sizes of dyes and protein-dye conjugates. Particles with diameters smaller than that of the pores of the membrane escape from the membrane and those with bigger diameters stay inside and a bulk of solvent outside makes the process easier and faster. Since PL **1** is 0.395 KDa, PL **2** is 0.881 KDa, and BSA is 66 KDa (1Da is equal to 1 g/mol), dyes are expected to be released from the membrane while keeping adduct inside.

4.5.3 Synthesis

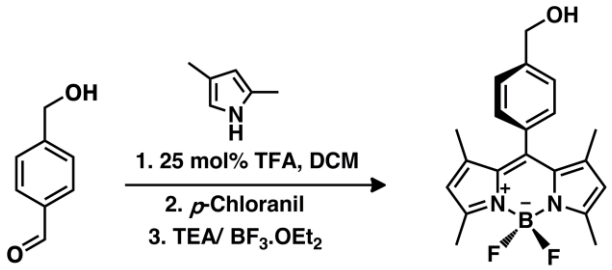

14

Synthesis of Compound 14: Trifluoroacetic acid (TFA; 1 drop) was added dropwise to a vigorously stirring solution of 4-(hydroxymethyl) benzaldehyde (0.5 g, 3.68 mmol) and 2,4-dimethylpyrrole (0.83 mL, 8.09 mmol) in 400 mL Ar-deaerrated dichloromethane (DCM). The resulting red solution was stirred at room temperature. The progress of the reaction was monitored by TLC and when TLC shows no starting material, *p*-Chloranil (0.903 g, 4.05 mmol) was then added in one portion and reaction was stirred for an additional hour. Triethyl amine (TEA) (5.0 mL) was then added dropwise to this mixture over a period of 15 min, and the resulting dark brown solution was allowed to stir for an additional 30 min at room temperature. BF_3•OEt_2 (5.0 mL) was then added dropwise to the reaction mixture over 15 min and it was left to stir at room temperature overnight. Combined organic phases were dried over anhydrous Na_2SO_4 and concentrated under vacuo. The crude product was subjected to F.C.C. by using DCM as the eluent. Compound 14 was obtained as dark orange solid (0.380 g, 29.2%).

^{1}H NMR (400 MHz, $CDCl_3$): δ_H 7.51 (d, J = 7.8 Hz, 2H), 7.38 (d, 2H), 6.04 (s, J = 31.5 Hz, 2H), 4.83 (s, 2H), 2.60 (s, J = 17.9 Hz, 6H), 1.46 (s, J = 51.7 Hz, 6H).

^{13}C NMR (100 MHz, $CDCl_3$): δ_C 155.5, 143.1, 141.9, 134.2, 128.2, 127.4, 121.2, 64.8, 14.5.

MS (TOF-ESI): m/z: Calcd. for $C_{20}H_{21}BF_2N_2O$: 353.17 $[M-H]^-$, Found:353.1673 $[M-H]^-$, Δ=-7.64 ppm.

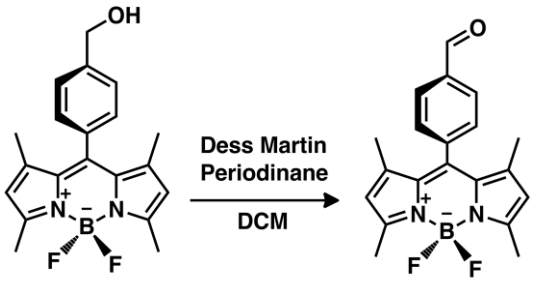

14 15

Synthesis of Compound 15: Dess-Martin periodinane (0.359 g, 0.84 mmol) dissolved in min. amount of Ar-degassed DCM was added dropwise to the mixture of compound **14** (0.150 g, 0.42 mmol) in a minimum amount of Ar-degassed DCM at 0 ^{o}C and it was left to stir at room temperature. The progress of the reaction was monitored by TLC and when TLC showed no starting material, the mixture was quenched with 20 mL sat'd $Na_2S_2O_3$ solution. Combined organic phases were then washed with sat'd $NaHCO_3$ solution (2x20 mL) and dried over anhydrous Na_2SO_4. After concentrated under vacuo, the crude product was subjected to the F.C.C. by using 95:5/ DCM: MeOH as the eluent. Compound **15** was obtained as dark orange solid (0.090 g, 60%).

^{1}H NMR (400 MHz, $CDCl_3$): δ_H 10.14 (s, J = 4.6 Hz, 1H), 8.04 (d, J = 6.2 Hz, 2H), 7.53 (d, J = 8.0 Hz, 2H), 6.019 (s, 2H), 2.58 (s, 6H), 1.37 (s, 6H).

^{13}C NMR (100 MHz, $CDCl_3$): δ_C 191.43, 156.25, 142.75, 141.40, 139.68, 136.68, 130.32, 129.15, 121.63, 121.60, 14.61, 14.50.

MS (TOF-ESI): m/z: Calcd. for $C_{20}H_{19}BF_2N_2O$: 351.16 $[M-H]^-$, Found:351.1548 $[M-H]^-$, Δ=-14.8 ppm.

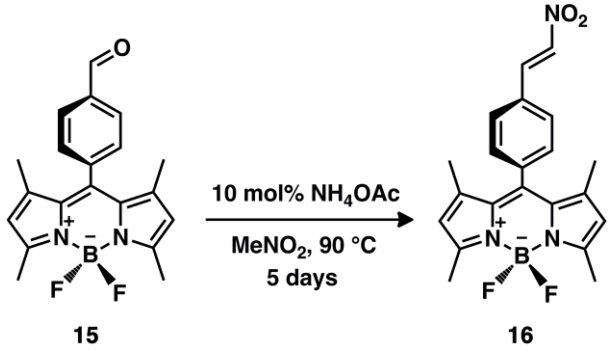

15 16

Synthesis of Compound 16: Solution of compound **15** (0.080 g, 0.23 mmol) and catalytic amount of NH_4OAc in nitromethane (4 mL) was immersed in an oil bath which was first stabilized at 90 ^oC. The mixture was stirred at 90 ^oC and the progress of the reaction was monitored by TLC. When TLC shows no starting material, nitromethane was evaporated and the crude product was subjected to F.C.C. by using 95:5/DCM: MeOH as the eluent. Compound **16** was obtained as red solid (0.045 g, 49.5%).

^1H NMR (400 MHz, d6-DMSO): δ_H 8.35(d, *J*=18.0 Hz, 1H), 8.25 (d, *J*=14.0 Hz, 1H), 8.1(d, *J*=8.0 Hz, 2H), 7.6(d, *J*=8.0 Hz, 2H), 6.2(s, 2H), 2.45(s, 6H), 1.4(s, 6H)

^{13}C NMR (100 MHz, d6-DMSO): δ_C 156.2, 142.7, 139.7, 139.0, 138.0, 137.9, 131.0, 130.8, 129.7, 129.5, 121.6, 14.6, 14.6.

MS (TOF-ESI): m/z: Calcd. for $C_{21}H_{20}BF_2N_3O_2$: 394.16 $[M-H]^-$, Found:394.1492 $[M-H]^-$,Δ=-2,74 ppm.

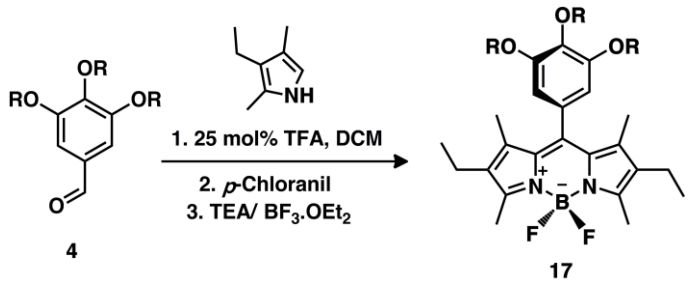

4 17

Synthesis of Compound 17: Trifluoroacetic acid (TFA; 1 drop) was added dropwise to a vigorously stirring solution of 3,4,5-tris(2-(2-(2-methoxyethoxy)ethoxy)benzaldehyde **4** (1.5 g, 2,55 mmol) and 23-ethyl-2,4-

dimethyl-pyrrole (528 mg, 5.61 mmol) in 350 mL Ar-deaerrated dichloromethane (DCM). The resulting red solution was stirred at room temperature and the reaction was monitored by TLC and when it showed no starting material, *p*-Chloranil (0.698 g, 2.79 mmol) was added in one portion and it was stirred for an additional hour. Triethyl amine (TEA) (8.0 mL) was then added dropwise to this mixture over a period of 15 min, and the resulting dark brown solution was allowed to stir for an additional 15 min. BF_3•OEt_2 (8.0 mL) was then added dropwise over a period of 15 min. and the resulting dark red solution was allowed to stir at room temperature overnight. The slurry reaction mixture was washed with water (3 × 300 mL) and dried over anhydrous Na_2SO_4. The solvent was evaporated and the residue was purified by silica gel flash column chromatography (F.C.C.) using DCM: MeOH (95:5, v/v) as the eluent. Compound **8** was obtained as a waxy dark orange solid (1.034 g, 46.7%).

^{1}H NMR (400 MHz, $CDCl_3$): δ_H 6.55 (s, *J* = 1.2 Hz, 2H), 4.24 (t, *J* = 7.4 Hz, 2H), 4.12 (t, *J* = 4.5 Hz, 4H), 3.85 (t, *J* = 4.7 Hz, 6H), 3.78 – 3.47 (m, 24H), 3.40 – 3.31 (m, 8H), 2.53 (s, 6H), 2.32 (q, *J* = 7.4 Hz, 4H), 1.42 (s, 6H), 1.00 (t, *J* = 7.4 Hz, 6H).

^{13}C NMR (100 MHz, $CDCl_3$): δ_C 153.8, 153.6, 139.7, 136.3, 132.7, 132.7, 72.7, 71.9, 70.9, 70.7, 70.6, 70.6, 69.7, 69.2, 59.0, 58.9, 17.1, 14.6, 12.5, 11.6.

MS (TOF-ESI): m/z: Calcd. for $C_{23}H_{24}BF_2N_2O_3$: 865.49 $[M-H]^-$, Found: 865.4904 $[M-H]^-$, Δ= -4.05 ppm.

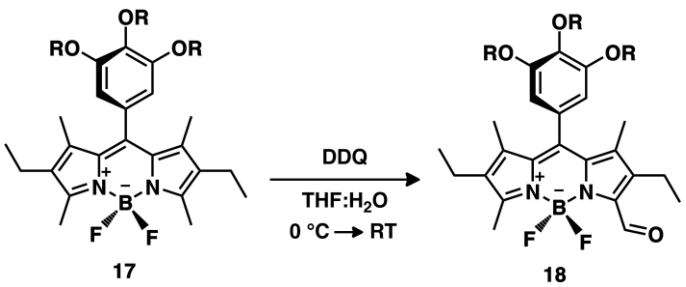

Synthesis of Compound 18: Compound **17** (0.40 g, 0.46 mmol) was dissolved in 18 mL, Ar-degassed THF containing 0.16 mL distilled water and it was cooled to 0 ^{o}C. DDQ (0.42 g, 0.54 mmol) was dissolved in Ar-degassed THF (6 mL) was added dropwise to the reaction under Ar while keeping the reaction at 0 ^{o}C. The reaction mixture was left to stir at room temperature for 3 days. When TLC showed no starting material, the resultant crude product was subjected to F.C.C. using EtOAc: MeOH (95:5, v/v) as eluent. Compound **18** was obtained as red solid (0.350 g, 86% yield).

^{1}H NMR (400 MHz, $CDCl_3$): δ_H 10.38 (s, 1H), 6.56 (s, 2H), 4.26 (s, 2H), 4.14 (s, 4H), 3.80-3.51 (m, 30H), 3.44 – 3.30 (m, 9H), 2.72 (s, 2H), 2.61(s, 3H), 2.36 (s,2H), 1.55 (s,3H), 1.41 (s, 3H), 1.05 (s, 6H).

^{13}C NMR (100 MHz, $CDCl_3$): δ_C 213.7, 185.9, 166.2, 153.9, 143.7, 141.5, 139.9, 139.2, 137.7, 137.0, 135.6, 134.3, 132.1, 129.6, 107.5, 77.4, 77.1, 76.7, 72.7, 71.9, 71.9, 70.8, 70.6, 70.6, 70.5, 70.5, 69.7, 69.2, 59.0, 59.0, 58.9, 17.6, 17.1, 14.3, 14.02, 13.7, 12.3, 10.4.

MS (TOF-ESI): m/z: Calcd. for $C_{23}H_{22}BF_2N_2O_4$: 879.47 $[M-H]^-$, Found:879.468 $[M-H]^-$, Δ= -2.52 ppm.

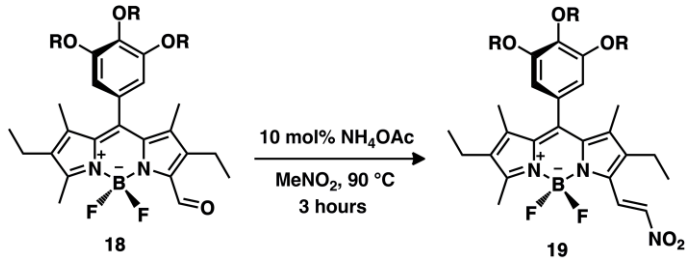

Synthesis of Compound 19: Solution of compound **18** (0.34 g, 0.39 mmol) and catalytic amount of NH_4OAc in nitromethane (5 mL) was immersed in an oil bath which was first stabilized at 90 ^{o}C. The mixture was stirred at 90 ^{o}C for 3 hrs and the progress of the reaction was monitored by TLC. When TLC shows no starting material, nitromethane was evaporated and the crude product was subjected to F.C.C.

by using 95:5/DCM: MeOH as the eluent. Compound **19** was obtained as red solid (0.090 g, 25.2 %).

^{1}H NMR (400 MHz, $CDCl_3$): δ_H 8.36 (d, *J* = 13.7 Hz, 1H), 7.84 (d, *J* = 13.8 Hz, 1H), 6.55 (s, 2H), 4.29 – 4.17 (m, 2H), 4.17 – 4.01 (m, 4H), 3.90 – 3.82 (m, 6H), 3.82 – 3.33 (m, 34H), 2.72 – 2.32 (m, 7H), 2.08 – 1.68 (m, 1H), 1.50 (s, 3H), 1.46 (d, *J* = 26.5 Hz, 6H), 1.07 (m, *J* = 19.8, 7.5 Hz, 6H).

^{13}C NMR (100 MHz, $CDCl_3$): δ_C 165.16, 153.95, 143.06, 140.18, 139.36, 137.86, 137.81, 137.76, 137.51, 137.47, 136.35, 135.43, 135.09, 133.94, 129.50, 127.51, 107.56, 77.37, 77.06, 76.74, 72.76, 71.95, 71.89, 70.85, 70.70, 70.65, 70.56, 69.70, 69.27, 59.03, 59.00.

MS (TOF-ESI): m/z: Calcd. for $C_{24}H_{23}BF_2N_3O_5$: 922.48 $[M\text{-}Na]^+$, Found: 946.47 $[M\text{-}Na]^+$, Δ= -8.73 ppm.

CHAPTER 5

5. Near IR Absorbing Bodipy Derivatives as Glutathione Activated Photosensitizers for Selective Photodynamic Action

Ilke Simsek Turan, Fatma Pir Cakmak, Deniz Cansen Yildirim, Rengul Cetin-Atalay and Engin U. Akkaya

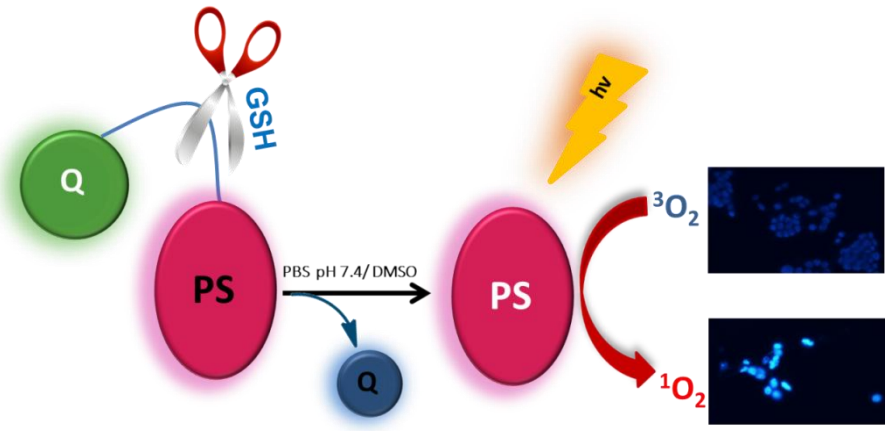

5.1 Objective

Since in practice, photosensitivity of the patient is still an issue often leading to painful edema in the patients undergoing PDT treatment, more selective PDT sensitizers are needed to remove any chance of off-target sensitization. In principle, this can be done in a number of ways. In this work, our goal was to design a quenched photosensitizer, which can only be capable of generating singlet oxygen after glutathione (GSH) mediated reaction resulting in the removal of the quencher moiety. Before the uncaging reaction, the PS-Q conjugate is expected to have little to negligible toxic activity on the selected cell cultures. GSH mediated uncaging results in a highly active photodynamic agent.

We are confident that as the stumbling blocks hindering the broader applicability of photodynamic therapy are removed, the methodology will be more effective competitor of the more established treatment protocols. We shall continue to do our part in providing chemical/photophysical avenues towards that end.

5.2 Introduction

Under physiological conditions, there is equilibrium between both cell death and division which maintain the tissue/organ homeostasis. The equilibrium is substantiated based on the unique mechanisms like cell cycle checkpoints, DNA repair and recombination, and cell death in which along with oxidation and reduction of proteins, the rate and nature of free radicals present significant roles. The term oxidative stress defines the equilibrium between NAD^+/NADH, $NADP^+$/NADPH, and/or GSH/GSSG and involves the relationship with different metabolites and control of cell metabolism.[76] Free radicals are the compounds having one or more electron pairs. Free radicals in mammals are called as reactive oxygen species which involve mainly, superoxide anions ($O_2^{\cdot -}$), hydroxyl radicals ($^{\cdot}OH$) and peroxide radicals ($ROO^{\cdot}$) however, H_2O_2 is a ROS-related compound with unpaired electrons. The increases in their levels can lead to increase in cellular defense systems and even

cell death unless damage is reversible. The changes in their levels can be attributed to the oxidation of nucleic acids, proteins, lipids, characteristics of carcinogens, DNA bases and sugar backbone of both DNA and RNA. The accumulation of oxidative damage on DNA contributes to the development of severe diseases like cancer, heart disease, cataracts, brain dysfunction, and aging. In normal functioning cells, these oxidative damages caused by ROS can be repaired by DNA repair enzymes effectively but, due to the increased ROS generation in cancer cells, oxidative products of DNA, proteins, lipids are accumulated and released into blood and tissue. The generated oxidative products of DNA and lipid peroxidation has been detected in several cancer tissues like colorectal adenocarcinomas, mammary ductal carcinomas, renal cell carcinoma, and blood samples from leukemia patients. The excessive generation of ROS is directly related with the development of cancer.[77,78]

However, healthy cells generate defense mechanisms involving proteins and molecules like glutathione to inactivate ROS. Glutathione (GSH) presents in the cells mainly in the reduced state (GSH) but it is oxidized to (GSSG) during the oxidative stress. Because of that, the measurement of GSH levels and the ratio of GSH/total GSH have been employed for the evaluation of redox status in biological systems. Maintenance of proper levels of GSH and its oxidation is very significant for cell functioning. As a result of ROS in unhealthy cells, imbalance in GSH has been detected in several diseases such as cancer, neurodegenerative disorders, cystic fibrosis, HIV, etc. The decreased levels of GSH designate the enhanced susceptibility to oxidative stress thus in turn, development of many disease states. However, the increase in GSH levels is related with the increased antioxidant capacity and resistance to oxidative stress that can be diagnosed in many cancer types. Besides, the elevated levels of GSH in tumor tissue develops the resistance and thus, leads to the alteration in the cytotoxicity of either chemotherapy drugs or radiation.[79,80]

5.3 Design of Photosensitizers

Among the numerous class of fluorescent dyes, Bodipy derivatives has spectroscopically risen in popularity due its considerable photophysical characteristics such that Bodipy dyes have high absorption coefficients, sharp fluorescence emission with high fluorescence quantum yields, high photostability, sensitivity to environmental conditions, high stability in physiological conditions. Use of Bodipy as a photosensitizer meets the requirements for a good photosensitizer since it has high singlet oxygen quantum yield, photostability, long wavelength absorption and low dark toxicity. Additionally, their spectroscopic properties can be modified with ease accordingly to the purpose of the study. Because of its outstanding properties, Bodipy dye constitutes the core of our target photosensitizers and contemplated target photosensitizer is shown in figure 43.

Photosensitizers have been designed to control their activity based on photoinduced electron transfer and because of that we have modified our core bodipy dye with the introduction of a 2,4-dinitrobenzenesulfonate (DNBS) group which was previously shown to be susceptible to thiol mediated cleavage. Electron sink 2,4-dinitrobenzenesulfonyl moiety is expected to quench the excited state through oxidative PeT. In order to ensure an enhanced spin-orbit coupling and faster the rates of inter-system crossing, and thus, translates into more efficient cytotoxic singlet oxygen generation, we have planned to incorporate heavy atoms like bromine into the structure. Since devised photosensitizers applied in PDT should have absorption at therapeutic window (600- 800 nm) and long-wavelength light is required for tissue penetration owing to the presence of endogenous absorbers, we have incorporated aromatic units via 3 and 5 positions of the core in order to extend the conjugation. Photosensitizers have been functionalized with the introduction of oligoethylene moieties in order to enhance the water solubility which is one of the vital characteristics of an ideal PS.

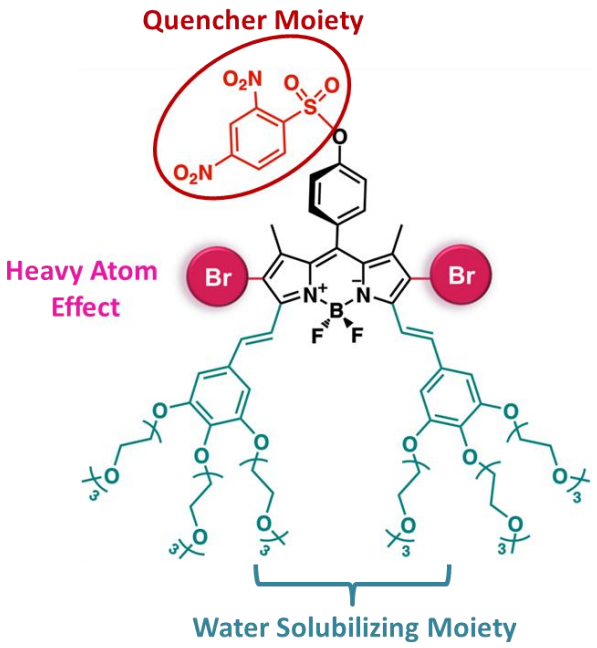

Figure 43: Structure of Designed Activatable Photosensitizer.

GSH-mediated activation of quenched photosensitizers should be achieved in a controlled manner with specifically and hastily. Because of that we have planned to synthesize three different photosensitizers which have differences in connectivity of the quencher moiety. We have planned to deduce the effect of connectivity differences of quencher in the activation, reactivity and stability of photosensitizers and thus, we can designate the ideal PS for PDT with controlled activity, reactivity and stability. In the case of PS **1**, we have incorporated quencher moiety on the para-position of the core bodipy whereas in the case of PS **2** and PS **3**, quencher moiety has been incorporated at the ortho to the core bodipy. We have expected that quenching via ortho substituted DNBS group will be more effective due to the closeness of the electron sink to the electron donor group. Additionally, we believed that ortho substitution increases the rate of thiol mediated activation of the quenched PS due to the enhanced steric hindrance between acceptor and donor groups. Correspondingly, substitution of extra heavy atom para to the electron sink increases the rate of reaction via weakening of the bond between phenoxide and sulfoxide

through electron withdrawing. On the other hand, the increased reactivity leads to decrease in the stability of PS thus in turn; the possibility of unspecific activation may be increased.

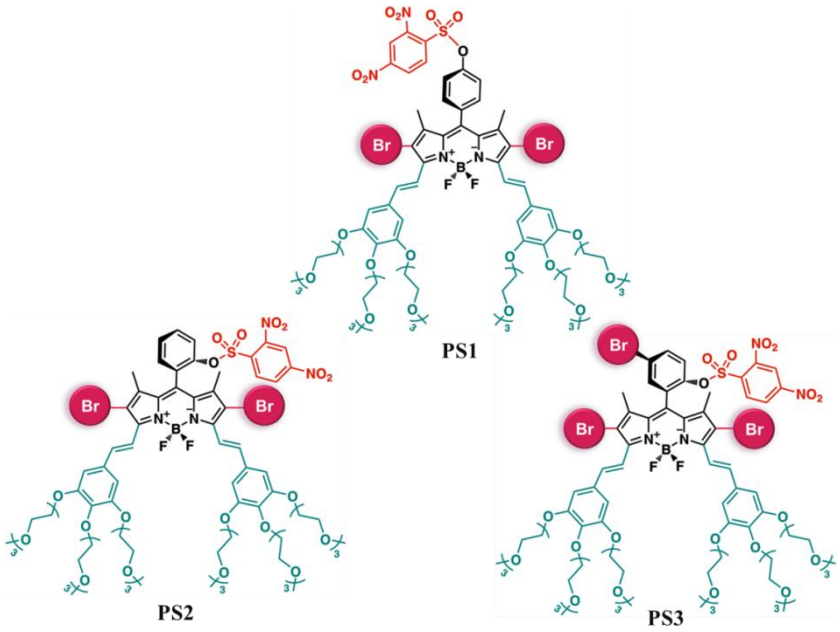

Figure 44: Target photosensitizers for GSH mediated activity control

5.4 Results and Discussion

5.4.1 Synthetic Approach

In order to incorporate PeT process for the activity control, we have devised our structures by incorporating quencher moiety to the meso position of the core. Phenol modified derivative of bodipy core is required for the introduction of DNBS group. Therefore, synthetic journey is begun with the synthesis of bodipy derivatives **20** and **21**. Bodipy skeleton can be formed via either acid catalyzed condensation of aldehyde with pyrrole or condensation of acylchloride derivatives of aldehydes with

excess pyrrole. We have preferred to construct bodipy skeleton through the use of aldehyde (4-hydroxybenzaldehyde for compound **20**, 2-hydroxybenzaldehyde for compound **21**) in the presence of acid catalysis. Formed air sensitive dipyyromethanes have been oxidized by *p*-Chloranil or DDQ to yield dipyrromethene. Abstraction of acidic proton through the use of excess base followed by borontrifluoride on the dipyrrin affords the target bodipy cores.

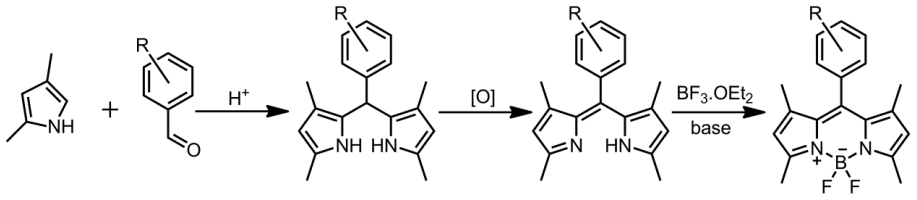

Figure 45: Synthesis of target bodipy core via acid catalyzed condensation of 4- and 2-hydroxybenzaldehydes with 2,4-dimethylpyrrole

After construction of the core, we have continued with the functionalization of core bodipy firstly with heavy atoms. Heavy atom modification must be done prior to extension of conjugation in order to eliminate side products generated from reaction of halogens with olefinic hydrogens. We have preferred to functionalize core with bromine as a ISC inducer instead of iodine due to the low stability of C-I bond whose lability increases during Knoevenagel condensation reaction. During NBS mediated bromination of bodipy **24**, the presence of mesomerically active hydroxyl group leads to the bromination of phenyl moiety from the para position according to the hydroxyl group. The yield of bromination reaction for the synthesis of compound **25** can be increased by performing the reaction in ice-cold environment unless we seek to synthesize both compounds **25** and **28**. Later, through the Knoevenagel condensation reaction with triethylene glycol modified aromatic aldehyde whose synthesis was stated in Chapter 3, we have been able to entitle the structures with both hydrophilicity and extended conjugation. Olefinic groups can be incorporated into the structure with condensation reactions which requires the removal of in situ generated water from the reaction medium via dean-stark apparatus. The synthesis of

activatable photosensitizers was completed with the introduction of quencher moiety via S_N2 type nucleophilic substitution reaction. Uncaged photosensitizers were deprotonated with excess triethylamine prior to addition of quencher. In order to prevent the hydrolysis of 2,4-dinitrobenzenesulfonyl chloride, dry THF was used and the reaction was performed under inert atmosphere in the catalysis of DMAP at 0 °C. Uncaged photosensitizers are all accepted as control compounds and each has been employed in live cell studies. In case of the possibility that control compounds could not be active in cells since they could not penetrate though cell membrane, we have synthesized another control compound **33** by following same synthetic route (figure 46).

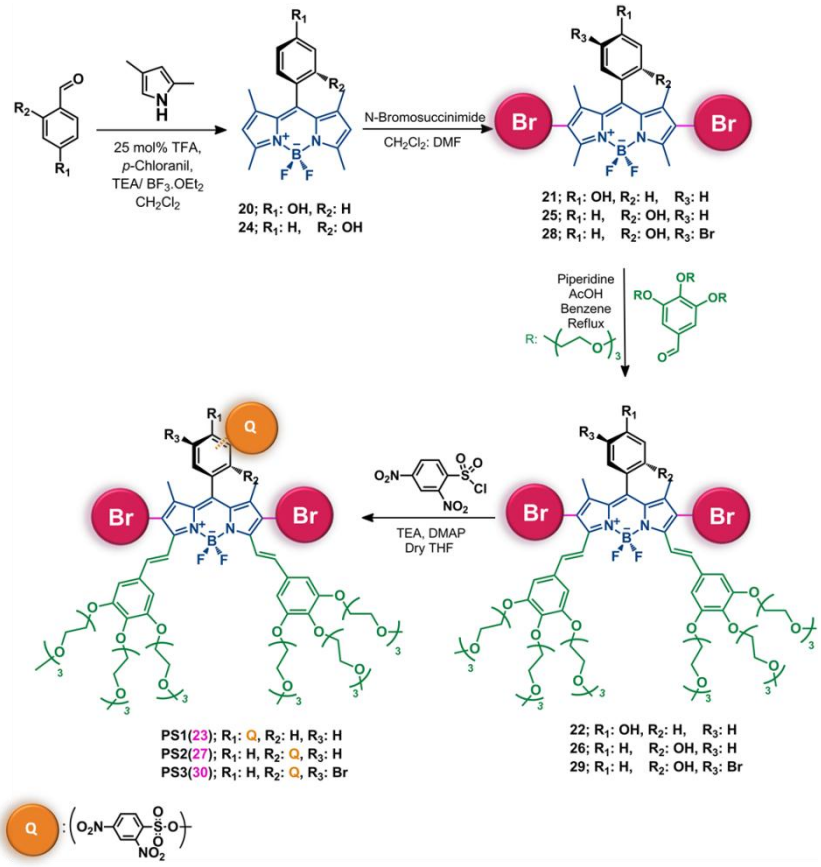

Figure 46: Synthetic Route for Activatable Photosensitizers

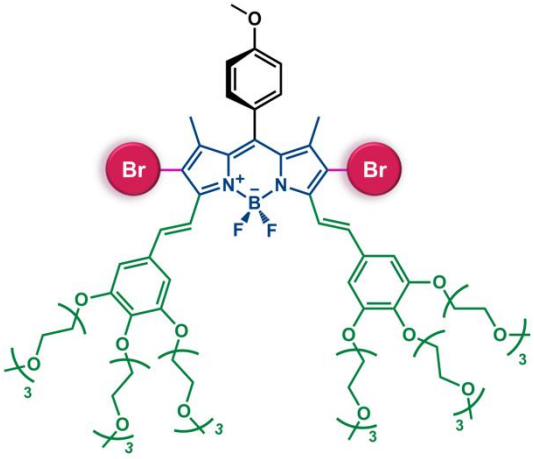

Figure 47: Chemical Structure of Control Photosensitizer **33.**

5.4.2 Working Principle

Our photosensitizers are quenched via oxidative PeT which is mediated by the introduction of electron sink DNBS moiety. Electron transfer occurs from electron rich bodipy core to electron poor quencher group and thus d-PeT becomes active. Since fluorescence of photosensitizers has been quenched, PS cannot produce singlet oxygen which enables us to control their cytotoxic activity. In the presence of cancer related cellular parameter glutathione, it attacks to the nucleophilic sulfonyl moiety of DNBS group and generates activated bodipy structure while releasing GSH-substituted 2,4-dinitrobenzene group and sulfur dioxide gas as a result of rearrangement. Once the photosensitizer is activated (d-PeT in off state), under light irradiation specific to bodipy, due to the enhanced spin orbit coupling and thus faster rates of inter-system crossing, PS starts to facilitates cytotoxic singlet oxygen generation which leads to cell death either by necrosis or apoptosis (figure 48).

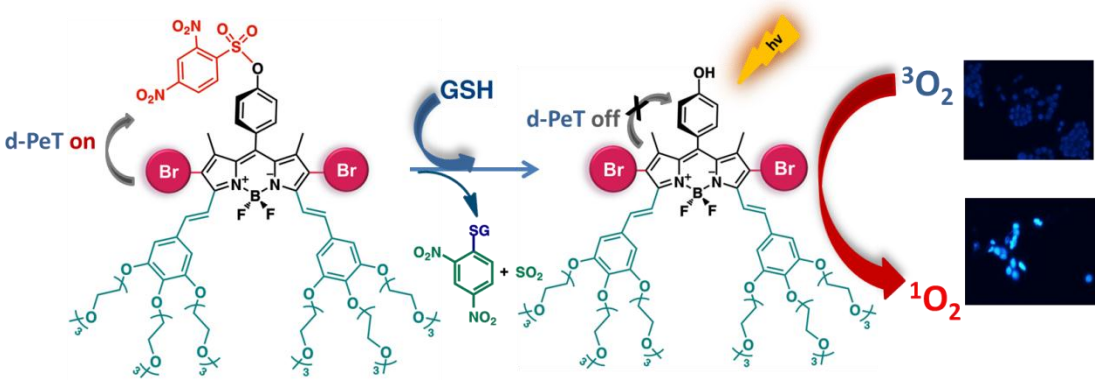

Figure 48: GSH-mediated activation of photosensitizers for the cytotoxic singlet oxygen generation

5.4.3 Spectral Proofs for Activation Process

We have started spectroscopic measurements in order to illustrate that our photosensitizers reacts with GSH to yield activated bodipy structures **22**, **26** and **29** through nucleophilic substitution reaction. The absorbance spectra belongs to GSH mediated reaction of PS **1-3** are shown in figure 48, it is obvious that the progress of the reaction can be followed spectroscopically. Since the electron sink DNBS group is removed, the conjugation over the structure decreases, uncaged photosensitizers are supposed to have absorbance higher in energy and lower in wavelength compared to photosensitizers **1-3** and spectra belongs to this conversion supports our expectations. It is clear that our quenched photosensitizers are susceptible to GSH mediated cleavage. When considering the wavelength that PS absorbing shows that they are active in the therapeutic window which is a vital parameter for PS to be used in PDT.

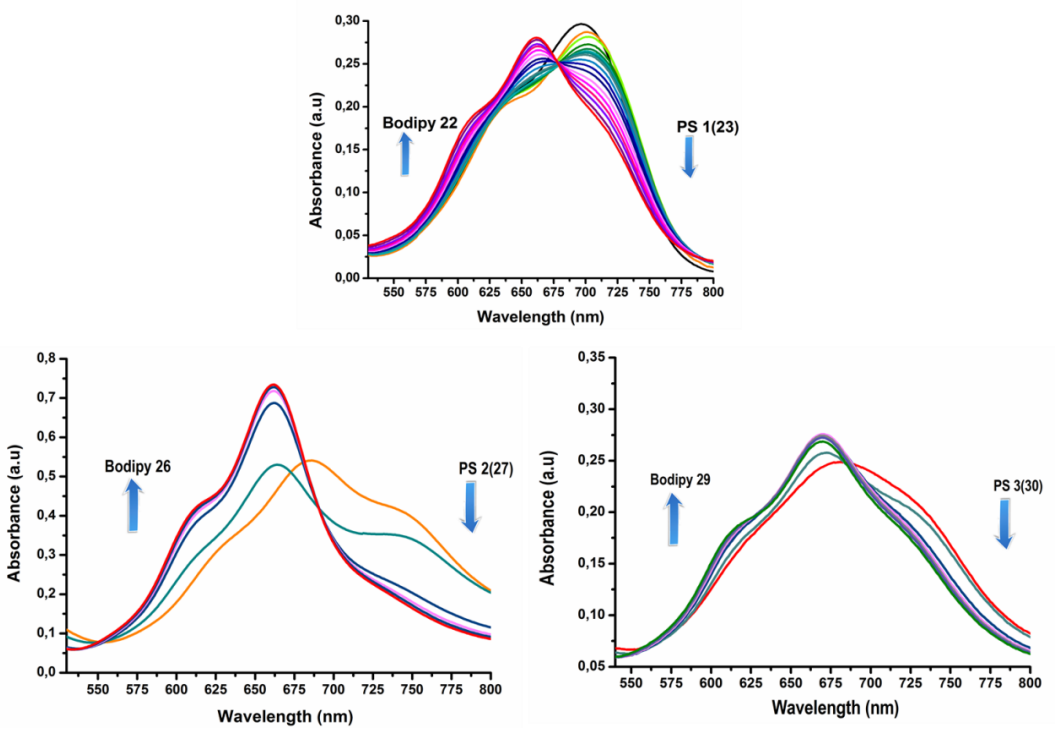

Figure 49: Absorbance Spectra of GSH-mediated Activation of Photosensitizers **2-3** in DMSO: 1X PBS (50:50, v/v, pH: 7.4, at 25 °C).

Fluorescence emission spectra of this reaction could prove that when quencher moiety is in close contact with PS, they should have little or no fluorescence emission due to the presence of d-PeT. On the other hand, when quencher group has been removed via GSH, the fluorescence emission should have been enhanced since d-PeT becomes inactive. When fluorescence spectra (figure 50) belong to this reaction is analyzed delicately, time dependent increment in emission proves our suggestion smoothly. As a result, these spectra substantiate that upon reaction with GSH, our quenched photosensitizers could be activated via blocking of d-PeT which enhances spin-orbit coupling, faster rates of inter-system crossing, and thus, enables the singlet oxygen generation. Increase in emission intensity will be different in each photosensitizer depending on the connectivity of quencher moiety. In the case of ortho substituted functionalization of electron sink, quenching could be more

effective due to the closeness of electron withdrawing DNBS moiety to the electron rich bodipy core which means that in PS **2**, quenching is more effective.

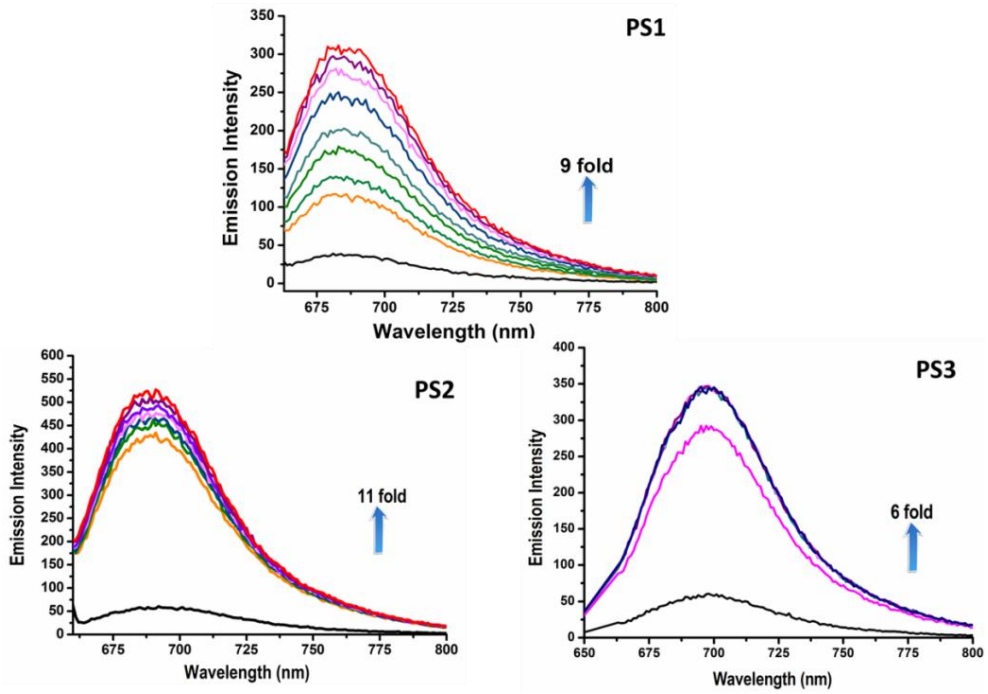

Figure 50: Fluorescence Emission Spectra of GSH-mediated Activation of Photosensitizers **2-3** in (4 μM) DMSO: 1X PBS (50:50, v/v, pH: 7.4, λ_{ex}: 655 nm at 25 °C).

Therefore, when it is activated, the enhancement in emission is expected to be higher. Since para connectivity is not as effective as ortho one due to the higher distance between electron sink and bodipy core, effect of d-PeT is lower and therefore, the enhancement in emission is lower compared to ortho one upon activation.

Although functionalization of electron sink in PS **3** is ortho to the donor, the presence of extra bromine in the para to the quencher decreases the effectiveness of d-PeT and because of that the enhancement in emission could be lower compared other photosensitizers. When comparing the fluorescence spectra belongs to each

photosensitizers, it can be concluded that PS **2** is a better candidate for GSH mediated activation of quenched PS for PDT compared to others. After fluorescence studies, we have continued with the singlet oxygen generation measurements first with caged photosensitizers and then with uncaged photosensitizers.

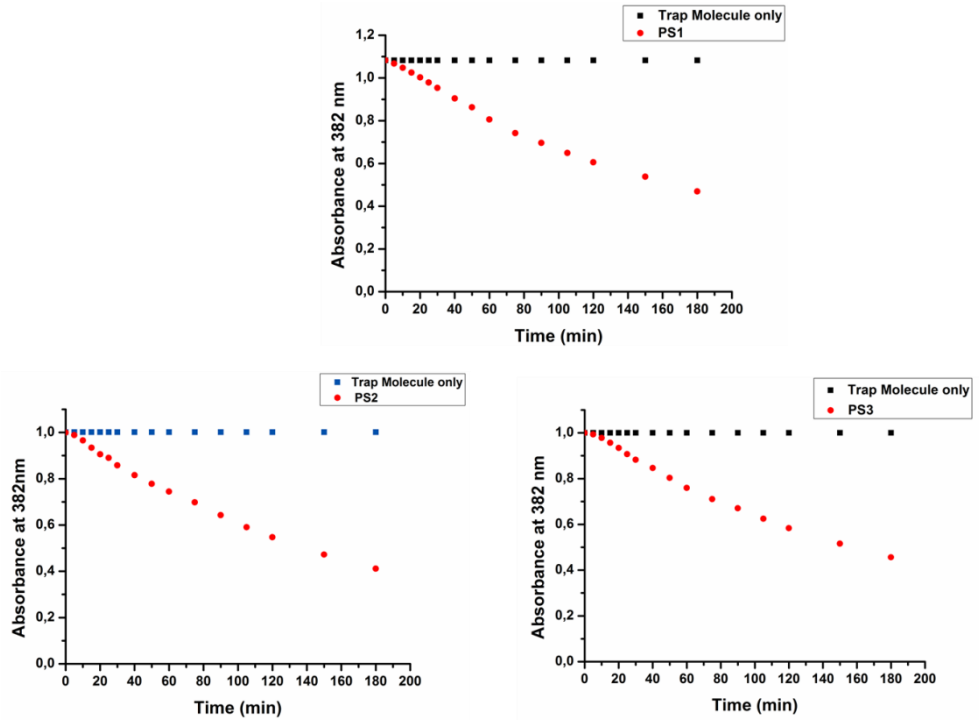

Figure 51: Absorbance spectrum of trap molecule (2,2'-(Anthracene-9,10-diyl)bis(methylene)dimalonic acid) with PS**1-2** (4 µM) in DMSO: 1X PBS (50:50, v/v, pH: 7.4, 25 °C) LED applied at 660 nm.

Since in the presence of reactive oxygen species, GSH would be in reduced form, the activation of the PS would be slow and less effective, therefore, singlet oxygen quantum yields would be lower. Due to reduction of GSH, there is not any significant difference between the ROS generation efficiencies (table 3) of PS in approximate reaction time. The decrease in the absorbance of trap molecule by the reaction with generated singlet oxygen via GSH mediated activation of PS needs more time compared to active form of them and PS could not be able to yield as much singlet oxygen as activated ones even in longer reaction times. When

considering the connectivity differences between PS, most active one PS **2**, generates high $^1O_2$ compared to others (table 4). However, owing to high reactivity and thus decreased stability, PS **2** would not be best candidate for PDT applications. PS **1** could be accepted as an ideal photosensitizer because singlet oxygen generation efficiency of uncaged compound **22** is close to most promising candidate with increased stability of the compound. Activation of quenched PS **1** could be controlled better and thus, decreases the possibility of healthy tissue damage.

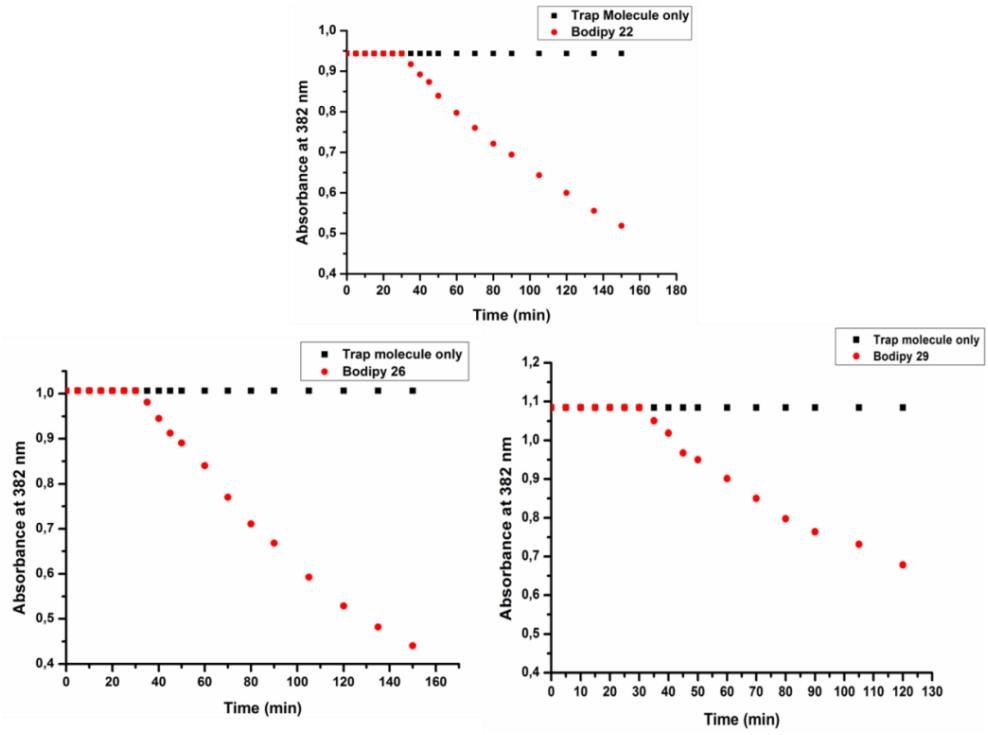

Figure 52: Absorbance spectrum of trap molecule (2,2'-(Anthracene-9,10-diyl)bis(methylene)dimalonic acid) with Bodipy **22, 26, 29** (4 µM) in DMSO: 1X PBS (50:50, v/v, pH: 7.4, 25 °C) LED applied at 660 nm.

It is clear from spectroscopic studies that GSH at physiologically relevant concentrations is capable of transforming an ineffective chromophores into a very effective sensitizer generating singlet oxygen when excited within the therapeutic

window (in this case at 660 nm). Next, we wanted to demonstrate the effectiveness of intracellular GSH in activating our "caged" photosensitizers. To that end, a number of human epithelial cancer cells in culture (Huh7, MCF7 and HCT116) were tested with the photosensitizers, and as a control, -Q (photosensitizers with no quencher group, or in other words, the active photosensitizers to be obtained when Q group is removed) were also included.

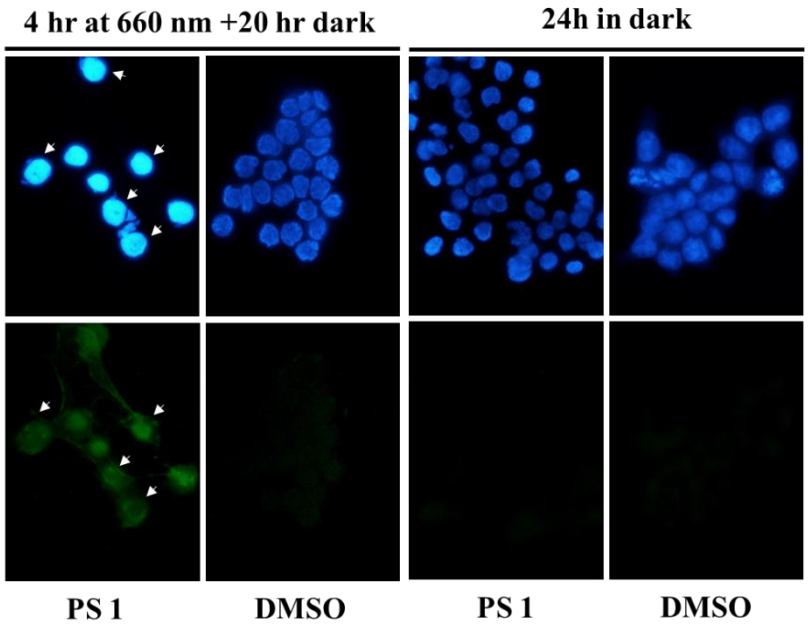

Figure 53: Fluorescence microscope images of Annexin-V-FITC stained HCT116 cells in the presence of 20 nM sensitizer **1**. Cells were either subjected to 4 hours of red LED irradiation at 660 nm for 4 hours, followed by 20 h incubation in the dark (**A**), or just 24 hours of dark incubation (**B**). Hoechst-33258 stains nuclear DNA in all conditions. Arrows point to the apoptotic cells with fragmented chromatin (bright blue) and Annexin V positive membrane (green). Images are captured at 40x.

Based on our results with chemical trap studies of singlet oxygen generation, we expected higher photocytotoxic activity on cancer cells with the control series. The cell culture studies were all done in triplicate with most of our caged photosensitizers were found to be effective. Some had relatively high dark toxicity which is checked by additional experiments to isolate the contribution of photocytotoxicity. The Bodipy dyes were tested both in dark and under irradiation with red LED light. The

results are presented in table 3. In one particular colon cancer cell line (HCT116), we obtained a remarkable IC_{50} of 20.0 nM under irradiation. The IC_{50} value without light is much higher suggesting that much lower concentrations will be effective under photodynamic regime. It is both surprising and noteworthy that when uncaged PS's were introduced, their photocytotoxicity is significantly lower. This may be due to reduced cell permeability and lipid solubility.

Table 3: IC_{50} values of sensitizers in HCT116 cell line

Sensitizers	Red LED irradiation for 4 h, IC_{50} μM	No light IC_{50} μM
BODIPY-**22**[a]	0.35±0.10	0.35±0.16
BODIPY-**26**[a]	0.64±0.11	0.42±0.27
BODIPY-**29**[a]	0.43±0.12	0.75±0.04
BODIPY-**33**[a]	0.04±0.02	0.20±0.03
PS1[a]	0.02±0.003	4.38±0.03
PS2[a]	0.02±0.004	0.29±0.11
PS3[a]	<0.06	0.36±0.10
NC[a]	no inhibition	no inhibition
PS1[b]	no inhibition	no inhibition

NC: Negative control. The experiments were performed in triplicate. [a]IC_{50} values of sensitizers with the HCT116 cell line after 72 hours of incubation with indicated sensitizers. NC: Negative control compound (1,3,5,7-tetramethyl-Bodipy). [b] The effect of **PS1** On the MRC-5 Human fetal lung fibroblast cells. The experiments were performed in triplicate

Nevertheless, considering the fact that **PS-Q** in the caged form is not capable of producing singlet oxygen, intracellular GSH is apparently cleaving the quencher module, and thus releasing the active photosensitizer. Using fluorescence microscopy, Annexin-V, Hoechst-33258 co-staining shows that cells clearly undergo apoptosis as evidenced by dense Hoechst-33258 incorporation of the nuclear stain and green Annexin-V labeling through the integrity-compromised cellular membranes. Same

compound without red light irradiation shows no such changes, cells keeping their usual appearance in the presence of 20 nM of sensitizer **1.**

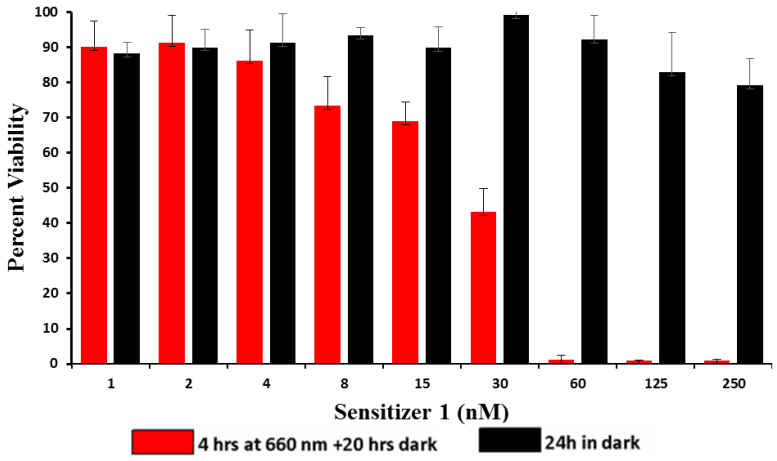

Figure 54: Growth inhibition of HCT116 cells was determined by NCI-SRB assay. Various concentrations of sensitizer **1** (1-250 nM) were used to determine cell death. Red bars show cell growth inhibition under 4 h irradiation with red LED, followed by 20 h incubation in the dark, black bars indicate cell growth inhibition following 24 h incubation in the dark.

Since we have observed that uncaged PS's were introduced, their photocytotoxicity is significantly lower due to reduced cell permeability and lipid solubility, we have synthesized new active photosensitizer **33** which does not bear hydroxyl group. Spectra in figure 54 shows that compound **33** are able to generate cytotoxic singlet oxygen as with other compounds. When this compound is employed in live cell studies unlike uncaged derivatives, PS **33** shows high activity (figure 55) which proves our suggestion that if uncaged photosensitizers should have high cell permeability, they could be able cause cell death.

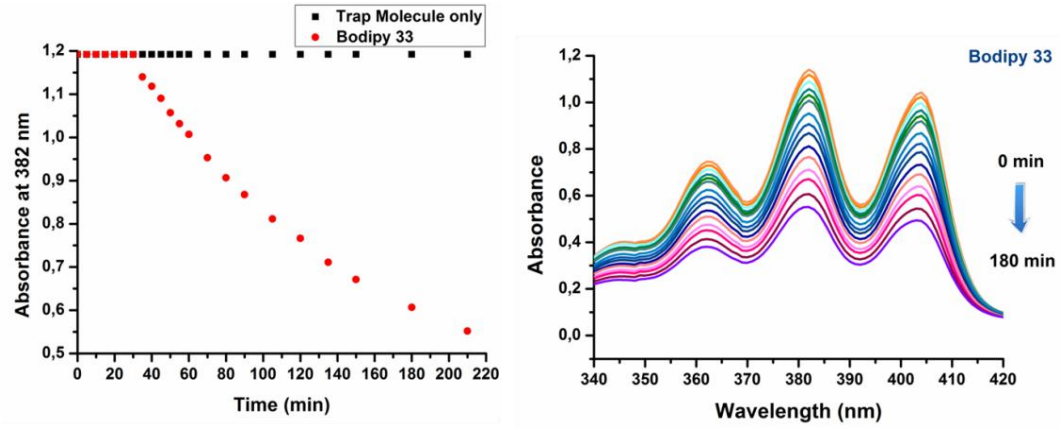

Figure 55: The decrease in absorbance spectrum of trap molecule (2,2'-(Anthracene-9,10-diyl)bis(methylene)dimalonic acid) in the presence of **Bodipy 33** (4 μM) in DMSO: 1X PBS (50:50, v/v, pH: 7.4, 25 °C) LED applied at 660 nm for 180 min.

5.5 Experimental Details

5.5.1 Singlet Oxygen Measurements

$^1O_2$ dependent degradation of water soluble trap, 2,2'-(anthracene-9,10 diylbis(methylene)dimalonic acid in the presence of photosensitizers (4 μM) in DMSO: 1X PBS (50:50, v/v, pH: 7.4) was studied to prove the photodynamic activity since the absorption of trap molecule decreases via photoxogenated [2+2] cycloaddition reaction of singlet oxygen. Prior to irradiation at 660 nm, solutions were incubated in dark for 30min and after that rapid degradation of trap molecule starts.

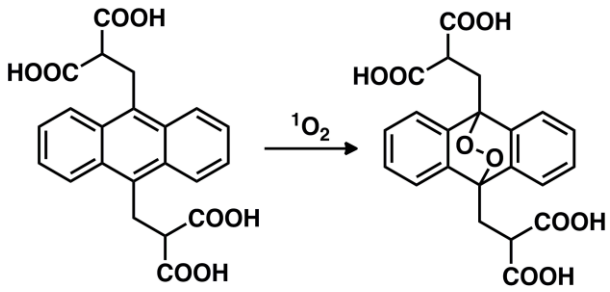

Figure 56: $^1O_2$ dependent degradation of trap molecule.

5.5.2 Singlet Oxygen Quantum Yield Studies

Singlet oxygen quantum yields were calculated according to the literature.[81] The relative quantum yields were calculated with reference to Methylene Blue (MB) in water as 0.52.[82,83] Quantum yields for singlet oxygen generation in DMSO: 1X PBS (50:50, v/v, pH: 7.4) were determined by monitoring the photooxidation of trap molecule (2,2'-(Anthracene-9,10-diyl)bis(methylene)dimalonic acid). Firstly, in order to have a reference in DMSO: 1X PBS (50:50, v/v, pH: 7.4), singlet oxygen

quantum yields of Methylene Blue were determined as 0.95. The quantum yields of singlet oxygen generation of the photosensitizers were calculated accordingly (table 4).

Oxygen saturated DMSO and 1X PBS (50:50, v/v, pH: 7.4) were obtained by bubbling oxygen for 15 minutes. The absorbance of trap molecule was adjusted around 1.0 in oxygen saturated solution. Then, the photosensitizer (4 μM) was added to cuvette and photosentizers' absorbance was adjusted around 0.2-0.3 in order to diminish the possibility of singlet oxygen quenching by the dyes. After, taking some measurements in dark, we exposed the cuvette to monochromatic light (660 nm) at the peak absorption wavelength. Absorbance was measured for several times after each irradiation. The graphics were plotted as the change in optical density (ΔOD) of trap molecule at 382 nm vs irradiation time for each photosensitizer.

The quantum yields of singlet oxygen generation were calculated by using the following equation:

$$\Phi(^1O_2)^{bod} = \Phi(^1O_2)^{MB} (m^{bod}. F^{MB} / m^{MB}. F^{bod}) \qquad \text{equation 2}$$

where superscripts 'bod' represents the photosensitizers, $\Phi(^1O_2)$ is the quantum yield of singlet oxygen, m is the slope of difference in change in the absorbance of the trap molecule (at 382 nm) with the irradiation time and F is the absorption correction factor, which is given by $F=1- 10^{-OD}$ (OD at the irradiation wavelength).

Table 4 : $\Phi(^1O_2)$ values of photosensitizers

Photosensitizers	**$\Phi(^1O_2)$**
BODIPY-22	0.35
BODIPY-26	0.40
BODIPY-29	0.37
BODIPY-33	0.25
MB	0.95
MB_{H2O}	0.52

5.5.3 Live Cell Studies

Cell culture

HCT116 human colon carcinoma cells (ATCC) were maintained in Dulbecco's Modified Eagle's Medium (DMEM) (Initrogen GIBCO), with 10% fetal bovine serum (FBS) (Invitrogen GIBCO), 2 mM L-glutamine, 0.1 mM nonessential amino acids, 100 units/mL penicillin and 100 g/mL streptomycin at 37 ˚C in a humidified incubator under 5% CO_2.

Sulforhodamine B assay

Cells were plated in 96-well plates (2000cell/well in 150 μL) and grown for 24 h at 37 ˚C prior to treatment with different concentrations of sensitizers and negative control (0.25-0.0005 μM for sensitizers 1, 2 and 3; 5.0-0.06 μM for BODIPYs dissolved in DMSO). After 72 h of incubation, the medium was aspirated, washed once with 1X PBS (Gibco, Invitrogen), followed by addition of 50 μL of a cold (4

˚C) solution of 10% (v/v) trichloroacetic acid (MERCK) for fixation. Then plates were washed five times with dd-H_2O and were left to air-dry. 50 µL of a 0.4% (m/v) of sulforhodamine (Sigma–Aldrich) in 1% acetic acid solution were then added to each well and left at room temperature for 10 min. The sulforhodamine B (SRB) solution was removed and the plates were washed five times with 1% acetic acid and left for air-drying. Protein Bound sulforhodamine B was solubilized in a 200 µL 10 mM Tris-base solution and the plates were shaken for 10 min on a plate shaker before the measurement of absorbance. The absorbance was read in a 96-well plate reader at 515 nm. Cells incubated in DMSO alone were used as controls for percent inhibition and IC_{50} calculations either in irradiated plate (for 4 h) or the plate kept in dark. Percent inhibition (%) values were calculated with the given formula: (1-(average (OD of treated wells)/ average (OD of DMSO treated cells)) X 100).

Detection of Apoptosis

Cells were seeded onto coverslips in 6-well plates. After 24 hours in culture, cells were treated with sensitizer **1** (20 nM/well). One group was irradiated with red LED at 625 nm for 4 hours and kept 20 hours in dark. Another group was incubated in dark for 24 hours. Apoptosis was determined with Annexin-V-Fluos (Roche) staining together with Hoechst-33258 (Sigma-Aldrich) counterstaining that shows the nuclear condensation. Cells were washed twice with ice-cold 1X PBS. Hoechts-33258 staining was performed by 1 µg/ml (final concentration) in each well followed by incubation for 10 minutes in dark. Cells were destained with 1X PBS for 5 minutes. Then Annexin-V-Fluos staining was carried out according to the manufacturer's recommendations (Roche). Slides were then analyzed under the fluorescence microscope (Nikon Eclipse 50i).

5.5.4 Synthesis

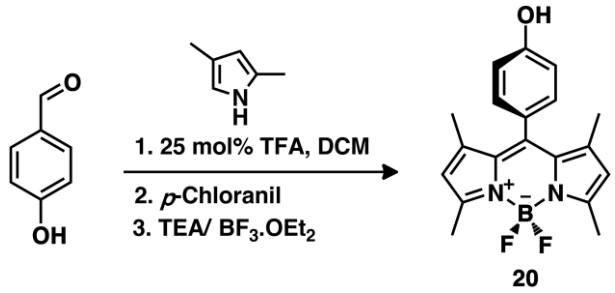

20

Synthesis of Compound 20: Two drops of trifluoroacetic acid was added to the solution of 4-hydroxy benzaldehyde (0.75 g, 6.0 mmol) and 2,4-dimethylpyrrole (1.17 g, 12.3 mmol) in 300 mL Ar-deaerrated dichloromethane (DCM). The reaction mixture was stirred at room temperature for 1 day. The stirring continued for further 2 hours after the addition of *p*-chloranil (0.77 g, 6.0 mmol) in one portion. Triethyl amine (5 mL) was added dropwise to the reaction mixture which was allowed to stir 30 min at room temperature. $BF_3.OEt_2$ (5 mL) was added dropwise to the reaction mixture which was allowed to stir at room temperature for 30 min. The resulting solution was extracted with water (3x100 mL) and combined organic phases were dried over anhydrous Na_2SO_4. After removal of the solvent, the residue was purified by silica gel flash column chromatography using DCM as the eluent. Compound **20** was obtained as orange-Red solid (0.65 g, 32%).

^{1}H NMR (400 MHz, $CDCl_3$): δ_H 7.14 (d, *J*= 8.6 Hz, 2H), 6.96 (d, *J*= 8.6 Hz, 2H), 5.99 (s, 2H), 2.57 (s, 6H), 1.46 (s, 6H).

^{13}C NMR (100 MHz, $CDCl_3$): δ_C 156.3, 155.3, 143.1, 132.0, 131.6, 129.3, 127.1, 121.1, 116.1, 14.5.

MS (TOF-ESI): m/z: Calcd.for $C_{19}H_{19}BF_2N_2O$: 338.1558 $[M-H]^-$, Found: 338.1493 $[M-H]^-$, Δ= 8.71ppm.

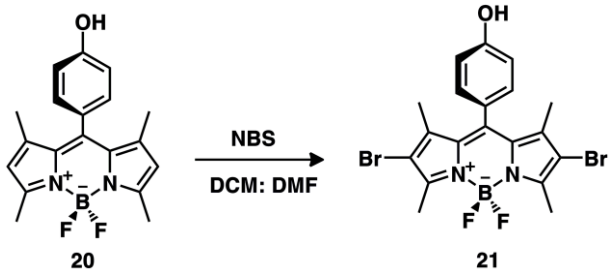

Synthesis of Compound 21: Compound **20** (0.060 g, 0.176 mmol) was dissolved in 20 mL mixture (DMF/DCM, 1:1, v/v). Then, *N*-Bromosuccinimide (0.066 g, 0.37 mmol) dissolved in DCM (10 mL) was added dropwise to reaction mixture at room temperature. The progress of the reaction was monitored by TLC. When TLC showed no starting material, the reaction was extracted with water (3x100 mL) and combined organic phases were dried over anhydrous Na_2SO_4. After removal of the solvent, the residue was purified by silica gel flash column chromatography using Acetone/ Hexane (1:4, v/v) as the eluent. Compound **21** was obtained as red solid (0.084 g, 95%).

^{1}H NMR (400 MHz, $CDCl_3$): δ_H 7.13 (d, *J* = 8.7 Hz, 2H), 7.00 (d, *J* = 8.6 Hz, 2H), 5.18 (s, H, OH), 2.62 (s, 6H), 1.47 (s, 6H).

^{13}C NMR (100 MHz, $CDCl_3$): δ_C 157.3, 152.5, 139.9, 130.0 128.1, 124.1, 115.3, 110.6 12.8, 12.5.

MS (TOF- ESI): m/z: Calcd for $C_{19}H_{17}BBr_2F_2N_2O$: 493.9769 $[M-H]^-$, Found: 493.9713 $[M-H]^-$, Δ=3.87 ppm.

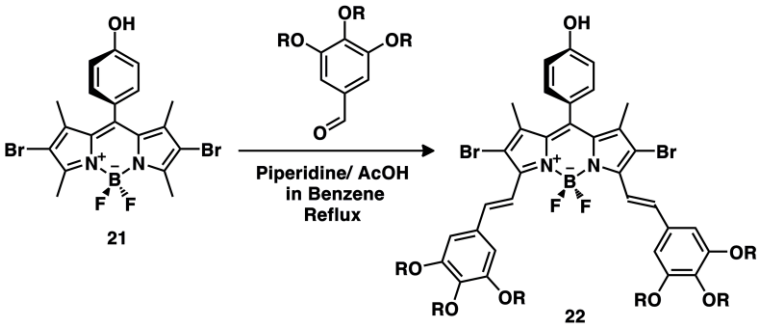

Synthesis of Compound 22: 3,4,5-tris(2-(2-(2-methoxyethoxy)ethoxy)benzaldehyde (0.233 g, 0.393 mmol) was added to a solution of compound **21** (0.093 g, 0.187 mmol) in 25 mL of benzene containing piperidine (0.2 mL) and acetic acid (0.2 mL). Mixture was refluxed until all the starting material was consumed and the progress of the reaction was monitored by TLC using DCM:MeOH (95:5) as the eluent. At the end of the reaction, crude product was concentrated and subjected to silica gel FCC using DCM:MeOH (95:5) as the eluent. Compound **22** was obtained as a green waxy solid (0.130 g, 42%).

^{1}H NMR (400 MHz, $CDCl_3$): δ_H 7.80 (d, *J* = 16.5 Hz, 2H), 7.35 (d, *J* = 16.5 Hz, 2H), 6.99 (d, *J* = 8.3 Hz, 2H), 6.84 (d, *J* = 8.3 Hz, 2H), 6.74 (s, 4H), 4.12 (t, *J* = 4.9 Hz, 12H), 3.78 (t, *J* = 4.9 Hz, 8H), 3.73 (t, *J* = 5.0 Hz ,4H), 3.64 – 3.67 (m, 12H), 3.53 – 3.60 (m, 24H), 3.42-3.49 (m, 12H), 3.30 (s, 6H), 3.26 (s, 12H), 1.31 (s, 6H).

^{13}C NMR (100 MHz, $CDCl_3$): δ_C 157.8, 152.8, 147.7, 141.2, 140.5, 140.0, 138.5, 132.8, 132.4, 129.6, 117.3, 116.4, 110.3, 107.5, 72.5, 71.9, 71.8, 70.7, 70.6, 70.5, 69.7, 69.0, 14.0.

MS (TOF- ESI): m/z: Calcd for $C_{75}H_{109}BBr_2F_2N_2O_{25}$: 1642.5747 $[M-H]^-$, Found: 1642.5585 $[M-H]^-$, Δ=9.86 ppm.

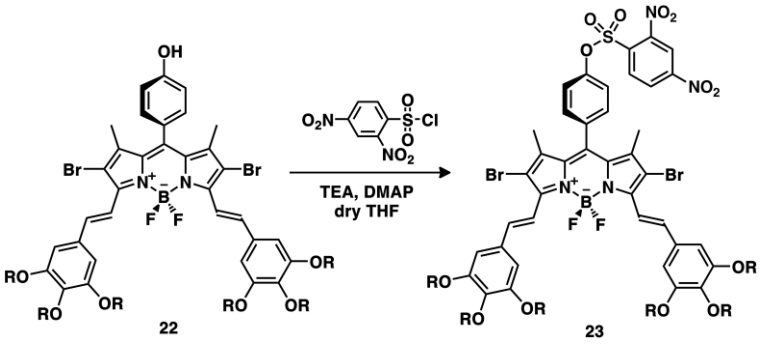

Synthesis of Compound 23: Dry triethyl amine (0.1 mL, 0.72 mmol) was added to a solution of compound **22** (0.40 g, 0.24 mmol) dissolved in dry THF (30 mL) and the reaction mixture was stirred at room temperature for 30min. 2, 4-dinitrobenzenesulfonyl chloride (0.160 g, 0.6 mmol) dissolved in dry THF (5 mL) was added dropwise to reaction mixture containing catalytic amount of DMAP at 0

°C and when it reached the room temperature, the mixture was stirred at room temperature overnight. The progress of the reaction was monitored by TLC (DCM/ MeOH, 95:5, v/v). When the starting material was consumed, crude product was concentrated and subjected to silica gel F.C.C. using (DCM/ MeOH, 95:5, v/v) as the eluent. Compound **23** was obtained as a green waxy solid (0.274 g, 60%).

^{1}H NMR (400 MHz, $CDCl_3$): δ_H 8.71 (d, *J*= 2.1 Hz, 1H), 8.57 (dd, *J* = 8.6, 2.2 Hz, 1H), 8.26 (d, *J* = 8.6 Hz, 1H), 7.98 (d, *J* = 16.5 Hz, 2H), 7.50-7.38 (m, 6H), 6.86 (s, 4H), 4.21 (m, 12H), 3.87 – 3.80 (m, 12H), 3.75 – 3.72 (m, 12H), 3.66 – 3.61 (m, 25H), 3.57 – 3.51 (m, 12H), 3.39 (s, 5H), 3.36 (s, 12H), 1.38 (s, 6H).

^{13}C NMR (100 MHz, $CDCl_3$): δ_C 152.9, 151.2, 149.5, 148.9, 140.5, 140.1, 136.6, 135.0, 133.8, 133.3, 132.1, 131.9, 130.7, 126.4, 123.3, 120.5, 116.9, 107.8, 72.5, 71.9, 71.9, 70.8, 70.7, 70.7, 70.6, 70.5, 70.5, 69.7, 69.1, 59.0, 58.9, 14.0.

MS (TOF- ESI): m/z: Calcd for $C_{81}H_{111}BBr_2F_2N_4O_{31}S$: 1872.53444 $[M-H]^-$, Found: 1872.54811 $[M-H]^-$, Δ=-7.3 ppm.

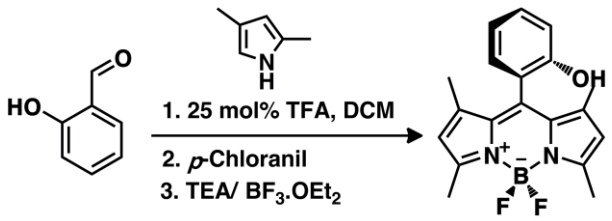

24

Synthesis of Compound 24: Two drops of trifluoroacetic acid was added to the solution of 2-hydroxy benzaldehyde (0.75 g, 6.0 mmol) and 2,4-dimethylpyrrole (1.17 g, 12.3 mmol) in 300 mL Ar-deaerrated dichloromethane (DCM). The reaction mixture was stirred at room temperature for 1 day. The stirring continued for further 2 hours after the addition of *p*-chloranil (0.77 g, 6.0 mmol) in one portion. Triethyl amine (5 mL) was added dropwise to the reaction mixture which was allowed to stir 30 min at room temperature. $BF_3.OEt_2$ (5 mL) was added dropwise to the reaction mixture which was allowed to stir at room temperature for 30 min. The resulting

solution was extracted with water (3x100 mL) and combined organic phases were dried over anhydrous Na_2SO_4. After removal of the solvent, the residue was purified by silica gel flash column chromatography using DCM as the eluent. Compound **24** was obtained as orange-red solid (0.51 g, 25%).

^{1}H NMR (400 MHz, $CDCl_3$): δ_H 7.40 (t, *J*= 7.5 Hz, 1H), 7.14 (d, *J*= 7.4 Hz, 1H), 7.08 (t, *J*= 7.4 Hz, 1H), 7.04 (d, *J*= 8.2 Hz, 1H), 6.02 (s, 2H), 2.58 (s, 6H), 1.53 (s, 6H).

^{13}C NMR (100 MHz, $CDCl_3$) δ 156.4, 152.2, 143.2, 135.0, 131.1, 129.1, 121.7, 121.6, 120.8, 14.6, 13.7.

MS (TOF- ESI): m/z: Calcd for $C_{19}H_{19}BF_2N_2O$: 338.1558 $[M-H]^-$, Found: 338.1523 $[M-H]^-$, Δ=0.1 ppm.

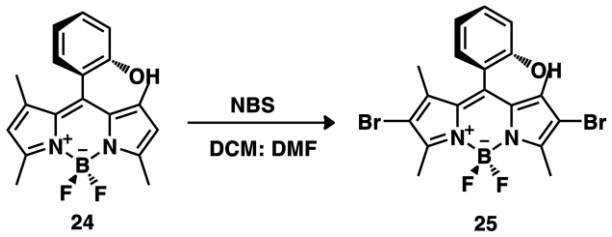

Synthesis of Compound 25: Compound **24** (0.060 g, 0.176 mmol) was dissolved in 20 mL mixture (DMF/DCM, 1:1, v/v). Then, *N*-Bromosuccinimide (0.066 g, 0.37 mmol) dissolved in DCM (10 mL) was added dropwise to reaction mixture at room temperature. The progress of the reaction was monitored by TLC. When TLC showed no starting material, the reaction was extracted with water (3x100 mL) and combined organic phases were dried over anhydrous Na_2SO_4. After removal of the solvent, the residue was purified by silica gel flash column chromatography using EtOAc/ Hexane (1:6, v/v) as the eluent. Compound **25** was obtained as red solid was obtained (0.031 g, 35%).

^{1}H NMR (400 MHz, $CDCl_3$): δ_H 7.45 (m, 1H), 7.11 (d, *J*= 4.3 Hz, 2H), 7.04 (d, *J*= 8.3 Hz, 1H), 4.96 (s, 1H, OH), 2.63 (s, 6H), 1.53 (s, 6H).

^{13}C NMR (100 MHz, $CDCl_3$): δ_C 131.6, 129.0, 122.0, 120.6, 116.8, 13.7, 13.0.

MS (TOF- ESI): m/z: Calcd for $C_{19}H_{17}BBr_2F_2N_2O$: 493.9769 $[M-H]^-$, Found: 493.9772 $[M-H]^-$, Δ=5.47 ppm.

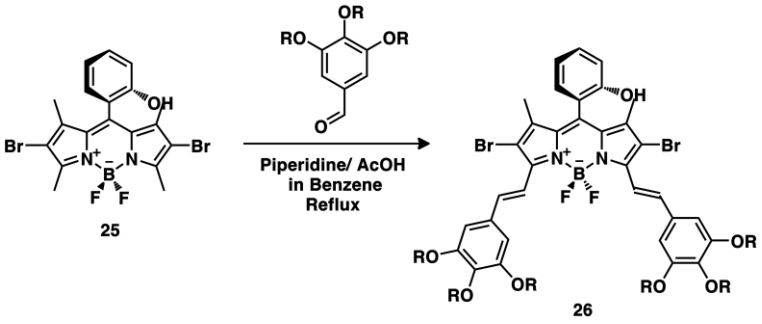

Synthesis of Compound 26: 3,4,5-tris(2-(2-(2-methoxyethoxy)ethoxy)benzaldehyde (0.240 g, 0.405 mmo) was added to a solution of compound **25** (0.096 g, 0.193 mmol) in 25 mL of benzene containing piperidine (0.2 mL) and acetateic acid (0.2 mL). Mixture was refluxed until all the starting material was consumed and the progress of the reaction was monitored by TLC using DCM:MeOH (95:5) as the eluent. At the end of the reaction, crude product was concentrated and subjected to silica gel FCC using DCM:MeOH (95:5) as the eluent. Compound **26** was obtained as a green waxy solid (0.134 g, 41%).

^{1}H NMR (400 MHz, $CDCl_3$): δ_H 7.95 (d, *J* = 16.5 Hz, 2H), 7.31 (m, 3H), 6.97 (m, 3H), 6.87 (s, 4H), 4.25 (t, *J*= 4.7 Hz, 8H), 4.19 (t, *J*=4.9 Hz, 4H), 3.88 (t, *J*= 4.8 Hz, 8H), 3.80 (t, *J*= 5.0 Hz, 4H), 3.72-3.75 (m, 12H), 3.68 – 3.61 (m, 24H), 3.56-3.51 (m, 12H), 3.38 (s, 6H), 3.35 (s, 12H), 1.26 (s, 6H, CH_3).

^{13}C NMR (100 MHz, $CDCl_3$): δ_C 153.1, 152.7, 148.0, 141.2, 140.2, 139.2, 132.6, 132.0, 132.0, 121.2, 120.8, 120.82, 116.9, 116.6, 110.5, 107.7,107.7, 71.9, 70.8, 70.6, 70.5, 70.3, 69.7, 69.0, 98.0,58.9, 12.8.

MS (TOF- ESI): m/z: Calcd for $C_{75}H_{109}BBr_2F_2N_2O_{25}$: 1642.5747 $[M-H]^-$, Found: 1642.5604 $[M-H]^-$, Δ=8.72 ppm.

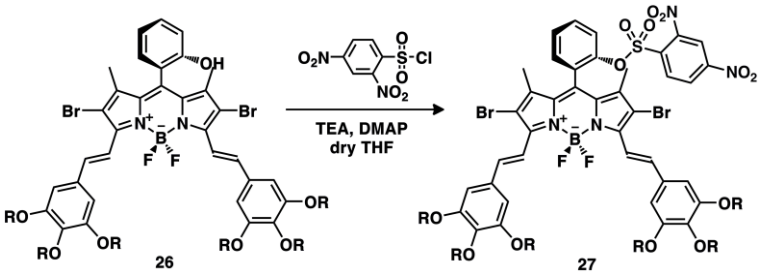

Synthesis of Compound 27: Dry triethyl amine (0.072 mL, 0.52 mmol) was added to a solution of compound **26** (0.230 g, 0.14 mmol) dissolved in dry THF (30 mL) and the reaction mixture was stirred at room temperature for 30min. 2, 4-dinitrobenzenesulfonyl chloride (0.093 g, 0.35 mmol) dissolved in dry THF (5 mL) was added dropwise to reaction mixture containing catalytic amount of DMAP at 0 $^{\circ}$C and when it reached the room temperature, the mixture was stirred at room temperature overnight. The progress of the reaction was monitored by TLC (DCM/ MeOH, 95:5, v/v). When the starting material was consumed, crude product was concentrated and subjected to silica gel FCC using (DCM/ MeOH, 95:5, v/v) as the eluent. Compound **27** was obtained as a green waxy solid (0.130 g, 35%).

^{1}H NMR (400 MHz, $CDCl_3$): δ_H 8.60 (s, 1H), 8.34- 8.24 (m, 1H), 7.95 (d, *J*= 16.2 Hz, 2H), 7.79- 7.65 (m, 2H), 7.55 (t, *J*= 7.5 Hz, 1H), 7.44 (d, *J*= 16.3 Hz, 1H), 7.35 (d, *J*= 7.5 Hz, 1H), 7.25 (d, *J*= 17.4 Hz, 2H), 6.85 (s, 4H), 4.26-4.22 (m, 12H), 3.90-3.86 (m, 8H), 3.85-3.82 (m, 4H), 3.75 (m, 12H), 3.67- 3.63 (m, 24H), 3.57- 3.53 (m, 12H), 3.39 (s, 6H), 3.36 (s, 12H), 1.5 (s, 6H).

^{13}C NMR (100 MHz, $CDCl_3$): δ_C 152.9, 152.89, 152.88, 150.2, 149.0, 147.7, 147.5, 141.0, 140.6, 134.3, 132.1, 131.9, 130.9, 128.6, 127.2, 126.0, 125.3, 121.5, 107.8, 72.54, 72.51, 71.96, 71.93, 70.8, 70.69, 70.68, 70.59, 70.54, 70.53, 69.7, 69.1, 69.0, 59.0, 58.9, 13.7, 13.5.

MS (TOF- ESI): m/z: Calcd for $C_{81}H_{111}BBr_2F_2N_4O_{31}S$: 1872.53444 $[M-H]^-$, Found: 1872.55020 $[M-H]^-$, Δ=-8.42 ppm.

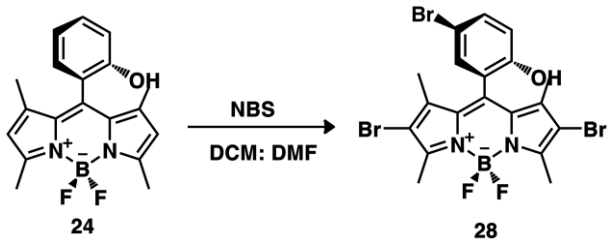

24 28

Synthesis of Compound 28: Compound 2**4** (0.060 g, 0.176 mmol) was dissolved in 20 mL mixture (DMF/DCM, 1:1, v/v). Then, *N*-Bromosuccinimide (0.066 g, 0.37 mmo) dissolved in DCM (10 mL) was added dropwise to reaction mixture at room temperature. The progress of the reaction was monitored by TLC. When TLC showed no starting material, the reaction was extracted with water (3x100 mL) and combined organic phases were dried over anhydrous Na_2SO_4. After removal of the solvent, the residue was purified by silica gel flash column chromatography using Acetone/ Hexane (1:4, v/v) as the eluent. Compound **28** was obtained as red solid was obtained (0.079 g, 90%).

^{1}H NMR (400 MHz, $CDCl_3$): δ_H 7.54 (dd, *J*= 8.7, 2.4 Hz, 1H), 7.26 (m, 1H), 6.95 (d, *J*= 8.7 Hz, 1H), 5.68 (s, 1H, OH), 2.53 (s, 6H), 1.59 (s, 6H).

^{13}C NMR (100 MHz, $CDCl_3$): δ_C 155.0, 151.7, 140.4, 134.4, 131.5, 130.2, 122.5, 118.7, 113.5, 112.2, 13.6, 13.2.

MS (TOF- ESI): m/z: Calcd for $C_{19}H_{16}BBr_3F_2N_2O$: 572.8874 $[M-H]^-$, Found: 572.8837 $[M-H]^-$, Δ=6.45 ppm.

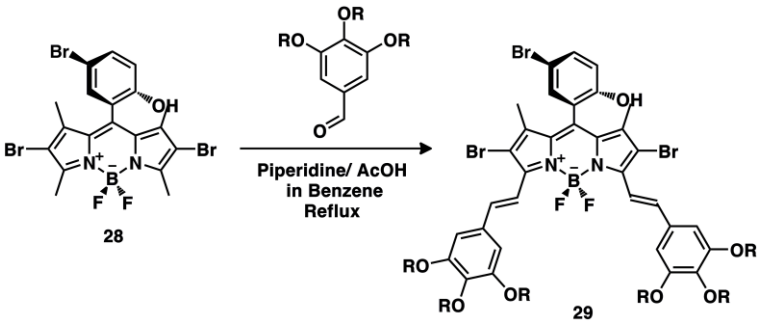

28 29

Synthesis of Compound 29: 3,4,5-tris(2-(2-(2-methoxyethoxy)ethoxy)benzaldehyde (0.433 g, 0.731 mmol) was added to a solution of compound **28** (0.20 g, 0.348 mmol)

in 25 mL of benzene containing piperidine (0.2 mL) and acetateic acid (0.2 mL). Mixture was refluxed until all the starting material was consumed and the progress of the reaction was monitored by TLC using DCM:MeOH (95:5) as the eluent. At the end of the reaction, crude product was concentrated and subjected to silica gel FCC using DCM:MeOH (95:5) as the eluent. Compound **29** was obtained as a green waxy solid (0.240 g, 40%).

^{1}H NMR (400 MHz, $CDCl_3$): δ_H 7.97 (d, *J*= 16.5 Hz, 2H), 7.45 (dd, *J*= 8.8, 2.5 Hz), 7.29 (d, *J*= 17.0 Hz, 2H), 7.12 (s, 1H), 6.95 (d, *J*= 8.8 Hz, 1H), 6.88 (s, 4H), 4.25 (m, 8H), 4.20 (t, *J*=4.52 Hz, 4H), 3.88 (t, *J*= 4.82 Hz, 8H), 3.80 (m, 4H), 3.73 (m, 12H), 3.69 – 3.62 (m, 24H), 3.57 – 3.51 (m, 12H), 3.38 (s, 6H), 3.34 (s, 12H), 1.28 (s, 6H).

^{13}C NMR (100 MHz, $CDCl_3$): δ_C 152.7 , 152.5 , 148.2 , 141.0 , 140.3 , 139.5 , 134.3 , 132.4 , 131.9 , 131.5 , 122.8 , 118.9 , 116.4 , 112.7 , 110.7 , 107.9, 72.4 , 71.9 , 70.8 , 70.6 , 70.53, 70.51, 69.7 , 69.0 , 58.99, 58.97, 13.1.

MS (TOF- ESI): m/z: Calcd for $C_{75}H_{108}BBr_3F_2N_2O_{25}$: 1720.4852 $[M-H]^-$, Found: 1720.4714 $[M-H]^-$, Δ=8.02 ppm.

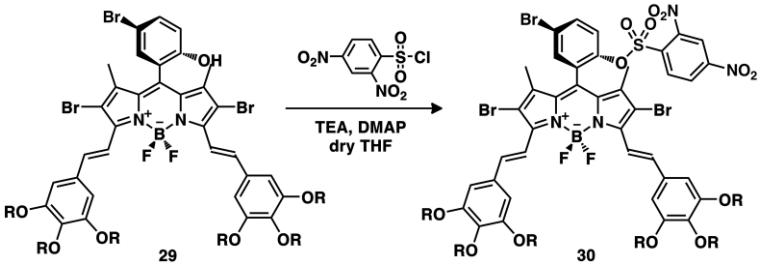

Synthesis of Compound 30: Dry triethylamine (0.72 mmol, 0.1 mL) was added to a solution of bodipy **29** (0.40 g, 0.24 mmol) dissolved in dry THF (30 mL) and the reaction mixture was stirred at room temperature for 30min. 2, 4-dinitrobenzenesulfonyl chloride (0.160 g, 0.6 mmol) dissolved in dry THF (5 mL) was added dropwise to reaction mixture containing catalytic amount of DMAP at 0 °C and when it reached the room temperature, the mixture was stirred at 40 °C for overnight. The progress of the reaction was monitored by TLC (DCM/ MeOH, 95:5,

v/v). When the starting material was consumed, crude product was concentrated and subjected to silica gel FCC using DCM/ MeOH (95:5, v/v) as the eluent. Compound **30** was obtained as a green waxy solid (0.274 g, 60%).

^{1}H NMR (400 MHz, $CDCl_3$): δ_H 8.61 (s, 1H), 8.26 (dd, *J*= 8.7, 2.2 Hz, 1H), 7.96 (d, *J*= 16.4 Hz, 2H), 7.83 (dd, *J*= 8.8, 2.5 Hz, 1H), 7.78 (d, *J*= 8.5 Hz, 1H), 7.55 – 7.51 (m, 2H), 7.24 (d, *J*= 16.4 Hz, 2H), 6.85 (s, 4H), 4.27 – 4.22 (m, 12H), 3.89 (t, *J*=4.88 Hz, 8H), 3.84 (t, *J*= 5.01 Hz, 4H), 3.76 – 3.73 (m, 12H), 3.69 – 3.62 (m, 24H), 3.58-3.52 (m, 12H), 3.39 (s, 6H), 3.36 (s, 12H), 1.57 (s, 6H).

^{13}C NMR (100 MHz, $CDCl_3$): δ_C 152.9, 150.3, 149.3, 147.3, 146.5, 141.3, 140.8, 134.0, 133.7, 131.8, 130.9, 129.2, 126.8, 116.2, 107.9, 72.5, 71.9, 70.8, 70.6, 70.59, 70.55, 69.7, 69.1, 59.0, 58.9, 13.8.

MS (TOF- ESI): m/z: Calcd for $C_{81}H_{110}BBr_3F_2N_4O_{31}S$: 1951.45223 $[M]^-$, Found: 1951.46175 $[M]^-$, Δ=-4.89 ppm.

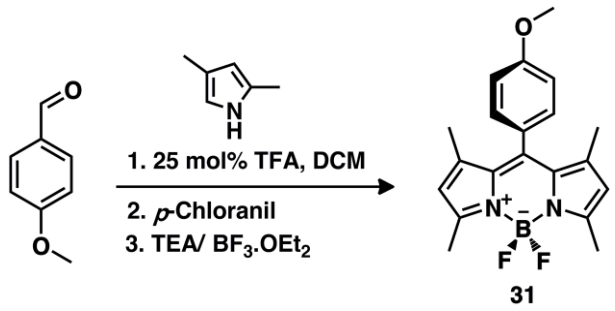

31

Synthesis of Compound 31: Two drops of trifluoroacetic acid was added to the solution of 4-methoxy benzaldehyde (1.0 g, 7.3 mmol) and 2,4-dimethylpyrrole (1.54 g, 16.1 mmol) in 300 mL Ar-deaerrated dichloromethane (DCM). The reaction mixture was stirred at room temperature for overnight. The stirring continued for further 2 hours after the addition of *p*-Chloranil (1.8 g, 7.3 mmol) in one portion. Triethyl amine (5 mL) was added dropwise to the reaction mixture which was allowed to stir 30 min at room temperature. $BF_3.OEt_2$ (5 mL) was added dropwise to the reaction mixture which was allowed to stir at room temperature for 30 min. The

resulting solution was extracted with water (3x100 mL) and combined organic phases were dried over anhydrous Na_2SO_4. After removal of the solvent, the residue was purified by silica gel flash column chromatography using DCM: Hexane (1:1, v/v) as the eluent. Compound **31** was obtained as orange-red solid (0.85 g, 33%).

^{1}H NMR (400 MHz, $CDCl_3$): δ_H 7.20 (d, *J*= 8.5 Hz, 2H), 7.03 (d, *J*= 8.5 Hz, 2H), 6.00 (s, 2H), 3.90 (s, 3H), 2.57 (s, 6H), 1.45 (s, 6H).

^{13}C NMR (100 MHz, $CDCl_3$): δ_C 160.1, 129.2, 127.9, 123.1, 121.1, 116.5, 114.5, 57.0, 55.3, 29.6, 14.5.

MS (TOF- ESI): m/z: Calcd for $C_{20}H_{21}BF_2N_2O$: $[M-H]^-$: 352.16786, Found: $[M-H]^-$: 352.16578, Δ=5.89 ppm.

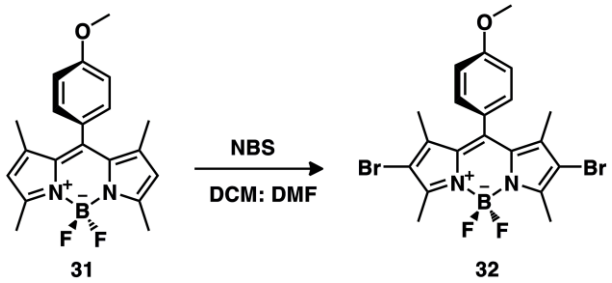

31 32

Synthesis of Compound 32: Compound **31** (0.087 g, 0.246 mmol) was dissolved in 20 mL mixture (DMF/DCM, 1:1, v/v). Then, *N*-Bromosuccinimide (0.105 g, 0.59 mmol) dissolved in DCM (10 mL) was added dropwise to reaction mixture at room temperature. The progress of the reaction was monitored by TLC. When TLC showed no starting material, the reaction was extracted with water (3x100 mL) and combined organic phases were dried over anhydrous Na_2SO_4. After removal of the solvent, the residue was purified by silica gel flash column chromatography using DCM/ Hexane (1:1, v/v) as the eluent. Compound **32** was obtained as red solid (0.0122 g, 97%).

^{1}H NMR (400 MHz, $CDCl_3$): δ_H 7.17 (d, *J* = 8.4 Hz, 2H), 7.05 (d, *J* = 8.4 Hz, 2H), 3.92 (s, 3H), 2.62 (s, 6H), 1.45 (s, 6H).

^{13}C NMR (100 MHz, $CDCl_3$): δ_C 160.5, 153.7, 140.6, 129.1, 126.3, 114.8, 55.3, 13.8, 13.6.

MS (TOF- ESI): m/z: Calcd for $C_{20}H_{19}BBr_2F_2N_2O$: $[M-H]^-$: 507.98888 , Found: $[M-H]^-$: 507.98641, Δ= 4.86 ppm.

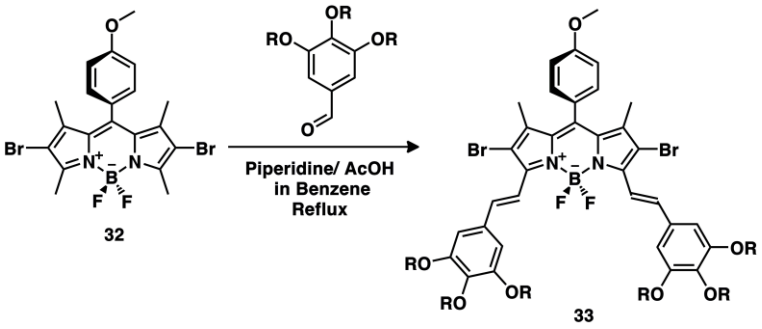

32 33

Synthesis of Compound 33: 3,4,5-tris(2-(2-(2-methoxyethoxy)ethoxy)benzaldehyde (0.364 g, 0.711 mmol) was added to a solution of compound **32** (0.125 g, 0.244 mmol) in 25 mL of benzene containing piperidine (0.2mL) and acetateic acid (0.2mL). Mixture was refluxed until all the starting material was consumed and the progress of the reaction was monitored by TLC using DCM:MeOH (95:5) as the eluent. At the end of the reaction, crude product was concentrated and subjected to silica gel F.C.C. using DCM:MeOH (95:5) as the eluent. Compound **33** was obtained as a green waxy solid (0.273 g, 67%).

^{1}H NMR (400 MHz, $CDCl_3$): δ_H 7.96 (d, *J*= 16.5 Hz, 2H), 7.50 (d, *J*= 16.5 Hz, 2H), 7.20 (d, *J*= 8.7 Hz, 2H), 7.07 (d, *J*= 8.7 Hz, 2H), 6.87 (s, 4H), 4.24-4.19 (m, 12H), 3.92 (s, 3H), 3.88 (t, *J*= 4.8 Hz, 8H), 3.80 (m, 4H), 3.73 (m, 12H), 3.69 – 3.62 (m, 24H), 3.57 – 3.51 (m, 12H), 3.39 (s, 6H), 3.37 (s, 12H), 1.50 (s, 6H).

^{13}C NMR (100 MHz, $CDCl_3$): δ_C 165.1, 160.6, 154.1, 152.8 , 149.8, 143.9, 141.2, 141.0 , 140.2 , 139.8 , 139.3, 136.9, 132.6 , 132.3 , 129.5 , 126.7 , 117.6 , 117.2 , 115.8, 114.8, 112.2, 109.0, 107.7, 71.9 , 70.8 , 70.69 , 70.67, 70.58, 70.54, 69.7 , 69.0 , 58.98, 55.41, 14.0.

MS (TOF- ESI): m/z: Calcd for $C_{76}H_{111}BBr_2F_2N_2O_{25}$: $[M-H]^-$: 1656.58673, Found: $[M-H]^-$: 1656.57938, Δ= 4.44ppm.

CHAPTER 6

6. BACKGROUND 2:

"LET THE LIGHT GLOW THERE"

6.1 Historical Evolution

Science is always fascinated by the magnificence of the nature. Mankind discovers notable ideas by observing it with wide open eyes and the questions are clarified by the whispers of the nature. Hereby, the term "Luminescence" takes part in the literature of the science.

Luminescence can be defined as the emission of light which occurs while an excited state molecule relaxes back to the ground state.[84] Historical evolution of the luminescence phenomena have grounded on Antiquity with the recognition of cold light in dead fish, fungi, luminous secretion of cuttle fish, luminous animals and insects, phosphorescent wood, etc. by Aristotle (384-322 B.C.). Radizeswki was the first one who reports the light emission produced in a synthetic way in 1877. He reported the luminescent compound lopine (2,4,5-triphenylimidazole) which emits green light upon reaction with a strong base in the presence of oxygen.[85] However, the term chemiluminescence was introduced to the luminescence literature first by Eilhardt Wiedemann in 1888 in order to distinguish the light emitted from thermal excitation of substances from the light emitted by molecules which are excited by other mechanisms without increasing their average kinetic energy. He characterized the luminescence as cold light after stating that phosphorescence and fluorescence means that the compounds emitting light without the need for heating.[9] Since then, luminescence was categorized into different classes based on the way of excitation

which can be listed as photoluminescence: caused by absorption of light, thermoluminescence: obtained by slight heating, electroluminescence: caused by electric field, crystalloluminescence: observed as a result of crystallization, triboluminescence: caused by friction and chemiluminescence: observed as a result of a chemical reaction.[3]

In this sense, chemiluminescence (CL) can be defined as the generation of electromagnetic radiation (UV, Vis or infrared) as a result of a chemical reaction producing electronically excited product which can either luminescence or donate its energy to another molecule luminescing later.[86]

6.2 General Principles

Chemiluminescence is based on the energy obtained by both the breaking and forming bonds during the chemical reaction. By considering the definition, two results can be inferred. Firstly, for a reaction to be chemiluminescent, one of the products must be fluorescent. Additionally, chemical reaction resulting in the formation of the emissive product must have sufficient energy for the formation of excited state. The transition of an electron from ground state to its excited state is generally in conjunction with both vibrational and rotational changes in the molecule. Additionally, the excited molecule can loss its energy through radiationless processes like chemical reactions, collisional deactivation, internal conversion or inter-system crossing that are undesirable since they are in competence with the chemiluminescence resulting in the decrease or loss of emission as in the case of other photophysical processes like fluorescence and phosphorescence.[84] Except for the excitation process, CL, FL and P returns to ground state (S_0) from the lowest singlet excited state (S_1) or from triplet excited state (T_1).

Chemiluminescent reactions are preceded over two different mechanisms which are direct and indirect (or sensitized) chemiluminescence. In a ***direct chemiluminescence*** (figure 57A), substrate and oxidant are reacted to form a

product or intermediate in electronically excited state which relaxes back to ground state with emission of light. In this type of chemiluminescence, the substrate is the CL precursor which can be converted into excited molecule responsible for light emission. The oxidant is generally the reagent of interest which has ability to initiate CL reaction. In direct reaction, catalyst, enzyme or metal ion can also be used to enhance CL efficiency output by reducing activation energy of the reaction. Additionally, cofactors can be applied to convert one or more of the substrates into a form which is capable of reacting or interacting with the catalyst, or to provide an efficient leaving group if bond cleavage is required to produce the excited emitter.[85] On the other hand, in the case of ***indirect or sensitized reaction*** (figure 57B), since the electronically excited product or intermediate does not have fluorescence, emission of light can be observed as a result of transfer of energy of the excited species to a fluorophore. When the energy is absorbed by the fluorophore, it is excited to an electronically energetic state, relaxing back to ground state results in the emission of photon.[86]

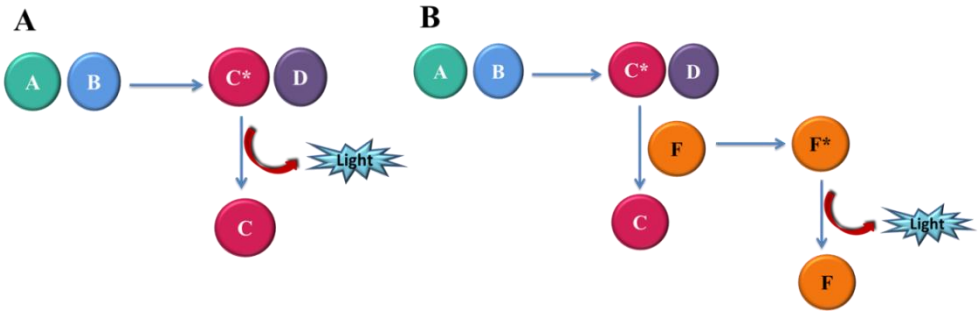

Figure 57: Schematic representation of direct and indirect CL. (*) indicates excited product

There are some critical requirements for a chemical reaction to emit light that can be listed as below:

The reaction must be exothermic to generate energy which is required to form electronically excited state. Generally, emissions from CL reactions fall in the range of 400 nm to 750 nm. Not only generation of electronically excited sates but also CL emission required an exothermic reaction generating 40-70 Kcal.mol^{-1} which is

associated with redox reactions employing either oxygen and hydrogen peroxide or similar oxidants.

The reaction pathway must be favorable so that the energy can be directed for the formation of an electronically excited state. The energy should not be lost via as heat, vibrational or rotational collisions. Otherwise, the reactions cannot be chemiluminescent. In addition, decaying process should be at a convenient rate in order to make the reactions emit photons. The longer the reaction time, the higher the loss of energy thus in turn, the lower the possibility for a reaction to be chemiluminescent.

Deactivation process favoring the photon emission must win the competition with the other nonradiative processes. In the case of sensitized CL, not only the energy transfer efficiency from excited intermediate or product to fluorophore but also the fluorescence efficiency of the dye must be high enough to favor light emission instead of non radiative processes.

Considering all luminescent processes, the intensity of produced emission depends on the efficiency of generating molecules in the excited state represented by quantum yield (Φ_{CL}) which can be defined as the fraction of molecules emitting a photon while returning to the ground state.

$$\Phi_{cl} = \Phi_c \,.\, \Phi_e \,.\, \Phi_f$$

where Φ_c represents the fraction of reacting molecules giving an excitable molecule and accounts for the yield of the chemical reaction; Φ_e represents the fraction of such molecules in an electronically excited state and relates to the efficiency of the energy transfer and Φ_f represents the fraction of these excited molecules that return to the ground state by emitting a photon.[87]

Although chemiluminescence is a strong analytical methodology, its efficiency depends on the several experimental factors such as temperature, pH, ionic strength, solvent, solution composition, concentration of the substrate, chemical structure of

the chemiluminescent precursor which is either the part responsible for electronic excitation or the side chain, nature and concentration of other substrates, the presence of energy transfer acceptors. When CL is used as an analytical technique, the parameters considered to be effective in emission intensity has to be optimized. The effect of these experimental factors has to be considered according to the type of chemiluminogenic precursor.

Chemiluminescence is a superior technique than other luminogenic ones since it offers several advantages. **1.** The light emission generated from a chemical reaction does not require any external light source for excitation which brings about low background signals.[88] **2.** Measurement of emitted light from a chemical reaction is very useful since the light intensity is directly related to the analyte concentration which in turn, enables the sensitive and accurate quantification. **3.** The high detectability of CL is a result of low background which is not affected by either warm-up or drift of light source, detector and by interferences from light scatterings as in the case of absorption and fluorescence methods. **4.** Additionally, emission of light is resulted from a specific reaction which is unique to the analyte of interest thus in turn; background emission, typical of fluorescence due to sample matrix components is avoided. **5.** Moreover, due to having wide dynamic range, samples can be measured over at least 5 decades of concentration depending on the instrument used without either dilution or modification of the sample cell. **6.** Furthermore, light emission occurs in a few seconds which makes the CL and BL very fast.[89] **7.** Other most common cited advantages of CL are the requirement of simple instrumentation, low detection limits due to the low background signal.[90] **8.** CL can be used for the determination of wide variety of species participating in the process like CL substrates, CL precursors, oxidant, species affecting the rate or efficiencies of CL reaction, activators such as catalyst, inhibitors like reductants that inhibit CL emission, fluorophores as in the case of sensitized CL, species which are not directly involved in the reaction however can react with other reagents in coupled reactions to generate a product which is a reactant in CL reaction, species can be modified with some CL precursors or fluorophores being determined by direct or

indirect CL. **9.** CL reactions can be coupled as a detection technique in chromatography, capillary electrophoresis or immunoassays in order to provide either qualitative or quantitative information.[85]

Although CL has several advantages, depending on the several environmental factors makes us to think about the possible disadvantages. For example, light emission is not specific for one unique analyte so, lack of selectivity may occur. Furthermore, since intensity of emission is dependent on the several factors like pH, ionic strength, temperature, solvent, they have to be optimized in order to prevent the fluctuations. Since CL emission is not constant but varying with time and also emission versus time profile can be varied according to the CL system, the signal has to be detected at strictly defined periods by applying strictly optimized environmental factors.[91]

6.3 Main Chemiluminescent Systems

6.3.1 Acyl Hydrazides

Reaction Mechanism: Oxidation of Luminol (5-amino-2,3-dihydro-1,4-phthalazinedione) in alkaline medium is the most famous examples in direct chemiluminescence reaction which was first reported by Albrecht in 1928. Direct CL mechanism of Luminol can be simplified as in figure 58 in which the key intermediate is the formation of α-hydroxyperoxide obtained by the oxidation of heterocyclic ring.

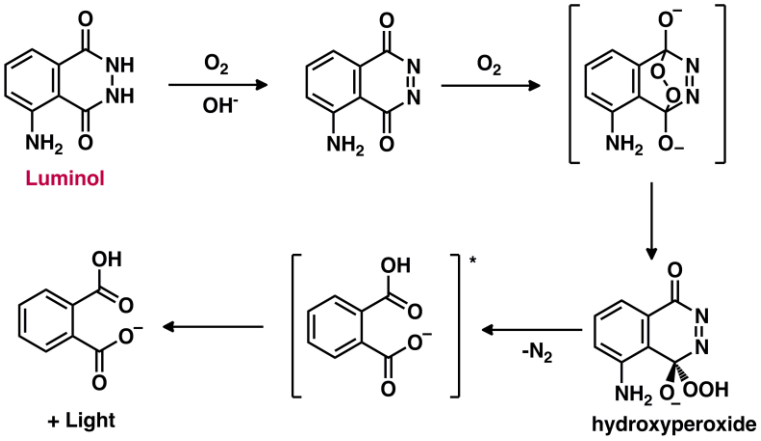

Figure 58: Reaction Mechanism of Luminol. [84]

Direct CL reaction mechanism follows the reaction of Luminol with either oxygen or any other alternative oxidizing agent in alkaline medium which forms an excited state of the α-hydroxyperoxide which yields CL while relaxing back to ground state.[92,93] Light is obtained by oxidation of luminol with an oxidizing agent like potassium ferricyanide in basic aqueous solutions containing oxygen however, enhanced emission is obtained when hydrogen peroxide was applied as an oxidizing agent which cause extensive degradation of the reaction products.[93] When decomposition mechanism is considered, the decomposition pattern and light emission depends on the pH of the system while the first step depends on the composition of medium. The CL in aprotic solvents like dimethylsulfoxide and dimethylformamide is easier and requires oxygen and a strong base. On the other hand, in protic solvents like water (water containing solvent mixtures or lower alcohols), various oxygen derivatives as molecular oxygen, peroxides, superoxide anion can oxidize luminol derivatives through the catalysis of either by enzymes or by minerals.[94]

Luminescent properties: The quantum yield of the luminol will be mostly 5% in DMSO [95] and 1,5% in aqueous solution.[94] The efficiency of the luminol system has been tried to be enhanced by structural modifications of the heterocyclic part

however, this leads to the complete loss of chemiluminescence. On the other hand, modifications in the nonheterocyclic part lead to enhancement of the emission. While electron donating substituents are better, electron withdrawing substituents leads to the loss of chemiluminescence.[95] Other methods used for the chemiluminescence enhancement is the use of enzymes. Although the chemiluminescence efficiency and the light intensity are not modified, more light is emitted after a long time due to the continuous recycling of enzyme.[84] Moreover, the use of carbonate and bicarbonate containing media are better for the determination of low concentration of peroxides. Additionally, the use of chemical enhancers is another way to enhance the emission of the system.

Applications: Luminol and its most commonly used derivative isolumniol has founded diverse applications in immunoassay or non-immunoassay diagnostics, monitoring techniques and biosensors.

Luminol and its derivatives have been reported in literature (figure 59) as chemiluminescent energy transfer cassettes (compound **A** and **B**) [96], chemiluminescent agents for photodynamic therapy (compound **C**)[97] and chemiluminescence based sensors (compound **D**).[98]

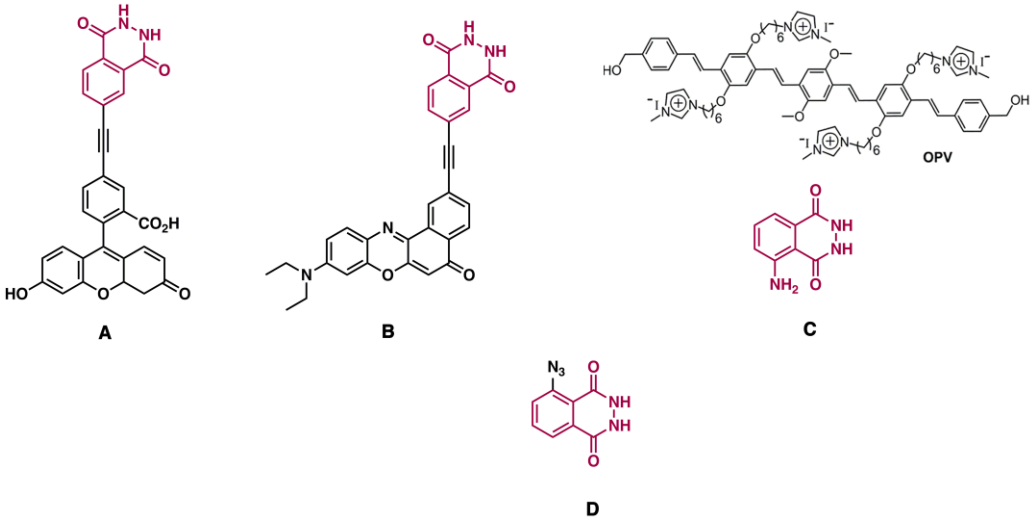

Figure 59: Structures of Luminol Derivatives.

6.3.2 Acridinium Esters

Reaction Mechanism: Another chemiluminescent compound is the Lucigenin (10,10′-dimethyl-9,9′- bisacridinium nitrate) which has an intense green light emission after oxidizing by hydrogen peroxide or oxygen an alkaline medium, was discovered by Gleu and Petsch in 1935.[99] Acridinium esters can produce light upon oxidation with hydrogen peroxide in alkaline medium through a mechanism shown in figure 60 since the acridinium derivatives are in equilibrium with the non chemiluminescent pseudobase obtained by hydroxyl substitution and this equilibrium can be shifted in alkaline medium. Since the half-life for the formation of pseudo base is 26 sec at pH, 8 sec. at pH 11 and 1 sec. at pH 13, chemiluminescence of acridinium esters could be triggered by sequential addition of hydrogen peroxide followed by addition of strong base.[84] There are different catalyst choices for the light emission like Co(II), Fe(II), Fe(III), Cu(II), Cr(III), Ni(II), Pb(II), Bi(III), Tl(III) and Hg(I) which contributes to the generation of more intense emission.[85]

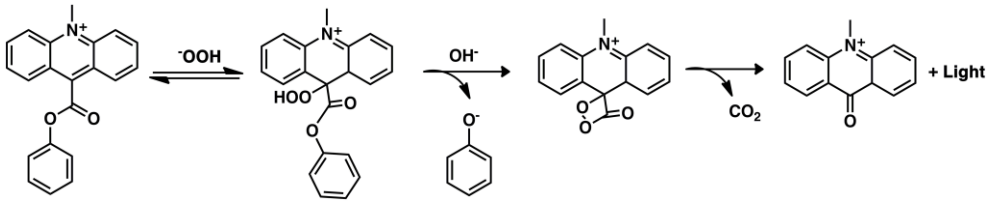

Figure 60: Most probable mechanism responsible for the chemiluminescence of acridinium esters and the alternative routes.[84]

Luminescent properties: Most acridinium derivatives are composed of two parts which are the acridinium heterocycle and leaving group. Each part has significant roles in the chemiluminescence. Acridinium esters emit light as a flash within 5 sec. periods just after the triggering of the chemical reaction due to rapid shift in the equilibrium toward the pseudo base. The rate of emission has been modified by the modifications on the leaving group. When considering phenol series, methylation of

acridinium ring slows the kinetic of light emission; monosubstitution slows the reaction slight however disubstitution slows more. Introduction of electron withdrawing groups into the phenyl ring increases the efficiency of light emission and reaction rate however, introduction of electron donating groups has the opposite effect.[100]

Chemiluminescence efficiency of the system has been developed by using epinephrine in cationic surfactant micelles containing periodate however, the use of enhancers has not been reported.[101] On the other hand, depending on the medium, luminescence efficiency of the system can be enhanced by using surfactants such that Triton X-100 and hexa-decyl trimethyl ammonium chloride which are repoted as the most effective ones.[102]

Applications: Due to the having high quantum yields with lowered background signals, no need for the use of catalysts, ease of coupling to proteins via esters or imidates[103,104], acridinium derivatives becomes best candidates that have been employed for the application in immunoassays of thyroid stimulating hormone (TSH)[105], tumor markers (a-fetoprotein)[106], immunoglobulins and related compounds. Additionally, acridinium compounds can be applied for DNA labeling to do chemiluminogenic DNA probes.[107]

6.3.3 Peroxalate Derivatives

Reaction Mechanism: Another type of chemiluminescent agent which gives glorious emission in the presence of a fluorophore is the oxalic acid derivatives. This type of CL reactions are referred as peroxalate chemistry (PO-CL) due to formation of excited states resulted from the decomposition of cyclic peroxides of oxalic acid derivatives like dioxetanes, dioxetanone, dioxetanediones. The first example of the peroxalate chemistry is the hydrogen peroxide oxidation of oxalic acid derivatives in the presence of a fluorescent compound like 9,10-diphenylanthracene giving a bright,

short lived blue emission which was reported in 1963 by Chandross.[108] CL emission resulting from peroxalates proceed via the sensitized or indirect mechanism so that the energy produced upon oxidation of the CL precursor was transferred to the fluorophore which emits a fluorescence while relaxing back to ground state from the lowest excited singlet state.[9]

The decomposition mechanism resulted from the light emission is suggested to follow a CIEEL (Chemically Initiated Electron Exchange Luminescence) which is explained in Section 2.3.4 in detail. Peroxalate derivatives is oxidized to decompose via a high energy intermediate 1,2-dioxetanedione (figure 61) which donates one electron to the fluorophore forming charge transfer complex. When this electron is transferred back to fluorophore, it was raised to an excited state and responsible for the emission of fluorescence.[86,109] Depending on the type of the fluorophore, the color of emission can be modulated.

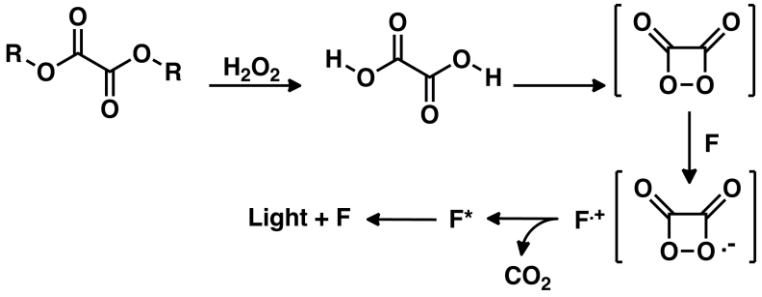

Figure 61: Possible reaction pathway for the PO-CL system.

Luminescent properties: Since PO-CL proceeds through the sensitized CL mechanism, the oxalate derivative and fluorophore can be chosen accordingly either to increase CL quantum yield or fluorescence quantum yield. Besides, they can modulated in a way as to meet the requirements of the assay such as medium (aqueous, non-aqueous), buffer composition and ratio, pH, wavelength of emission and conjugate synthesis.[84]

PO-CL systems gives long lasting emission with CL quantum yields in the range of 22-27% upon oxidation with hydrogen peroxide when the reaction are carried out under optimum conditions. The most popular examples of oxalate derivatives are known as *bis*-(2,4,6-trichlorophenyl)oxalate (TCPO) and *bis*-(2,4-dinitrophenyl) oxalate shown in figure 62. Additionally, the fame oxalate esters are culminated with discovery of the trifluoromethlsulfonyl derivative of the oxamide A whose CL quantum yield is 0.34.[110] Chemiluminescence quantum can be increased linearly with increase in hydrogen peroxide concentration due to the increase in the number of oxidized molecules while the rate of light emission remained constant. Beside this, concentration of oxalate esters is also crucial in a way that increasing the concentration of oxalate esters leads to the decrease in the overall efficiency of the system.

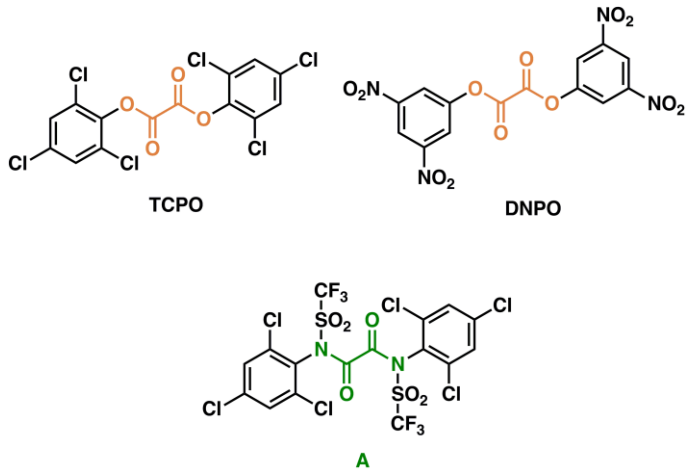

Figure 62: Structures of Peroxalate based Chemiluminogenic Compounds

When considering mechanism of the reaction, chemical structure of the leaving group has considerable effect on the efficiency of PO-CL. Not only high CL quantum yields but also the ease of preparation and the stability towards the hydrolysis makes the oxalic esters derivatives bearing electron withdrawing substituents on leaving groups standard reagents for PO-CL system.[110] Additionally, the presence of electron withdrawing substituents increases the rate of light emission due to the increased stability of leaving groups with extended conjugations.

Although any appreciable light is not reported in acidic medium, the optimum pH is close to neutrality. However, since light emission is generated by upon oxidation with hydrogen peroxide, alkaline conditions are required to activate the system.

Applications: The formation and decomposition of CL intermediates in PO-CL system seems to be responsible for the observed high background emission which can be diminished with the continuous addition of reagents.[84] Another disadvantage of this system is the low solubility of esters in water and high susceptibility to the hydrolysis which bring about the use of organic cosolvents like acetonitrile, dioxane, tert-butanol, ethyl acetate.[86] Additionally, the use of organic cosolvent bring along another parameter such that the type of solvent affects the fluorescence emission of the fluorophore. PO-CL system has been applied for the detection of hydrogen peroxide forming enzymes like uricase, choline oxidase, cholesterol oxidase, xanthine oxidase and glucose oxidase.[84,111]

In the literature, novel multifunctional HPOX micelles are designed to either image hydrogen peroxide or serve as therapeutic agents with potent antioxidant and antiapoptic activity **A**.[112] Additionally, chemiluminescent miscelles were prepared via the self-assembly of amphiphilic PCL-PEG which sequester peroxalate and fluorescent dye in their hydrophobic core that can be used to detect hydrogen peroxide in biological environment **B**.[113,114]

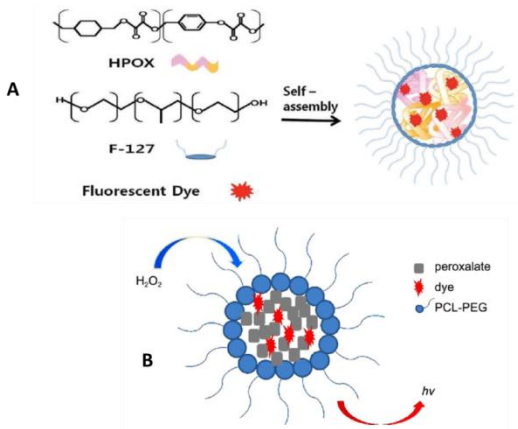

Figure 63: Literature examples for PO-CL system

2.3.4 Dioxetane Derivatives

Reaction Mechanism: When the decomposition mechanisms of previously mentioned chemiluminescent compounds and the bioluminescent compound luciferin/luciferase have been examined, one can realize that the emission is resulted from an energetic 1,2-dioxetanone intermediate. After this, a major breakthrough in chemiluminogenic substances comes with the introduction of four-membered ring peroxides namely 1,2-dioxetanes.

1,2-Dioxetanes bear high strain energy as expected from the comparison of their bond angle ((∠CCO) and dihedral angle (COOC) with those of hydrogen peroxide.[115]

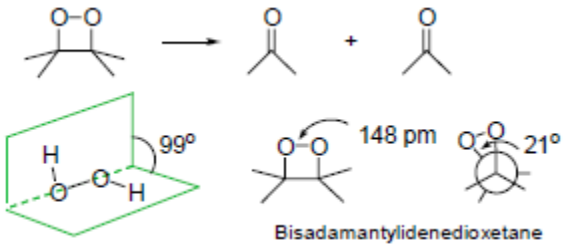

Figure 64: Properties of dioxetane structure[115]

When heated gently, the decomposition reaction is initiated to give two formaldehyde fragments. Some of which is in excited state resulting from the emission of a photon of light while decaying to ground state.[116] The criterion behind the chemiluminescence of dioxetanes comes from the fulfillment of energetic criterion which enables the decomposition of the precursor into an electronically excited product.

The simplest and smallest chemiluminescent precursor is tetramethyldioxetane can be thermally initiated to decompose into two acetone molecules for which the heat of reaction (ΔH^0) and activation enthalpy ($\Delta H^{\ddagger}$) have been determined experimentally as −61 and ca. 25 kcal mol^{-1}, respectively (figure 65). The total of ca. 86 kcal mol^{-1} is enough to produce one of the acetone molecules in its nπ* excited state since the singlet and triplet energies are 84 and 78 kcal mol^{-1} respectively which means that

the most important criterion is gratified. Thus in turn, these chemiluminescent precursors has been proved to bear enough energy for the chemiexcitation of a fragment in the transition state for thermal decomposition.[115]

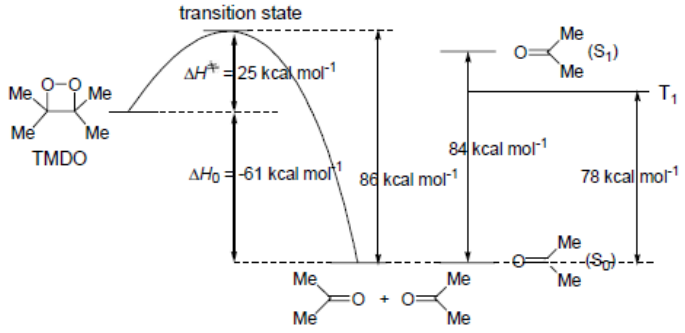

Figure 65: Production of an electronically excited acetone for thermal decomposition of tetramethyldioxetane[115]

Decomposition Mechanisms: New generation dioxetane derivatives have been synthesized to have remarkable thermostabilities up to even years. The most stable derivative has been synthesized whose activation energy is 37 kcal/mol with half-life even more than 20 years.[117,118] The decomposition of chemiluminescent precursor to excited state intermediate can be triggered only by heat which limits their applications. On the other hand, the reactivity and thermostability of the dioxetanes can be governed both by the chemical structure and by the mechanism at which high energy peroxide bond is cleaved.[119]

Thermal decomposition of sterically less hindered simple dioxetanes leads to the formation of triplet excited carbonyls along with the less amount of singlet excited carbonyl compounds. As a result, direct emission of light could not be expected.[115]

1,2-dioxetanes have been decomposed thermally via competing mechanisms which are concerted, biradical and an alternative mechanism The *concerted mechanism* follows the thermally induced simultaneous and homolytic cleavage of C-C and O-O bonds of four membered ring directly leading to the formation of two carbonyl compounds of which one is in the excited state (figure 66a). Whereas in the case of

biradical mechanism, O-O bonds to form an intermediate can proceed through two different ways. In the case of first possibility, some of the intermediate can be excited to singlet state while others still in the ground state. However, in the case of second possibility, some of the intermediate molecules can undergo triplet excited state via intersystem crossing while some stays still in the ground state. But, both processes is end up with C-C bond cleavage, thus in turn, two different carbonyl compounds are produced (figure 66b).[120] Concerted and biradical mechanisms have proceeded over one common feature which is twisting of dioxetane ring in transition state, thus in turn clearly puckered transition states are involved.

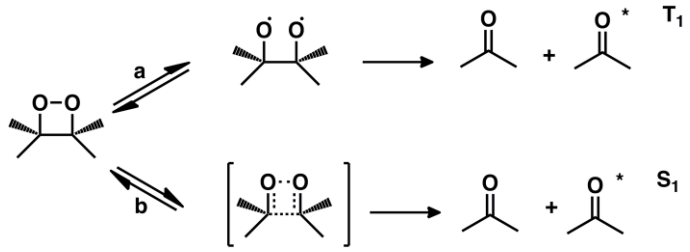

Figure 66: The two modes of decomposition of 1,2-dioxetanes: (I) the diradical mechanism and (II) the chemically initiated electron exchange chemiluminescence (CIEEL). The diradical mechanism most often generates triplet excited states (T1) while CIEEL generally results in singlet states (S1).[84]

In the case of third phenomenon known as *chemically initiated electron exchange luminescence mechanism (CIEEL)*, the decomposition reaction starts with electron transfer from an oxidizable donor like phenoxide ion which leads to the formation of a solvent caged biradical pair and the cleavage of dioxetane. Due to the back electron transfer, excited state phenoxide intermediate is formed while relaxing back to the ground state, it produces photon of light (figure 67).[121] 1,2-dioxetanes bearing an easily oxidizable substituents especially an aromatic electron donor decomposes via CIEEL mechanism and singlet excited state formation efficiency is remarkably higher.

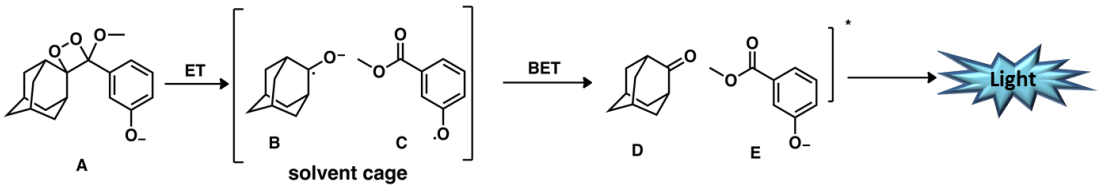

Figure 67: Decomposition mechansim of adamantyl subtituted dioxetane derivatives[121]

Luminescent properties: The structure of chemiluminogenic dioxetanes can be divided into five parts (figure 68):

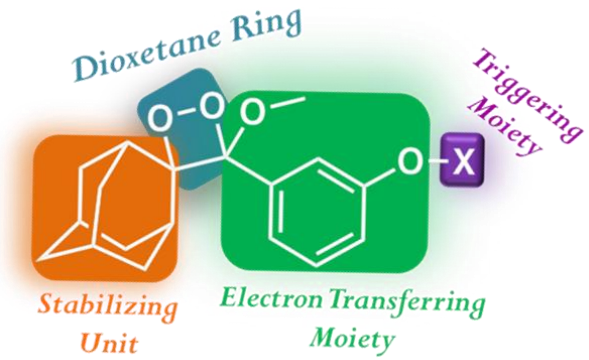

Figure 68: Design parameters of Chemiluminogenic Dioxetane Derivatives

1. Dioxetane Ring: is responsible for the luminescence as a result of the decomposition of four membered cyclic rings.
2. Triggering Moiety: can be designed according to the analyte of interest which contributes to the initiation of decomposition reaction by activating the aromatic moiety.
3. Aromatic-electron transferring moiety: triggers the ring opening of 1,2-dioxetane ring via electron transfer when it is activated. Additionally, it is responsible for the emission.
4. Alkoxy Group: During the synthesis of four membered ring, alkoxy group activates the olefinic function so as to enable singlet oxygen addition.

5. Adamantyl Moiety: increases the stability of dioxetane ring. Together with the aromatic and alkoxy groups, it prevents the twisting about C-C bond of dioxetane. Thus in turn, thermal stability is increased.[115]

Although it seems that there are only five parameters which are effective in luminescence, there are additional significant features that must be considered. The position of the triggering unit is very important since it defines the CL quantum yield, emission wavelength of excited intermediate, rate of decomposition and the rate of light emission. High singlet excitation efficiencies are observed when the triggering unit is connected to the aryl moiety on meta position rather than ortho or para to the dioxetane ring since the largest amount of charge can be transferred to ring if meta relationship exists thus in turn, CL quantum yield has been improved due to the increase in chemiexcitation quantum yield.[119]

The modification of aromatic moiety with aniline has negative effects on the dioxetane ring. Since the basicity of amino group is higher, it keeps the electrons and prevents their transfer during the decomposition reaction which leads to the decrease in emission intensity.[122]

Since the rate determining step is decomposition of dioxetane anion which is initiated by the electron transfer from aromatic moiety, pH of the medium is very important in terms of emission rate, quantum yield and so on. Chemiluminescence from a dioxetane modified with phenolic substituent can be triggered in aprotic solvents with the help of a base since the decomposition rate of deprotonated dioxetane is 4.4×10^6 times faster than the unprotonated one. This brings another point, even triggering moiety has been removed by the analyte, due to the type of solvent and the pH of the medium, emission could not be observed. For example, in the presence of water, emission intensity and rate are lowered due to the protonation of aryloxy group whose pKa is around 9. Because of that, decomposition reaction must be performed in aprotic solvents which stabilize but not protonate the phenoxide ion with the pH of either 9 or above it.[119]

The phenoxide anion is moderately stable having a half-life between 2 to 30 min depending on the solvent, pH, etc. of the medium. Actually, the light emission is two step processes. In the first step, analyte has removed the triggering moiety X and this removal proceeds at a constant rate depending on the concentration of the analyte of interest. In the second step, due to the constant production of excited state intermediate alkoxy ester which is decomposing slowly, there is a lag phase. After a while, CL reaction has reached a plateau. So that decomposition of 1,2-dioxetanes leads to "glow" emission (figure 69) whereas others " flash" emission.[119]

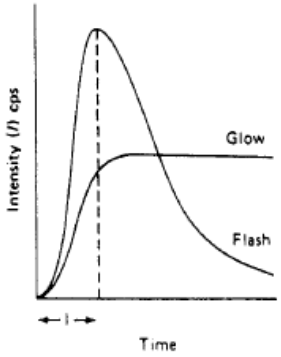

Figure 69: Emission Spectra of Dioxetanes

Applications: Due to some of the derivatives' thermal instability, quenching of emission in aqueous medium, quenching of emission in the absence of alkaline medium and the difficulty to luminescence processes, 1,2-dioxetane derivatives have been accepted as unsuitable for diagnostic applications so many years. However, enhanced dependency on S_1 vs T_1 ratios and the half-life on the molecule substituents attract attention of researchers to look for more stable dioxetanes. Additionally, in the sense of practical uses, thermal stability of dioxetanes makes them easy to handle in bioanalytical and clinical applications. Moreover, thorough the modification of the triggering unit, these reactive compounds can be used to detect different type of analytes like phosphatase enzymes[123], β-galactosidase [124], etc.[84]

New types of 1,2-dioxetanes have been designed and synthesized for chemiluminescent detection of choline esterase activity **A** [125], glutathione transferase **B** [77] and for protease activity **C** (figure 70).[122]

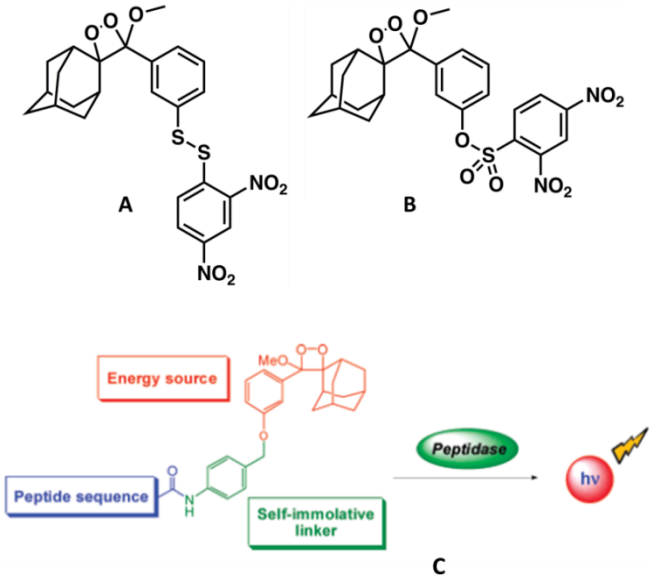

Figure 70: Literature examples for Dioxetane Chemiluminescence

CHAPTER 7

7. Chemiluminescence Sensing of Fluoride Ions Using a Self-Immolative Amplifier

This work is partially described in the following publication

Ilke Simsek Turan, Engin U. Akkaya

Org. Lett., ***2014***, *16(6), 1680-1683*

7.1. Objective

In this work, we wanted to incorporate a self immolative linker to trigger two chemiluminescence processes at the same time, in response to single fluoride mediated deprotection event. This approach offers a chemical avenue for enhancing the signal produced in response to a given analyte. Considering the fact that chemiluminescence in principle can provide a rapid, qualitative and/or quantitative test for analytes of interest, we are confident that other probes combining the power of self-immolation and chemiluminescence will emerge. Rapid assessment of fluoride concentrations in drinking water could be a possible application, and the bright chemiluminescence of the probe or structurally related derivatives could provide a promising alternative.

7.2. Introduction

7.2.1 Self Immolative Amplifiers

Promising advancements in biological and chemical sensors and drug delivery are implemented through the development of self immolative molecular structures (dendrimers and polymers) that are embodied with trigger unit sensitive to an analyte, a reporter unit giving information about the disassembly process and a reagent unit behaving as free analyte after transformation. These structures offer an improvement both in signal amplification due to the multiple releases of reporter groups and drug delivery due to the attachment of location specific groups and also specific triggering units.

Classical prodrug approach involves the direct connection of protecting moieties to the active compound through a scissle bond which can be cleaved under specific conditions. This classical prodrug approach works well when the linkage is easily accessible but when the active compound (trigger and or reporter) is sterically bulky,

its release is prevented. In order to overcome these problems, scissle linkers are incorporated between the trigger and reporter units. Under specific conditions, domino like reaction is initiated by the removal of protecting groups that leads to the disassembly of active compound in its components. This linker technology is known as self immolative linkers and coupled systems (trigger-linker-reporter) can be referred to as self immolative molecular systems. Single activation event promoted chain reaction of these molecular systems may lead to the release of single reporter unit which is called as nonamplified whereas that may lead to the release of multiple reporter units which is called as amplified (figure 71).[126]

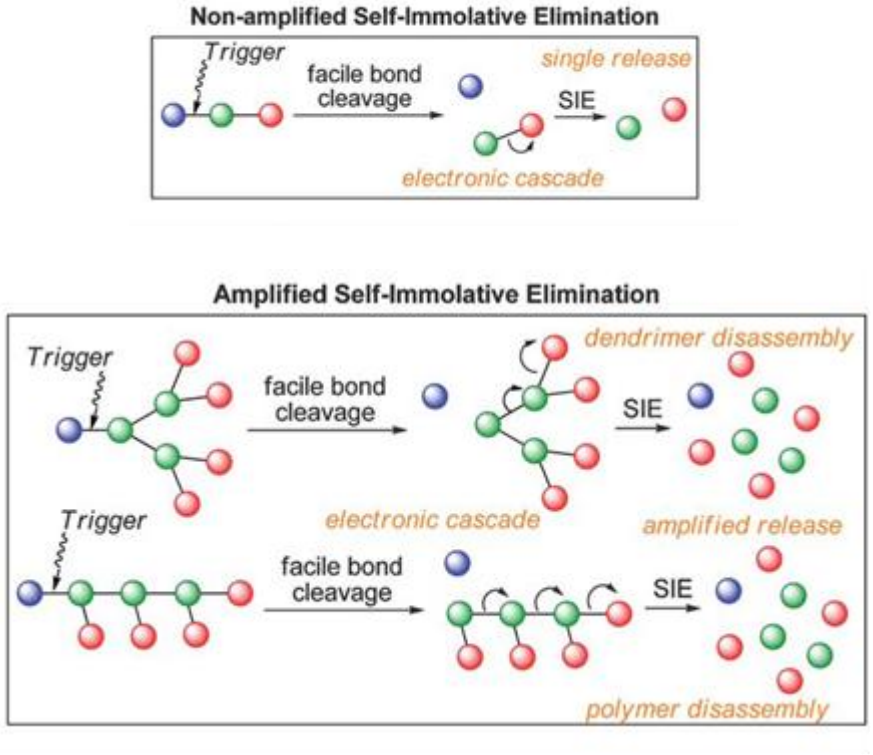

Figure 71: Schematic Representation of Non-Amplified and Amplified Eliminations[126]

7.2.1.1 Self Immolative Dendrimers

Self immolative molecular systems have been applied in the development of molecular sensors and probes which involve the detection of a specific analyte upon the release of chromogenic molecules through domino like reaction. Exponential release of chromogenic molecule increases the sensitivity of diagnostic methods and this signal amplification also forms the indispensible building blocks of imaging and drug delivery. The increasing need for effective signal amplification in diagnostic, imaging and drug delivery brings about the development of self immolative molecular systems through dendrimeric or polymeric platforms.[127,128]

Dendrimers, monodispersed macromolecules, have well defined finite structures of hyperbranched polymers that are composed of three parts as multivalent surface, outer shell and the core. As the dendrimer grows through branching, different compartments of it will show different characteristics and the properties of these compartments can be modified to a desired molecular property or a function of it as drug delivery, molecular sensors and so on.[129-131] These molecules are modified to use as sensors in which the dendrimeric structure is equipped with a *triggering unit* that is sensitive to specific analyte, *scissle linker* that forms the core of the dendrimeric structure and chromogenic reporter.[132,133] When triggering unit is activated, dendrimer is fragmented into its building blocks through domino like reaction to release a reporter unit and reagents (figure 72).[134,135] The process continues till the molecule releases all of the reporter and reagent units from the probe.

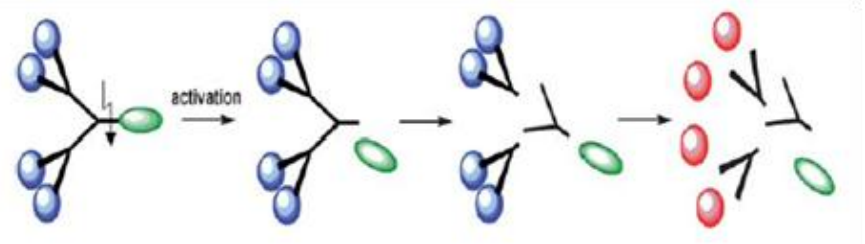

Figure 72: Self Immolative Dendrimer Fragmentation [129]

These molecules are termed as self immolative dendrimers since they sacrifice themselves to implement their essential function.[129] Upon activation of the trigger, molecule can disassemble through 1,4 or 1,6- quinone methide eliminations to release the reporter units (figure 73). The eliminations proceeds through 1,4 or 1,6 pathways since phenyl moiety can be substituted from para position which leads to 1,6 eliminations and/or ortho position which leads to 1,4-eliminations.

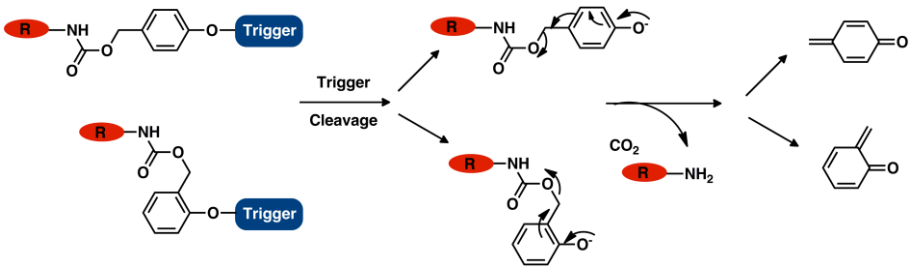

Figure 73: 1,4- and 1,6- Quinone Methide Eliminations [129]

Since the reaction of analyte with the trigger leads to exponential evolution of diagnostic signal, self immolative dendrimers are viewed as molecular amplifiers and they are used for signal amplification in the field of diagnostics, imaging, sensors and drug delivery.[132]

7.2.2 Anion Sensing

Anion detection has been extensively studied due to the significance of anions in biological processes and in nature which brings the consideration of industrial and agricultural pollution. Optical signaling systems for the selective recognition of anions have attracted great attention in recent years. Over the past decade, optical systems based on fluorescence due to its high sensitivity at low analyte concentration have been designed to implement selective recognition.[136,137]

7.2.2.1 Fluoride Ion Sensing

Optical sensing of fluoride ions, especially in aqueous solutions is very challenging, because of their highly efficient hydration, reducing effective nucleophilicity and basicity. Although fluoride ion offers several beneficial effects in the sense of either dental health or the treatment of osteoporosis, high intake of fluoride may bring about the increased possibility of fluorosis, nephrotoxic changes and kidney failure.[138] On the other hand, considering its presence in water, commercial products, and its implication in a number of health problems, monitoring of fluoride concentration is an important public priority. At present, ion selective electrodes are an option, but low-cost and straightforward assessment of fluoride ions requires other methodologies. There are many proposals for detection of fluoride by using chromogenic and fluorogenic probes, some working in organic solvents, and others operating in aqueous mixtures, all with acknowledged limitations, such as low affinity, inhibition of response by water, limited spectral changes, or lack of selectivity.[139] Most fluorescent detection systems operate through the strong interaction between fluoride ion and silyl group so that more specific probes have been designed based on the introduction of silyl containing groups as shown in figure 74.[138,140-144]

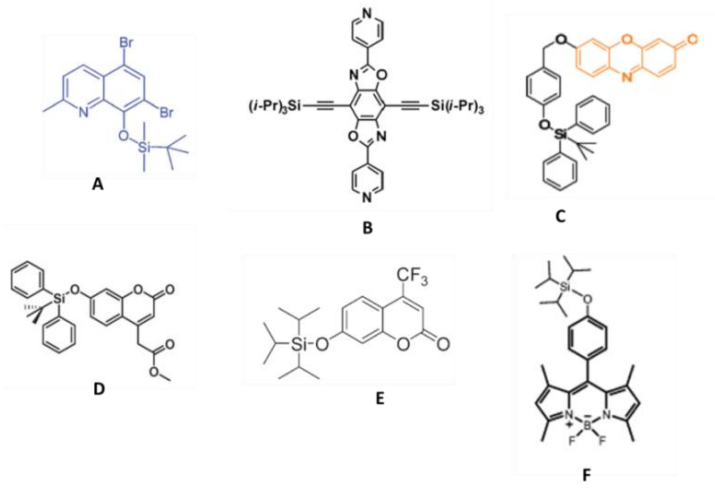

Figure 74: Literature Examples for Fluoride Anion Sensors

7.3 Design of Chemiluminescent Probe

When considering both structure and parameters affecting the emission intensity of 1,2-dioxetanes, adamantyl group was chosen to raise the thermal stability of the compound which enables the ease of use during the spectroscopic measurements. Moreover, self immolative amplifier was modified with *tert*-butyldimethylsilyl group as triggering moiety since the strong and specific affinity between fluoride ion and silyl group initiates the decomposition reaction hastily which is one of the most significant requirements for a chemiluminogenic reaction to come out with the light emission. Phenoxide ion was chosen to trigger the ring opening reaction of dioxetane ring when the fragmentation is initiated. In the sense of activation of olefinic function, methoxy group was preferred.

Triggering unit is directly introduced to the core in order to contribute to the acceleration of the fragmentation reaction. The decomposition reaction was devised in a way as to fragment into its building blocks via 1,4-quinone methide elimination which enables the consequent release of tail units swiftly compared to 1,6-elimination.

In the literature, mostly designed 1,2-dioxetane derivatives decompose to give light emission upon reaction with fluoride ion. However, fluoride ion catalyzed decomposition has never been studied as analytically. Additionally, chemiluminescence quantum yield of designed 1,2-dioxetane derivatives could not exceed the value of 0.29 in DMSO. In this work, chemiluminogenic precursor was designed so as to be activated by a single cleavage event resulting in the fragmentation of amplifier to release duet of tail units. Thus in turn, high quantum yield from this domino reaction was expected since two chemiluminogenic dioxetane derivatives could be released upon activation by a single event.

This study is expected to be pioneer in chemiluminescence based sensors due to its analytical perspective.

7.4 Results and Discussion

In this work, we wanted to incorporate a self immolative linker to trigger two chemiluminescence processes at the same time, in response to single fluoride mediated deprotection event. Since the fluoride ion mediated decomposition of a dioxetane was studied (but not analytically) and chemiluminescence quantum yield of designed 1,2-dioxetane derivatives could not exceed the value of 0.29 in DMSO, we have intended to construct this work as a comparison base at first. For this, we have synthesized the reference compound **39** and the probe separately **44**. Beside, we have studied their fluoride ion induced decomposition individually.

7.4.1 Synthetic Approach

We have synthesized the reference compound (RC) and the probe as shown in figure 75 some in close analogy to the literature procedures.

In the literature, for the synthesis of dioxetane derivatives most generally, McMurry Coupling reactions between a ketone and an ester are preferred. When this reaction has been considered, there are three possible products which are coupled ketone, coupled ester and coupled ketone and an ester. Thus, the yield of this reaction was very low as expected and the reaction favors the formation of coupled ketone. Additionally, when performing the reaction, we have almost no control over it and also, the reaction proceed superficially for the synthesis of dioxetane derivatives. Because of that, we have designed a synthetic scheme which proceeds via Wadworth-Emmons Wittig Olefination reaction.

We have begun the synthesis with the protection of 3-hydroxybenzaldehyde in order to prevent its polymerization reaction during the course of acetal formation. After the protection of the benzaldehyde with benzoyl chloride, we have continued with the synthesis of acetal formation reaction in the catalysis of *p*-toluenesulfonic acid in

order to establish the alkoxy part of the dioxetane that is either responsible for the activation of olefinic function for singlet oxygen addition reaction or necessary for the introduction of olefinic group. Since we have devised to introduce olefinic group via Horner-Emmons Wittig Reaction, we have continued with incorporation of phosphonate functionality which is Wittig Olefination precursor and synthesized via Michaleis-Arbusov Reaction in the catalysis of titanium tetrachloride. Titanium tetrachloride is a Lewis acid which hastens the reaction at low temperatures and enables the simple isolation of the desired product. Subsequent treatment of phosphonate derivative with LDA abstracts the acidic proton in order to generate ylide of compound **36** which was then reacted with adamantanone to form the olefin **37**. Compound **37** is a joint partner of RC and probe.

We have continued with the modification of the conjoint by *tert*-butyl dimethylsilyl (TBDMS) group which is the triggering unit of dioxetane and specific for the fluoride ion. The introduction of triggering unit was mediated via simple nucleophilic substitution reaction. Dioxetane ring was supposed to introduce at the last step of synthesis due to the sensitivity and reactivity of four membered units. Oxygen molecule founds in nature as in triplet state however, singlet oxygen is the reactive one for the cycloaddition reaction that can be obtained by photooxidation of it in the presence of photosensitizers. In this work, we have used methylene blue (MB) as photosensitizer which is excited via the irradiation. While MB relaxes back to ground state, it transfers its energy to triplate state oxygen and generates singlet oxygen which is then reacts with olefin **37** through [2+2] cycloaddition reaction to form RC **39** (figure 76) .

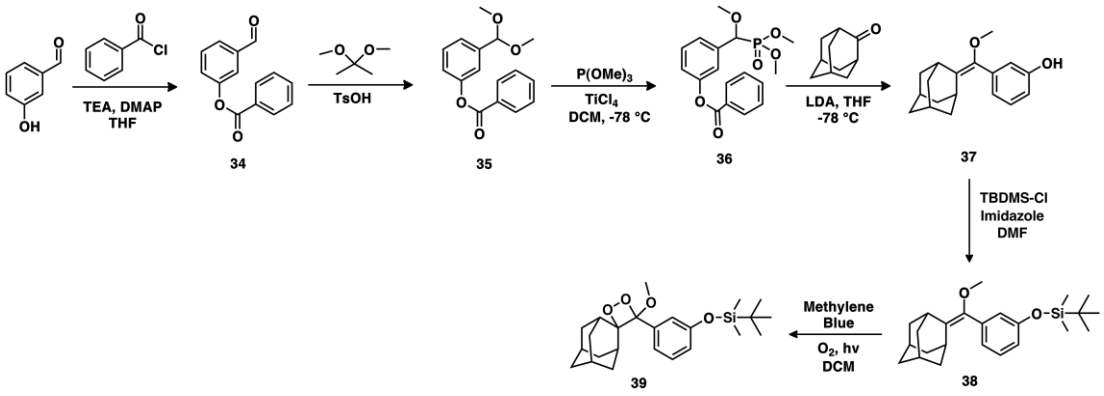

Figure 75: Pursued synthetic route for the synthesis of 1,2-dioxetane derivative.

Synthesis of probe **44** was started with the protection of 2,6-bis(hydroxymethyl)-*p*-cresol with TBDMS group in order to introduce triggering unit. The protection was performed with three hydroxyl groups since the protection could not be preceded selectively on the other hand, hydrolysis can be achieved specifically on the benzylic group. Thus in turn, we could be able to introduce the triggering unit to the self immolative amplifier. Through the subsequent treatment of the compound **41** with *p*-nitrochloroformate in the catalysis of DMAP, carbonate groups would be introduced to the structure. Chemiluminogenic precursor was inserted into the structure via simple nucleophilic substitution reaction and the synthesis of the structure was completed with [2+2] cycloaddition reaction of singlet oxygen.

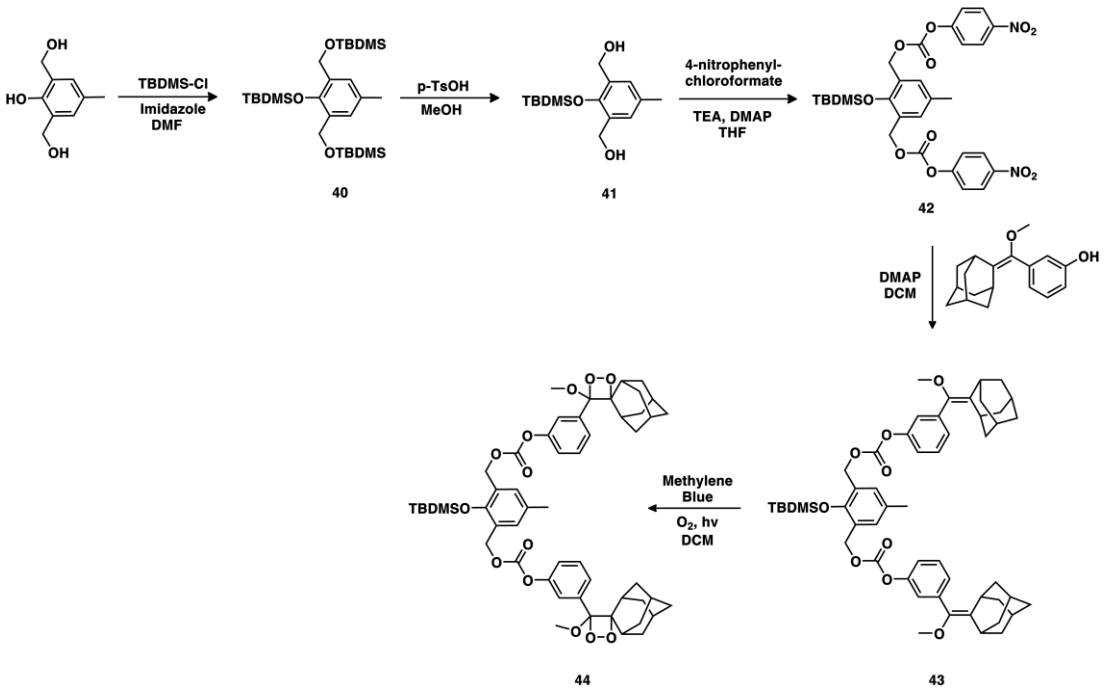

Figure 76: Synthesis of the self-immolative chemiluminogenic Fluoride sensor

7.4.2 Working Principle

In order to investigate optimized conditions for light emission, we believe that first we must understand the decomposition of the self immolative amplifier whose suggested decomposition mechanism was shown in figure 77. Upon addition of fluoride ion to the medium, it attacks to TBDMS group and leads to the formation of compound **A** via the removal of triggering group. When phenoxide ion is formed on the self immolative amplifier, it starts to sacrifice itself to release chemiluminogenic tail units **B** while CO_2 is released from the fragmentation reaction. When structure **B** is formed which is the activated form of 1,2-dioxetane, transfers electron to the four membered rings to initiates its decomposition for the generation of excited state molecule **C** while it relaxes back to ground state **D**, results in the emission of photon.

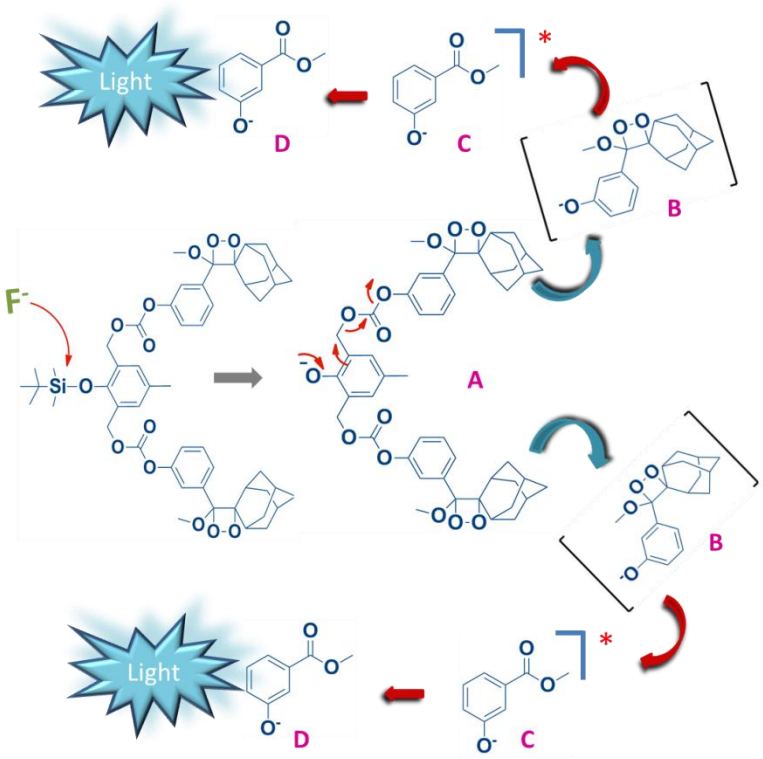

Figure 77: Self-immolation mechanism and multivalent response

7.4.3 Spectral Proofs for Chemiluminogenic Fragmentation

Since chemiluminescence quantum yields of 1,2-dioxetane derivatives are reported high when DMSO was the solvent of choice as in the case of decomposition of RC, we have preferred to start with titration in DMSO. Since the emission intensity and the rate of fragmentation are decreased as a result of deprotonation of phenoxide group whose pKa is around 9 which brings about the use of aprotic solvent in order to stabilize but not protonate phenoxide ion.

Also, we have wanted to observe fluoride ion mediated chemiluminescence in water while using DMSO as a cosolvent. For this, after working in DMSO, we have continued with titration in DMSO/buffer mixture. However, in the case of buffer/organic solvent mixture, we have to use high concentration of the probe since

in the presence of water, possibility of phenoxide-protonation is enhanced which leads to termination of fragmentation reaction leading light emission. When we compare the CL emission spectra, almost same emission intensity was obtained when probe was used as five times more concentrated than in the case of DMSO (figure 78). Additionally, fluoride ion concentration is also changed due to the competitive hydrogen bonding between fluoride and water molecules. As the concentration of active analyte decreases, either the rate of fragmentation reaction or the emission intensity decreases.

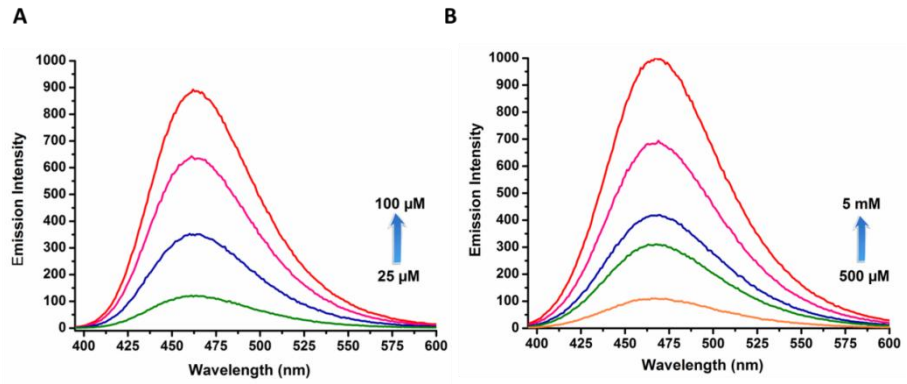

Figure 78: A) Chemiluminescence spectra of probe+F^- in the presence of increasing F^- concentrations. Probe concentration is 100 µM in DMSO. **B**) Chemiluminescence spectra of probe+F^- in the presence of increasing F^- concentrations. Probe concentration is 500 µM in DMSO/PBS (1X, 90/10, pH 7.2).

Although we have desired to perform this emission in physiological conditions, mechanism of light emission prevents this. After attempting to use 5% buffer, we have tried to increase the buffer percentages in DMSO and when considering the mechanism with explanations mentioned above, the higher in the buffer percentage in DMSO, the lower the emission intensity as in figure 79.

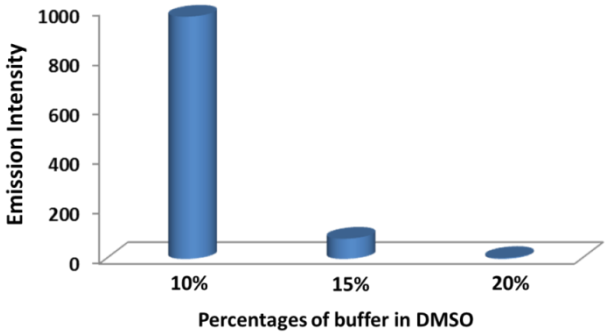

Figure 79: Chemiluminescence Intensity of Probe at different percentages of buffer (PBS 1X, pH 7.2) in DMSO. Probe concentration is 500 µM

Since the emission intensity and rate of fragmentation are decreased as a result of deprotonation of phenoxide group whose pKa is around 9 which brings about the use of aprotic solvent in order to stabilize the but not protonate the phenoxide ion. Even though buffer percentage in DMSO is 5%, we have wanted to work in physiological conditions and but we have the emission intensity in acidic pH. As expected, the higher the probability of protonation, the lower the rate of fragmentation and the emission intensity.

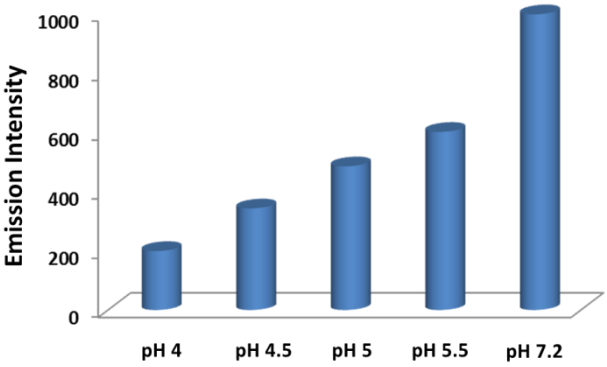

Figure 80: pH-dependent chemiluminescence intensity of Probe in the presence of F^- (5mM). Probe concentration is 500 µM in DMSO/Buffer (90/10 for pH 4-5.5, NaOAc buffer 50 mM, for pH 7.2, PBS 1X).

Since have observed emission at acidic pH, we have checked whether compound has been decomposed under acidic conditions due to presence of easily hydrolysable

carbonate groups (figure 81). However, when comparing with the other results at different pH values, emission is not the result of labile carbonate linkages instead it is the result of reaction between silyl moiety and fluoride ion which triggers the decomposition of amplifier into its chemiluminogenic tail units.

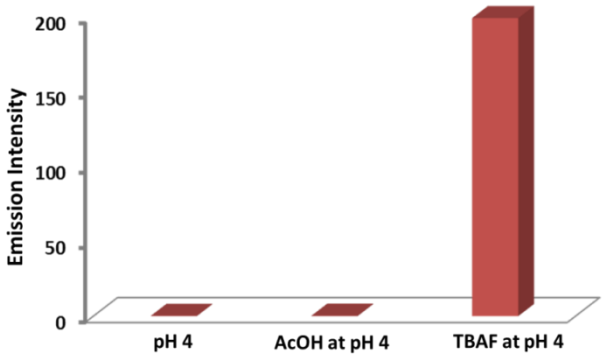

Figure 81: Chemiluminescence intensity of probe in the presence of AcOH (5 mM) and F^- (5 mM). Probe concentration is 500 μM in DMSO/NaOAc (50 mM, 90/10, pH 4).

As the selectivity of the reaction between fluoride ion and silyl group has been reported, we have tested the selectivity in the sense of CL based self immolative amplifier. For this, we have applied *tetra*-butyl ammonium salts of several anions and as expected, the fragmentation reaction could be triggered only with the addition of fluoride ion and there is no background emission observed depends on the type of the medium preferred (figure 82).

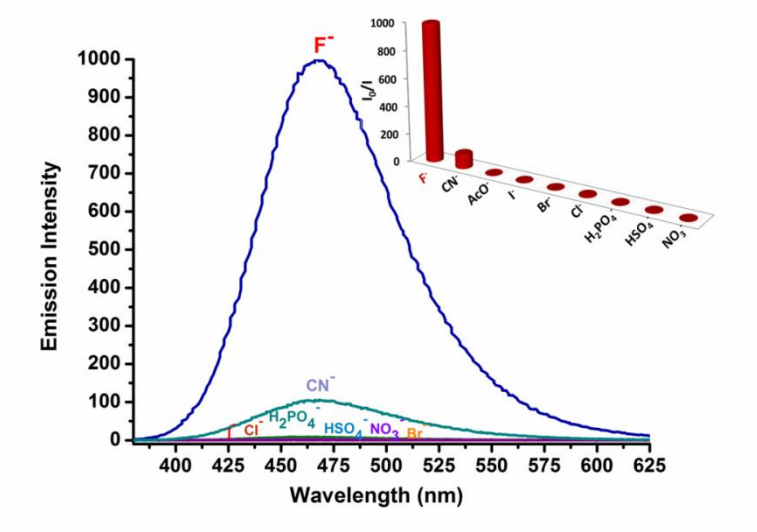

Figure 82: Chemiluminescence spectra of probe upon addition of 10 equiv. of I^-, Br^-, Cl^-, CN^-, AcO^-, $H_2PO_4^-$, HSO_4^-, NO_3^-, F^- and Probe concentration is 500 µM in DMSO/PBS (1X, 90/10, pH 7.2).

Digital photographs of the solutions show the selectivity of chemiluminescence under ambient light. Fluoride in DMSO or DMSO-buffer mixture, elicits clear response with luminescence intensity reflecting fluoride concentration.

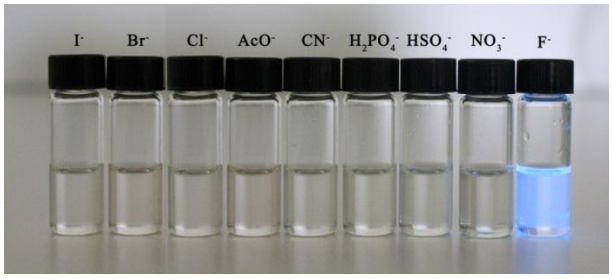

Figure 83: Selective chemiluminescent response of the fluoride probe **9** under ambient light.

We also wanted to demonstrate the response to aqueous fluoride solution in the form of test strips. To that end, we impregnated PMMA with the chemiluminogenic probe. The polymer strips on glass were prepared. These probes when dipped into

fluoride solutions in THF, chemiluminescence is triggered. Again, the luminescence intensity is related to the fluoride concentration in solution. The photograph was digitized and the brightness of the strips was quantified (figure 84 and 85). The plot of brightness as a function of fluoride concentration shows a reproducible relation. The effect of water content was also investigated by varying the percentage of buffer in DMSO. The polymer strips because of the thickness of the polymeric layers and inhomogeneity of diffusion of fluoride, shows bright and dark patches except for the high fluoride case, but the integrated luminescence of produced on the strips provides usable analytical data.

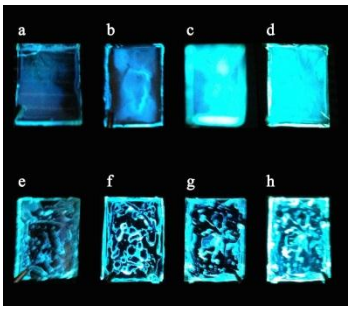

Figure 84: PMMA on glass impregnated with probe, exposed to increasing concentrations of F^- (12.5 mM to 100 mM) in THF (top, a-d). Same strips exposed to 250 mM fluoride and in varying concentrations of buffer (PBS, pH 7.2) DMSO (e-h, 40, 30, 20, 10 %).

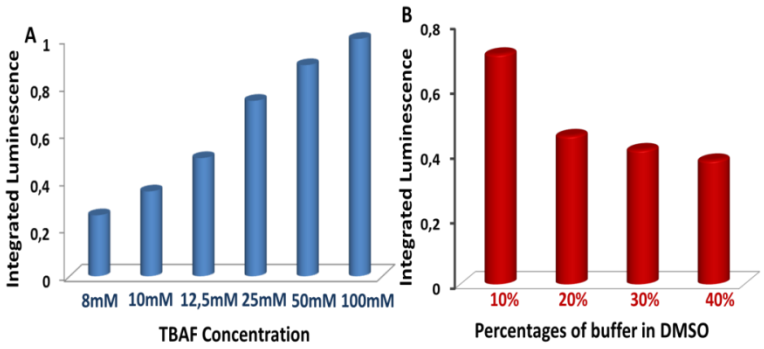

Figure 85: Integrated luminescence from the PMMA strips showing the response to increasing fluoride (A) and water (B) concentrations.

When we have completed the analytical study of probe, we have continued with the reference compound (figure 86). As in the case of probe, when we have used water, the emission intensity is also changed. However, when we compare the results of probe and RC in the identical conditions, self immolative chemiluminogenic amplifier presents higher emission intensity which proves that we can enhance signal in response to given analyte concentration by using a self immolative approach.

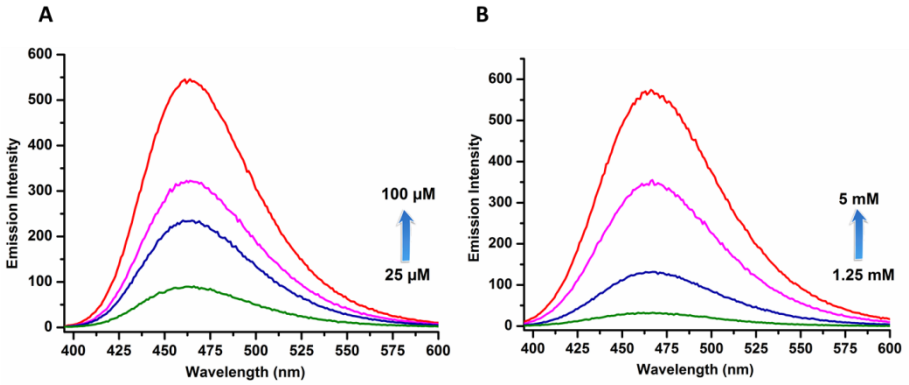

Figure 86: A) Chemiluminescence spectra of RC in the presence of increasing F^- concentrations. Probe concentration is 100 µM in DMSO. B) Chemiluminescence spectra of RC in the presence of increasing F^- concentrations. Probe concentration is 500 µM in DMSO/PBS (1X, 90/10, pH 7.2).

When we examine the figure 87 and 88, it is obvious that our self immolative amplifier is way better than RC both in DMSO and DMSO/buffer mixture. Additionally, with the calculation of quantum yield for both compounds, we would confirm that the amplifier can release two chemiluminogenic precursors upon activation by a single event.

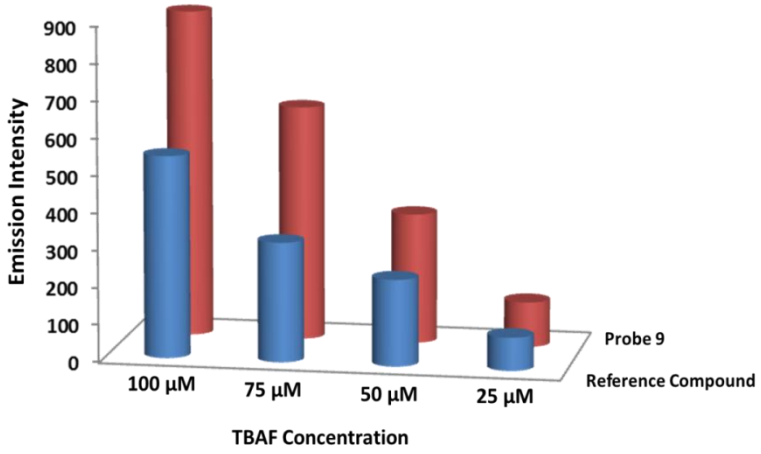

Figure 87: Comparison of chemiluminescence intensity of Probe and reference compound in the presence of increasing F^- concentrations. Probe concentration is 100 µM in DMSO.

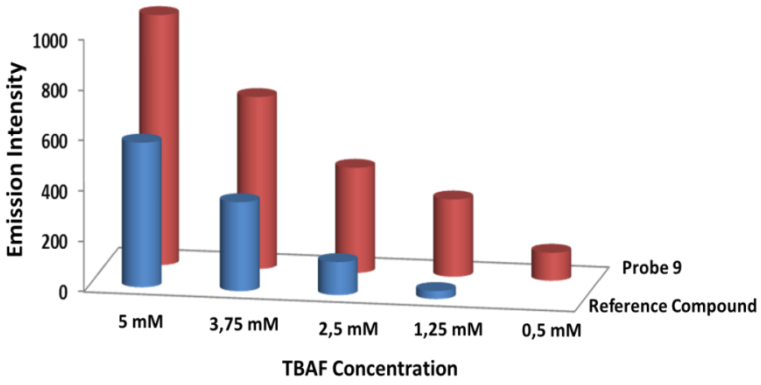

Figure 88: Comparison of chemiluminescence intensity of Probe and RC in the presence of increasing F^- concentrations. Probe concentration is 500 µM in DMSO/PBS (1X, 90/10, pH 7.2).

In order to prove the single event activated release of two chemiluminogenic tails, we have determined the quantum yield of both RC and probe. Quantum yield of RC is 0.29 in DMSO whereas quantum yield of our self immolative amplifier is 0.46 (figure 89).

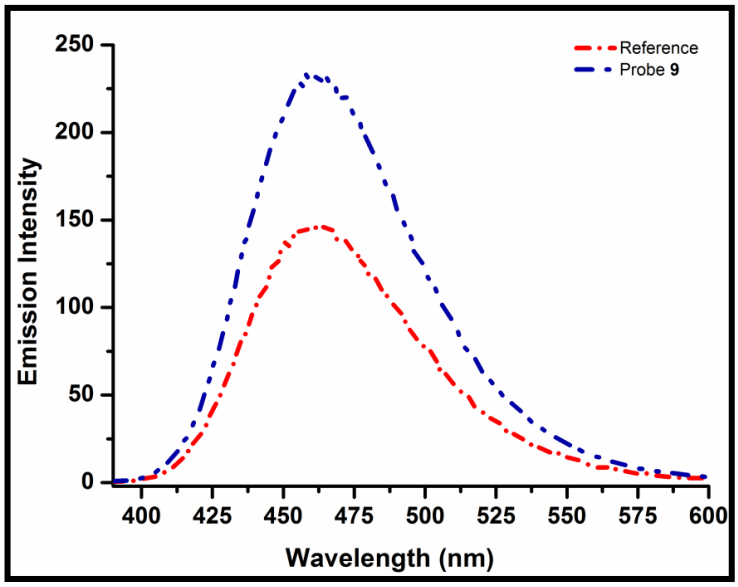

Figure 89: Chemiluminescence decomposition spectra of RC and Probe.

Furthermore, we have studied the detection limit of both compounds either in DMSO and DMSO/buffer mixtures. Detection Limit was calculated for probe in

DMSO as $4{,}70x10^{-5}M$ (σ=0.004108),

DMSO/PBS (1X, pH 7.2) as $6{,}72\ x10^{-4}M$ (σ= 0.094838)

On the other hand, detection limit was calculated for reference compound in

DMSO as $5{,}29x10^{-5}M$ (σ=0.077144),

DMSO/PBS (1X, pH 7.2) as $1.80x10^{-3}M$ (σ=0.111555)

7.5 Experimental Details

7.5.1 Preparation of Test Strips

Test strips were prepared as follows: 4 mg of PMMA and 10 mg of compound **9** was dissolved in 0.2 mL of THF. 30 μL from this solution was impregnated into the glass plate which was left to dry at room temperature. Then, TBAF from related stock solutions in THF were impregnated into the plate which was left to dry at room temperature.

7.5.2 Detection Limit Measurements

The detection limits for probe and reference compound were calculated based on chemiluminescence titration. In order to determine the S/N ratio, the chemiluminescence emission intensity of the blanks without F^- was measured 10 times and standard deviation of these blanks was calculated. Chemiluminescence emission intensities of the probe and reference compound in the presence of F^- were plotted as a concentration of F^- in order to determine the slopes.

$$\text{Detection limit: } 3\sigma/m$$

where σ represents the standard deviation of the blank measurements, m represents the slope between intensity versus sample concentration.

7.5.3 Synthesis

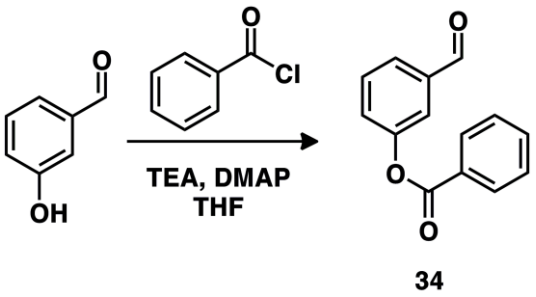

34

Synthesis of Compound 34: 3-hydroxy benzaldehyde (1 g, 8.19 mmol) was dissolved in dry THF. When reaction mixture was cooled to 0 °C, TEA (1.71 mL, 12.2 mmol) was added and mixed for 20 min. After the addition of catalytic amount of DMAP, benzoyl chloride (1.38 mL, 12.2 mmol) was added dropwise to the reaction mixture and it was left to stir at room temperature. The progress of the reaction was monitored by TLC. When TLC showed no starting material, reaction was concentrated to half of it. The residue was diluted with EtOAc and extracted with brine. Combined organic phases were dried over anhydrous Na_2SO_4. After removal of the solvent, the residue was purified by silica gel flash column chromatography using EtOAc/ Hexane (1:5, v/v) as the eluent. Compound **34** was obtained as white solid (1.41 g, 76%).

^{1}H NMR (400 MHz, $CDCl_3$): δ_H 10.04 (s, 1H), 8.23 (d, *J* = 8.4 Hz, 2H), 7.78-7.82 (m, 2H), 7.57-7.69 (m, 2H), 7.51-7.57 (m, 3H).

^{13}C NMR (100 MHz, $CDCl_3$): δ_C 191.1, 164.8, 151.5, 137.8, 133.9, 130.24, 130.21, 129.0, 128.71, 128.69, 127.9, 127.3, 122.5.

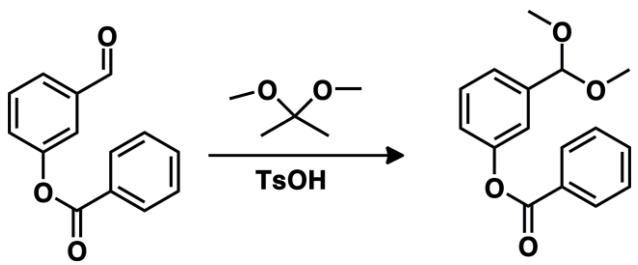

34 **35**

Synthesis of Compound 35: Compound **34** (1 g, 4.42 mmol), 2,2-dimethoxy propane (1.2 mL) and catalytic amount of *p*-toluenesulfonic acid was mixed at 75 °C. The progress of the reaction was monitored by TLC. When TLC showed no starting material, reaction was concentrated to half of it. The residue was diluted with EtOAc and extracted with brine. Combined organic phases were dried over anhydrous Na_2SO_4. After removal of the solvent, the residue was purified by silica gel flash column chromatography using EtOAc/ Hexane (1:5, v/v) as the eluent. Compound **35** was obtained as pale yellow liquid (0.745 g, 62%).

^{1}H NMR (400 MHz, $CDCl_3$): δ_H 8.24 (d, J = 8.5 Hz, 2H), 7.65 (t, J= 7.4 Hz, 1H), 7.39-7.55 (m, 5H), 7.23 (d, J= 8.0 Hz, 1H), 5.48 (s, 1H), 3.37 (s, 6H).

^{13}C NMR (100 MHz, $CDCl_3$): δ_C 165.1, 151.0, 140.0, 133.6, 130.1, 129.5, 129.3, 128.6, 124.2, 121.7, 120.2, 102.2, 52.5.

MS (TOF- ESI): m/z: Calcd for $C_{16}H_{16}O_4$: 295.09408 $[M+Na]^+$, Found: 295.09078 $[M+ Na]^+$, Δ= 11.18 ppm.

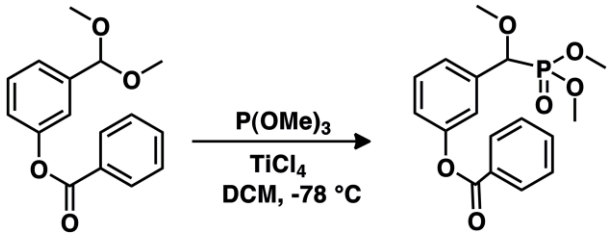

35 **36**

Synthesis of Compound 36: Trimethyl phosphite (0.3 mL, 2.58 mmol) was added to the solution of compound **35** (0.50 g, 1.84 mmol) in DCM at -78 °C under Ar. 15 min later, $TiCl_4$ (0.3 mL, 2.58 mmol) was added dropwise to the reaction mixture at -78 °C. The mixture was stirred for 30 min before allowing it to room temperature and stirred at room temperature for further 1 hour. After the addition of aqueous methanol (2:1), reaction mixture was diluted with DCM and extracted first with saturated solution of $NaHCO_3$ then with brine. Combined organic phases were dried over anhydrous Na_2SO_4. After removal of the solvent, the residue was purified by

silica gel flash column chromatography using EtOAc as the eluent. Compound **36** was obtained as white solid (0.583 g, 91%).

^{1}H NMR (400 MHz, $CDCl_3$): δ_H 8.22 (d, *J*=8.3 Hz, 2H), 7.66-7.68 (m, 1H), 7.52-7.55 (m, 2H), 7.48 (t, *J*= 7.8 Hz, 1H), 7.38 (d, *J*= 7.7 Hz, 1h), 7.34 (s, 1H), 7.24 (d, *J*=8.0 Hz, 1H), 4.60 (d, *J*=15.8 Hz, 1H), 3.74 (dd, *J*=7.1, 6H), 3.45 (s, 3H).

^{13}C NMR (100 MHz, $CDCl_3$): δ_C 165.0, 151.2, 151.2, 136.1, 133.6, 130.1, 129.6, 129.5, 128.6, 125.4, 125.3, 122.0, 121.9, 121.2, 121.14, 80.7, 79.0, 59.0, 58.8, 53.98, 53.92, 53.8, 53.7.

MS (TOF- ESI): m/z: Calcd for $C_{19}H_{17}O_6P$: 373.07657 $[M+ Na]^+$, Found: 373.07657 $[M+ Na]^+$, Δ=12.27 ppm.

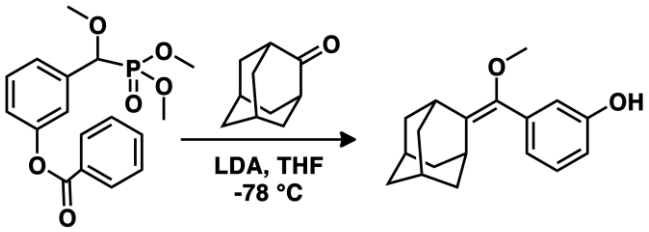

36 **37**

Synthesis of Compound 37: Lithiumdiisopropyl amide (1.8 mL, 3.07 mmol) was added dropwise to the reaction mixture of compound **36** (0.43 g, 1.23 mmol) dissolved in 1 mL dry THF at -78 °C under Ar. After stirring of the reaction mixture for 45 min, 2-adamantanone (0.166 g, 1.11 mmol) dissolved in dry THF was added dropwise to the reaction mixture at -78 °C under Ar. Reaction was left to stir at room temperature overnight. After pouring it into phosphate buffer (0.2 M, pH 7), it was extracted with EtOAc. Combined organic phases were dried over anhydrous Na_2SO_4. After removal of the solvent, the residue was purified by silica gel flash column chromatography using EtOAc/ Hexane (1:5, v/v) as the eluent. Compound **37** was obtained as white solid (0.312 g, 94%).

^{1}H NMR (400 MHz, $CDCl_3$): δ_H 7.23 (t, *J*= 7.8 Hz, 1H), 6.88-6.91 (m, 2H), 6.80-6.83 (m, 1H), 6.11 (s, br, 1H), 3.36 (s, 3H), 3.27 (s, 1H), 2.68 (s, 1H), 1.80-1.98 (m, 12H).

^{13}C NMR (100 MHz, $CDCl_3$): δ_C 155.8, 142.8, 136.7, 132.4, 129.1, 121.8, 115.9, 114.6, 57.7, 39.1, 39.0, 37.1, 32.2, 30.3, 28.2.

MS (TOF- ESI): m/z: Calcd for $C_{18}H_{22}O_2$: 271.16926 $[M+H]^+$, Found: 271.16357 $[M+H]^+$, Δ=13.59 ppm.

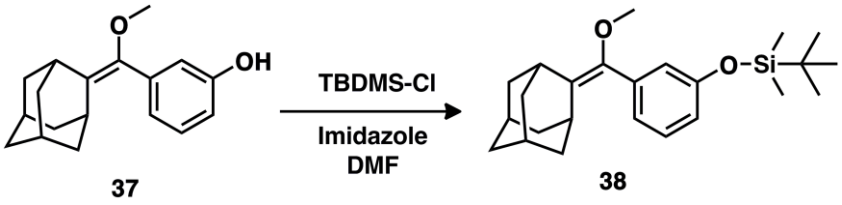

37 38

Synthesis of Compound 38: Compound **37** (0.10 g, 0.37 mmol) and TBDMS-Cl (0.089 g, 0.59 mmol) were dissolved in 2 mL dry DMF and reaction was started with the addition of imidazole (0.050 g, 0.74 mmol) and it was strirred at room temperature overnight. The progress of the reaction was monitored by TLC using DCM as the eluent. When TLC shows no starting material, it was extracted with EtOAc. Combined oganic phases were dried over $NaSO_4$ and concentrated under vacuo. The crude product was subjected to silica gel F.C.C. using DCM: as the eluent. Compound **38** was obtained as a colorless liquid (0.121 g, 85%).

^{1}H NMR (400 MHz, $CDCl_3$): δ_H 7.22 (t, *J*= 7.9 Hz, 1H), 6.95-6.93 (m, 1H), 6.83-6.82 (m, 1H), 6.81-6.78 (m, 1H), 3.32 (s, 3H), 3.27 (s, 1H), 2.0-1.81 (m, 12H), 1.01 (s, 9H), 0.22 (s, 6H).

^{13}C NMR (100 MHz, $CDCl_3$): δ_C 155.3, 143.3, 136.8, 131.2, 128.9, 122.5, 121.0, 119.3, 57.6, 39.2, 39.0, 37.2, 32.2, 30.1, 28.3, 26.7, -4.4.

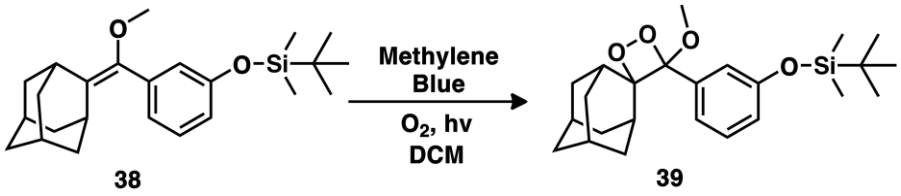

38 39

Synthesis of Compound 39: Compound **38** (0.10 g, 0.26 mmol) was dissolved in DCM. Methylene blue (5 mg) was added to the reaction mixture which was irradiated while oxygen gas was passing through it. The progress of the reaction was monitored by TLC. When TLC showed no starting material, the mixture was concentrated under vacuo and the residue was subjected to the silica gel flash column chromatography by using DCM as the eluent. Compound **39** was obtained as white solid (0.105 g, 97%).

^{1}H NMR (400 MHz, $CDCl_3$): δ_H 7.32-7.05 (br m, 3H), 6.92-6.89 (m, 1H), 3.26 (s, 3H), 3.05 (s, 1H), 2.26 (s, 1H), 1.96-1.25 (m, 12H), 1.01 (s, 9H), 0.22 (s, 6H).

^{13}C NMR (100 MHz, $CDCl_3$): δ_C 140.5, 136.5, 133.6, 132.7, 129.1, 126.9, 125.7, 99.8, 54.2, 40.8, 39.1, 37.5, 37.3, 36.8, 35.9, 34.1, 30.4, 30.3, 30.0, 5.4.

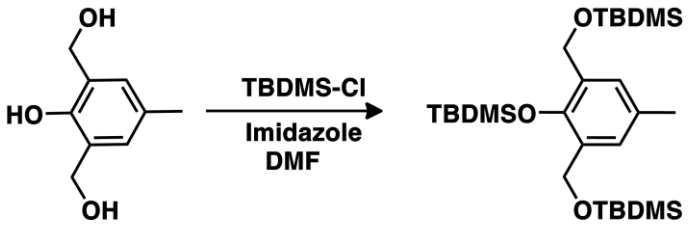

40

Synthesis of Compound 40: Imidazole (0.776 g, 11.4 mmol) was added to the reaction mixture of 2,6-bis(hydroxymethyl)-*p*-cresol (0.50 g, 2.97 mmol) dissolved in DMF at 0 °C. Then, *tert*-butyl dimethylsilyl chloride (1.69 g, 11.3 mmol) was added to reaction and it was left to stir at room temperature overnight. When starting material was consumed, diluted with diethyl ether and washed with saturated NH_4Cl solution. After washing with brine, combined organic phases were dried over anhydrous Na_2SO_4. After removal of the solvent, the residue was purified by silica

gel flash column chromatography using EtOAc/ Hexane (1:5, v/v) as the eluent as the eluent. Compound **40** was obtained as colorless waxy oil (1.29 g, 86%).

^{1}H NMR (400 MHz, $CDCl_3$): δ_H 7.19 (s, 2H), 4.75 (s, 4H), 2.35 (s, 3H), 1.06 (s, 9H), 0.97 (s, 18H), 0.22 (s, 6H), 0.13 (s, 12H).

^{13}C NMR (100 MHz, $CDCl_3$): δ_C 145.7, 131.2, 130.7, 126.5, 60.6, 26.0, 21.0, 18.7, 18.4, 2.9, 3.4, -5.4.

MS (TOF- ESI): m/z: Calcd for $C_{27}H_{54}O_3Si_3$: 533.3273 $[M+Na]^+$, Found: 533.3283 $[M+Na]^+$, Δ=-10.38 ppm.

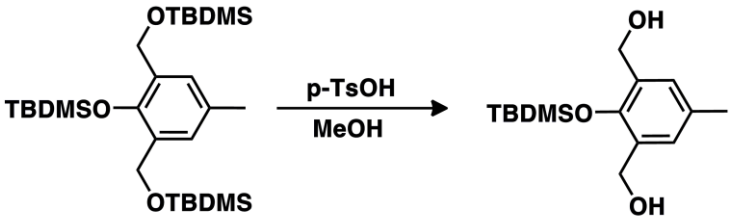

40 **41**

Synthesis of Compound 41: Compound 40 (1 g, 1.96 mmol) was dissolved in 3 mL of methanol. After adding catalytic amount of *p*-toluenesulfonic acid, reaction was stirred at room temperature. The progress of the reaction was monitored by TLC. When TLC showed no starting material, the reaction was diluted with EtOAc and extracted first with saturated solution of $NaHCO_3$ and with brine. Combined organic phases were dried over anhydrous Na_2SO_4. After removal of the solvent, the residue was purified by silica gel flash column chromatography using EtOAc/ Hexane (1:5, v/v) as the eluent. Compound **41** was obtained as pale yellow solid (0.53 g, 96%).

^{1}H NMR (400 MHz, CDCl3): δ_H 7.16 (s, 2H), 4.67 (d, *J*= 5.9 Hz, 4H), 2.33 (s, 3H), 1.06 (s, 9H), 0.22 (s, 6H).

^{13}C NMR (100 MHz, CDCl3): δ_C 131.6, 129.0, 61.0, 26.0, 20.6, 18.6, -3.6.

MS (TOF- ESI): m/z: Calcd for $C_{15}H_{26}O_3Si$: 305.15434 $[M+Na]^+$, Found: 305.15781 $[M+Na]^+$, Δ=-11.36 ppm.

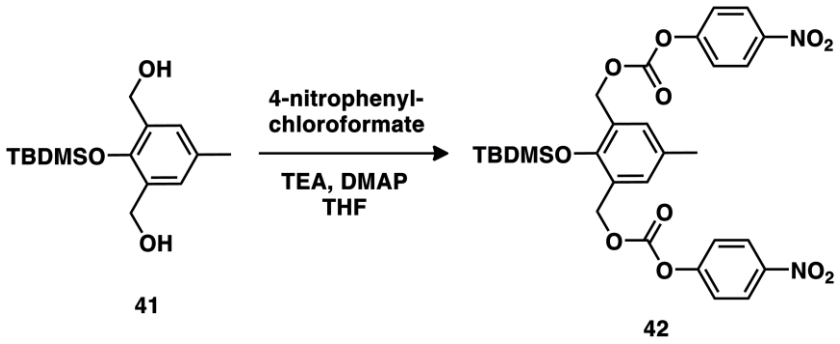

41 42

Synthesis of Compound 42: A solution of compound **41** (0.386 g, 1.37 mmol) in dry THF was cooled to 0 °C. Triethyl amine (766 μL, 5.5 mmol) and catalytic amount of DMAP were added. Then, 4-nitrophenyl chloroformate (1.10 g, 5.5 mmol) dissolved in dry THF was added drop wise to the reaction at 0 °C. The reaction mixture was allowed to stir at room temperature. The progress of the reaction was monitored by TLC. When TLC showed no starting material, the reaction was diluted with EtOAc and extracted first with saturated solution of NH_4Cl and with brine. Combined organic phases were dried over anhydrous Na_2SO_4. After removal of the solvent, the residue was purified by silica gel flash column chromatography using EtOAc/ Hexane (1:5, v/v) as the eluent. Compound **42** was obtained as pale yellow solid (0.435 g, 52%).

^{1}H NMR (400 MHz, $CDCl_3$): δ_H 8.30 (d, *J*= 9.2 Hz, 4H), 7.41 (d, *J*= 9.2 Hz, 4H), 7.29 (s, 2H), 5.33 8s, 4H), 2.36 (s, 3H), 1.09 (s, 9H), 0.27 (s, 6H).

^{13}C NMR (100 MHz, $CDCl_3$): δ_C 155.5, 152.4, 149.5, 145.4, 131.9, 131.7, 125.4, 125.3, 121.7, 66.4, 31.5, 25.8, 22.6, 20.5, 18.7, 14.1, -3.7.

MS (TOF- ESI): m/z: Calcd for $C_{29}H_{32}N_2O_{11}Si$: 635.16676 $[M+Na]^+$, Found: 635.17570 $[M+Na]^+$, Δ=-12.5 ppm.

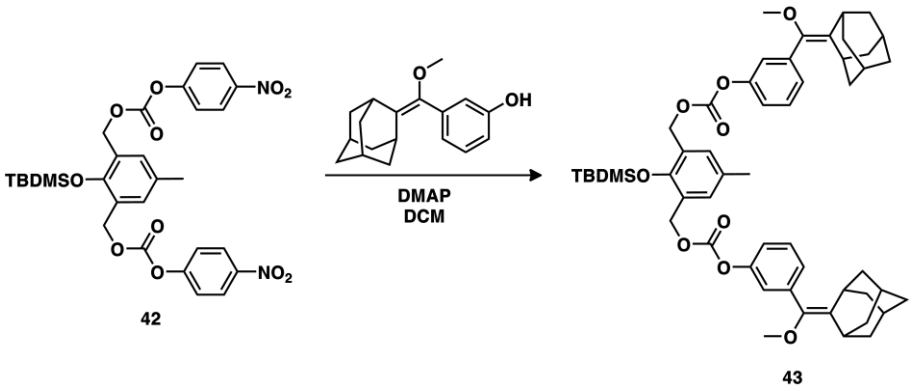

Synthesis of Compound 43: Compound **42** (0.15 g, 0.245 mmol) was dissolved in DCM. After the addition of compound **4** (0.159 g, 0.588 mmol) and DMAP (0.05 g, 0.588 mmol), the reaction mixture was stirred at room temperature overnight. When the starting material was consumed, the mixture was concentrated under vacuo and the residue was subjected to the silica gel flash column chromatography using EtOAc/ Hexane (1:5, v/v) as the eluent. Compound **43** was obtained as white solid (0.174 g, 81%).

^{1}H NMR (400 MHz, $CDCl_3$): δ_H 7.43 (t, *J*= 7.9 Hz, 2H), 7.26 (s, 2H), 7.20 (d, *J*= 7.8 Hz, 2H), 7.14 (m, 2H), 7.10 (dq, *J*= 2.3, 8.04 Hz, 2H) 5.27 (s, 4H), 3.29 (s, 6H), 3.25 (s, 2H), 2.66 (s, 2H), 2.32 (s, 3H), 1.78-1.96 (m, 24H), 1.06 (s, 9H), 0.24 (s, 6H).

^{13}C NMR (100 MHz, $CDCl_3$): δ_C 153.6, 151.0, 149.2, 137.1, 132.7, 131.5, 131.4, 128.9, 126.9, 125.7, 121.8, 119.9, 65.8, 57.9, 39.2, 39.0, 37.1, 32.1, 31.6, 30.3, 28.2, 25.9, 22.6, 2.5, 18.7, 14.1, -3.7.

MS (TOF- ESI): m/z: Calcd for $C_{53}H_{66}O_9Si$: 897.43683 $[M+Na]^+$, Found: 897.44856 $[M+Na]^+$, Δ=-13.07 ppm.

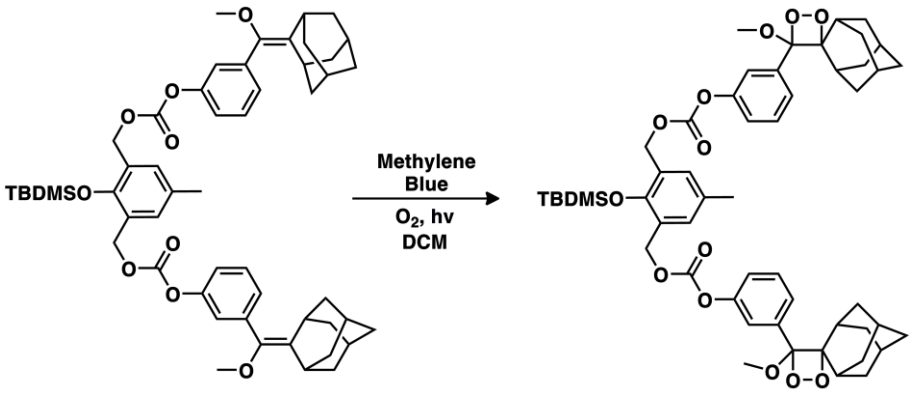

43 44

Synthesis of Compound 44: Compound **43** (0.174 g, 0.19 mmol) was dissolved in DCM. Methylene blue (5 mg) was added to the reaction mixture which was irradiated while oxygen gas was passing through it. The progress of the reaction was monitored by TLC. When TLC showed no starting material, the mixture was concentrated under vacuo and the residue was subjected to the silica gel flash column chromatography by using DCM as the eluent. Compound **44** was obtained as white solid (0.171 g, 96%).

^{1}H NMR (400 MHz, $CDCl_3$): δ_H 7.84-7.34 (br m, 4H), 7.48 (t, *J*= 7.7 Hz, 2H), 7.26-7.28 (m, 4H), 5.31 (s, 4H), 3.25 (s, 6H), 3.05 (s, 2H), 2.36 (s, 3H), 2.16 (s, 2H), 1.25-1.91 (m, 24H), 1.08 (s, 9H), 0.27 (s, 6H).

^{13}C NMR (100 MHz, $CDCl_3$): δ_C 153.4, 151.2, 149.2, 136.6, 131.6, 131.5, 129.3, 125.6, 122.0, 111.4, 95.4, 65.9, 53.4, 50.0, 36.3, 34.7, 33.1, 32.8, 32.2, 31.7, 31.5, 25.9, 25.8, 20.3, 18.7, -3.7.

CHAPTER 8

8. Chemiluminogen Probes for Palladium ion in Polar Organic Media

Ilke Simsek Turan, Ozge Yilmaz, Engin U. Akkaya

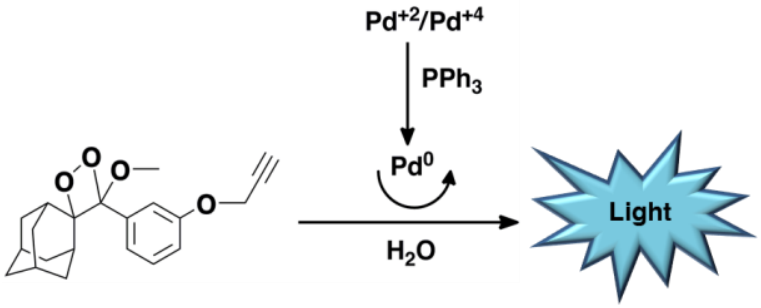

8.1. Objective

In this work, we have wanted to develop a new perspective for the sensing of Pd ions by using chemiluminescent precursor in regardless of their oxidation states and sources. Considering the fact that chemiluminescence in principle can provide a rapid, qualitative and/or quantitative test for analytes of interest, we are confident that other probes combining the power of chemiluminescence will emerge. Chemiluminogenic assessment of Pd concentrations in water, soil, etc. could be a possible application, and the bright chemiluminescence of the probe or structurally related derivatives could provide a promising alternative.

We believe that this study is expected to be pioneer in the development of chemiluminescence based Pd(0) sensors due to its analytical perspective.

8.2. Introduction

8.2.1 Palladium Sensing

C-C bond forming reactions are very substantial since it enables the construction of new substances for variety of purposes. For example, Buchwald-Hartwig, Heck, Sonogashira, Suzuki-Miyaura Reactions attract considerable attention due to their power of forming covalent bonds which are not easy to construct. These reactions proceed based on the use of palladium (Pd) as a catalyst that can be applied for the synthesis of many drugs.[145] Due to its subsequent use in pharmaceutical industry, residual Pd has been detected in the final compound even after extensive purification.

Additionally, beside their use as catalysts, Pd together with other platinum group elements like Pt, Rh, Ru have been used in the vehicle exhaust catalyst systems in order to reduce the emissions of gaseous pollutants like carbon monoxide, hydrocarbons and nitrogen oxides. Emissions resulted from vehicle catalytic

converters leads to the increase in the concentrations of Pd as with other platinum group elements in environmental areas like soil, plants, and rivers, coastal and oceanic environments. Thus in turn, Pd ions can be transported to the biological materials via the accumulation in food chain.[146]

When considering both the existence of Pd ions in the final product of pharmaceutical industry and the accumulation of them in biological materials, they represent the potential health hazards since proposed dietary intake of palladium is <1.5-15 μg/day per person and its threshold in drugs is 5-10 ppm. Products obtained as a result of Pd catalyzed reactions exceeds this threshold since they contain 300-2000 ppm residual palladium.[146]

Excessive intake of palladium and platinum group elements could lead to the development of several diseases like asthma, nausea, hair loss, increased spontaneous abortion and dermatitis. Moreover, palladium can lead to the impairment of various cellular processes by binding to thiol containing amino acids, proteins, DNA and biochemical like vitamin B_6. Beside, even low amount of Pd can cause severe allergic reactions.[147]

Therefore, methods are urgently required either for the sensitive or the selective detection of palladium ions. Till now, conventional methods like atomic absorption spectrometry, plasma emission spectrometry, solid phase micro-extraction-high performance liquid chromatography, X-ray fluorescence and inductively coupled plasma mass spectrometry have been applied due to their high sensitivity, fast measurement.[148] However, application of these methods requires the large and expensive equipment, sophisticated sample preparation techniques, precautions to prevent cross contamination form prior analysis and well-trained operators.

8.2.1.1 Fluorescent Detection of Palladium ions

When compared with the conventional methods, fluorescent detection methods would be more desirable due to their simplicity, low cost and low detection limits. In the literature, there are numerous examples for the detection of palladium ions via colorimetric and fluorescent methods.

Colorimetric probes have been developed based on detection of mostly Pd^{+2} ions. Which were designed based on the use of derivatives of *p*-nitrosophenylamino[149], azo compounds[150], oximes[151], hydrazones[152] and mercapto receptors.[153,154] Furthermore, in the case of fluorescent based methods, probes are designed based on the coordination induced fluorescence quenching[155], coordination induced fluorescence enhancement[156], reaction based detection, fluorophore formation[157] since these probes can be used to detect the analyte of interest in living cells and in living tissues microscopically upon combination with imaging techniques.

The fluorescent probes designed based on the coordination mechanism are quenched as a result of paramagnetic nature of palladium ions with a drawback of varying degrees of interferences from other transition metals. On the other hand, reaction based probes represent remarkable selectivity since the detection mechanism is preceded based on a specific reaction which enable the control of parameters effectively.[158] The probes containing allyl ether moiety proceed via Tsuji-Trost reaction which is a Pd(0) catalyzed nucleophilic substitution reaction with a substrate containing a leaving group in an allylic position.[159-161] Another type of reaction has been applied for specific detection of Pd ions is the depropargylation reaction. Propargyl ether modified probes could be hydrolyzed via two different mechanisms (figure 90) depending on the palladium source such that either via an allenyl-Pd intermediate which is resulted from the oxidative addition of Pd^{0} to the alkyne moiety or via Pd^{+2}/Pd^{+4} catalyzed hydration intermediates. The probes designed based on the depropargylation reaction is shown in figure 91 which represent remarkable results upon reaction with Pd ions.[158,162-164]

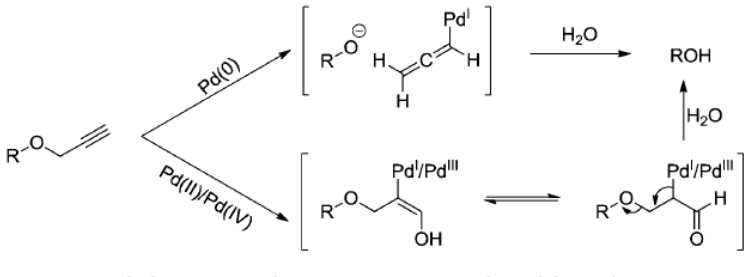

Figure 90: Pd-catalyzed depropargylation reaction[147]

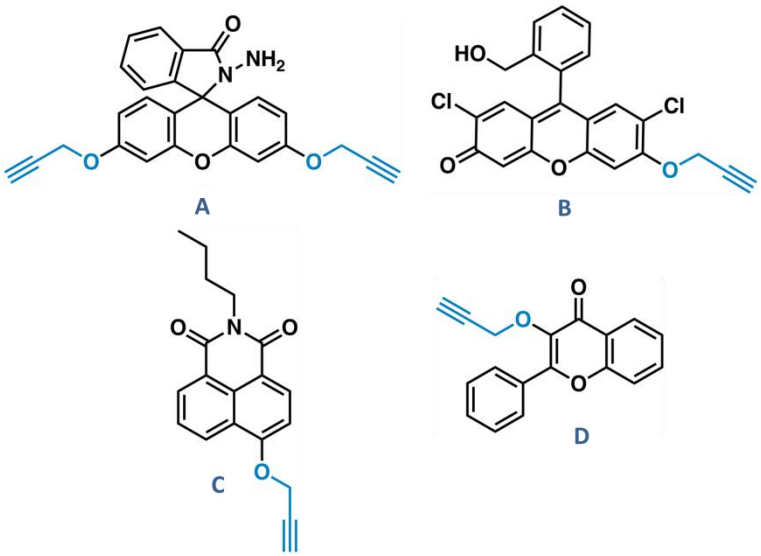

Figure 91: Fluorescent detection of Pd ion via depropargylation reaction

8.3 Design of Chemiluminescent Probe

When considering both structure and parameters affecting the emission intensity of 1,2-dioxetanes, adamantyl group was chosen to rise the thermal stability of the compound which enables the ease of use during the spectroscopic measurements. Moreover, one probe is modified with propargyl ether moiety and other probe is modified with allyl ester moiety as triggering units since the strong and specific

depropargylation reaction and Tsuji-Trost reaction initiates the decomposition reaction hastily. Phenoxide ion was chosen to trigger the ring opening reaction of dioxetane ring when the fragmentation is initiated. In the sense of activation of olefinic function, methoxy group was preferred. Triggering unit is directly introduced to the aryl moiety in order to contribute to the acceleration of the chemiluminogenic reaction.

Up to now, to the best of our knowledge, chemiluminescence based detection of palladium ions has not been published yet and we believe that this study is expected to be pioneer in chemiluminescence based sensors due to its analytical perspective.

8.4 Results and Discussion

8.4.1 Synthetic Approach

For the synthesis of our probe, we have used Wadworth-Emmons Wittig Olefination reaction other than McMurry coupling reaction which enables the formation of three possible products as coupled ketone, coupled ester and coupled ketone-ester. Because of the formation of three possible products, the yield of the reaction is very low and it favors the formation of coupled ketone. Additionally, when performing the reaction, we have almost no control over it and also, the reaction proceed superficially for the synthesis of dioxetane derivatives. In the case of Wittig Olefination, we construct the structure gradually starting with the protection of 3-hydroxybenzaldehyde as benzoyl ester derivative in order to prevent polymerization reaction during the acetal formation. For the construction of alkoxy part of the probe that is either responsible for the activation of olefinic function for singlet oxygen addition reaction or necessary for the introduction of olefinic group, acetal functionally is introduced to the structure via *p*-toluenesulfonic acid catalyzed addition of 2,2-dimethoxypropane. For the generation of double bond in the final structure via Wittig olefination, as it is understood from its name, we have to introduce phosphonate functionality to the structure via Michaleis-Arbusov Reaction

in the catalysis of titanium tetrachloride. Titanium tetrachloride is Lewis acid which hastens the reaction at low temperatures and enables the simple isolation of the desired product. Subsequent treatment of phosphonate derivative with LDA abstracts the acidic proton in order to generate ylide of compound **36** which was then reacted with adamantanone to form the olefin **37**.

For the synthesis of probe **46**, propargyl unit has to be introduced before photooxidation reaction due to the sensitivity and reactivity of the four membered units. Propargylation of compound **37** was achieved via nucleophilic substitution reaction of propargyl bromide. Finally, the synthesis of the probe was accomplished with the photooxidation of the dioxetane **45**. Oxygen molecule founds in nature as in triplet state however, singlet oxygen is the reactive one for the cycloaddition reaction that can be obtained by photooxidation of it in the presence of photosensitizers. In this work, we have used methylene blue (MB) as photosensitizer which is excited via the irradiation. While MB relaxes back to ground state, it transfers its energy to triplate state oxygen and generates singlet oxygen which is then reacts with olefin **45** through [2+2] cycloaddition reaction to form **46** (figure 92) . When we examine the structure of the probe in terms of organic functionalities, oxygen is preferentially is added to the double instead of the alkyne unit since the electron density of the double bond due to the presence of electron pumping methoxy unit is higher compared to the alkyne unit.

For the synthesis of the second probe **48**, we have modified the compound **37** through nucleophilic substitution reaction of allylchloroformate in the catalysis of DMAP. Subsequent photooxidation of compound **47** with MB under irradiation, compound **48** could be synthesized. We have performed photooxidation reactions at -78 °C but during the synthesis of probe **48**, we have performed the reaction deliberately due to either the high sensitivity of carbonate functionally or the sensitivity of allyl group which comes from the ease of CO_2 elimination from the structure.

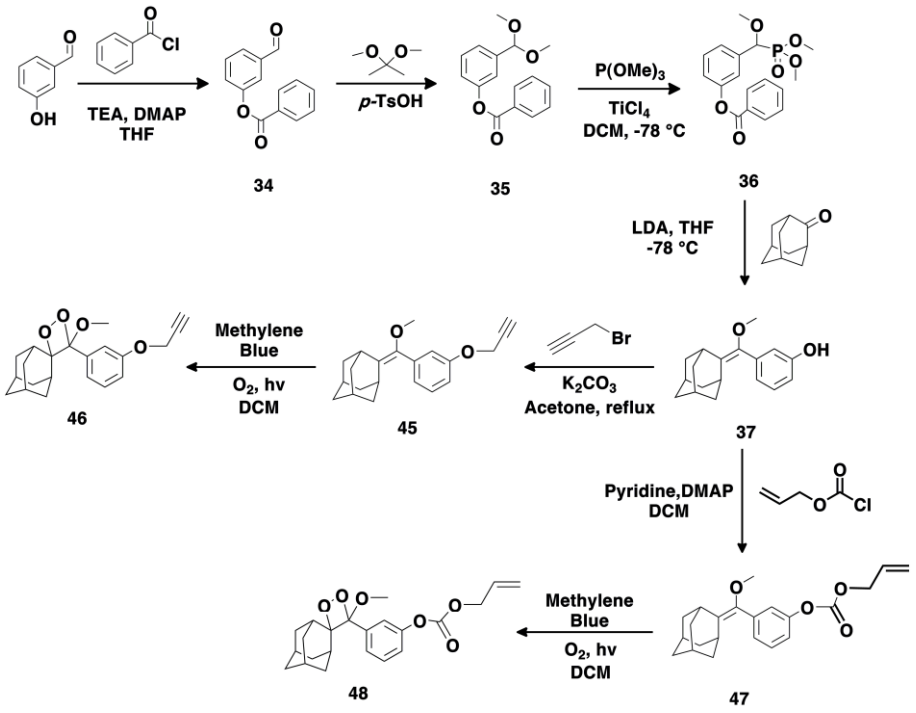

Figure 92: Synthetic scheme for chemiluminescent palladium probes **46** and **48**

8.4.2 Working Principle

We have designed the probe **46** which detects the palladium ions as a result of depropargylation reaction. At the beginning, we have expected that the decomposition mechanism has been preceded as the classical depropargylation reaction however, as a result of the nature of chemiluminescence; we have observed depropargylation reaction regardless of the charge of palladium ions. The proposed chemiluminescent depropargylation reaction has been initiated with the oxidative addition of Pd(0) to the alkyne moiety which results in the formation of allenyl-Pd intermediate **A**. Thus in turn, in the act of water molecules as nucleophile, the intermediate **A** leads to the formation of compound **B**. Since the pKa of phenoxide ion is around 9, it is in equilibrium with its phenolic form. Because of that through the addition of strong base to the medium, the equilibrium is driven to the formation of activated form of 1,2-dioxetane which transfers electron to the four membered

ring to initiates its decomposition for the generation of excited state molecule **D** while it relaxes back to ground state **E**, results in the emission of photon.

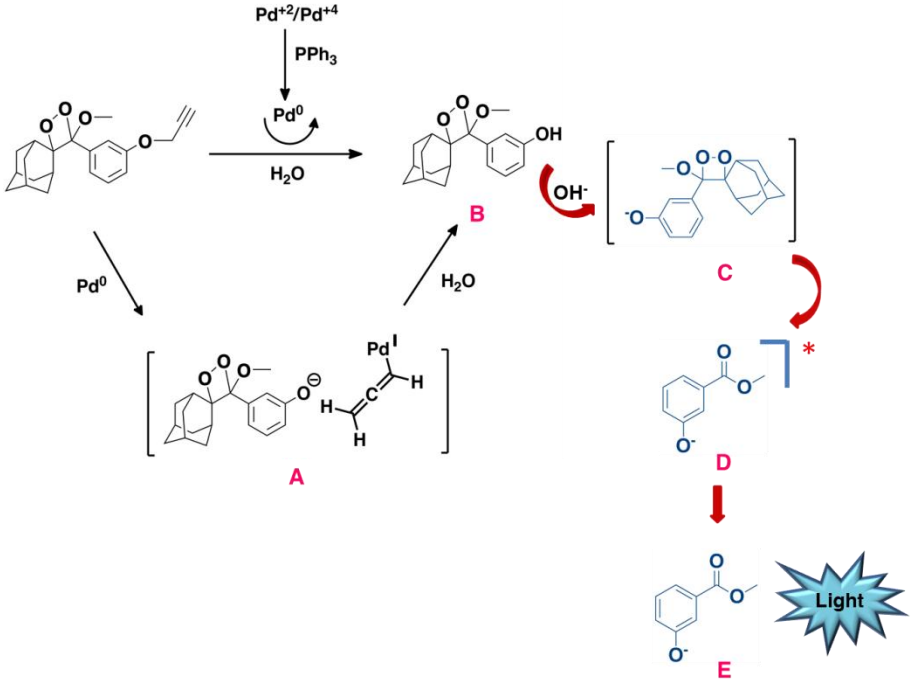

Figure 93: Proposed chemiluminescent depropargylation process catalyzed by Pd ions

In the case of probe **2** (**48**), we have expected that it works through Tsuji-Trost reaction which is started with the allylic oxidative insertion of Pd(0) **A** which leads to the formation of compound **B** as a result of nucleophilic addition water. Since the pKa of phenoxide ion is around 9, it is in equilibrium with its phenolic form. Because of that through the addition of strong base to the medium, the equilibrium is driven to the formation of activated form of 1,2-dioxetane which transfers electron to the four membered ring to initiates its decomposition for the generation of excited state molecule **D** while it relaxes back to ground state **E**, results in the emission of photon. However, we could not be able to prevent the background emission resulted from the addition of strong base to the medium due to the lability of formate moiety to

nucleophilic attack. Because of that, probe **2** does not work specifically as we expected at the beginning.

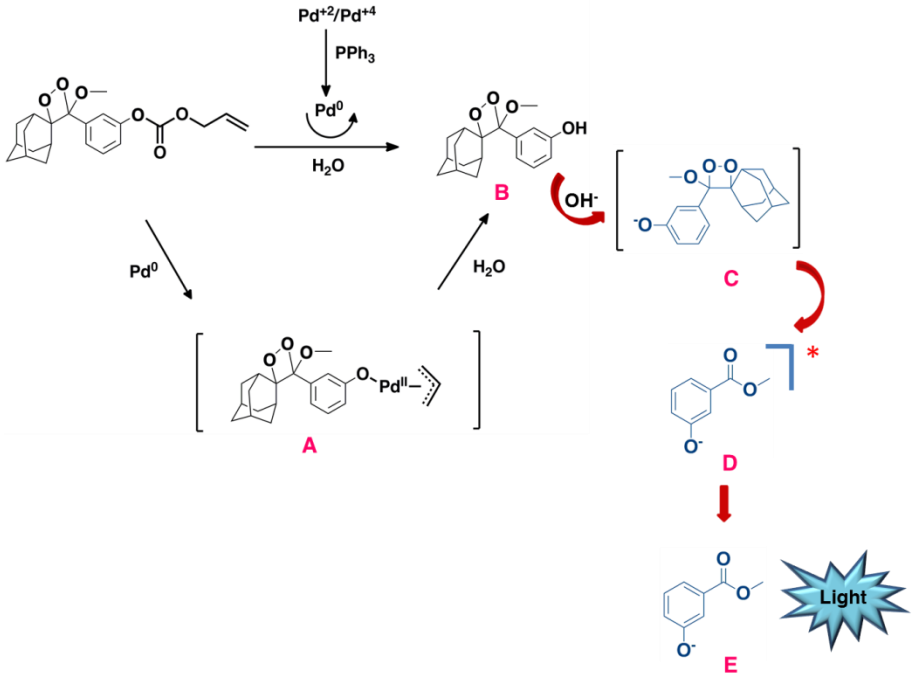

Figure 94: Proposed chemiluminescent Pd^0 catalyzed Tsuji-Trost reaction

8.4.3 Spectral Proofs for Chemiluminogenic Fragmentation

During the analytical survey of the palladium probes, we have used $PdCl_2$ as the representative palladium species since it is the most toxic among them. In order to understand the fragmentation process of our Pd probes, we have wanted to figure out depropargylation reaction proceeds through whether Pd(0) or not Pd(II)/Pd(IV). For this, we have used $PdCl_2$ either in the presence or absence of PPh_3 which is used for the in situ generation of Pd(0). Then, we have realized that the depropargylation reaction of our chemiluminogenic probe is decomposed via Pd(0). Since the emission intensity of dioxetane derivatives can be controlled with the changes in pH of the medium or with the reduction of activation energy necessary for the fragmentation reaction, we have wanted to enhance emission intensity by playing along with both

parameters. In the literature, chemiluminogenic reactions require the use of strong base since the fragmentation of phenoxide ion is faster than phenol group. By considering this, we have used strong base in a way that it will not create any background emission in the absence of Pd ions. In our case, strong base addition is necessary in order to eliminate the effect of acidic units as a result of ligand exchange during in situ generation of Pd(II)/Pd(IV). Additionally, in order to increase the rate of depropargylation reaction thus in turn fragmentation reaction ending up with light emission, the reaction temperature was optimized as the 70 °C. After the determination of these parameters, we have continued with Pd ion titration of chemiluminogenic probe **46**. Since the emission intensity is correlated with the concentration of analyte of interest, we have observed that the higher the concentration of Pd(0), the stronger the emission as shown in figure 95. This is also related with the enhancement of the reaction rate with increase in analyte concentration which is responsible for the initiation of depropargylation reaction.

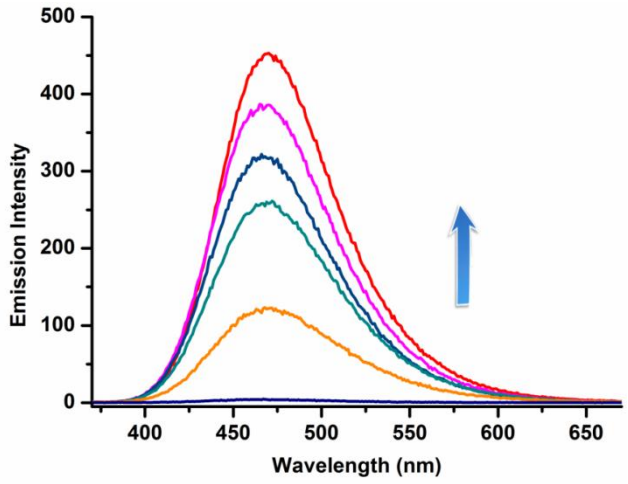

Figure 95: Chemiluminescence Spectra of probe **46** (200 μM) in the presence of increasing concentrations of $PdCl_2$ (concentrations: 0.1, 0.2, 0.3, 0.4, 0.5, 0.6 mM) in DMSO-H_2O (95:5, v/v) solution with Na_2CO_3-$NaHCO_3$ Buffer (50 mM, pH: 9.0) involving PPh_3 (1 mM) at 70 °C.

At the very beginning, we have figured out that chemiluminogenic depropargylation reaction occurs via Pd(0) ion so that the amount of PPh_3 as reducing is also crucial for the light emission. After the titration of the probe in the presence of varying

concentrations of PPh_3, we have identified that 1mM PPh_3 works well as shown in figure 96. The concentration of PPh_3 is critical because excess PPh_3 stabilizes the catalytically inactive, coordinately saturated palladium species Pd^0L_4. Therefore, it leads to decrease in the concentration of reactive palladium species but shifting the equilibrium from PdL_{4-n} to PdL_4 and thus in turn retards the depropargylation reaction.[146]

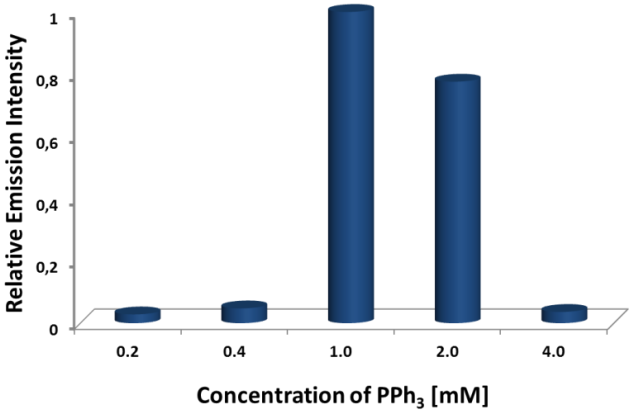

Figure 96: Chemiluminescence Spectra of pH dependent deallylation of Dioxetane **46** (200 µM) in the presence of varying concentrations of PPH_3 in DMSO-H_2O (95:5, v/v) solution with Na_2CO_3-$NaHCO_3$ Buffer (50 mM, pH: 9.0) involving $PdCl_2$ (0.4 mM), at 70 °C.

Furthermore, when we consider the reaction mechanism, nucleophile is needed during the depropargylation reaction that is H_2O in our case. In order to obtain optimized emission intensity, the amount of water used in the reaction is also critical due to the possibility of protonation of phenoxide ion which is responsible for the fragmentation process. Therefore, we have made spectroscopic measurements by using different buffer percentages in DMSO as shown in figure 97. It can be concluded that the higher the percentages of buffer in DMSO, the higher possibility of protonation of phenoxide ion and the lower the emission intensity.

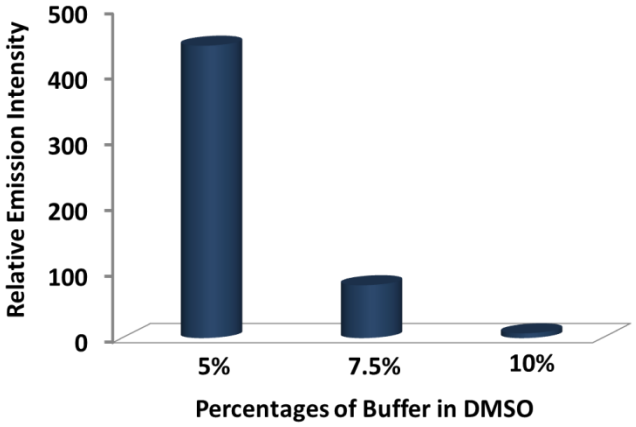

Figure 97: Chemiluminescence Intensity of Dioxetane **46** (200 μM) at different percentages of buffer (Na_2CO_3-$NaHCO_3$ buffer, 50 mM, pH: 9.0) involving $PdCl_2$ (0.4 mM), PPh_3 (1 mM) at 70 °C.

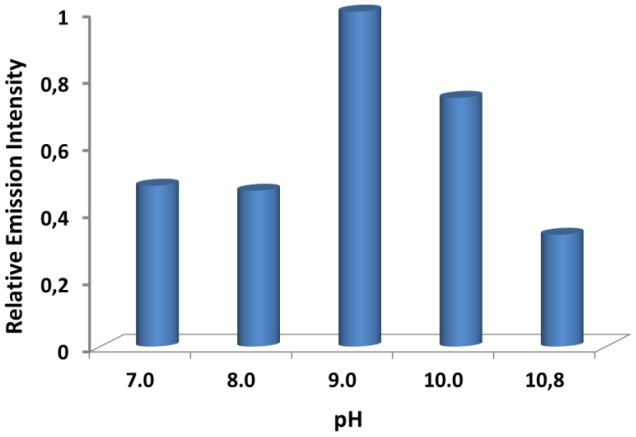

Figure 98: Chemiluminescence Spectra of pH dependent deallylation of Dioxetane **46** (200 μM) in the presence of $PdCl_2$ (0.4 mM), PPh_3 (1 mM) in DMSO-H_2O (95:5, v/v) solution with Kpi Buffer (50 mM for pH: 7.0, 8.0) (Na_2CO_3-$NaHCO_3$ Buffer (50 mM for pH: 9.0-10.8) involving PPh_3 (1 mM) at 70 °C

Although we have used strong base for the enhancement of decomposition of dioxetane, pH of the medium is very significant since nucleophilicity is increased in basic pH (figure 99). Moreover, pH of phenoxide ion is around 9 so that it is in equilibrium with its phenol form. When the pH is lowered, the possibility of protonation of phenoxide ion is increased which leads to increase in the possibility of

reduced emission intensity. When the pH of the medium is above 9 although it seems that it is better for chemiluminescent decomposition reaction, the emission intensity is lowered due to the chelation of palladium.[146] There is a detrimental equilibrium between the number of parameters affecting either reaction conditions or emission intensity and the conditions which are needed to be optimized.

Since we have figured out that chemiluminogenic depropargylation reaction fragmented via the in situ generated Pd(0), we have wanted to prove this with the analytical measurement after the optimization of reaction conditions. It is clear from the figure 98 that in the sense of fragmentation of chemiluminogenic precursor, Pd(0) is the active ion and it is free from the palladium source. When we examine the figure, emission intensity is lowered in the case of Pd $(PPh_3)_4$ which can be attributed to the air sensitivity of the reagent. Therefore, in situ generation of Pd(0) is more effective in terms of the generation of active palladium species.

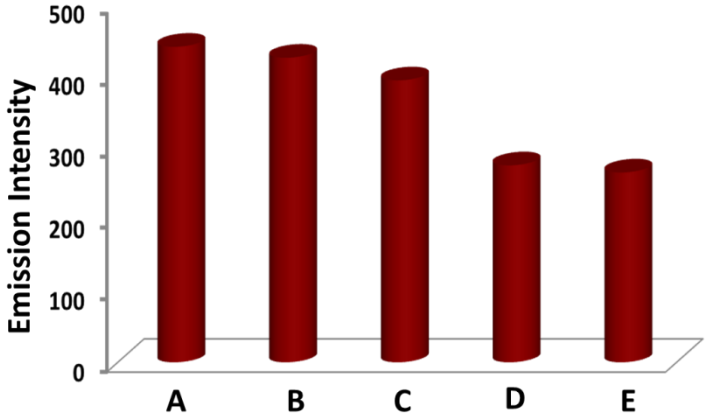

Figure 99: Chemiluminogenic response of the probe toward various Pd species A= $PdCl_2$, B= Na_2PdCl_4, C= Na_2PdCl_6, D=$Pd(OAc)_2$, E=$Pd(PPh_3)_4$

After the optimization of analytical conditions, we have proved the specificity of our probe to Pd ions. For this, we have made chemiluminescent measurement of our probe in the presence of different ions and as shown from figure 100, we have

proved that chemiluminescent depropargylation reaction of 1,2-dioxetanes can only be decomposed in the presence of Pd(0) ions.

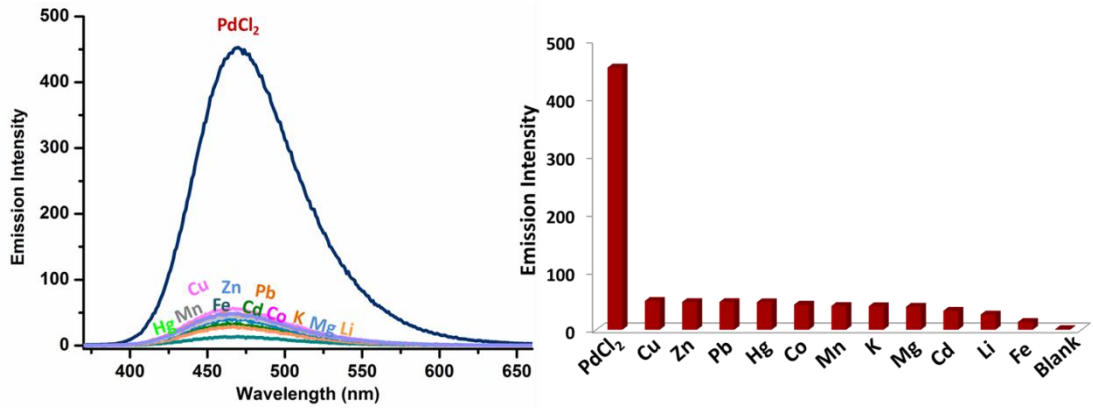

Figure 100: Chemiluminescence Emission Intensity of Dioxetane **46** (200 µM) upon addition of different metal ions in DMSO-H_2O (95:5, v/v) solution with Na_2CO_3-$NaHCO_3$ Buffer (50 mM, pH: 9.0) involving PPh_3 (1 mM) at 70 °C. Metals ions were used as perchlorate salts.

Furthermore, we have studied the detection limit of the probe in DMSO/buffer mixtures. We have founded standard deviation as 0.026268 and the slope of the graph as 885,92 thus in turn, detection limit was calculated according to the equation as 88µM.

When we have considered the probe **48** which decomposes via Tsuji-Trost reaction, we have not observed any specific emission resulted from the compounds' Pd(0) deallylation reaction. Due to the presence of carbonate functionality, addition of strong base leads to background emission in the absence of palladium ion.

1,2-dioxetane modified with propargyl ether unit is suitable for the Chemiluminogenic detection in situ generated Pd(0) ions due to the strength of the ether bond against the strong base and also the lability of this bond Pd(0) catalyzed depropargylation reaction. The strength of the ether bond introduces selectivity at some point compared with the allylic allie **48**.

8.5 Experimental Details

8.5.1 Detection Limit Measurements

The detection limit for probe and reference compound was calculated based on chemiluminescence titration. In order to determine the S/N ratio, the chemiluminescence emission intensity of the blanks without Pd was measured 10 times and standard deviation of these blanks was calculated. Chemiluminescence emission intensities of the probe in the presence of Pd ions were plotted as a concentration of Pd in order to determine the slopes. The linear relationship between emission intensity and Pd(0) concentration were determined and detection limits were calculated according to the equation,

Detection limit: $3\sigma/m$

where σ represents the standard deviation of the blank measurements, m represents the slope between intensity versus sample concentration.

8.5.2 Synthesis

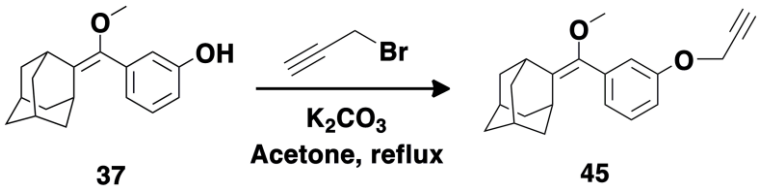

37 45

Synthesis of Compound 45: K_2CO_3 (0.107 g, 0.78 mmol) was added to the reaction mixture of compound **37** (0.070 g, 0.26 mmol) and propargyl bromide (45 µL, 0.52 mmol) dissolved in 5 ml acetone. After the addition of catalytic amount of KI, reaction mixture was refluxed at 65 °C. The progress of the reaction was monitored by TLC. When TLC showed no starting material, the reaction was extracted with water (3x100 mL) and combined organic phases were dried over anhydrous Na_2SO_4.

After removal of the solvent, the residue was purified by silica gel flash column chromatography using EtOAc / Hexane (1:5, v/v) as the eluent. Compound **45** was obtained as colorless solid (0.075 g, 94%).

^{1}H NMR (400 MHz, $CDCl_3$): δ_H 7.29 (td, *J*=8.1, 1.1 Hz, 1H), 6.99-6.97 (m, 2H), 6.94-6.91 (m, 1H), 4.72 (s, 2H), 3.32 (s, 1H), 3.28 (s, 1H), 2.65 (s, 1H), 2.55-2.54 (m, 1H), 2.00-1.81 (m, 12H).

^{13}C NMR (100 MHz, $CDCl_3$): δ_C 157.3, 143.2, 136.9, 131.7, 128.9, 122.7, 115.6, 114.0, 75.5, 57.7, 55.7, 39.25, 39.07, 37.2, 32.2, 30.2, 28.3.

MS (TOF- ESI): m/z: Calcd for $C_{21}H_{24}O_2$: 309.18491 $[M+H]^+$, Found: 309.18983 $[M+H]^+$, Δ=-1.68 ppm.

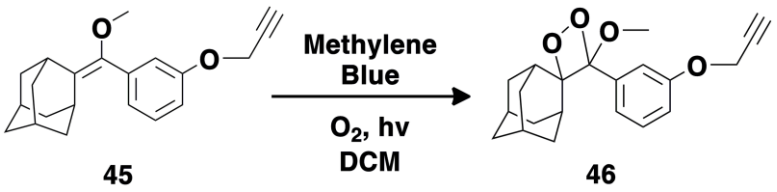

Synthesis of Compound 46: Compound **45** (0.10 g, 0.32 mmol,) was dissolved in DCM. Methylene blue (5 mg) was added to the reaction mixture which was irradiated while oxygen gas was passing through it. The progress of the reaction was monitored by TLC. When TLC showed no starting material, the mixture was concentrated under vacuo and the residue was subjected to the silica gel flash column chromatography by using DCM as the eluent. Compound **46** was obtained as white solid (0.108 g, 98%).

^{1}H NMR (400 MHz, $CDCl_3$): δ_H 7.37-7.13 (br, m, 3H), 7.05-7.02 (m, 1H), 4.74 (s, 2H), 3.24 (s, 3H), 3.04 (s, 1H), 2.52 (s, 1H), 2.22 (s, 1H), 1.92-1.01 (m, 12H).

^{13}C NMR (100 MHz, $CDCl_3$): δ_C 157.5, 136.3, 129.3, 122.8, 121.3, 120.2, 119.1, 116.2, 111.9, 95.4, 75.7, 55.8, 49.9, 36.4, 34.7, 33.1, 32.9, 32.3, 31.6, 31.5, 26.0, 25.9.

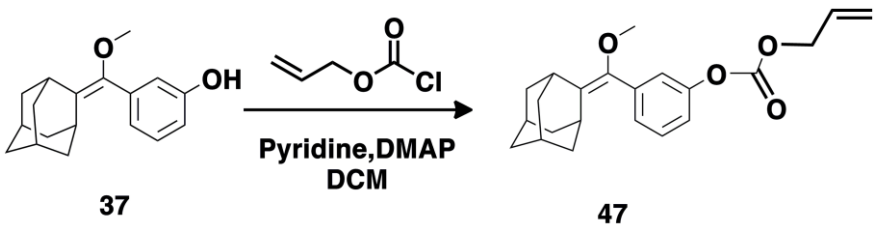

Synthesis of Compound 47: Pyridine (56 µL, 0.7 mmol) was added to the reaction mixture of compound **37** (0.135 g, 0.5 mmol) dissolved in DCM and the reaction mixture was stirred at room temperature for 10 min. After the addition of catalytic amount of DMAP, allyl chloroformate (0.72 g ,0.6 mmol) dissolved in DCM was added dropwise to the reaction mixture while it was kept at 0 °C and left to stir at room temperature overnight. When TLC shows no starting material, the reaction mixture was concentrated under vacuo and crude product was subjected to the flash column chromatography by using EtOAc/Hexane (1:5, v/v) as the eluent. Compound **47** was obtained as colorless solid (0.150 g, 85%).

^{1}H NMR (400 MHz, $CDCl_3$): δ_H 7.37 (t, *J*=7.8 Hz, 1H), 7.22 (d, *J*=7.6 Hz, 1H), 7.16 (s, 1H), 7.12 (d, *J*=8.1 Hz, 1H), 6.07-5.99 (m, 1H), 5.45 (d, *J*=14.4 Hz, 1H), 5.34 (d, *J*= 9.2 Hz, 1H), 4.77 (m, 2H), 3.32 (s, 3H), 3.27 (s, 1H), 2.68 (s, 1H), 2.00-1.81 (m, 12H).

^{13}C NMR (100 MHz, $CDCl_3$): δ_C 153.4, 150.9, 142.5, 137.1, 132.6, 131.1, 128.9, 126.9, 121.7, 119.8, 119.4, 69.1, 57.8, 39.1, 39.0, 37.1, 32.1, 30.2, 26.2.

MS (TOF- ESI): m/z: Calcd for $C_{22}H_{26}O_4$: 355.19039 $[M+H]^+$, Found: 355.19886 $[M+H]^+$, Δ=-1.52 ppm.

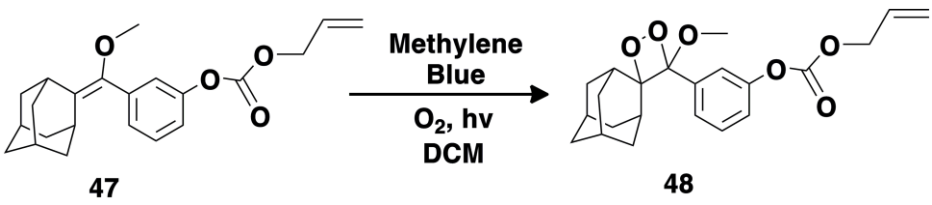

Synthesis of Compound 48: Compound **47** (0.12 g, 0.34 mmol,) was dissolved in DCM. Methylene blue (5 mg) was added to the reaction mixture which was irradiated while oxygen gas was passing through it. The progress of the reaction was monitored by TLC. When TLC showed no starting material, the mixture was concentrated under vacuo and the residue was subjected to the silica gel flash column chromatography by using DCM as the eluent. Compound **48** was obtained as white solid (0.124 g, 95%).

^{1}H NMR (400 MHz, $CDCl_3$): δ_H 7.46 (br, m, 3H), 7.25 (dd, *J*= 9.1, 2.40 Hz, 1H), 6.06-5.96 (m, 1H), 5.47-5.41 (m, 1H), 5.36-5.33 (m, 1H), 4.76 (d, *J*= 5.8 Hz, 2H), 3.23 (s, 3H), 3.04 (s, 1H), 2.15 (s, 1H), 1.82-0.99 (m, 12H).

^{13}C NMR (100 MHz, $CDCl_3$): δ_C 153.2, 151.1, 136.6, 131.0, 129.3, 127.2, 125.6, 122.3, 122.0, 119.5, 117.5, 95.3, 69.2, 49.9, 36.3, 34.7, 33.1, 32.8, 32.2, 31.7, 31.5, 26.0, 25.8.

CHAPTER 9

9. CONCLUSION

In this thesis, we have proposed novel approaches for the design and synthesis of fluorescent compounds as for fluorescent probes, protein labeling agents, and photodynamic therapy agents. They have been developed by considering biologically important thiols like cysteine (Cys), homocysteine (HCys) and gluthathione (GSH) since the abnormal levels of biological thiols are associated with many human diseases and even with cancer. Besides, since there is a growing need for the development of sensitive, selective and rapid detection of biologically important anions and metals like fluoride and palladium, we have tried to devise new sensing methodology like chemiluminescence due to its fascinating advantages.

In the first project of the journey, we have devised and evaluated two nitroolefin-BODIPY conjugates (**1** and **7**) operating at different wavelengths in order to sense and detect biothiols (Cys, Hcy and GSH) in aqueous solutions and met with success. Both probes acted as colorimetric (blue shift) and fluorometric (turn on) dual sensors for the selective, sensitive and rapid detection of biologically significant thiols. Based on our findings, practicality of present protocol was highlighted and wherein our rewarding multi-faceted design was successfully realized. Our works along these areas are in progress. In combination with thiol sensing project, we have devised new nitroolefin functionalized Bodipy derivatives for labeling applications of proteins which has thiol moieties. Thorough the colorimetric (blue shift) and fluorometric changes (turn on) via conjugate addition; probes designed to label proteins in biological systems with high selectivity and sensitivity in a developed response range. Our works covering the design of new labeling agents and strategies are in progress. In the sense of third project (chapter 5), we took advantage of activating

(uncaging) a photosensitizer by a cancer-related cellular parameter Glutathione. Before the uncaging reaction, the PS-Q conjugate has little to negligible toxic activity on the selected cell cultures. GSH mediated uncaging results in a highly active photodynamic agent. We are confident that as the stumbling blocks hindering the broader applicability of photodynamic therapy are removed, the methodology will be more effective competitor of the more established treatment protocols. We shall continue to do our part in providing chemical/photophysical avenues towards that end.

In case of sensing projects, we have taken the advantage of chemiluminescence to devise new structures for biologically important anion (fluoride) and metal (palladium). In the case of chemiluminescent sensing of fluoride ions, we demonstrated that using self-immolative linkers multiple chemiluminescence events can be triggered. This approach offers a chemical avenue for enhancing the signal produced in response to a given analyte. Considering the fact that chemiluminescence in principle can provide a rapid, qualitative and/or quantitative test for analytes of interest, we are confident that other probes combining the power of self-immolation and chemiluminescence will emerge. Rapid assessment of fluoride concentrations in drinking water could be a possible application, and the bright chemiluminescence of the designed and synthesized probe or structurally related derivatives could provide a promising alternative. There are several literature works for fluorescent sensing of palladium ions either depending or regardless of the charge however, the only innovation of these studies are the fluorophores that they use and detection sensitivity of the system. On the other hand, we have tried to develop new perspective for sensing of palladium ions in terms of the method that we have preferred to apply. With this radical reform, we have proved that with the power of chemiluminescence which combine rapid, qualitative and/or quantitative test for analytes of interest, we have analyzed the palladium ions regardless of their charge and source in aqueous environment. Although detection limit of the probe is 88 μM which is higher compared to fluorogenic ones, this idea inspires the scientists for the development of new chemiluminescent probes for highly sensitive and

selective detection of palladium ions. As a future work, sensitive and water soluble type of the probe with enhanced signal emission can be designed, synthesized and characterized. Considering the convenience of the method and substantial results, we are confident that other chemiluminogenic probes will emerge.

REFERENCES

(1) Wainwright, M.: *Photosensitisers in biomedicine*; John Wiley & Sons, 2009.

(2) Steiner, U. E.: Fundamentals of Photophysics, Photochemistry, and Photobiology. In *Photodynamic Therapy*; Springer, 2014; pp 25-58.

(3) Sauer, M.; Hofkens, J.; Enderlein, J. Basic Principles of Fluorescence Spectroscopy. *Handbook of Fluorescence Spectroscopy and Imaging: From Single Molecules to Ensembles* **2011**, 1-30.

(4) Wayne, R. P.; Wayne, R. P. Principles and applications of photochemistry. **1988**.

(5) Itoh, T. Fluorescence and phosphorescence from higher excited states of organic molecules. *Chemical reviews* **2012**, *112*, 4541-4568.

(6) Ye, R.; Barron, A. R. Photoluminescence Spectroscopy and its Applications.

(7) Deshpande, S. Principles and applications of luminescence spectroscopy. *Critical reviews in food science and nutrition* **2001**, *41*, 155-224.

(8) Valeur, B.; Berberan-Santos, M. N.: *Molecular fluorescence: principles and applications*; John Wiley & Sons, 2012.

(9) Garcia-Campana, A. M.: *Chemiluminescence in analytical chemistry*; CRC Press, 2001.

(10) Lakowicz, J. R.; Masters, B. R. Principles of fluorescence spectroscopy. *Journal of Biomedical Optics* **2008**, *13*, 9901.

(11) Song, L.; Hennink, E.; Young, I. T.; Tanke, H. J. Photobleaching kinetics of fluorescein in quantitative fluorescence microscopy. *Biophysical Journal* **1995**, *68*, 2588-2600.

(12) Homocianu, M. Solvent effects on the electronic absorption and fluorescence spectra. *Journal of Advanced Research in Physics* **2011**, *2*.

(13) Li, X.; Gao, X.; Shi, W.; Ma, H. Design strategies for water-soluble small molecular chromogenic and fluorogenic probes. *Chemical reviews* **2013**, *114*, 590-659.

(14) Morris, M. C. Spotlight on Fluorescent Biosensors · Tools for Diagnostics and Drug Discovery. *ACS Medicinal Chemistry Letters* **2013**, *5*, 99-101.

(15) Boens, N.; Leen, V.; Dehaen, W. Fluorescent indicators based on BODIPY. *Chem. Soc. Rev.* **2012**, *41*, 1130-1172.

(16) Valeur, B.; Leray, I. Design principles of fluorescent molecular sensors for cation recognition. *Coordination Chemistry Reviews* **2000**, *205*, 3-40.

(17) Silva, A. P. Fluorescent PET (Photoinduced Electron Transfer) sensors as potent analytical tools. *Analyst* **2009**, *134*, 2385-2393.

(18) Matsumoto, T.; Urano, Y.; Shoda, T.; Kojima, H.; Nagano, T. A thiol-reactive fluorescence probe based on donor-excited photoinduced electron transfer: key role of ortho substitution. *Organic letters* **2007**, *9*, 3375-3377.

(19) Li, X.; Qian, S.; He, Q.; Yang, B.; Li, J.; Hu, Y. Design and synthesis of a highly selective fluorescent turn-on probe for thiol bioimaging in living cells. *Org. Biomol. Chem.* **2010**, *8*, 3627-3630.

(20) Jun, M. E.; Roy, B.; Ahn, K. H. “Turn-on” fluorescent sensing with “reactive” probes. *Chemical Communications* **2011**, *47*, 7583-7601.

(21) Han, J.; Loudet, A.; Barhoumi, R.; Burghardt, R. C.; Burgess, K. A ratiometric pH reporter for imaging protein-dye conjugates in living cells. *Journal of the American Chemical Society* **2009**, *131*, 1642-1643.

(22) Nakata, E.; Nazumi, Y.; Yukimachi, Y.; Uto, Y.; Maezawa, H.; Hashimoto, T.; Okamoto, Y.; Hori, H. Synthesis and photophysical properties of new SNARF derivatives as dual emission pH sensors. *Bioorganic & medicinal chemistry letters* **2011**, *21*, 1663-1666.

(23) Best, Q. A.; Xu, R.; McCarroll, M. E.; Wang, L.; Dyer, D. J. Design and investigation of a series of rhodamine-based fluorescent probes for optical measurements of pH. *Organic letters* **2010**, *12*, 3219-3221.

(24) Zhu, H.; Fan, J.; Xu, Q.; Li, H.; Wang, J.; Gao, P.; Peng, X. Imaging of lysosomal pH changes with a fluorescent sensor containing a novel lysosome-locating group. *Chemical Communications* **2012**, *48*, 11766-11768.

(25) Jokic, T.; Borisov, S. M.; Saf, R.; Nielsen, D. A.; Kühl, M.; Klimant, I. Highly photostable near-infrared fluorescent pH indicators and sensors based on BF2-chelated tetraarylazadipyrromethene dyes. *Analytical chemistry* **2012**, *84*, 6723-6730.

(26) Gareis, T.; Huber, C.; Wolfbeis, O. S.; Daub, J. Phenol/phenolate-dependent on/off switching of the luminescence of 4, 4-difluoro-4-bora-3a, 4a-diaza-s-indacenes. *Chemical Communications* **1997**, 1717-1718.

(27) Baruah, M.; Qin, W.; Basaric, N.; De Borggraeve, W. M.; Boens, N. BODIPY-based hydroxyaryl derivatives as fluorescent pH probes. *The Journal of organic chemistry* **2005**, *70*, 4152-4157.

(28) Murtagh, J.; Frimannsson, D. O.; O'Shea, D. F. Azide conjugatable and pH responsive near-infrared fluorescent imaging probes. *Organic letters* **2009**, *11*, 5386-5389.

(29) Yu, F.; Song, P.; Li, P.; Wang, B.; Han, K. Development of reversible fluorescence probes based on redox oxoammonium cation for hypobromous acid detection in living cells. *Chemical Communications* **2012**, *48*, 7735-7737.

(30) Tang, B.; Yu, F.; Li, P.; Tong, L.; Duan, X.; Xie, T.; Wang, X. A near-infrared neutral pH fluorescent probe for monitoring minor pH changes: imaging in living HepG2 and HL-7702 cells. *Journal of the American Chemical Society* **2009**, *131*, 3016-3023.

(31) Tang, B.; Liu, X.; Xu, K.; Huang, H.; Yang, G.; An, L. A dual near-infrared pH fluorescent probe and its application in imaging of HepG2 cells. *Chem. Commun.* **2007**, 3726-3728.

(32) Gee, K. R.; Zhou, Z.-L.; Qian, W.-J.; Kennedy, R. Detection and imaging of zinc secretion from pancreatic β-cells using a new fluorescent zinc indicator. *Journal of the American Chemical Society* **2002**, *124*, 776-778.

(33) Lee, K.-S.; Kim, H.-J.; Kim, G.-H.; Shin, I.; Hong, J.-I. Fluorescent chemodosimeter for selective detection of cyanide in water. *Organic letters* **2008**, *10*, 49-51.

(34) Rusin, O.; St. Luce, N. N.; Agbaria, R. A.; Escobedo, J. O.; Jiang, S.; Warner, I. M.; Dawan, F. B.; Lian, K.; Strongin, R. M. Visual detection of cysteine and homocysteine. *Journal of the American Chemical Society* **2004**, *126*, 438-439.

(35) HoáLee, J. Fluorescence turn-on probe for homocysteine and cysteine in water. *Chemical Communications* **2008**, 6173-6175.

(36) Huang, S.-T.; Ting, K.-N.; Wang, K.-L. Development of a long-wavelength fluorescent probe based on quinone–methide-type reaction to detect physiologically significant thiols. *Analytica chimica acta* **2008**, *620*, 120-126.

(37) Maeda, H.; Matsuno, H.; Ushida, M.; Katayama, K.; Saeki, K.; Itoh, N. 2, 4-Dinitrobenzenesulfonyl Fluoresceins as Fluorescent Alternatives to Ellman's Reagent in Thiol-Quantification Enzyme Assays. *Angewandte Chemie* **2005**, *117*, 2982-2985.

(38) Pires, M. M.; Chmielewski, J. Fluorescence imaging of cellular glutathione using a latent rhodamine. *Organic letters* **2008**, *10*, 837-840.

(39) Uchinomiya, S.; Ojida, A.; Hamachi, I. Peptide Tag/Probe Pairs Based on the Coordination Chemistry for Protein Labeling. *Inorganic chemistry* **2013**, *53*, 1816-1823.

(40) Miller, L. W.; Cornish, V. W. Selective chemical labeling of proteins in living cells. *Current opinion in chemical Biology* **2005**, *9*, 56-61.

(41) Waggoner, A. Fluorescent labels for proteomics and genomics. *Current opinion in chemical biology* **2006**, *10*, 62-66.

(42) Jung, D.; Min, K.; Jung, J.; Jang, W.; Kwon, Y. Chemical biology-based approaches on fluorescent labeling of proteins in live cells. *Molecular BioSystems* **2013**, *9*, 862-872.

(43) Marks, K. M.; Nolan, G. P. Chemical labeling strategies for cell biology. *Nature methods* **2006**, *3*, 591-596.

(44) O'Hare, H. M.; Johnsson, K.; Gautier, A. Chemical probes shed light on protein function. *Current opinion in structural biology* **2007**, *17*, 488-494.

(45) Keppler, A.; Gendreizig, S.; Gronemeyer, T.; Pick, H.; Vogel, H.; Johnsson, K. A general method for the covalent labeling of fusion proteins with small molecules in vivo. *Nature biotechnology* **2002**, *21*, 86-89.

(46) Soh, N. Selective chemical labeling of proteins with small fluorescent molecules based on metal-chelation methodology. *Sensors* **2008**, *8*, 1004-1024.

(47) Calloway, N. T.; Choob, M.; Sanz, A.; Sheetz, M. P.; Miller, L. W.; Cornish, V. W. Optimized fluorescent trimethoprim derivatives for in vivo protein labeling. *ChemBioChem* **2007**, *8*, 767-774.

(48) Dougherty, T. J.; Gomer, C. J.; Henderson, B. W.; Jori, G.; Kessel, D.; Korbelik, M.; Moan, J.; Peng, Q. Photodynamic therapy. *Journal of the National Cancer Institute* **1998**, *90*, 889-905.

(49) Buytaert, E.; Dewaele, M.; Agostinis, P. Molecular effectors of multiple cell death pathways initiated by photodynamic therapy. *Biochimica et Biophysica Acta (BBA)-Reviews on Cancer* **2007**, *1776*, 86-107.

(50) Majumdar, P.; Nomula, R.; Zhao, J. Activatable triplet photosensitizers: Magic bullets for targeted photodynamic therapy. *Journal of Materials Chemistry C* **2014**.

(51) Triesscheijn, M.; Baas, P.; Schellens, J. H.; Stewart, F. A. Photodynamic therapy in oncology. *The oncologist* **2006**, *11*, 1034-1044.

(52) Lovell, J. F.; Liu, T. W.; Chen, J.; Zheng, G. Activatable photosensitizers for imaging and therapy. *Chemical reviews* **2010**, *110*, 2839-2857.

(53) Kamkaew, A.; Lim, S. H.; Lee, H. B.; Kiew, L. V.; Chung, L. Y.; Burgess, K. BODIPY dyes in photodynamic therapy. *Chemical Society Reviews* **2013**, *42*, 77-88.

(54) Awuah, S. G.; You, Y. Boron dipyrromethene (BODIPY)-based photosensitizers for photodynamic therapy. *RSC Advances* **2012**, *2*, 11169-11183.

(55) Kuimova, M. K.; Yahioglu, G.; Ogilby, P. R. Singlet oxygen in a cell: spatially dependent lifetimes and quenching rate constants. *Journal of the American Chemical Society* **2008**, *131*, 332-340.

(56) Dolmans, D. E.; Fukumura, D.; Jain, R. K. Photodynamic therapy for cancer. *Nature Reviews Cancer* **2003**, *3*, 380-387.

(57) Juarranz, Á.; Jaén, P.; Sanz-Rodríguez, F.; Cuevas, J.; González, S. Photodynamic therapy of cancer. Basic principles and applications. *Clinical and Translational Oncology* **2008**, *10*, 148-154.

(58) Ormond, A. B.; Freeman, H. S. Dye sensitizers for photodynamic therapy. *Materials* **2013**, *6*, 817-840.

(59) Celli, J. P.; Spring, B. Q.; Rizvi, I.; Evans, C. L.; Samkoe, K. S.; Verma, S.; Pogue, B. W.; Hasan, T. Imaging and photodynamic therapy: mechanisms, monitoring, and optimization. *Chemical reviews* **2010**, *110*, 2795-2838.

(60) Ogilby, P. R. Singlet oxygen: there is still something new under the sun, and it is better than ever. *Photochemical & Photobiological Sciences* **2010**, *9*, 1543-1560.

(61) Choi, Y.; Weissleder, R.; Tung, C.-H. Selective antitumor effect of novel protease-mediated photodynamic agent. *Cancer research* **2006**, *66*, 7225-7229.

(62) Chen, J.; Stefflova, K.; Niedre, M. J.; Wilson, B. C.; Chance, B.; Glickson, J. D.; Zheng, G. Protease-triggered photosensitizing beacon based on singlet oxygen quenching and activation. *Journal of the American Chemical Society* **2004**, *126*, 11450-11451.

(63) Lo, P.-C.; Chen, J.; Stefflova, K.; Warren, M. S.; Navab, R.; Bandarchi, B.; Mullins, S.; Tsao, M.; Cheng, J. D.; Zheng, G. Photodynamic molecular beacon triggered by fibroblast activation protein on cancer-associated fibroblasts for diagnosis and treatment of epithelial cancers. *Journal of medicinal chemistry* **2008**, *52*, 358-368.

(64) Cló, E.; Snyder, J. W.; Voigt, N. V.; Ogilby, P. R.; Gothelf, K. V. DNA-programmed control of photosensitized singlet oxygen production. *Journal of the American Chemical Society* **2006**, *128*, 4200-4201.

(65) McDonnell, S. O.; Hall, M. J.; Allen, L. T.; Byrne, A.; Gallagher, W. M.; O'Shea, D. F. Supramolecular photonic therapeutic agents. *Journal of the American Chemical Society* **2005**, *127*, 16360-16361.

(66) Peng, H.; Chen, W.; Cheng, Y.; Hakuna, L.; Strongin, R.; Wang, B. Thiol reactive probes and chemosensors. *Sensors* **2012**, *12*, 15907-15946.

(67) Pace, N. J.; Weerapana, E. Diverse functional roles of reactive cysteines. *ACS chemical biology* **2012**, *8*, 283-296.

(68) Chen, X.; Zhou, Y.; Peng, X.; Yoon, J. Fluorescent and colorimetric probes for detection of thiols. *Chemical Society Reviews* **2010**, *39*, 2120-2135.

(69) Jung, H. S.; Chen, X.; Kim, J. S.; Yoon, J. Recent progress in luminescent and colorimetric chemosensors for detection of thiols. *Chemical Society Reviews* **2013**, *42*, 6019-6031.

(70) MarasanapalliáKalle, A.; JayasreeáVarma, S. A chromenoquinoline-based fluorescent off–on thiol probe for bioimaging. *Chemical Communications* **2012**, *48*, 2722-2724.

(71) Sun, Y.-Q.; Chen, M.; Liu, J.; Lv, X.; Li, J.-f.; Guo, W. Nitroolefin-based coumarin as a colorimetric and fluorescent dual probe for biothiols. *Chemical Communications* **2011**, *47*, 11029-11031.

(72) Kwon, H.; Lee, K.; Kim, H.-J. Coumarin–malonitrile conjugate as a fluorescence turn-on probe for biothiols and its cellular expression. *Chem. Commun.* **2011**, *47*, 1773-1775.

(73) JungáKim, M. A thiol-specific fluorescent probe and its application for bioimaging. *Chemical Communications* **2010**, *46*, 2751-2753.

(74) Ulrich, G.; Goze, C.; Guardigli, M.; Roda, A.; Ziessel, R. Pyrromethene dialkynyl borane complexes for “Cascatelle” energy transfer and protein labeling. *Angewandte Chemie* **2005**, *117*, 3760-3764.

(75) Niu, S. L.; Massif, C.; Ulrich, G.; Ziessel, R.; Renard, P.-Y.; Romieu, A. Water-solubilisation and bio-conjugation of a red-emitting BODIPY marker. *Organic & biomolecular chemistry* **2011**, *9*, 66-69.

(76) Ortega, A. L.; Mena, S.; Estrela, J. M. Glutathione in cancer cell death. *Cancers* **2011**, *3*, 1285-1310.

(77) Ito, M.; Shibata, A.; Zhang, J.; Hiroshima, M.; Sako, Y.; Nakano, Y.; Kojima-Aikawa, K.; Mannervik, B.; Shuto, S.; Ito, Y. Universal Caging Group for the in-Cell Detection of Glutathione Transferase Applied to 19F NMR and Bioluminogenic Probes. *ChemBioChem* **2012**, *13*, 1428-1432.

(78) Forman, H. J.; Fukuto, J. M.; Torres, M. Redox signaling: thiol chemistry defines which reactive oxygen and nitrogen species can act as second messengers. *American Journal of Physiology-Cell Physiology* **2004**, *287*, C246-C256.

(79) Rahman, I.; MacNee, W. Oxidative stress and regulation of glutathione in lung inflammation. *European Respiratory Journal* **2000**, *16*, 534-554.

(80) Yeh, C. C.; Hou, M. F.; Wu, S. H.; Tsai, S. M.; Lin, S. K.; Hou, L. A.; Ma, H.; Tsai, L. Y. A study of glutathione status in the blood and tissues of patients with breast cancer. *Cell biochemistry and function* **2006**, *24*, 555-559.

(81) Cakmak, Y.; Kolemen, S.; Duman, S.; Dede, Y.; Dolen, Y.; Kilic, B.; Kostereli, Z.; Yildirim, L. T.; Dogan, A. L.; Guc, D. Designing Excited States: Theory-Guided Access to Efficient Photosensitizers for Photodynamic Action. *Angewandte Chemie* **2011**, *123*, 12143-12147.

(82) Bonacin, J. A.; Engelmann, F. M.; Severino, D.; Toma, H. E.; Baptista, M. S. Singlet oxygen quantum yields (Φd) in water using beetroot extract and an array of LEDs. *Journal of the Brazilian Chemical Society* **2009**, *20*, 31-36.

(83) Ronzani, F.; Trivella, A.; Arzoumanian, E.; Blanc, S.; Sarakha, M.; Richard, C.; Oliveros, E.; Lacombe, S. Comparison of the photophysical properties of three phenothiazine derivatives: transient detection and singlet oxygen production. *Photochemical & Photobiological Sciences* **2013**, *12*, 2160-2169.

(84) Dodeigne, C.; Thunus, L.; Lejeune, R. Chemiluminescence as diagnostic tool. A review. *Talanta* **2000**, *51*, 415-439.

(85) Garcia-Campana, A.; Baeyens, W.; Cuadros-Rodriguez, L.; Ales, B. F.; Bosque-Sendra, J.; Gamiz-Gracia, L. Potential of chemiluminescence and bioluminescence in organic analysis. *Current Organic Chemistry* **2002**, *6*, 1-20.

(86) García-Campaña, A.; Baeyens, W. Principles and recent analytical applications of chemiluminescence. *Analusis* **2000**, *28*, 686-698.

(87) Fereja, T. H.; Hymete, A.; Gunasekaran, T. A Recent Review on Chemiluminescence Reaction, Principle and Application on Pharmaceutical Analysis. *ISRN Spectroscopy* **2013**, *2013*.

(88) Jimenez, A.; Navas, M. Chemiluminescence methods (present and future). *Grasas y Aceites* **2002**, *53*, 64-75.

(89) Roda, A.; Pasini, P.; Guardigli, M.; Baraldini, M.; Musiani, M.; Mirasoli, M. Bio-and chemiluminescence in bioanalysis. *Fresenius' journal of analytical chemistry* **2000**, *366*, 752-759.

(90) Baeyens, W.; Schulman, S.; Calokerinos, A.; Zhao, Y.; Garćia Campaña, A. M.; Nakashima, K.; De Keukeleire, D. Chemiluminescence-based detection: principles and analytical applications in flowing streams and in immunoassays. *Journal of pharmaceutical and biomedical analysis* **1998**, *17*, 941-953.

(91) Baeyens, W.; Bruggeman, J.; Lin, B. Enhanced chemiluminescence detection of some dansyl amino acids in liquid chromatography. *Chromatographia* **1989**, *27*, 191-193.

(92) White, E. H.; Bursey, M. M. Chemiluminescence of luminol and related hydrazides: the light emission step. *Journal of the American Chemical Society* **1964**, *86*, 941-942.

(93) White, E. H.; Zafiriou, O.; Kagi, H. H.; Hill, J. H. Chemilunimescence of luminol: The chemcial reaction. *Journal of the American Chemical Society* **1964**, *86*, 940-941.

(94) Schroeder, H. R.; Yeager, F. M. Chemiluminescence yields and detection limits of some isoluminol derivatives in various oxidation systems. *Analytical Chemistry* **1978**, *50*, 1114-1120.

(95) McCapra, F.; Behesti, I. Bioluminescence and Chemiluminescence: Instruments and Applications, ed. by K. van Dyke. *CRC Press: Boca Raton, FL* **1985**, *1*, 9-42.

(96) Han, J.; Jose, J.; Mei, E.; Burgess, K. Chemiluminescent Energy-Transfer Cassettes Based on Fluorescein and Nile Red. *Angewandte Chemie International Edition* **2007**, *46*, 1684-1687.

(97) Yuan, H.; Chong, H.; Wang, B.; Zhu, C.; Liu, L.; Yang, Q.; Lv, F.; Wang, S. Chemical molecule-induced light-activated system for anticancer and antifungal activities. *Journal of the American Chemical Society* **2012**, *134*, 13184-13187.

(98) Bailey, T. S.; Pluth, M. D. Chemiluminescent Detection of Enzymatically Produced Hydrogen Sulfide: Substrate Hydrogen Bonding Influences Selectivity for H2S over Biological Thiols. *Journal of the American Chemical Society* **2013**, *135*, 16697-16704.

(99) Schuster, G. B.; Schmidt, S. P. *Chemiluminescence of Organic Compounds*1981.

(100) Nelson, N. C.; Cheikh, A. B.; Matsuda, E.; Becker, M. M. Simultaneous detection of multiple nucleic acid targets in a homogeneous format. *Biochemistry* **1996**, *35*, 8429-8438.

(101) Kamidate, T.; Ichihashi, H.; Segawa, T.; Watanabe, H. Enhanced chemiluminescence of lucigenin with epinephrine in cationic surfactant micelles containing periodate. *Journal of bioluminescence and chemiluminescence* **1995**, *10*, 55-61.

(102) Bagazgoitia, F. J.; Garcia, J. L.; Diéquez, C.; Weeks, I.; Woodhead, J. S. Effect of surfactants on the intensity of chemiluminescence emission from acridinium ester labelled proteins. *Journal of bioluminescence and chemiluminescence* **1988**, *2*, 121-128.

(103) Hart, R. C.; Taaffe, L. R. The use of acridinium ester-labelled streptavidin in immunoassays. *Journal of immunological methods* **1987**, *101*, 91-96.

(104) Batmanghelich, S.; Brown, R. C.; Stuart Woodhead, J.; Weeks, I.; Smith, K. Preparation of a chemiluminescent imidoester for the non-radioactive labelling of proteins. *Journal of Photochemistry and Photobiology B: Biology* **1992**, *12*, 193-201.

(105) Berry, D.; Clark, P.; Price, C. A laboratory and clinical evaluation of an immunochemiluminometric assay of thyrotropin in serum. *Clinical chemistry* **1988**, *34*, 2087-2090.

(106) Weeks, I.; Beheshti, I.; McCapra, F.; Campbell, A. K.; Woodhead, J. S. Acridinium esters as high-specific-activity labels in immunoassay. *Clinical chemistry* **1983**, *29*, 1474-1479.

(107) Paradh, A.; Hill, A.; Mitchell, W. Detection of beer spoilage bacteria< i> Pectinatus</i> and< i> Megasphaera</i> with acridinium ester labelled DNA probes using a hybridisation protection assay. *Journal of microbiological methods* **2014**, *96*, 25-34.

(108) Chandross, E. A. A new chemiluminescent system. *Tetrahedron Letters* **1963**, *4*, 761-765.

(109) Schuster, G. B. Chemiluminescence of organic peroxides. Conversion of ground-state reactants to excited-state products by the chemically initiated electron-exchange luminescence mechanism. *Accounts of Chemical Research* **1979**, *12*, 366-373.

(110) Jonsson, T. Peroxyoxalate Chemiluminescence for Miniaturized Analytical Flow Systems. **2003**.

(111) Nakashima, K.; Kuroda, N.; Kawaguchi, S.; Wada, M.; Akiyama, S. Peroxyoxalate chemiluminescent assay for oxidase activities based on detecting enzymatically formed hydrogen peroxide. *Journal of bioluminescence and chemiluminescence* **1995**, *10*, 185-191.

(112) Cho, S.; Hwang, O.; Lee, I.; Lee, G.; Yoo, D.; Khang, G.; Kang, P. M.; Lee, D. Chemiluminescent and Antioxidant Micelles as Theranostic Agents for Hydrogen Peroxide Associated-Inflammatory Diseases. *Advanced Functional Materials* **2012**, *22*, 4038-4043.

(113) Lee, I.; Hwang, O.; Yoo, D.; Khang, G.; Lee, D. Detection of hydrogen peroxide in vitro and in vivo using peroxalate chemiluminescent micelles. *Bull Korean Chem Soc* **2011**, *32*, 2187-2192.

(114) Lee, D.; Khaja, S.; Velasquez-Castano, J. C.; Dasari, M.; Sun, C.; Petros, J.; Taylor, W. R.; Murthy, N. In vivo imaging of hydrogen peroxide with chemiluminescent nanoparticles. *Nature materials* **2007**, *6*, 765-769.

(115) Matsumoto, M. Advanced chemistry of dioxetane-based chemiluminescent substrates originating from bioluminescence. *Journal of Photochemistry and Photobiology C: Photochemistry Reviews* **2004**, *5*, 27-53.

(116) De Vico, L.; Liu, Y.-J.; Krogh, J. W.; Lindh, R. Chemiluminescence of 1, 2-dioxetane. Reaction mechanism uncovered. *The Journal of Physical Chemistry A* **2007**, *111*, 8013-8019.

(117) Wieringa, J.; Strating, J.; Wynberg, H.; Adam, W. Adamantylideneadamantane peroxide, a stable 1, 2-dioxetane. *Tetrahedron Letters* **1972**, *13*, 169-172.

(118) Schuster, G. B.; Turro, N. J.; Steinmetzer, H. C.; Schaap, A. P.; Faler, G.; Adam, W.; Liu, J. Adamantylideneadamantane-1, 2-dioxetane. Chemiluminescence and decomposition kinetics of an unusually stable 1, 2-dioxetane. *Journal of the American Chemical Society* **1975**, *97*, 7110-7118.

(119) Beck, S.; Koster, H. Applications of dioxetane chemiluminescent probes to molecular biology. *Analytical chemistry* **1990**, *62*, 2258-2270.

(120) Hummelen, J. C.; Luider, T. M.; Oudman, D.; Koek, J. N.; Wynberg, H. 1, 2-dioxetanes: Luminescent and nonluminescent decomposition, chemistry, and potential applications. *Order* **1991**, *501*, 1008.

(121) Adam, W.; Bronstein, I.; Trofimov, A. V. Solvatochromic effects on the electron exchange chemiluminescence (CIEEL) of spiroadamantyl-substituted dioxetanes

and the fluorescence of relevant oxyanions. *The Journal of Physical Chemistry A* **1998**, *102*, 5406-5414.

(122) Richard, J.-A.; Jean, L.; Romieu, A.; Massonneau, M.; Noack-Fraissignes, P.; Renard, P.-Y. Chemiluminescent probe for the in vitro detection of protease activity. *Organic letters* **2007**, *9*, 4853-4855.

(123) Schaap, A.; Akhavan, H.; Romano, L. Chemiluminescent substrates for alkaline phosphatase: application to ultrasensitive enzyme-linked immunoassays and DNA probes. *Clinical chemistry* **1989**, *35*, 1863-1864.

(124) Beale, E.; Deeb, E.; Handley, R.; Akhavan-Tafti, H.; Schaap, A. A rapid and simple chemiluminescent assay for Escherichia coli beta-galactosidase. *BioTechniques* **1992**, *12*, 320-323.

(125) Sabelle, S.; Renard, P.-Y.; Pecorella, K.; de Suzzoni-Dézard, S.; Créminon, C.; Grassi, J.; Mioskowski, C. Design and synthesis of chemiluminescent probes for the detection of cholinesterase activity. *Journal of the American Chemical Society* **2002**, *124*, 4874-4880.

(126) Blencowe, C. A.; Russell, A. T.; Greco, F.; Hayes, W.; Thornthwaite, D. W. Self-immolative linkers in polymeric delivery systems. *Polymer Chemistry* **2011**, *2*, 773-790.

(127) Sagi, A.; Weinstain, R.; Karton, N.; Shabat, D. Self-immolative polymers. *Journal of the American Chemical Society* **2008**, *130*, 5434-5435.

(128) Avital-Shmilovici, M.; Shabat, D. Dendritic chain reaction: Responsive release of hydrogen peroxide upon generation and enzymatic oxidation of methanol. *Bioorganic & medicinal chemistry* **2010**, *18*, 3643-3647.

(129) Avital-Shmilovici, M.; Shabat, D. Self-immolative dendrimers: A distinctive approach to molecular amplification. *Soft Matter* **2010**, *6*, 1073-1080.

(130) Klajnert, B.; Bryszewska, M. Dendrimers: properties and applications. *Acta Biochimica Polonica* **2000**, *48*, 199-208.

(131) Balzani, V.; Ceroni, P.; Gestermann, S.; Kauffmann, C.; Gorka, M.; Vögtle, F. Dendrimers as fluorescent sensors with signal amplification. *Chemical Communications* **2000**, 853-854.

(132) Shamis, M.; Shabat, D. Single-Triggered AB6 Self-Immolative Dendritic Amplifiers. *Chemistry-A European Journal* **2007**, *13*, 4523-4528.

(133) Sella, E.; Weinstain, R.; Erez, R.; Burns, N. Z.; Baran, P. S.; Shabat, D. Sulfhydryl-based dendritic chain reaction. *Chem. Commun.* **2010**, *46*, 6575-6577.

(134) Sella, E.; Shabat, D. Self-immolative dendritic probe for direct detection of triacetone triperoxide. *Chemical Communications* **2008**, 5701-5703.

(135) Amir, R. J.; Shabat, D. Self-immolative dendrimer biodegradability by multi-enzymatic triggering. *Chem. Commun.* **2004**, 1614-1615.

(136) Ashokkumar, P.; Weißhoff, H.; Kraus, W.; Rurack, K. Test-Strip-Based Fluorometric Detection of Fluoride in Aqueous Media with a BODIPY-Linked Hydrogen-Bonding Receptor. *Angewandte Chemie International Edition* **2014**, *53*, 2225-2229.

(137) Veale, E. B.; Gunnlaugsson, T. Fluorescent sensors for ions based on organic structures. *Annual Reports Section" B"(Organic Chemistry)* **2010**, *106*, 376-406.

(138) Kim, S. Y.; Park, J.; Koh, M.; Park, S. B.; Hong, J.-I. Fluorescent probe for detection of fluoride in water and bioimaging in A549 human lung carcinoma cells. *Chemical Communications* **2009**, 4735-4737.

(139) Turan, I. S.; Akkaya, E. U. Chemiluminescence Sensing of Fluoride Ions Using a Self-Immolative Amplifier. *Organic letters* **2014**, *16*, 1680-1683.

(140) Bao, Y.; Liu, B.; Wang, H.; Tian, J.; Bai, R. A “naked eye” and ratiometric fluorescent chemosensor for rapid detection of F− based on combination of desilylation reaction and excited-state proton transfer. *Chemical Communications* **2011**, *47*, 3957-3959.

(141) Sokkalingam, P.; Lee, C.-H. Highly sensitive fluorescence “turn-on” indicator for fluoride anion with remarkable selectivity in organic and aqueous media. *The Journal of organic chemistry* **2011**, *76*, 3820-3828.

(142) Jo, M.; Lim, J.; Miljanic, O. S. Selective and sensitive fluoride detection through alkyne cruciform desilylation. *Organic letters* **2013**, *15*, 3518-3521.

(143) Kim, S. Y.; Hong, J.-I. Chromogenic and fluorescent chemodosimeter for detection of fluoride in aqueous solution. *Organic letters* **2007**, *9*, 3109-3112.

(144) Bozdemir, O. A.; Sozmen, F.; Buyukcakir, O.; Guliyev, R.; Cakmak, Y.; Akkaya, E. U. Reaction-based sensing of fluoride ions using built-in triggers for intramolecular charge transfer and photoinduced electron transfer. *Organic letters* **2010**, *12*, 1400-1403.

(145) Song, F.; Garner, A. L.; Koide, K. A highly sensitive fluorescent sensor for palladium based on the allylic oxidative insertion mechanism. *Journal of the American Chemical Society* **2007**, *129*, 12354-12355.

(146) Garner, A. L.; Song, F.; Koide, K. Enhancement of a catalysis-based fluorometric detection method for palladium through rational fine-tuning of the palladium species. *Journal of the American Chemical Society* **2009**, *131*, 5163-5171.

(147) Li, H.; Fan, J.; Peng, X. Colourimetric and fluorescent probes for the optical detection of palladium ions. *Chemical Society Reviews* **2013**, *42*, 7943-7962.

(148) Liu, B.; Bao, Y.; Du, F.; Wang, H.; Tian, J.; Bai, R. Synthesis and characterization of a fluorescent polymer containing 2, 6-bis (2-thienyl) pyridine moieties as a highly efficient sensor for Pd 2+ detection. *Chemical Communications* **2011**, *47*, 1731-1733.

(149) Overholser, L. G.; Yoe, J. H. The Colorimetric Detection and Determination of Palladium with Compounds Containing the p-Nitrosophenylamino Group1. *Journal of the American Chemical Society* **1941**, *63*, 3224-3229.

(150) Blanco, M.; Maspoch, S. 5-phenylazo-8-aminoquinoline as a sensitive reagent for the extraction-spectrophotometric determination of palladium (II). *Microchimica Acta* **1983**, *81*, 11-20.

(151) Menis, O.; Rains, T. Colorimetric Determination of Palladium with α-Furildoxime. *Analytical Chemistry* **1955**, *27*, 1932-1934.

(152) Mukherjee, S.; Chowdhury, S.; Chattapadhyay, A. P.; Bhattacharya, A. Spectroscopic, cytotoxic and DFT studies of a luminescent palladium (II) complex of a hydrazone ligand that induces apoptosis in human prostate cancer cells. *Inorganica Chimica Acta* **2011**, *373*, 40-46.

(153) Safavi, A.; Gholivand, M.; Dastghaib, S. R. Selective Extraction–Spectrophotometric Determination of Traces of Palladium in Catalysts. *Microchemical journal* **1997**, *57*, 288-293.

(154) Sahu, R.; Sondhi, S.; Gupta, B. Extraction and spectrophotometric determination of Pd (II) with 3, 4, 4a, 5-tetrahydro-3, 3, 4a-trimethyl-7-(substituted)-pyrimido (1, 6-< i> a</i>)-benzimidazole-1-thiol (PBT). *Talanta* **1995**, *42*, 401-405.

(155) Kubo, K.; Miyazaki, Y.; Akutsu, K.; Sakurai, T. Synthesis and emission behavior of double-armed tetrathiacrown carrying two naphthalenes. *Heterocycles* **1999**, *51*, 965-968.

(156) Schwarze, T.; Dosche, C.; Flehr, R.; Klamroth, T.; Löhmannsröben, H.-G.; Saalfrank, P.; Cleve, E.; Buschmann, H.-J.; Holdt, H.-J. Combination of a CT modulated PET and an intramolecular excimer formation to quantify PdCl2 by large fluorescence enhancement. *Chemical Communications* **2010**, *46*, 2034-2036.

(157) Wu, Q.; Anslyn, E. V. Heavy metal analysis using a Heck-catalyzed cyclization to create coumarin. *J. Mater. Chem.* **2005**, *15*, 2815-2819.

(158) Wei, G.; Wang, L.; Jiao, J.; Hou, J.; Cheng, Y.; Zhu, C. Cu< sup> 2+</sup> triggered fluorescence sensor based on fluorescein derivative for Pd< sup> 2+</sup> detection. *Tetrahedron Letters* **2012**, *53*, 3459-3462.

(159) Jiang, J.; Jiang, H.; Liu, W.; Tang, X.; Zhou, X.; Liu, W.; Liu, R. A colorimetric and ratiometric fluorescent probe for palladium. *Organic letters* **2011**, *13*, 4922-4925.

(160) Garner, A. L.; Koide, K. Studies of a fluorogenic probe for palladium and platinum leading to a palladium-specific detection method. *Chemical Communications* **2009**, 86-88.

(161) Li, D.; Campbell, L. D.; Austin, B. A.; Koide, K. Detection of trace palladium in flasks and metal reagents using a fluorogenic Tsuji–Trost reaction. *ChemPlusChem* **2012**, *77*, 281-283.

(162) Santra, M.; Ko, S.-K.; Shin, I.; Ahn, K. H. Fluorescent detection of palladium species with an O-propargylated fluorescein. *Chemical Communications* **2010**, *46*, 3964-3966.

(163) Liu, B.; Wang, H.; Wang, T.; Bao, Y.; Du, F.; Tian, J.; Li, Q.; Bai, R. A new ratiometric ESIPT sensor for detection of palladium species in aqueous solution. *Chem. Commun.* **2012**, *48*, 2867-2869.

(164) Zhu, B.; Gao, C.; Zhao, Y.; Liu, C.; Li, Y.; Wei, Q.; Ma, Z.; Du, B.; Zhang, X. A 4-hydroxynaphthalimide-derived ratiometric fluorescent chemodosimeter for imaging palladium in living cells. *Chemical Communications* **2011**, *47*, 8656-8658.

APPENDIX

^{1}H-NMR, ^{13}C-NMR and HrMS SPECTRA OF THE SYTHESIZED COMPOUNDS

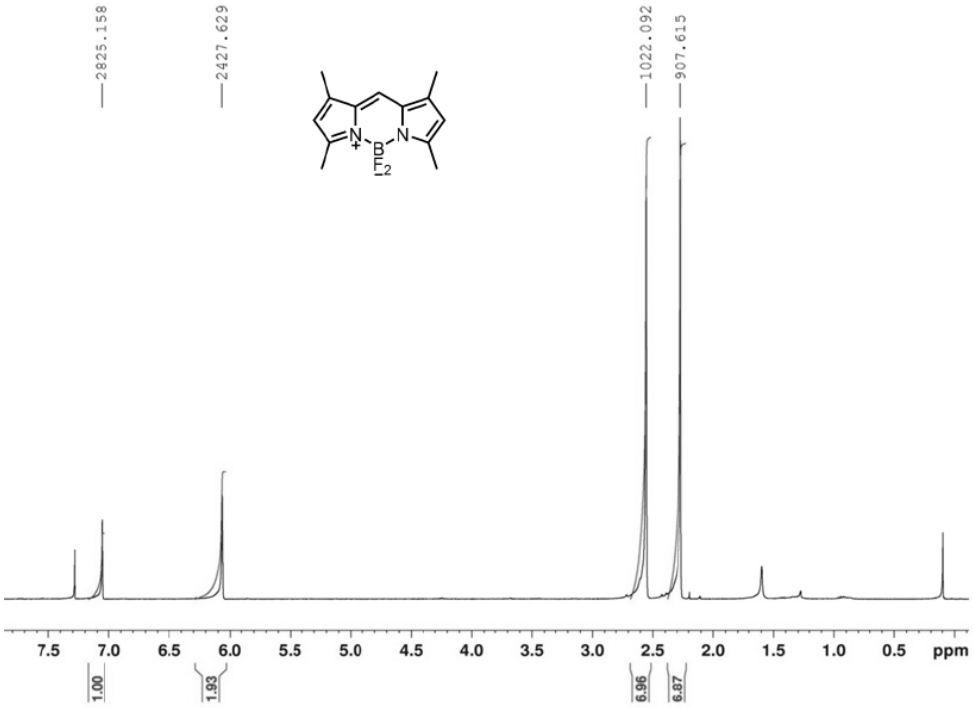

^{1}H-NMR Spectrum of compound **5**

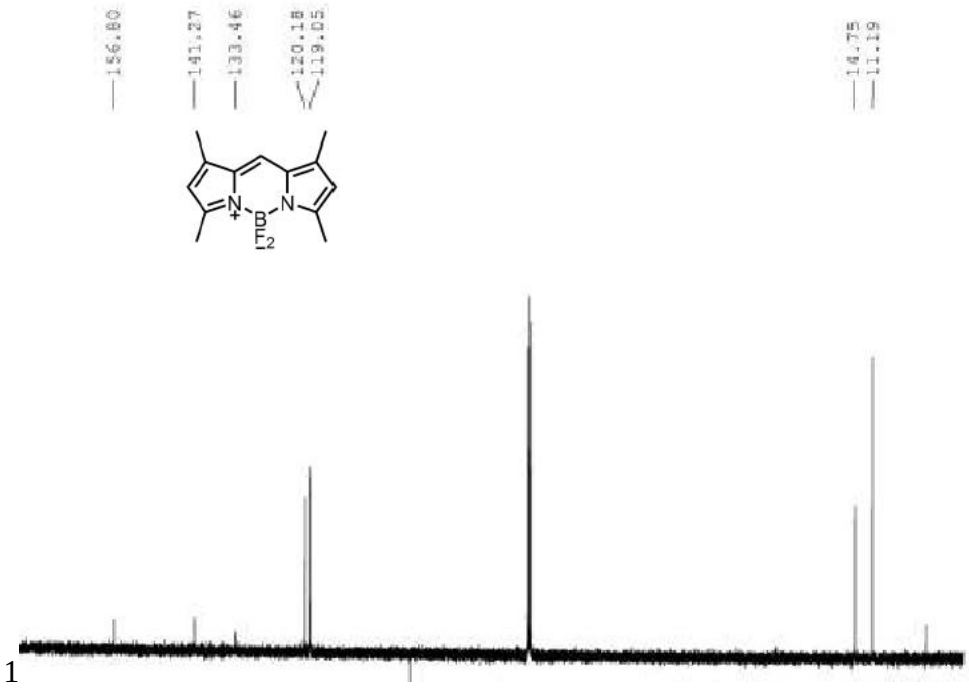

^{13}C-NMR Spectrum of Compound **5**

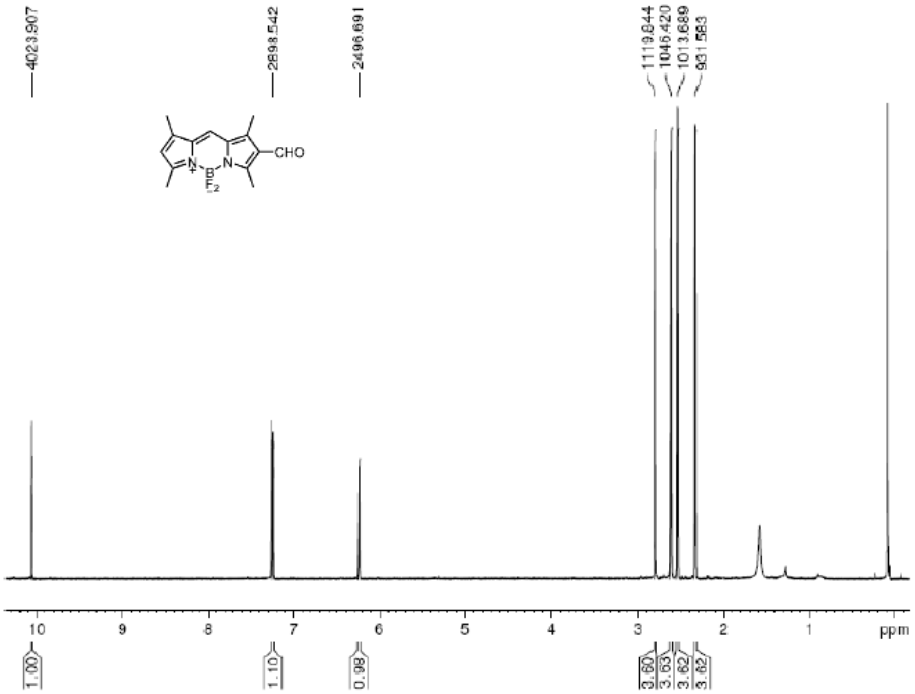

^{1}H-NMR Spectrum of compound **6**

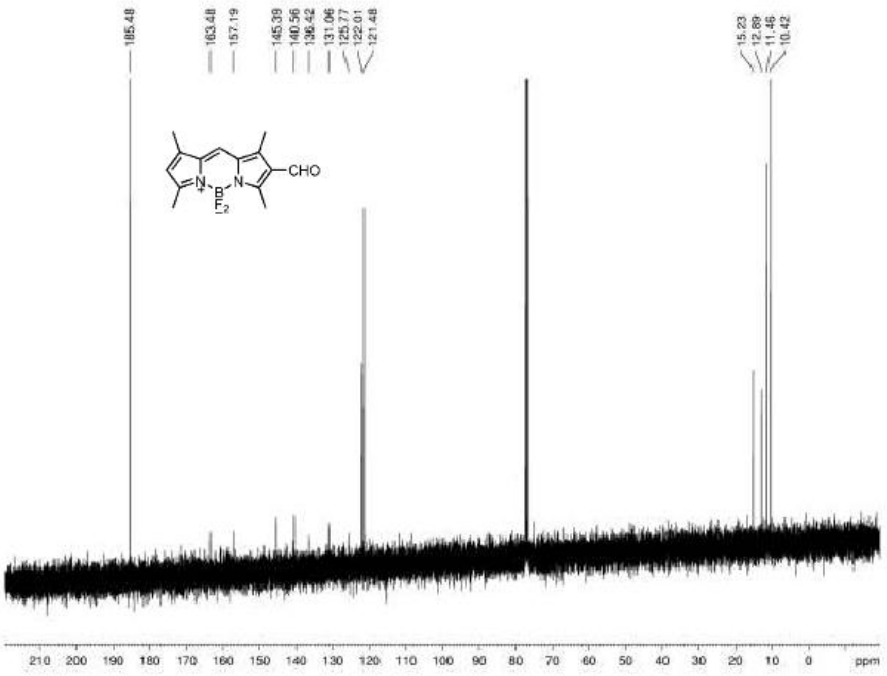

^{13}C-NMR Spectrum of Compound **6**

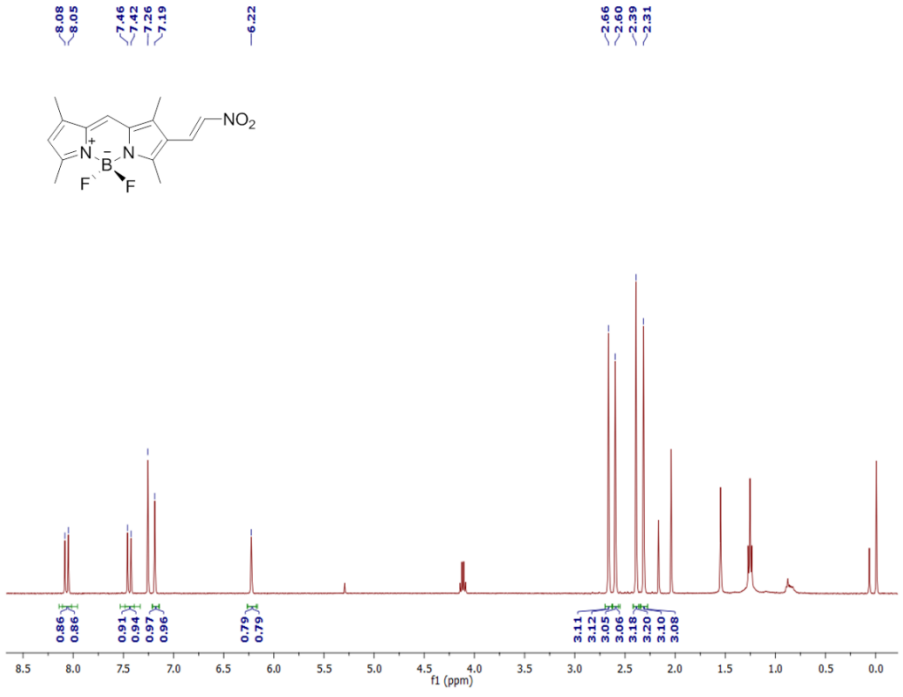

^{1}H-NMR Spectrum of compound **7**

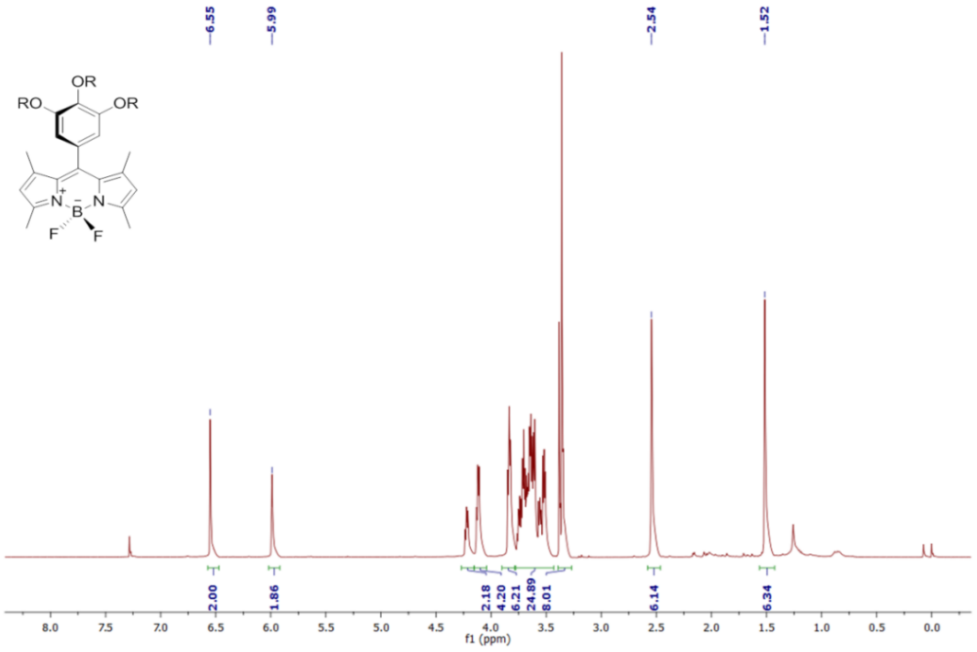

^{1}H-NMR Spectrum of compound **8**

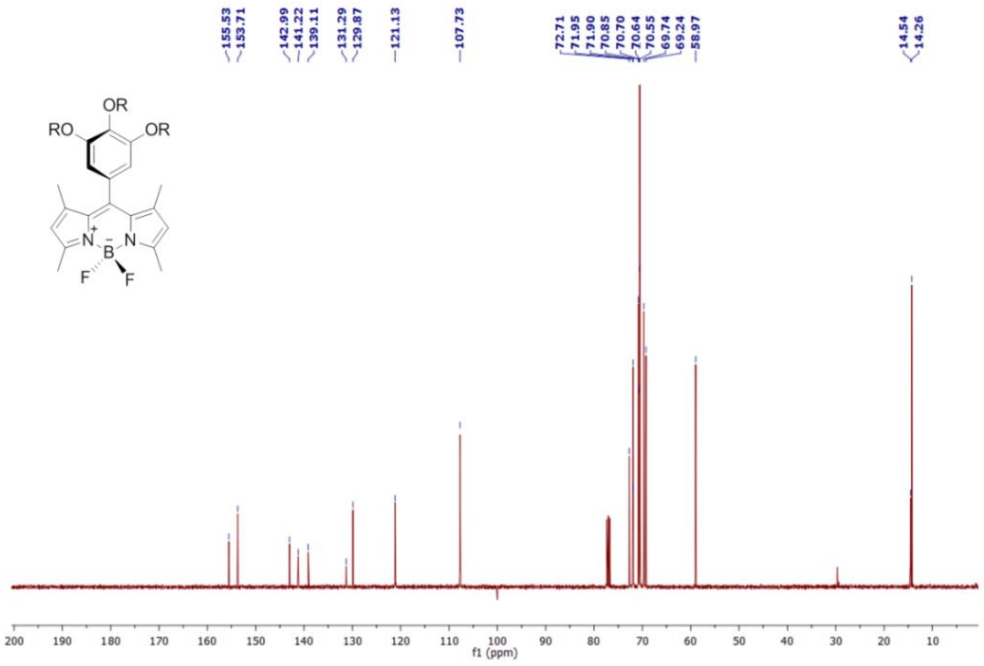

^{13}C-NMR Spectrum of Compound **8**

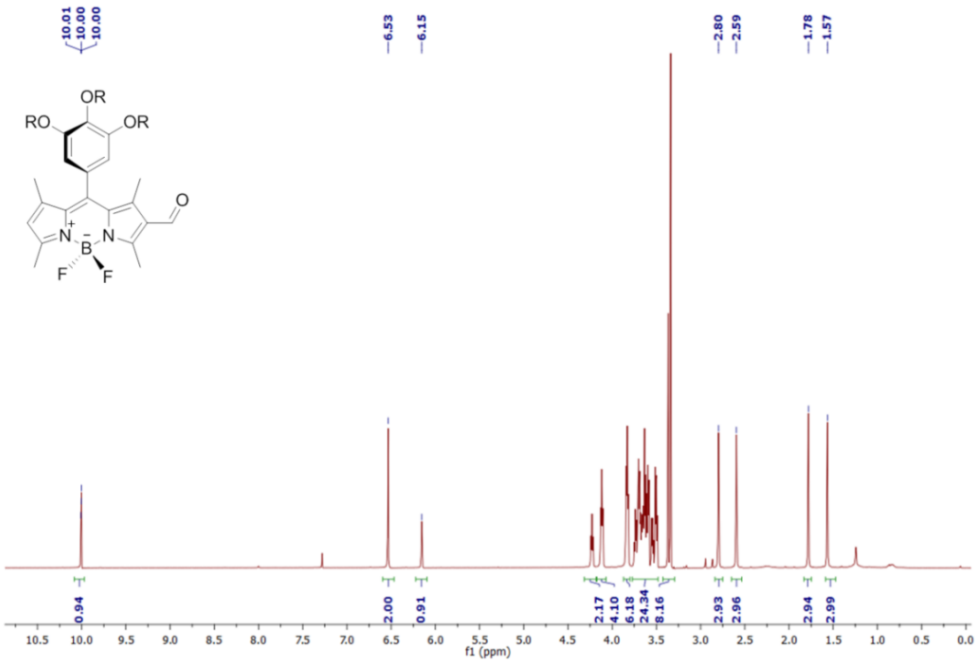

^{1}H-NMR Spectrum of compound **9**

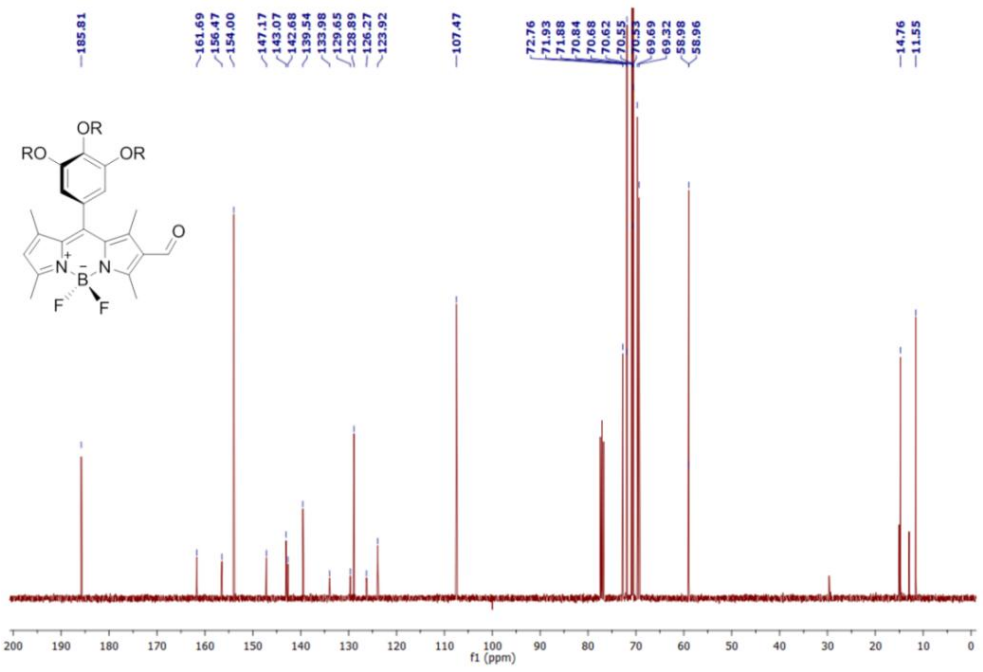

^{13}C-NMR Spectrum of Compound **9**

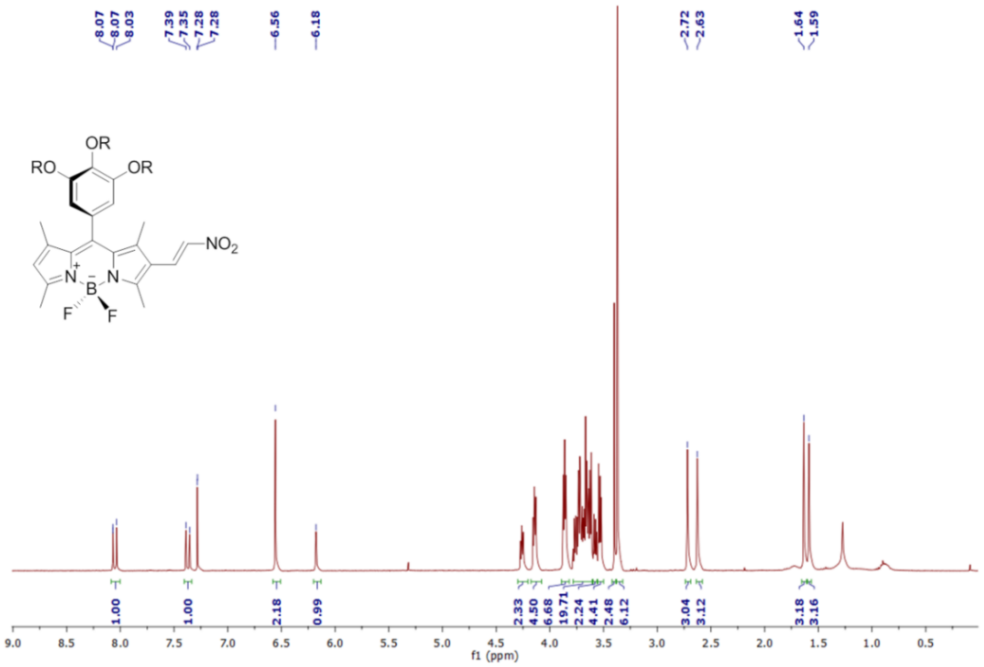

^{1}H-NMR Spectrum of compound **10**

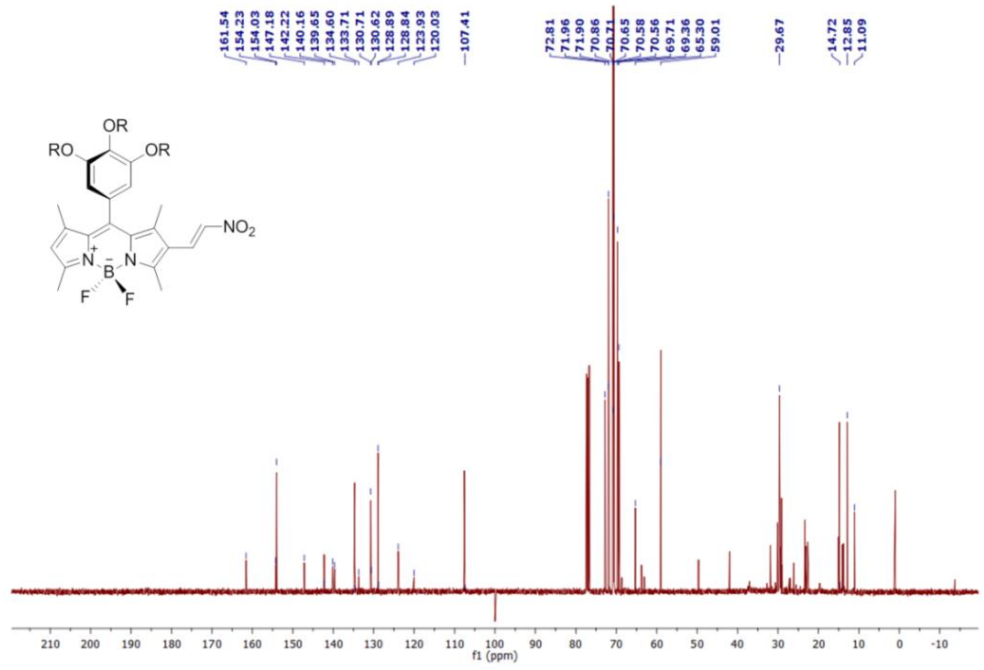

^{13}C-NMR Spectrum of Compound **10**

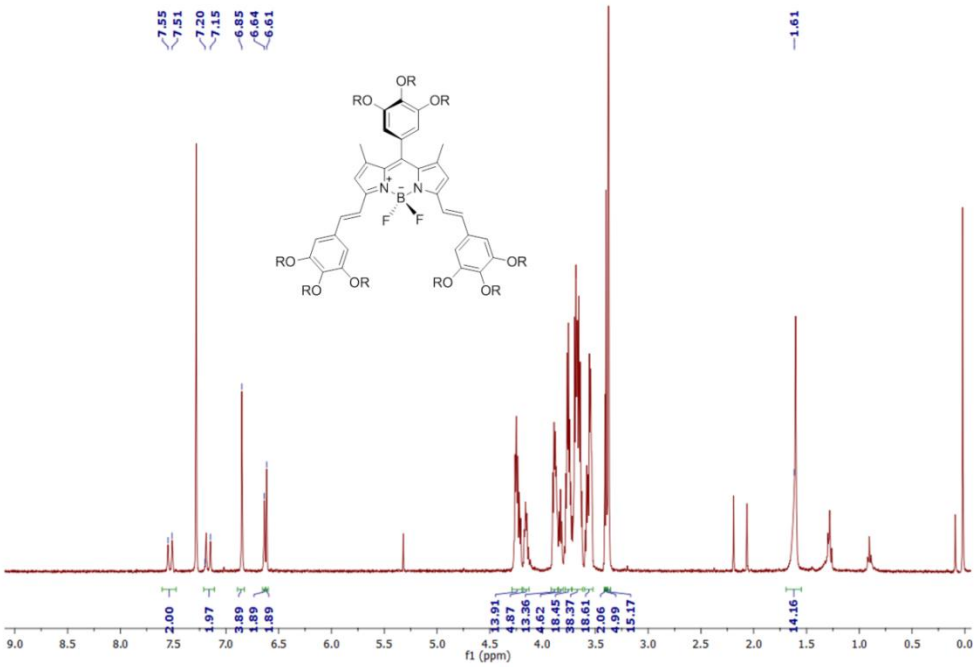

^{1}H-NMR Spectrum of compound **11**

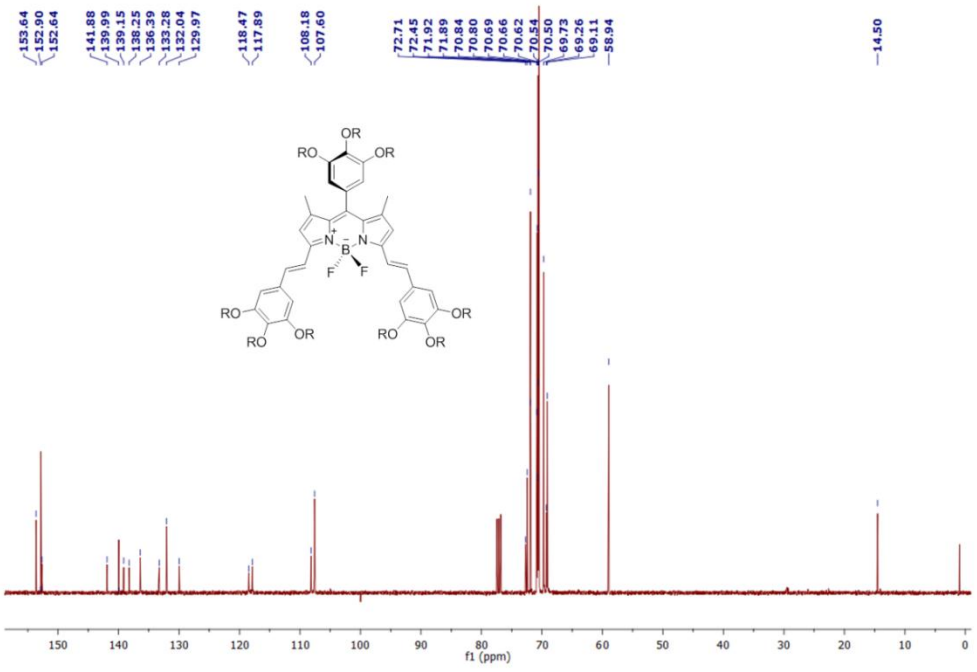

^{13}C-NMR Spectrum of Compound **11**

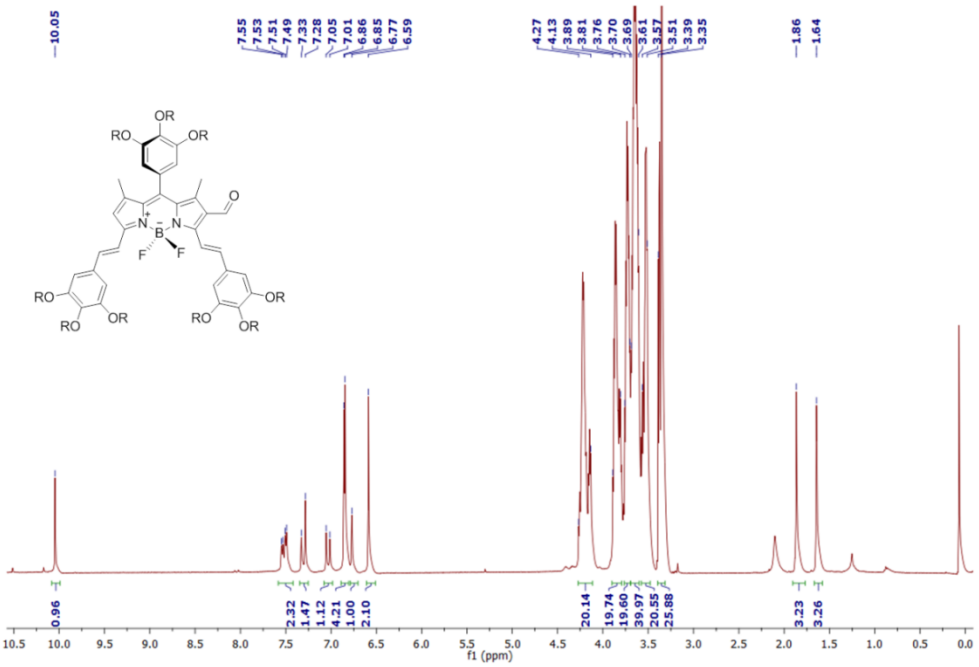

^{1}H-NMR Spectrum of compound **12**

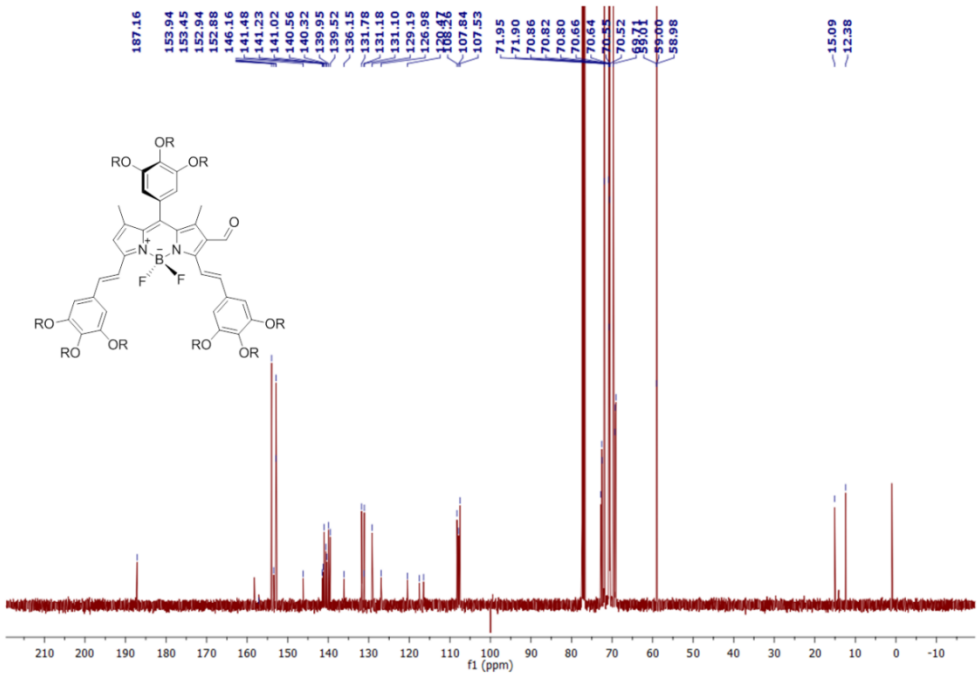

^{13}C-NMR Spectrum of Compound **12**

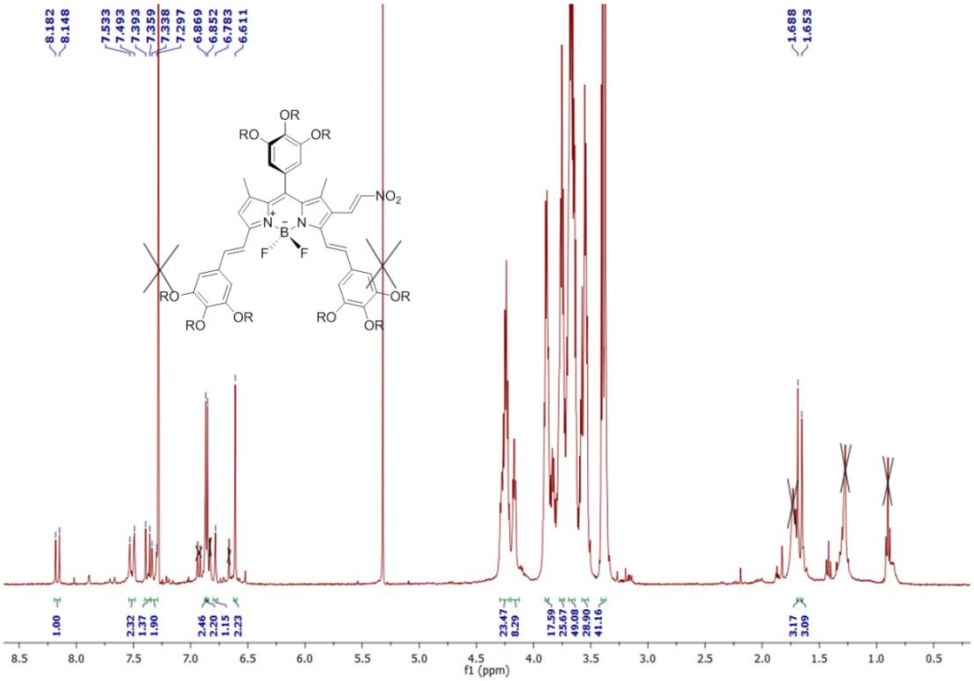

[1]H-NMR Spectrum of compound **13**

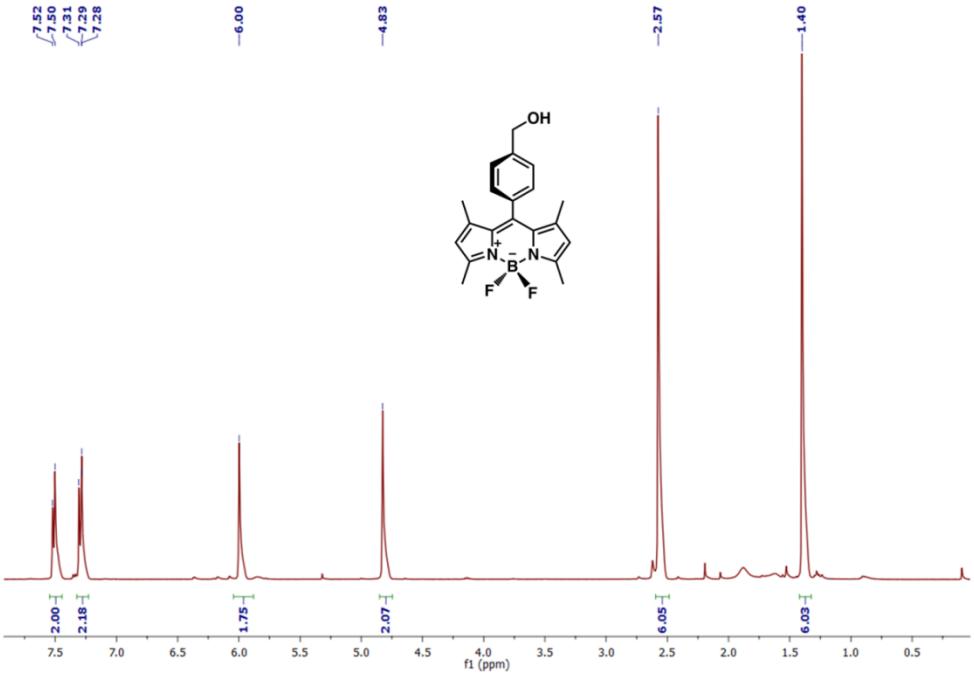

[1]H-NMR Spectrum of compound **14**

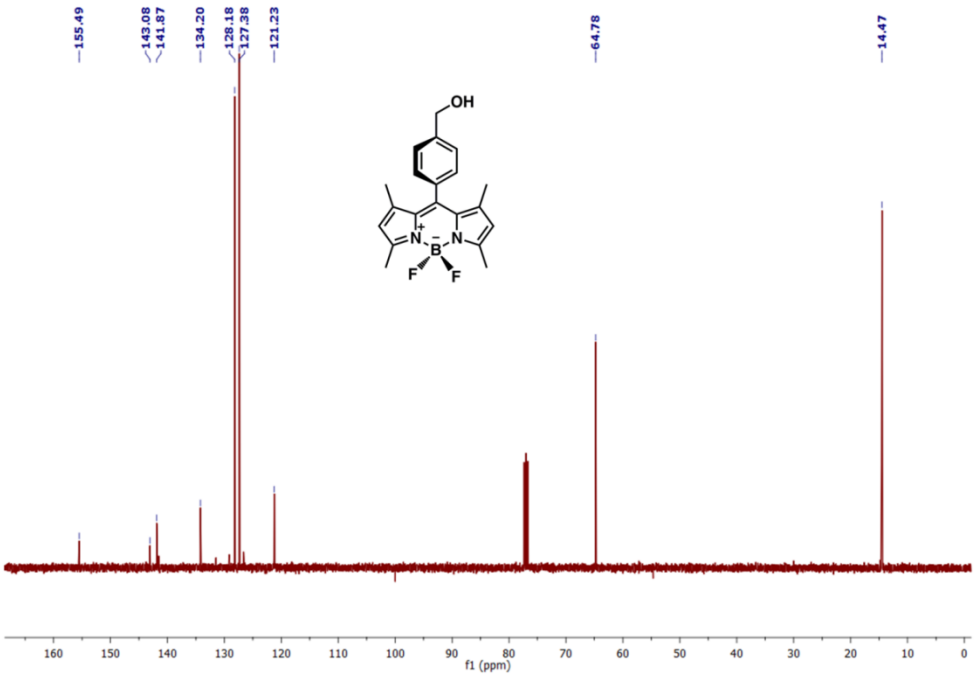

^{13}C-NMR Spectrum of Compound **14**

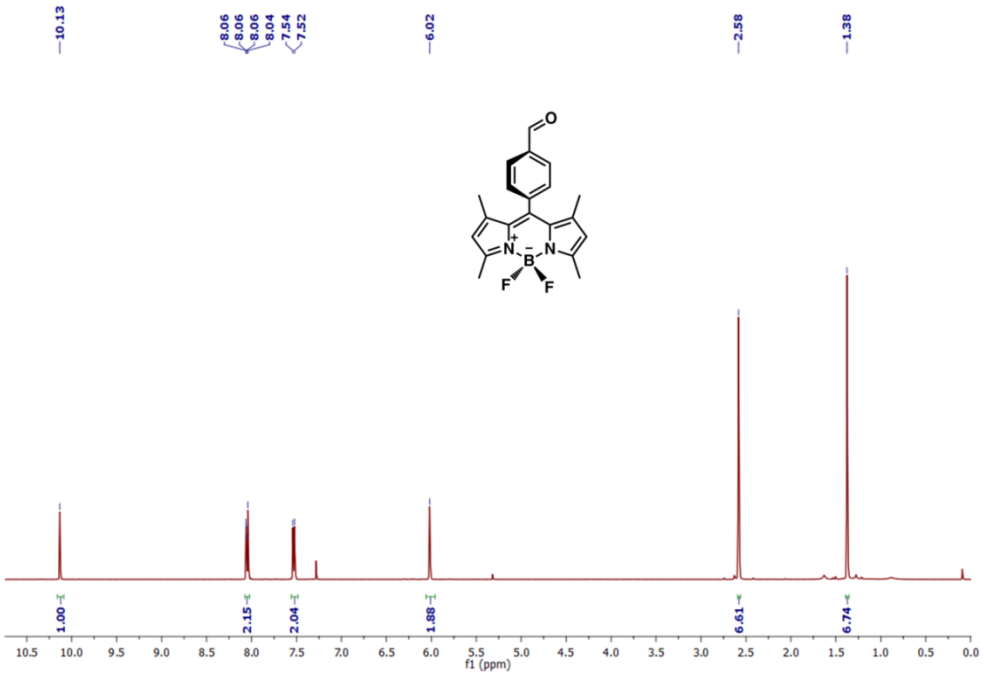

^{1}H-NMR Spectrum of compound **15**

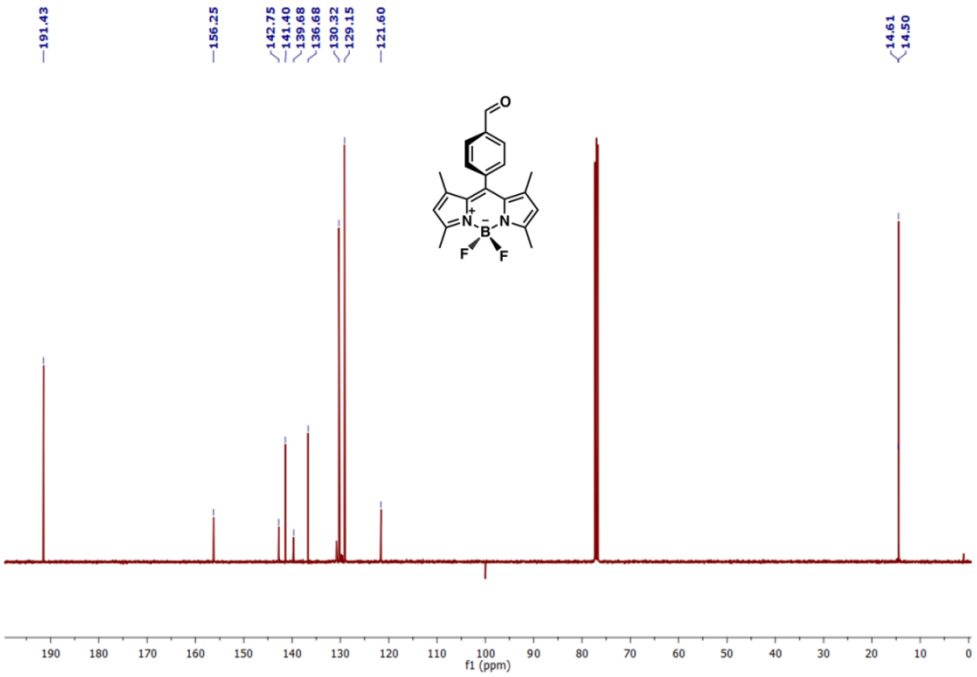

^{13}C-NMR Spectrum of Compound **15**

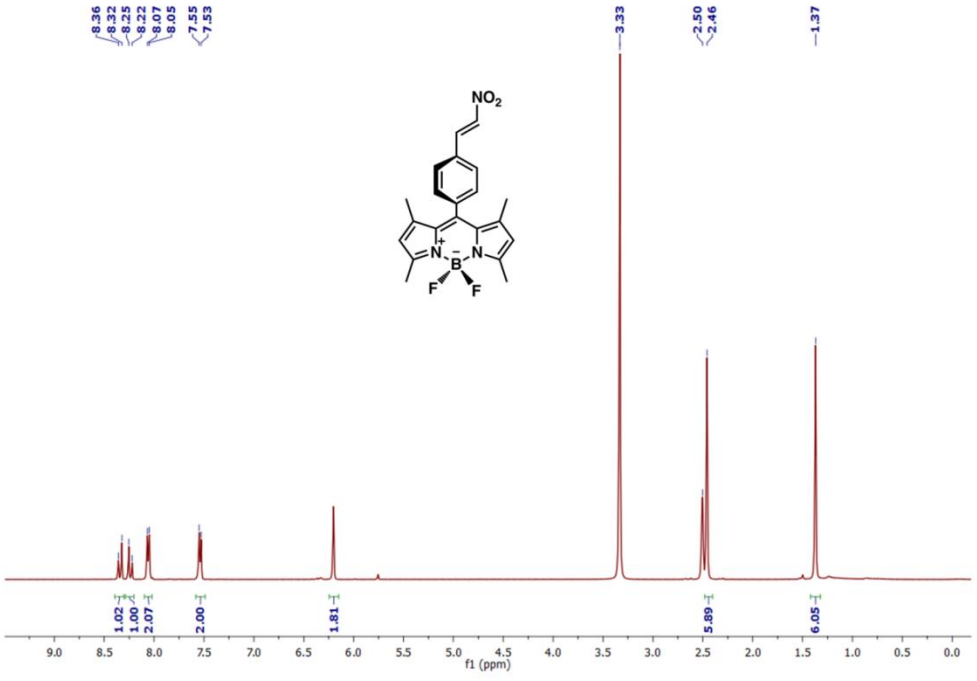

^{1}H-NMR Spectrum of compound **16**

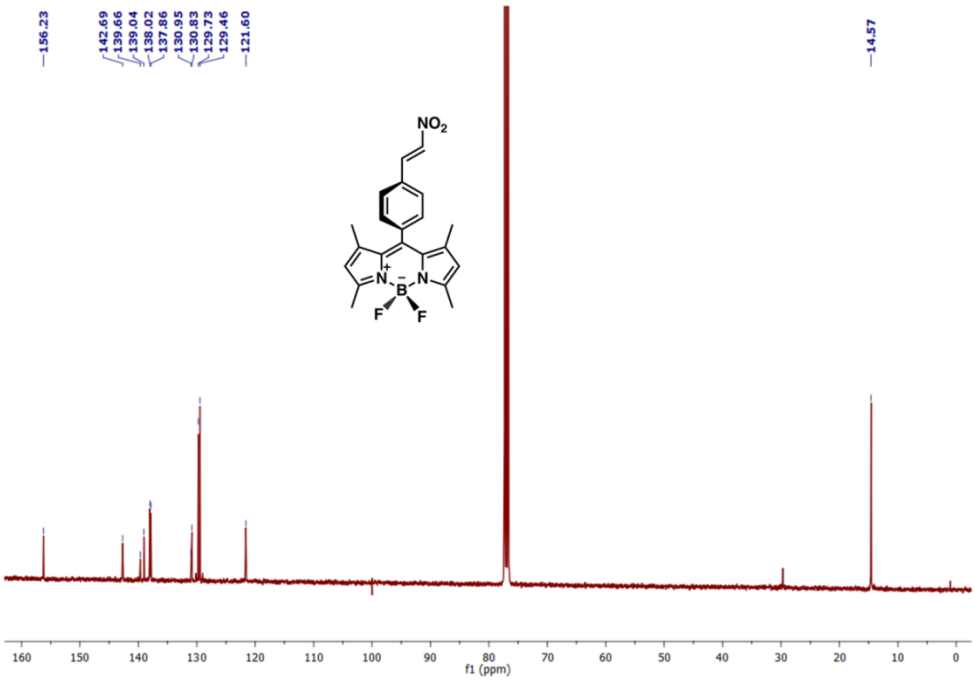

^{13}C-NMR Spectrum of Compound **16**

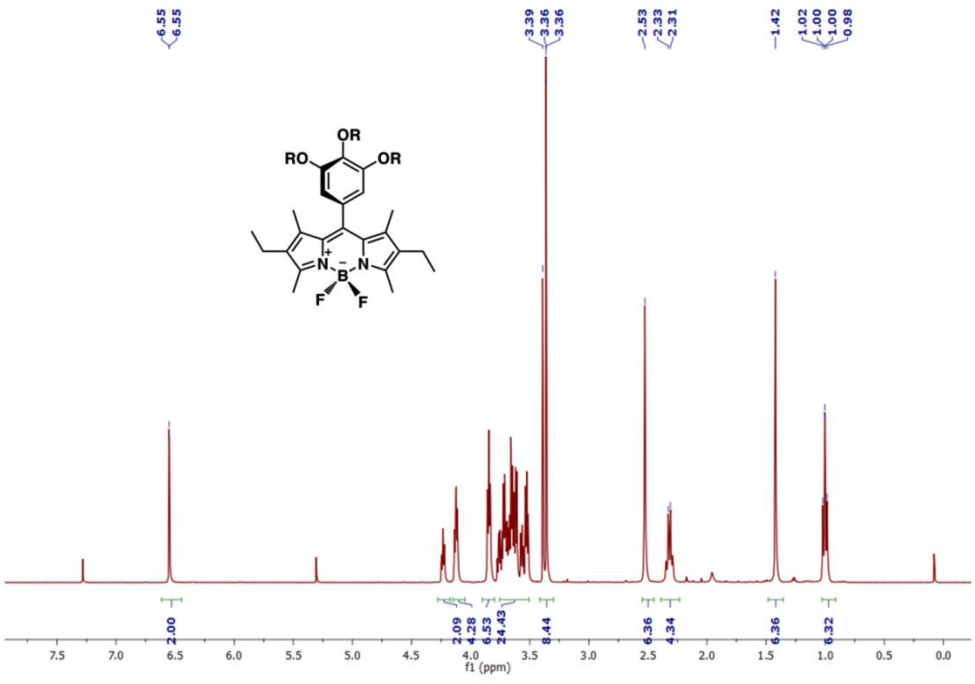

^{1}H-NMR Spectrum of compound **17**

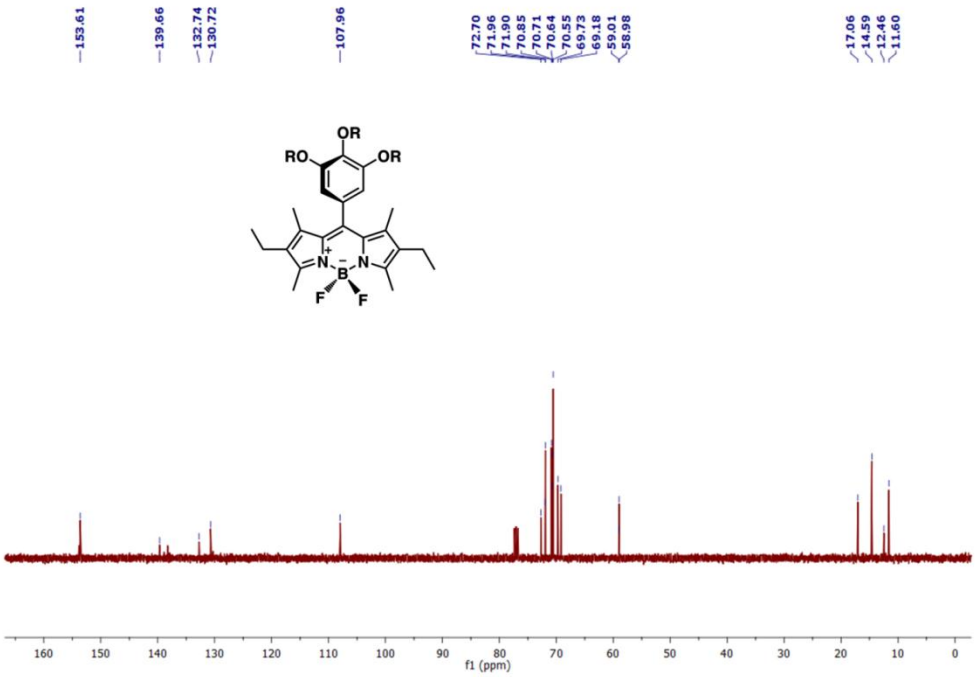

^{13}C-NMR Spectrum of Compound **17**

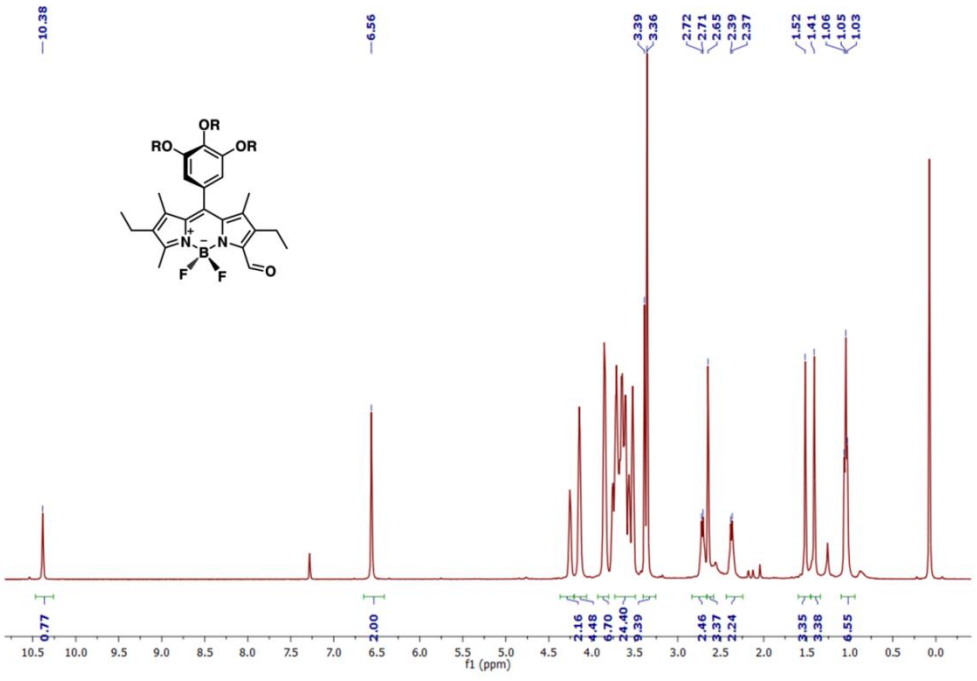

^{1}H-NMR Spectrum of compound **18**

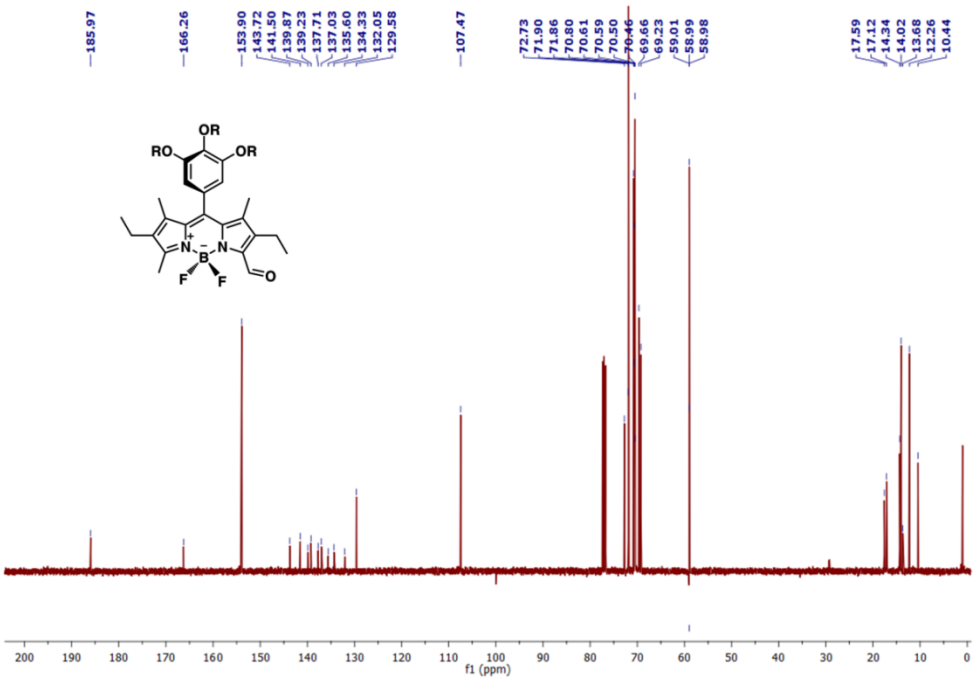

^{13}C-NMR Spectrum of Compound **18**

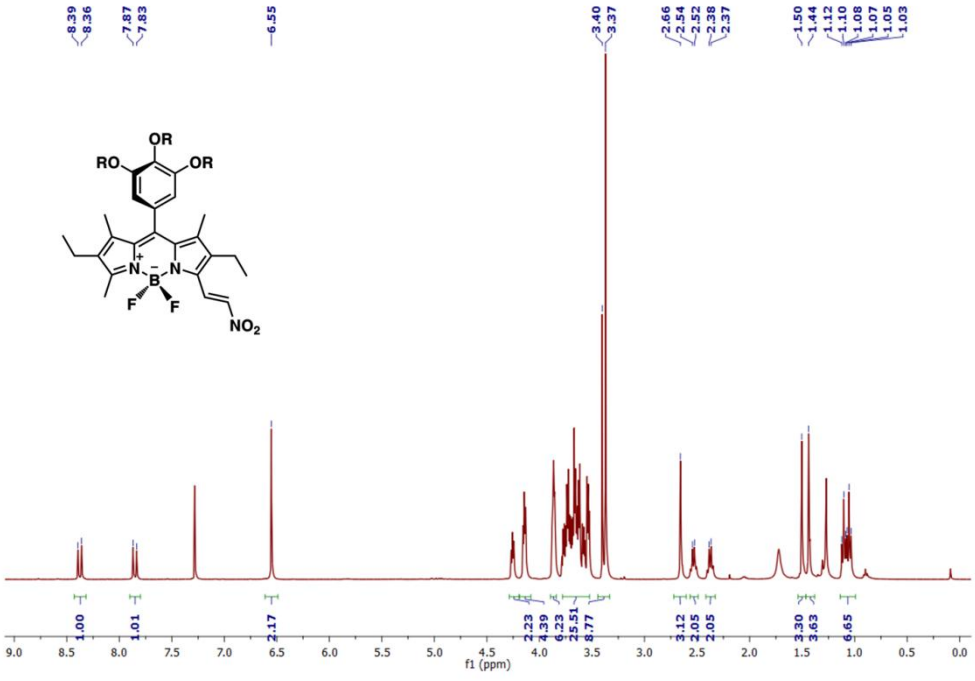

^{1}H-NMR Spectrum of compound **19**

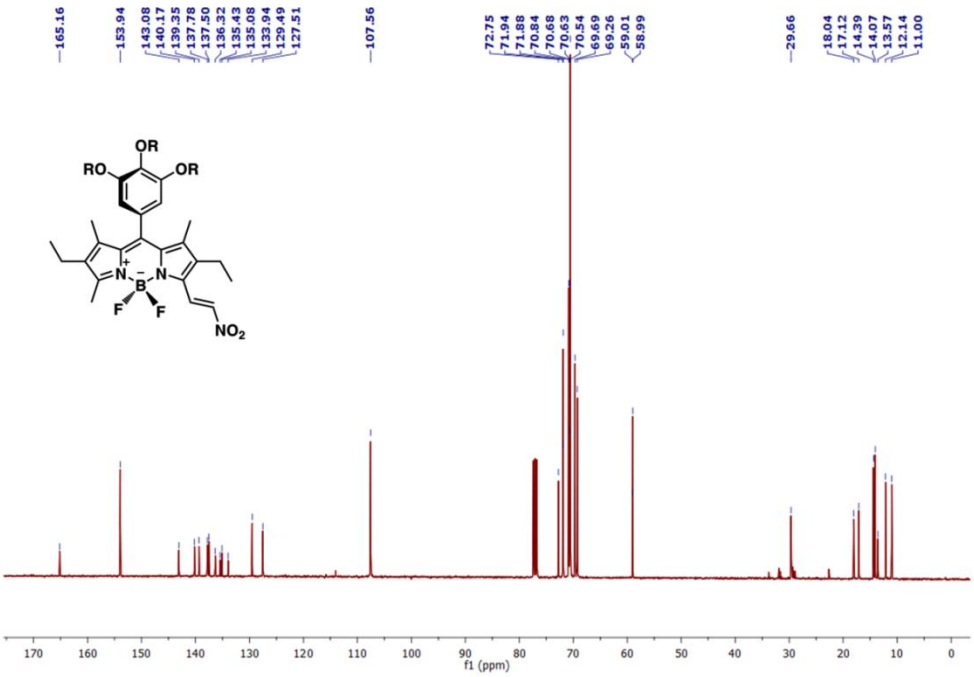

^{13}C-NMR Spectrum of Compound **19**

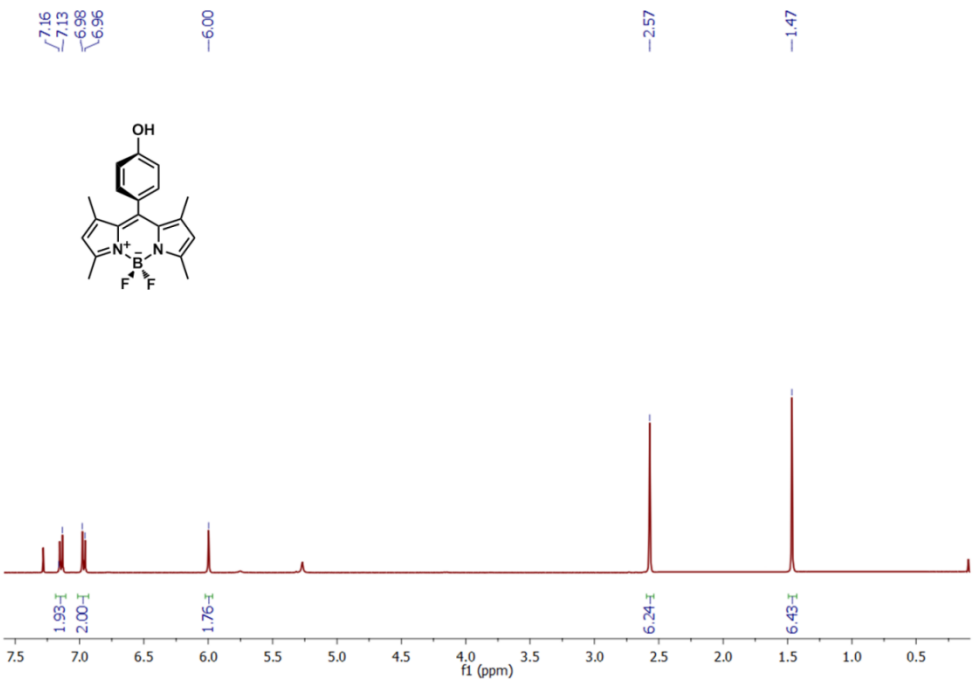

^{1}H-NMR Spectrum of compound **20**

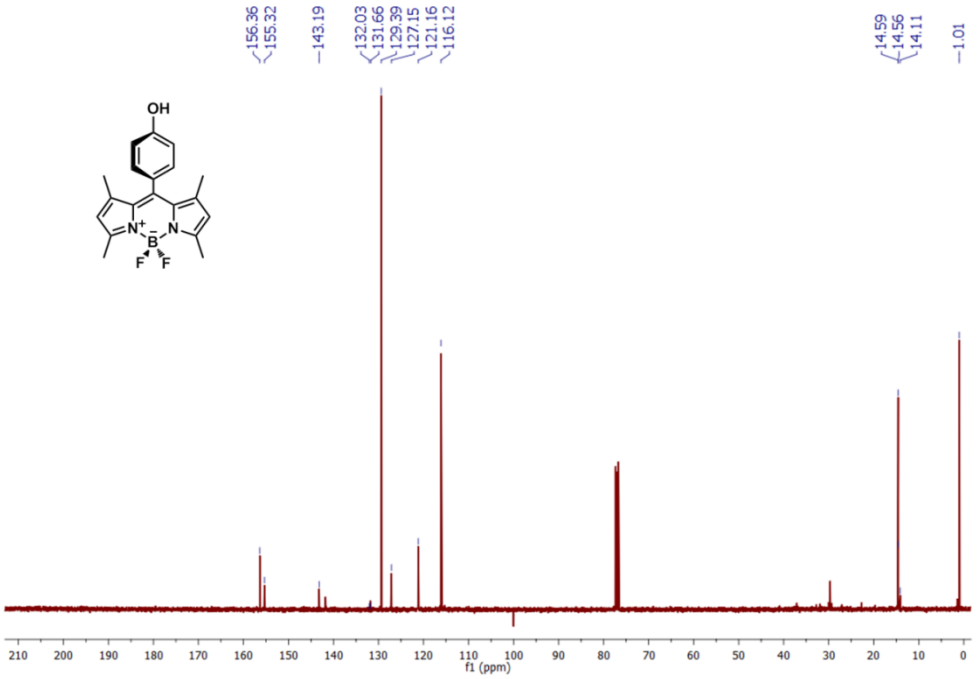

^{13}C-NMR Spectrum of Compound **20**

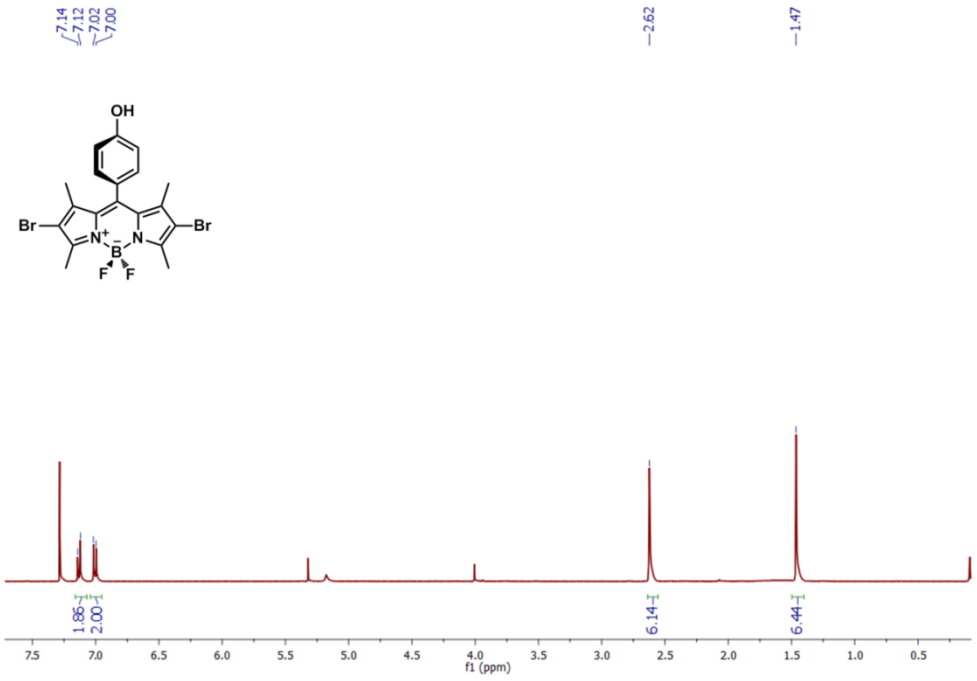

^{1}H-NMR Spectrum of compound **21**

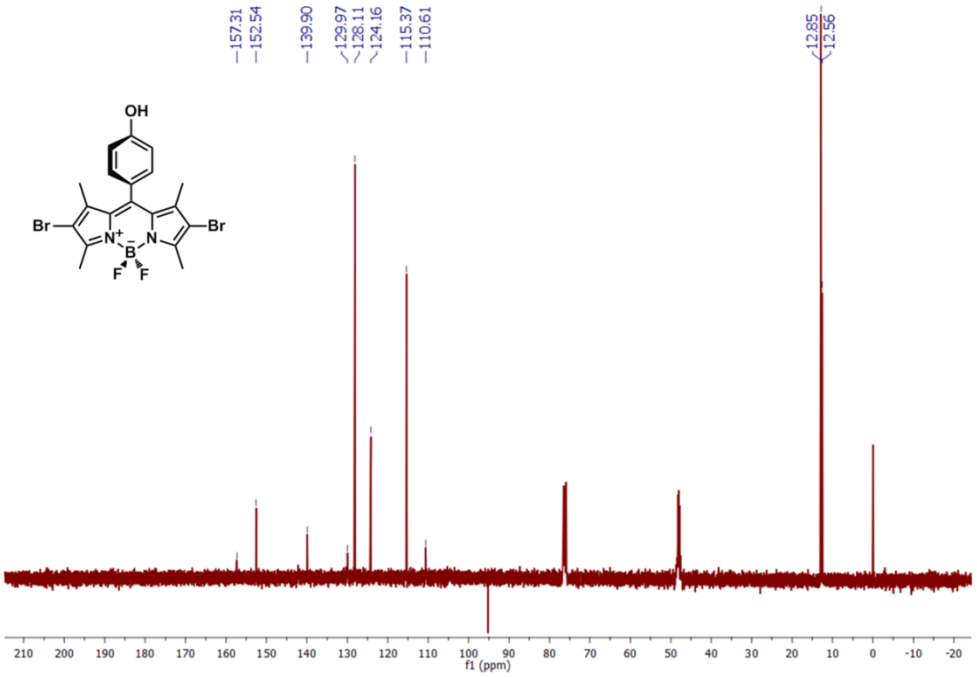

^{13}C-NMR Spectrum of Compound **21**

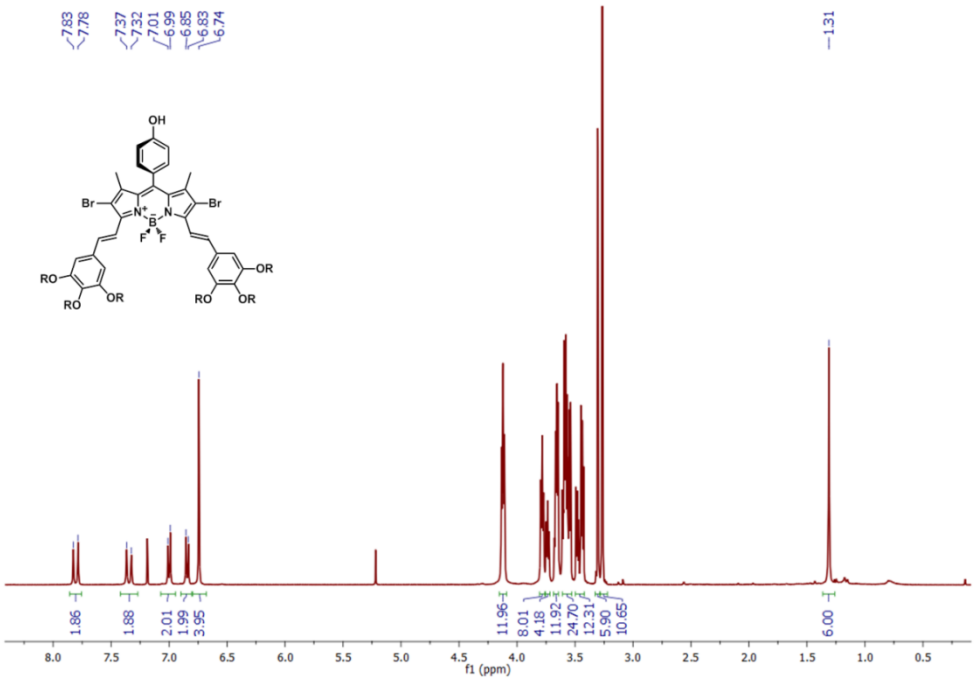

^{1}H-NMR Spectrum of compound **22**

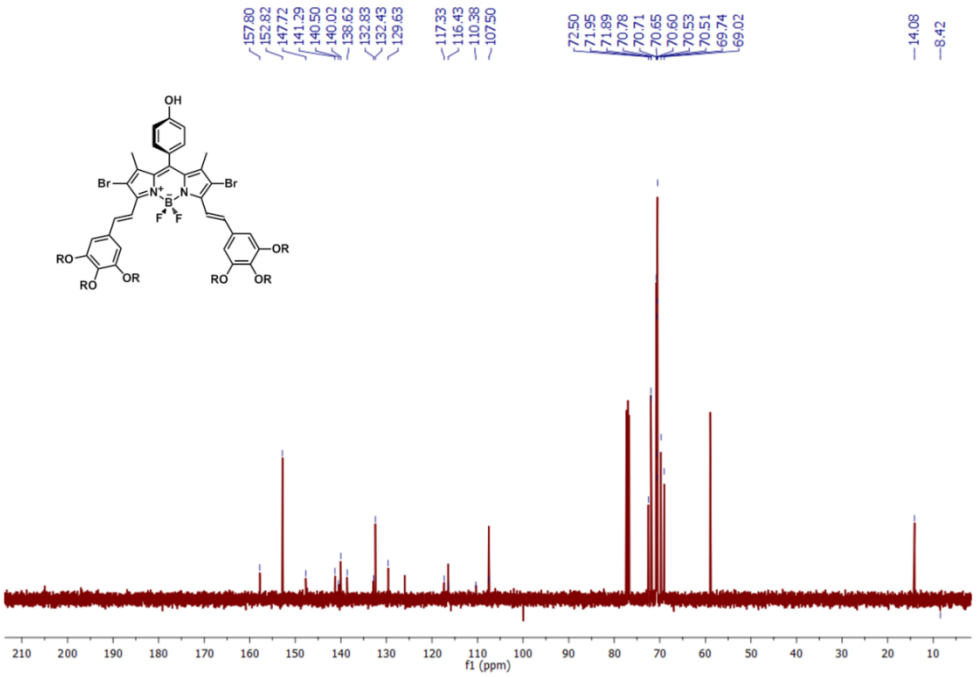

^{13}C-NMR Spectrum of Compound **22**

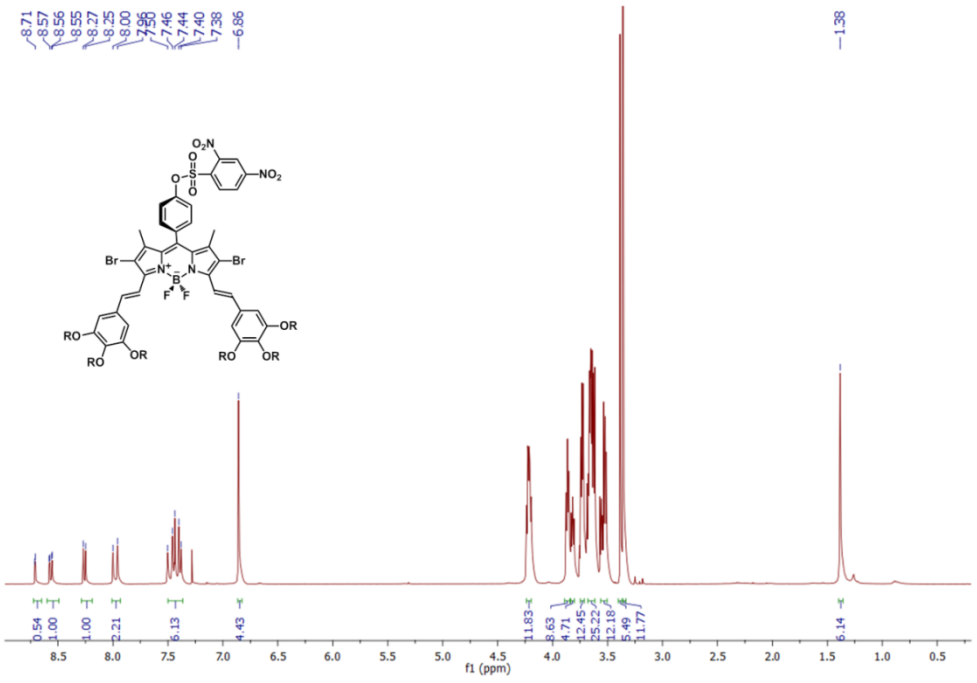

^{1}H-NMR Spectrum of compound **23**

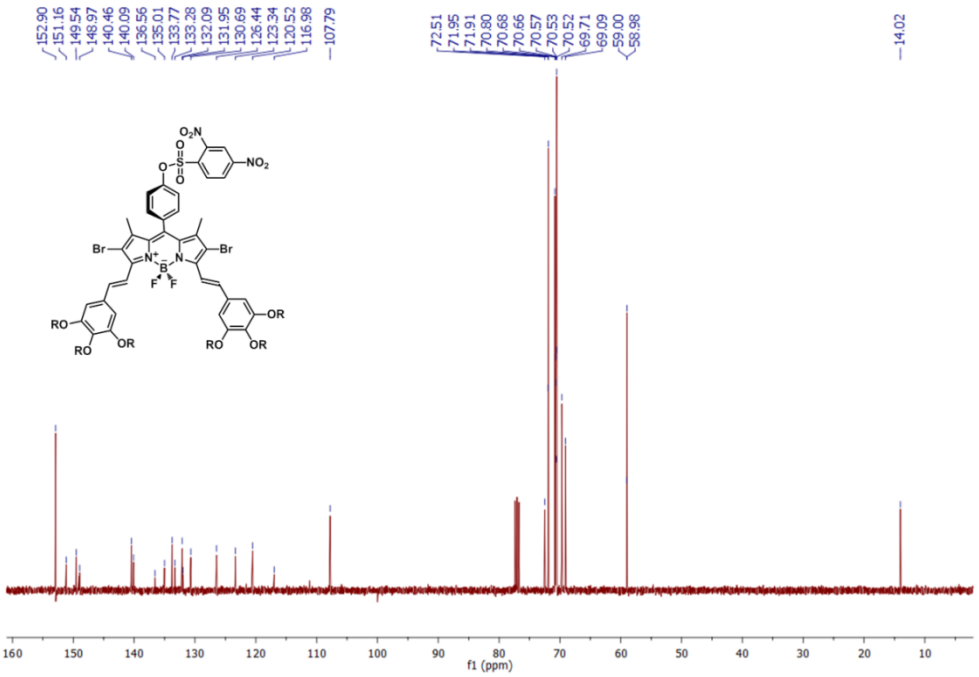

^{13}C-NMR Spectrum of Compound **23**

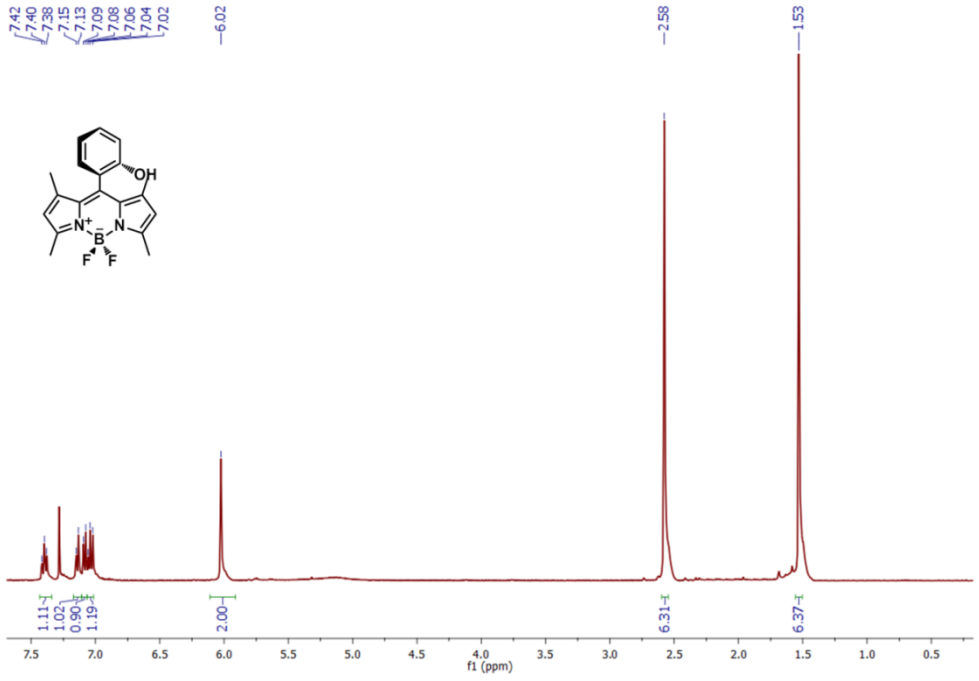

^{1}H-NMR Spectrum of compound **24**

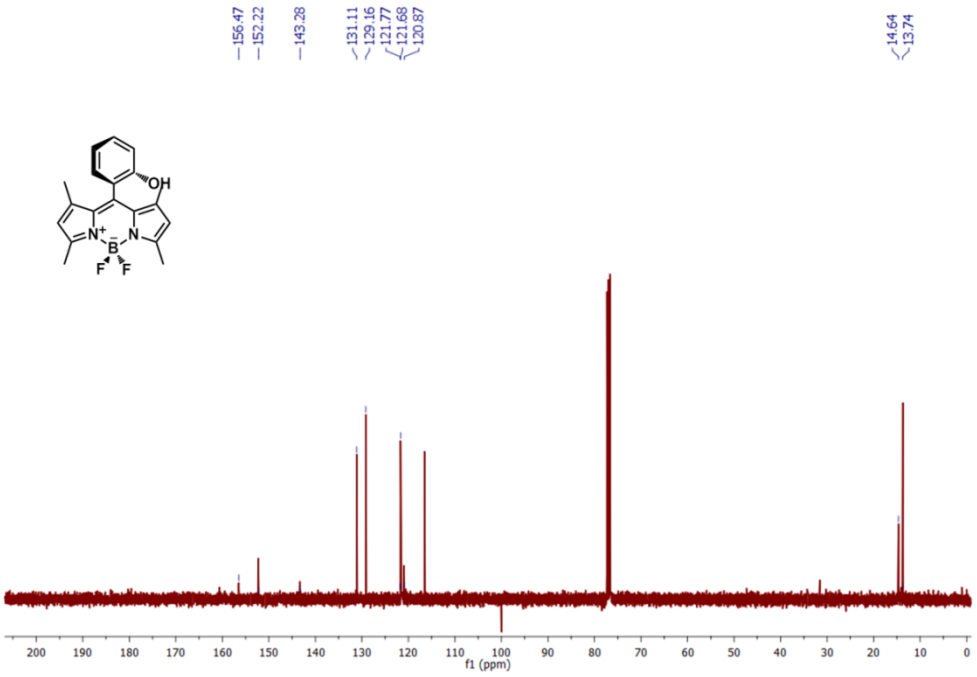

^{13}C-NMR Spectrum of Compound **24**

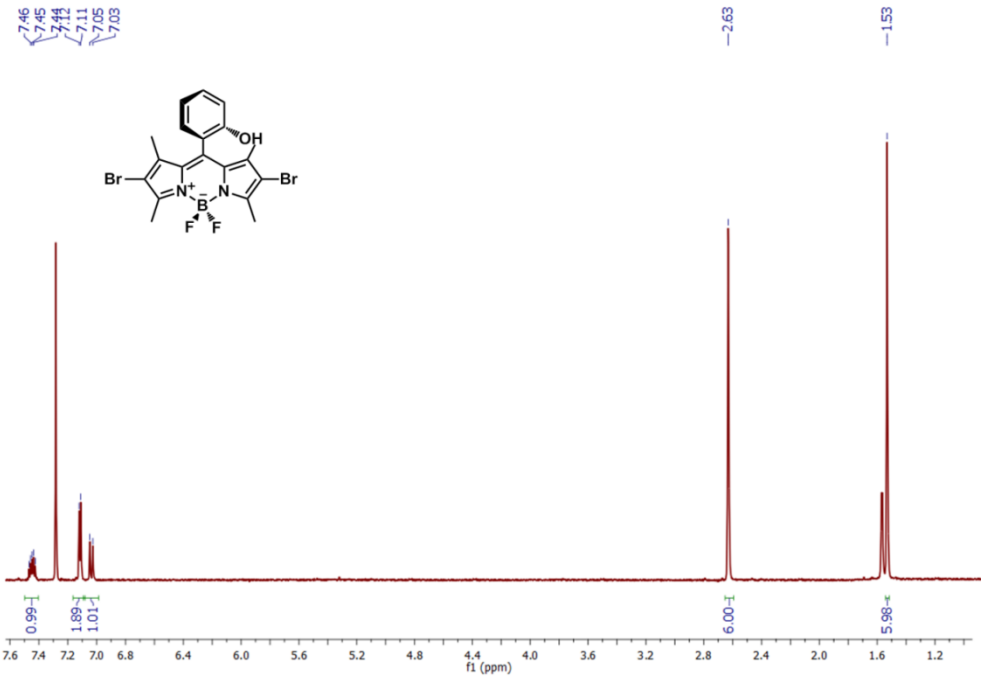

^{1}H-NMR Spectrum of compound **25**

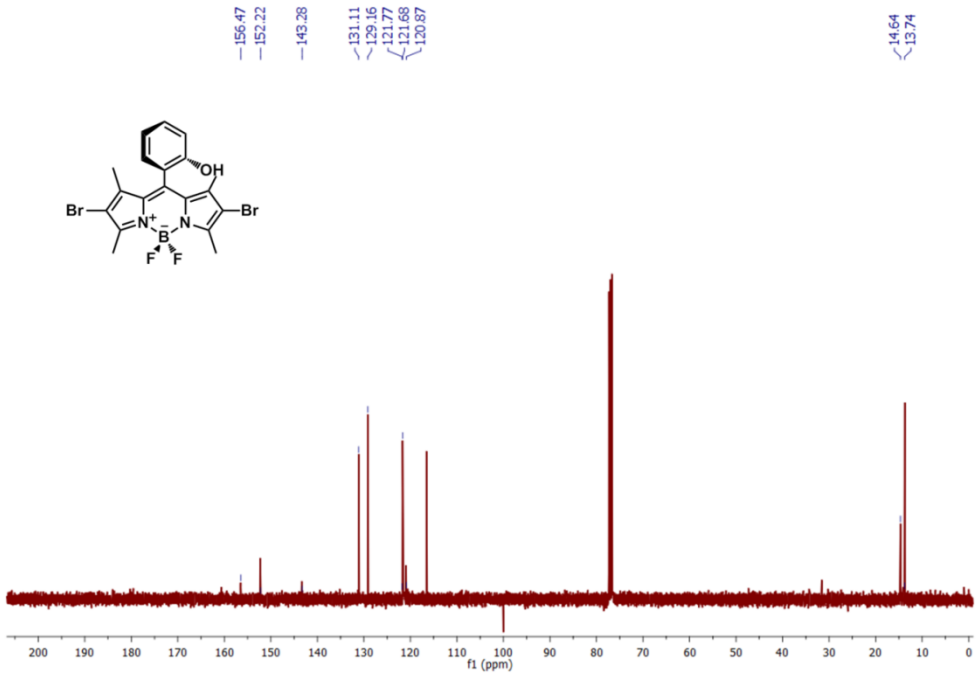

^{13}C-NMR Spectrum of Compound **25**

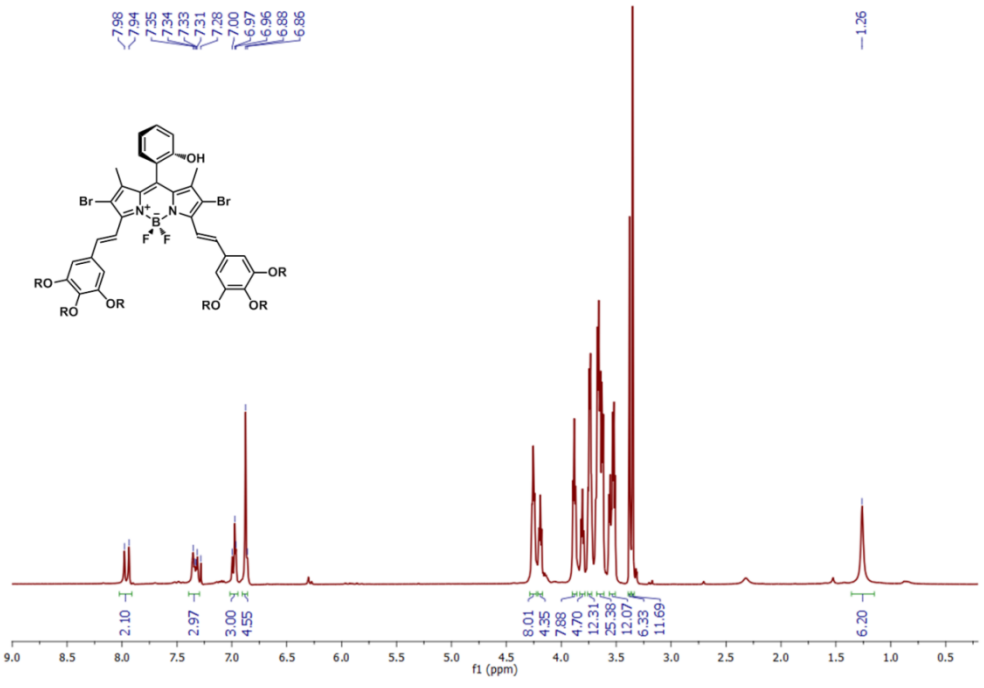

^{1}H-NMR Spectrum of compound **26**

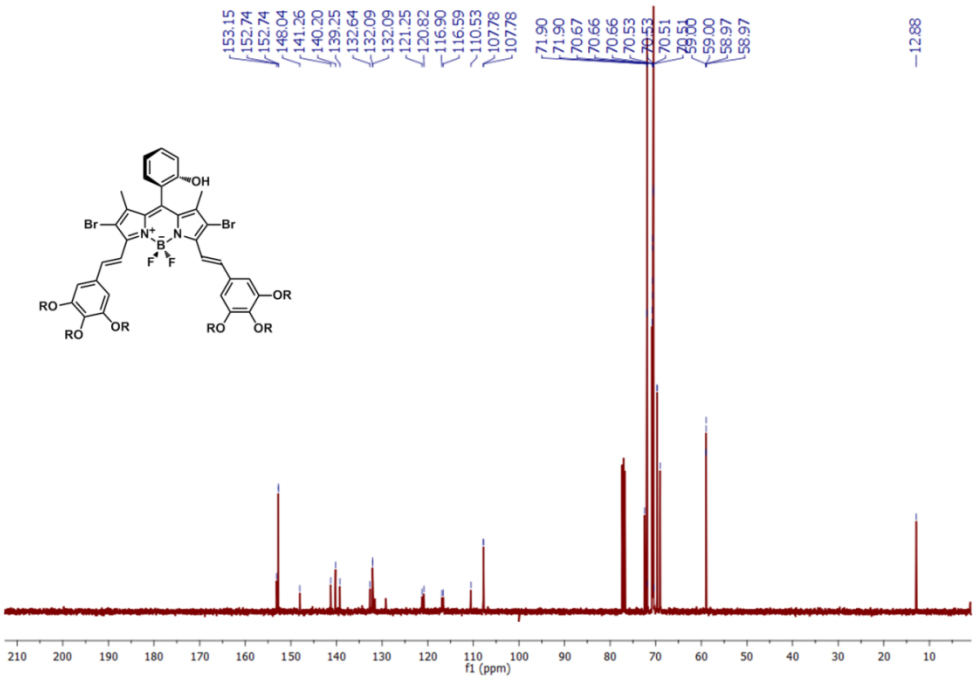

^{13}C-NMR Spectrum of Compound **26**

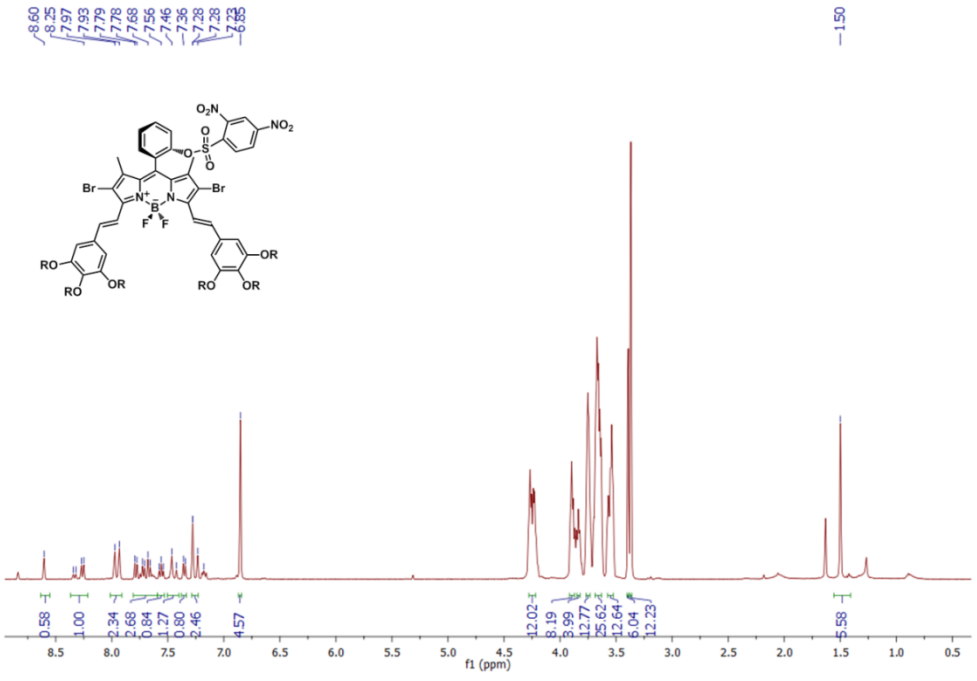

^{1}H-NMR Spectrum of compound **27**

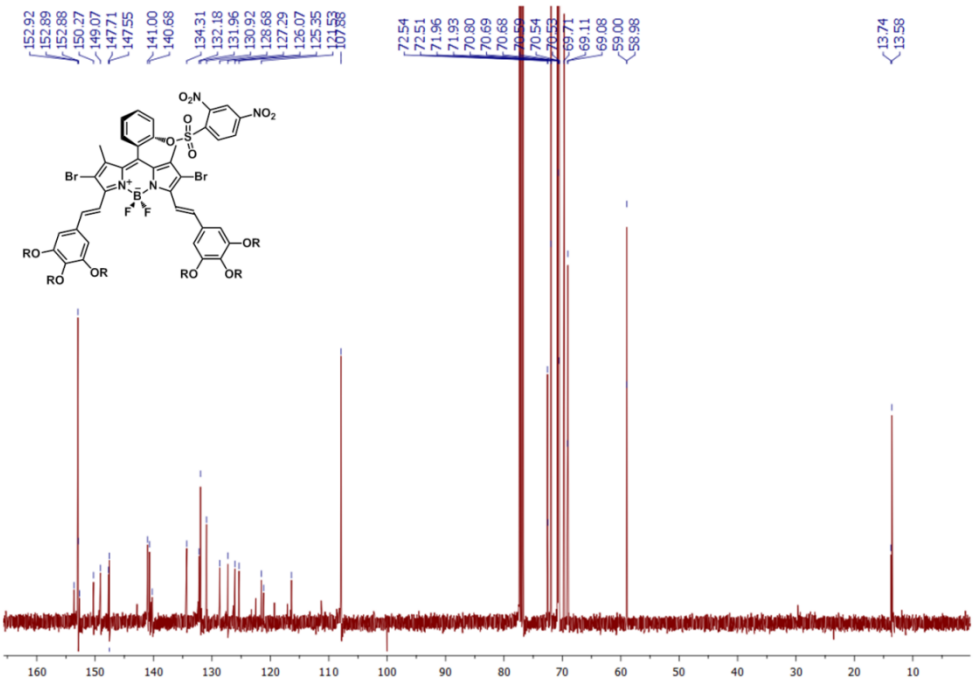

^{13}C-NMR Spectrum of Compound **27**

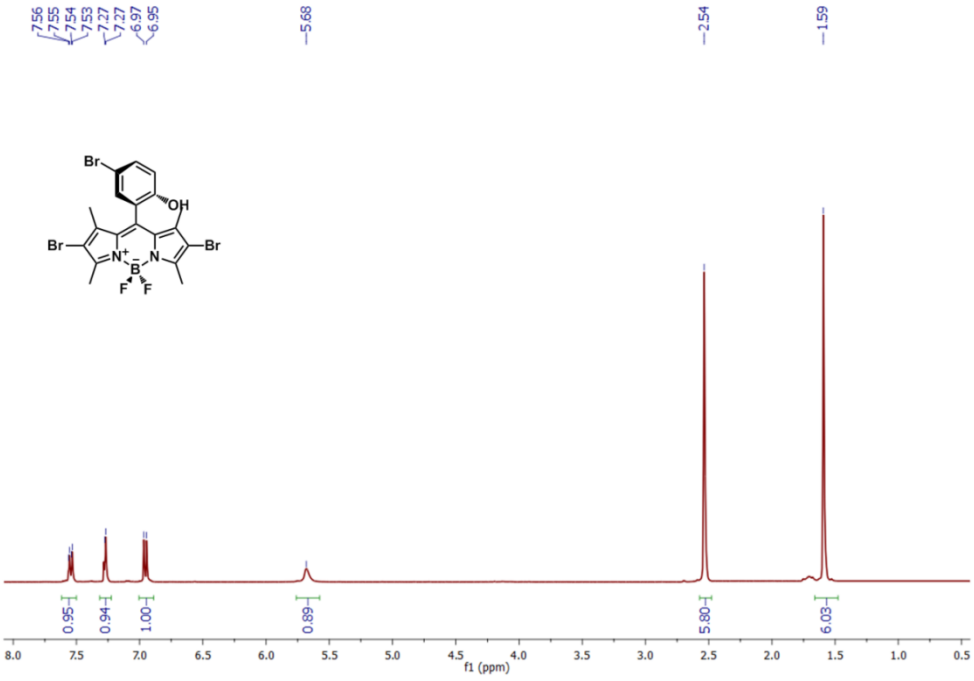

^{1}H-NMR Spectrum of compound **28**

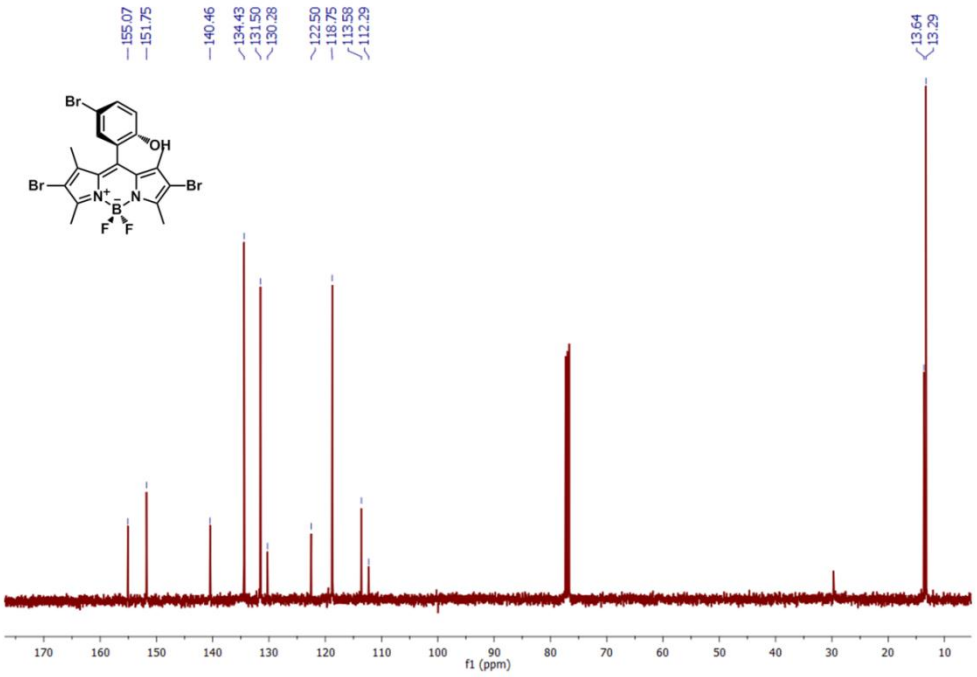

^{13}C-NMR Spectrum of Compound **28**

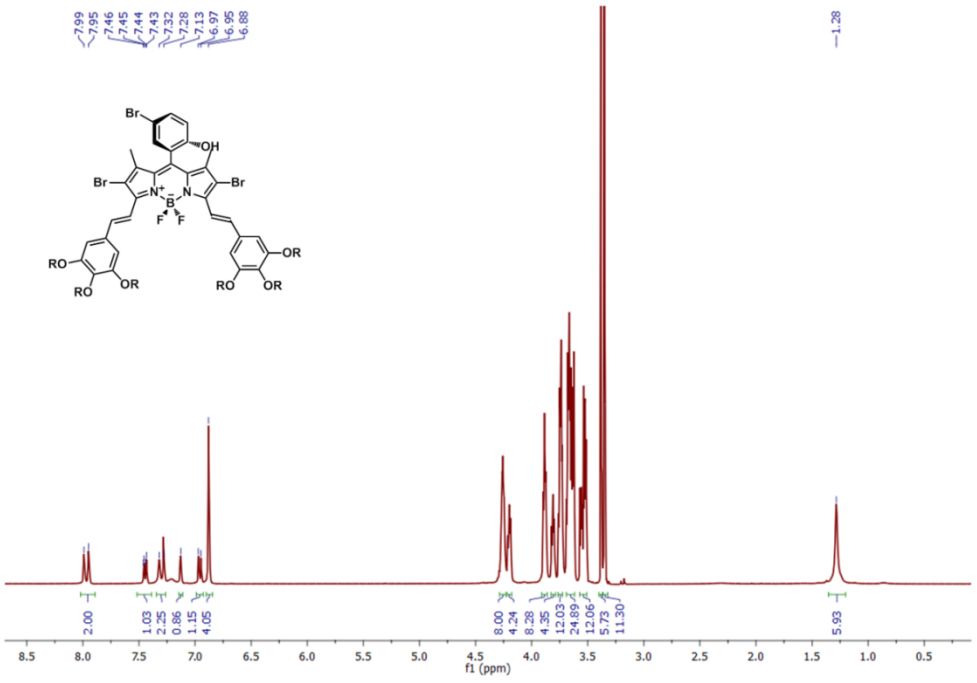

^{1}H-NMR Spectrum of compound **29**

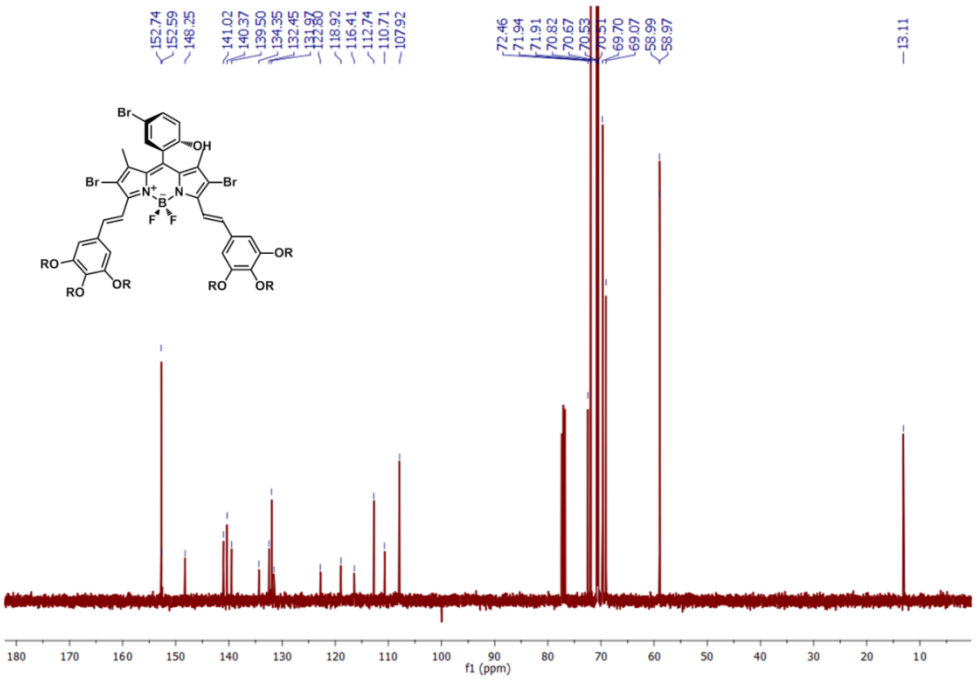

^{13}C-NMR Spectrum of Compound **29**

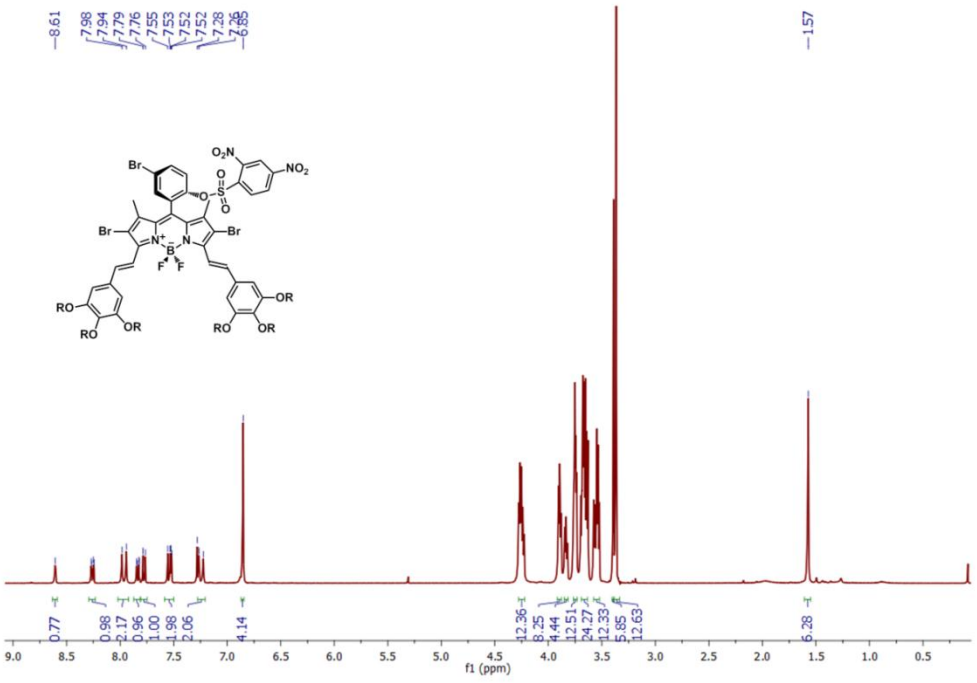

^{1}H-NMR Spectrum of compound **30**

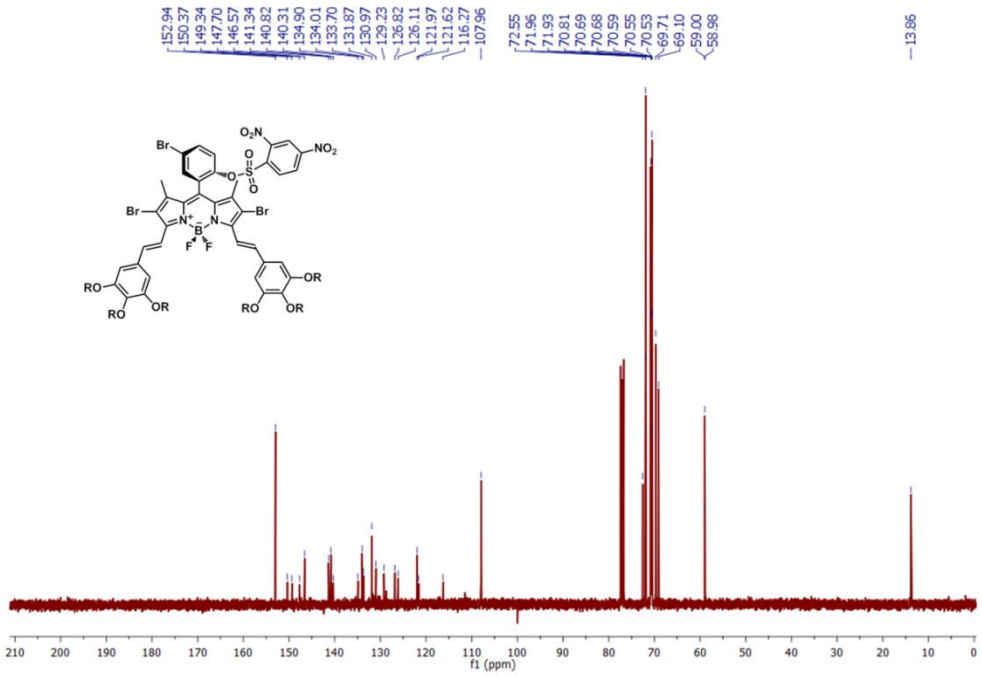

^{13}C-NMR Spectrum of Compound **30**

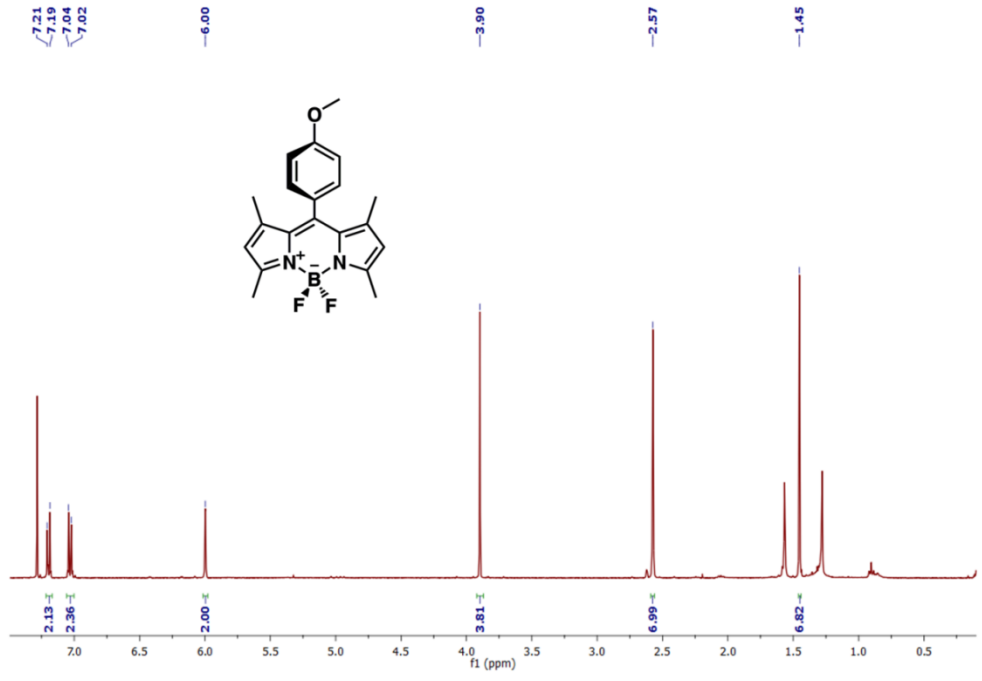

^{1}H-NMR Spectrum of compound **31**

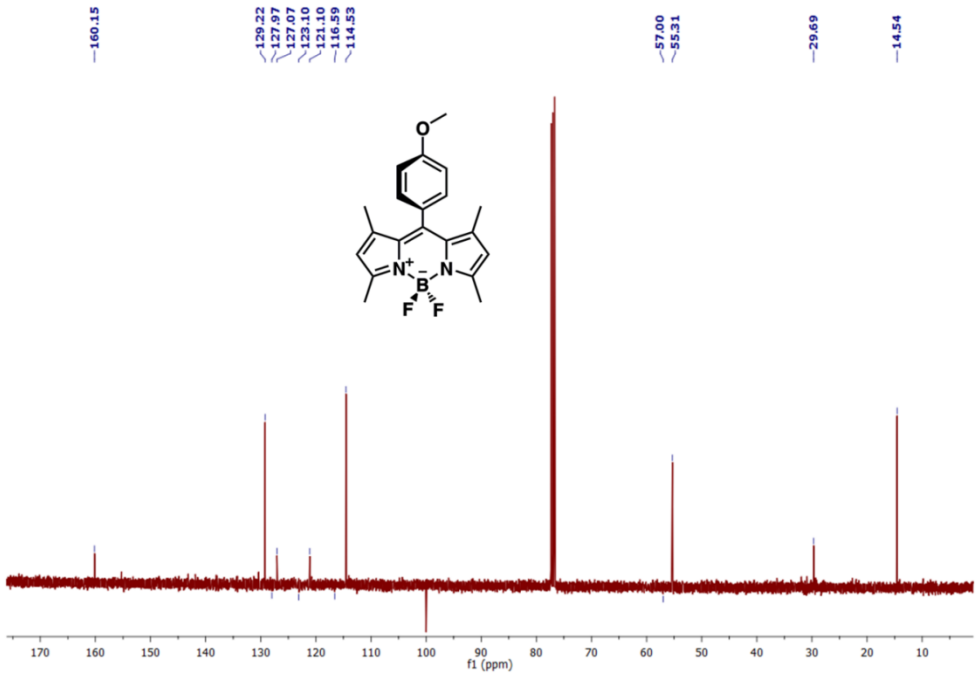

^{13}C-NMR Spectrum of Compound **31**

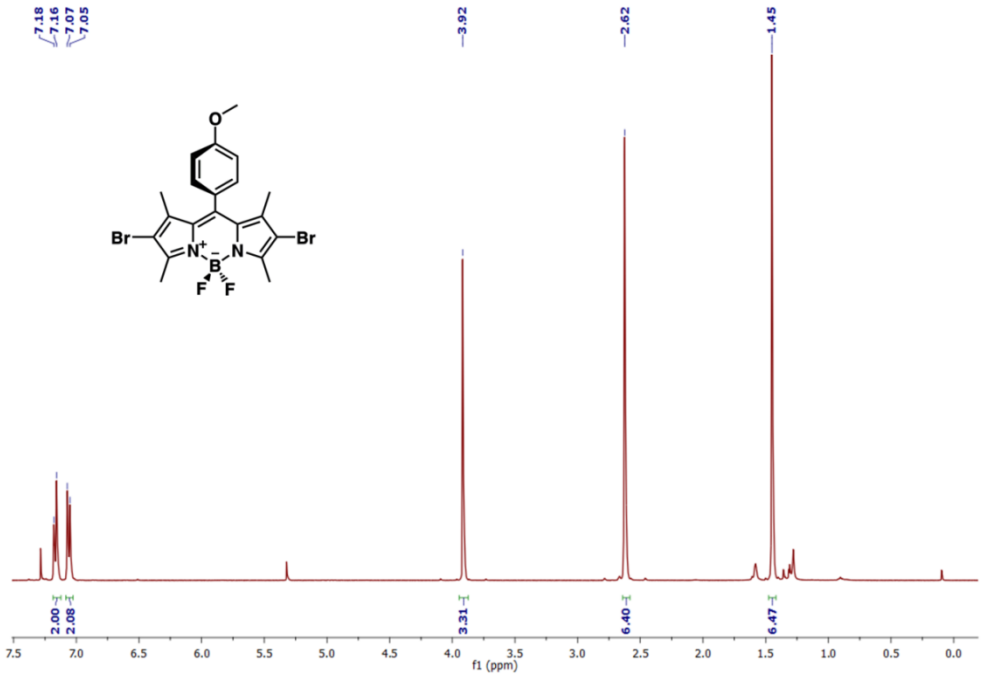

^{1}H-NMR Spectrum of compound **32**

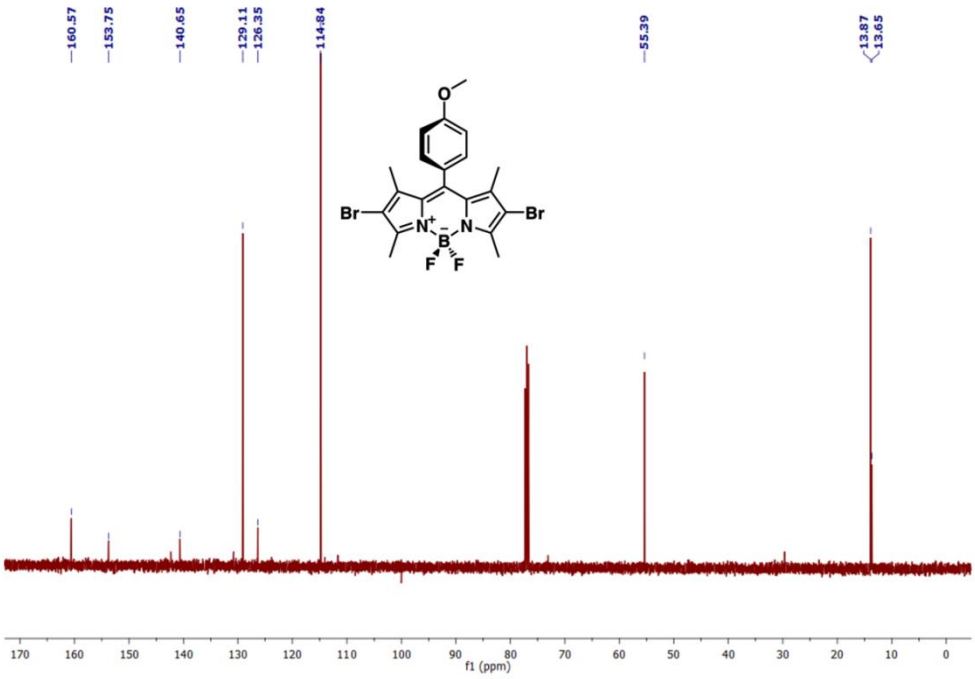

^{13}C-NMR Spectrum of Compound **32**

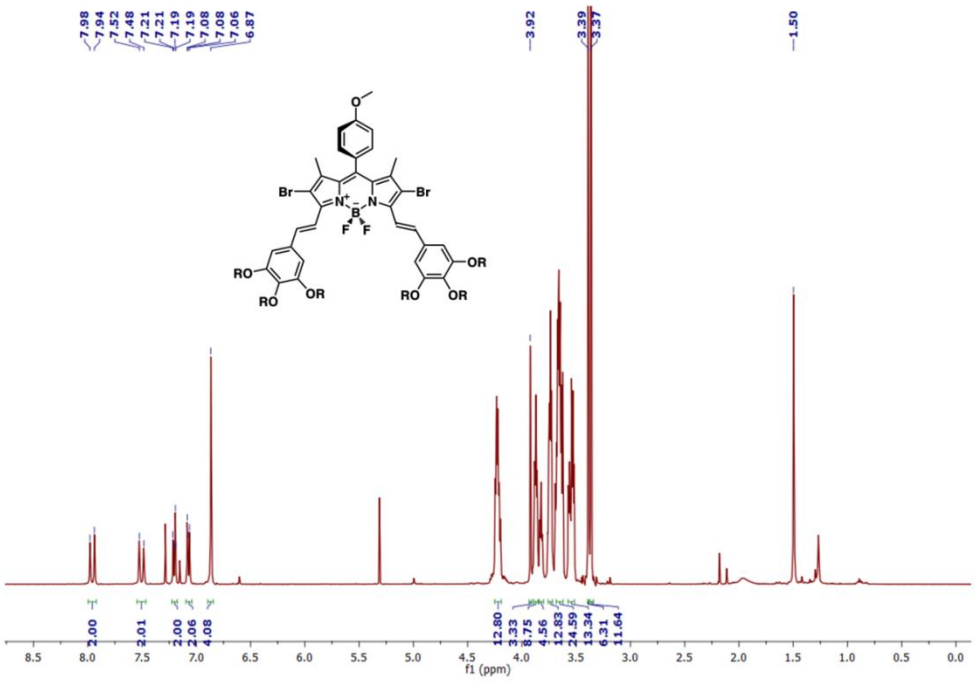

^{1}H-NMR Spectrum of compound **33**

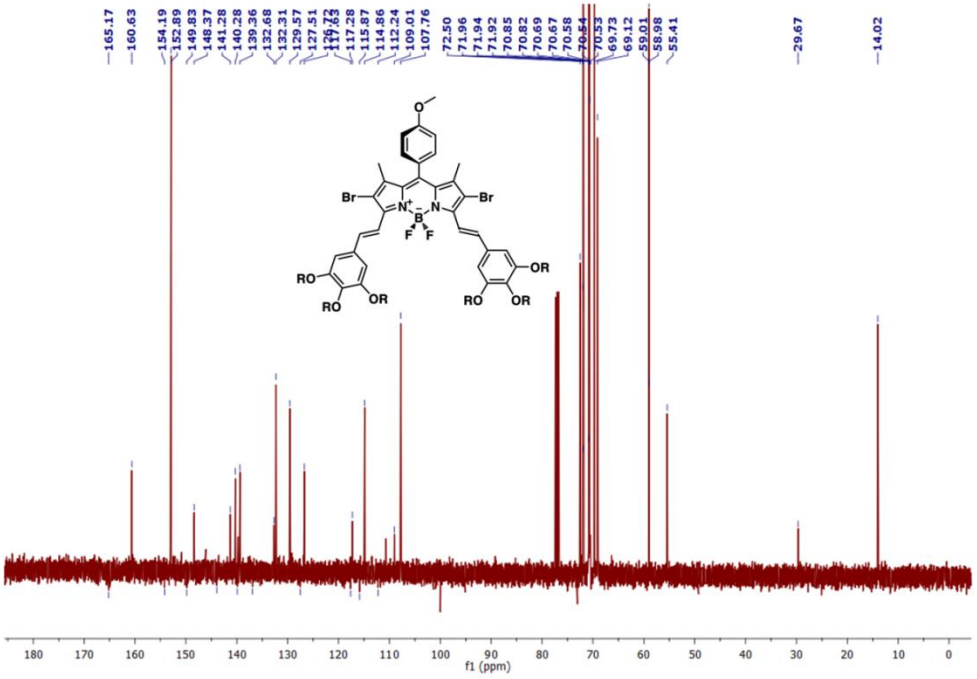

^{13}C-NMR Spectrum of Compound **33**

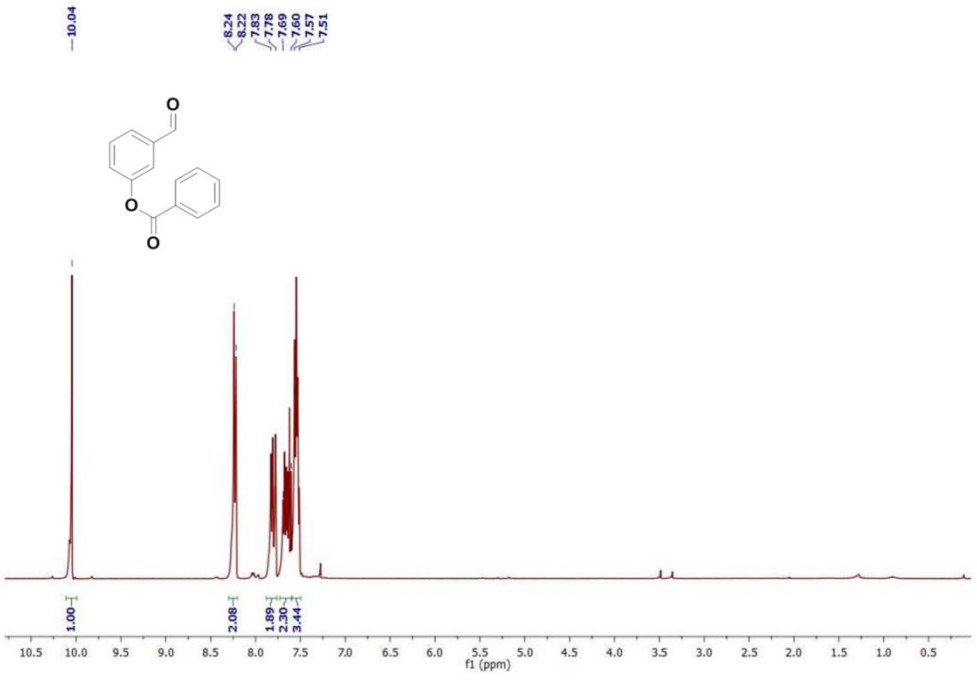

^{1}H-NMR Spectrum of compound **34**

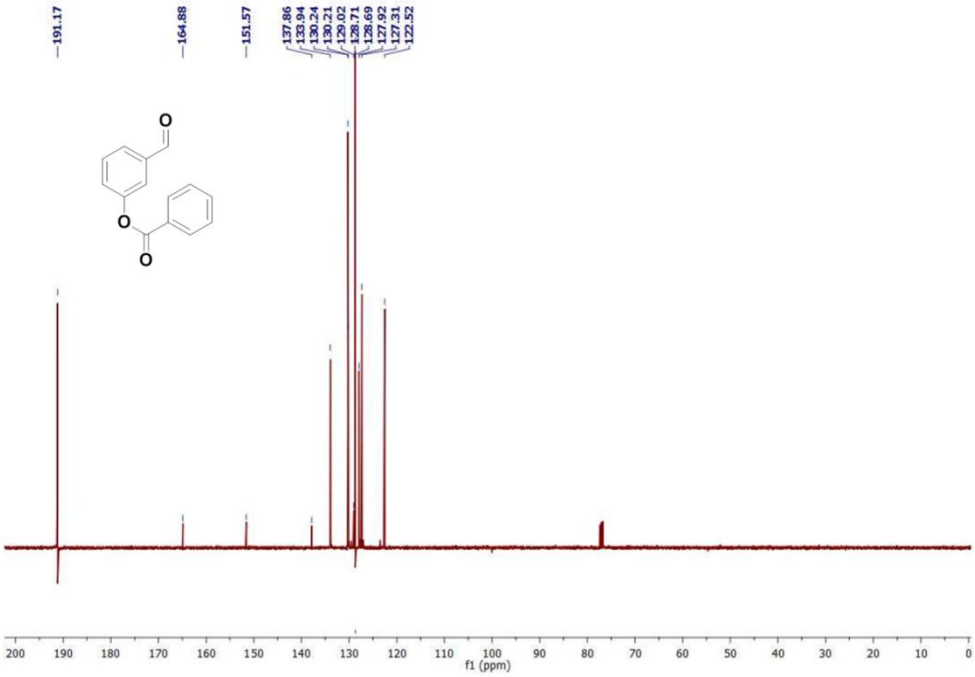

^{13}C-NMR Spectrum of Compound **34**

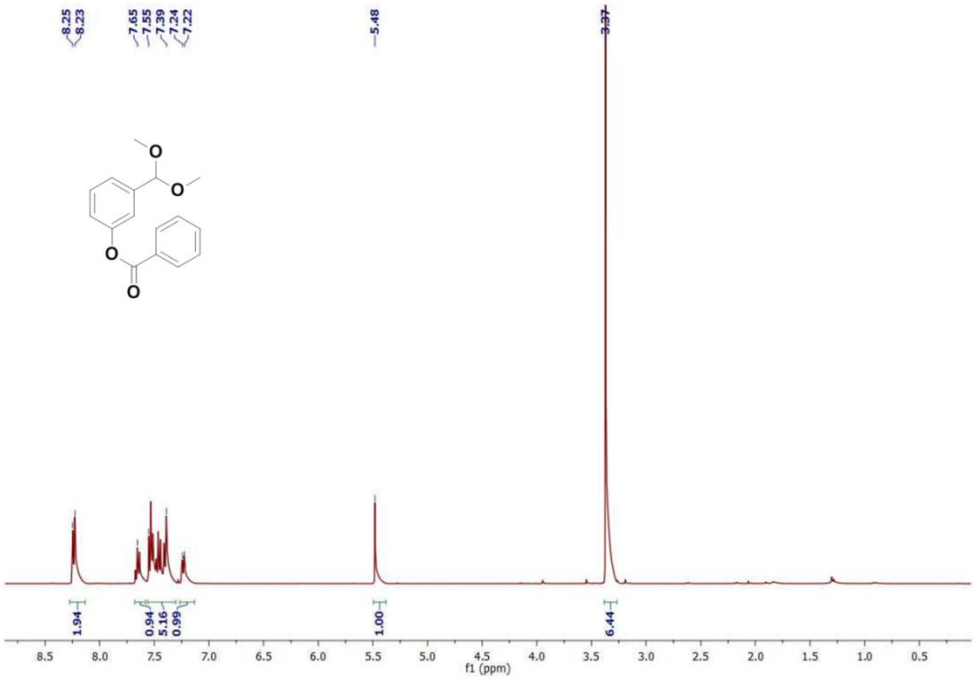

^{1}H-NMR Spectrum of compound **35**

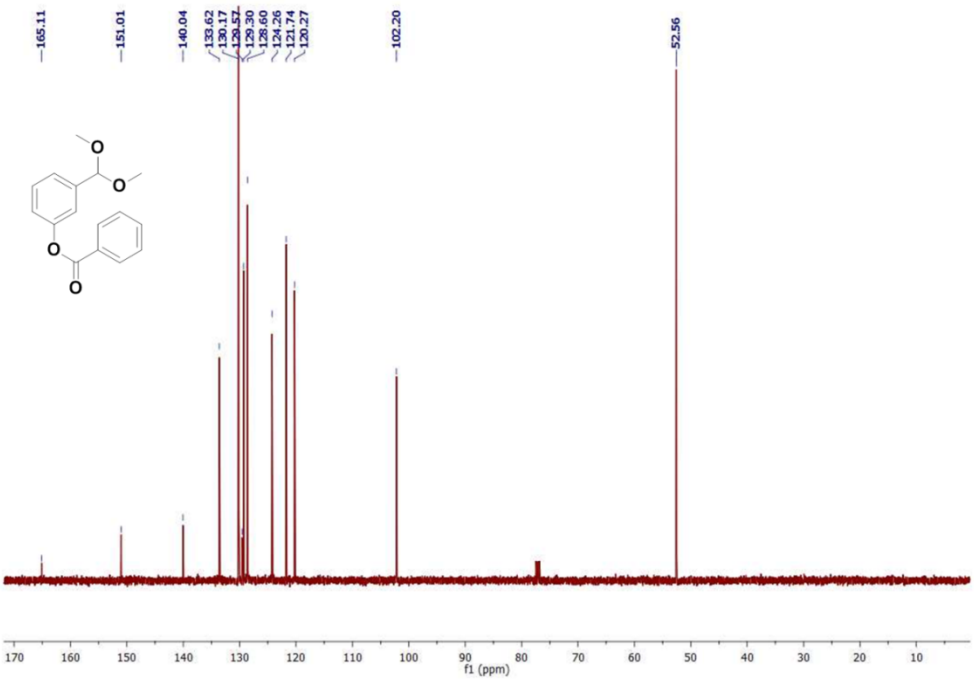

^{13}C-NMR Spectrum of Compound **35**

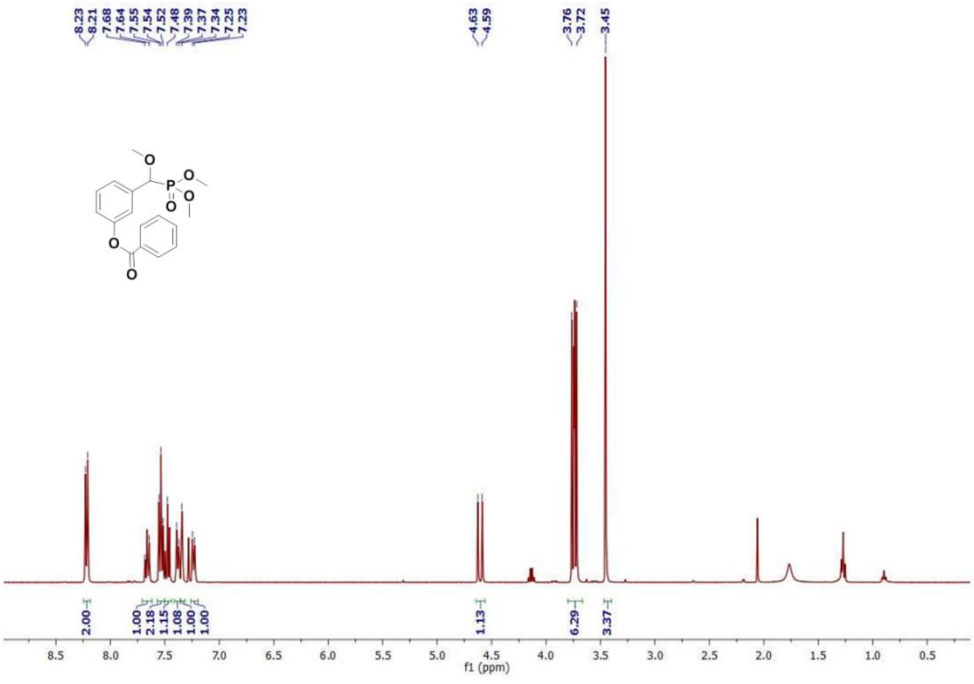

^{1}H-NMR Spectrum of compound **36**

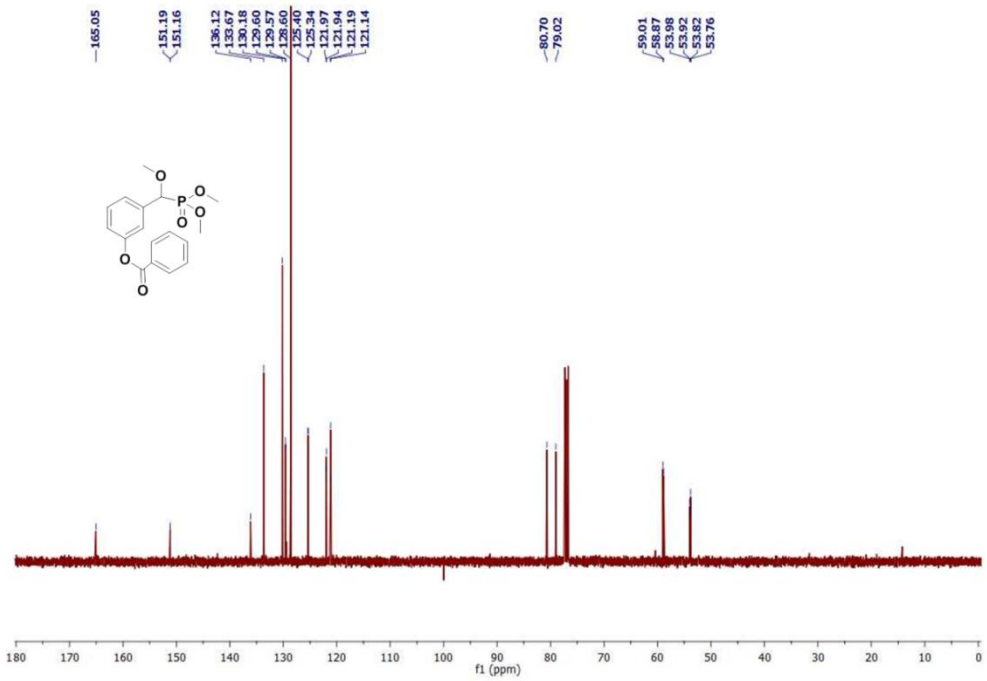

^{13}C-NMR Spectrum of Compound **36**

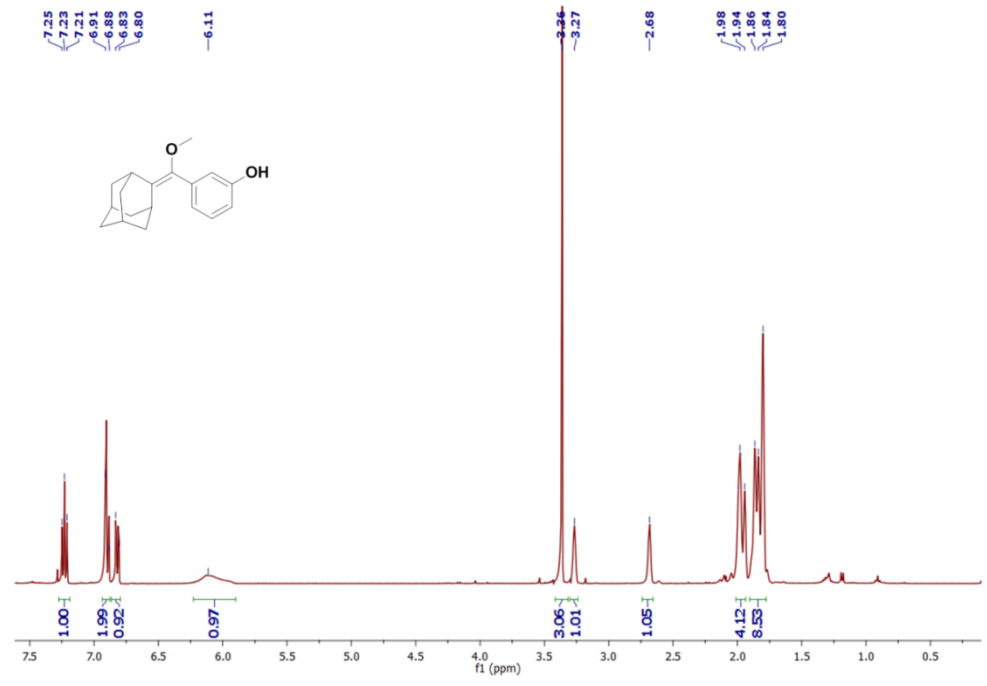

^{1}H-NMR Spectrum of compound **37**

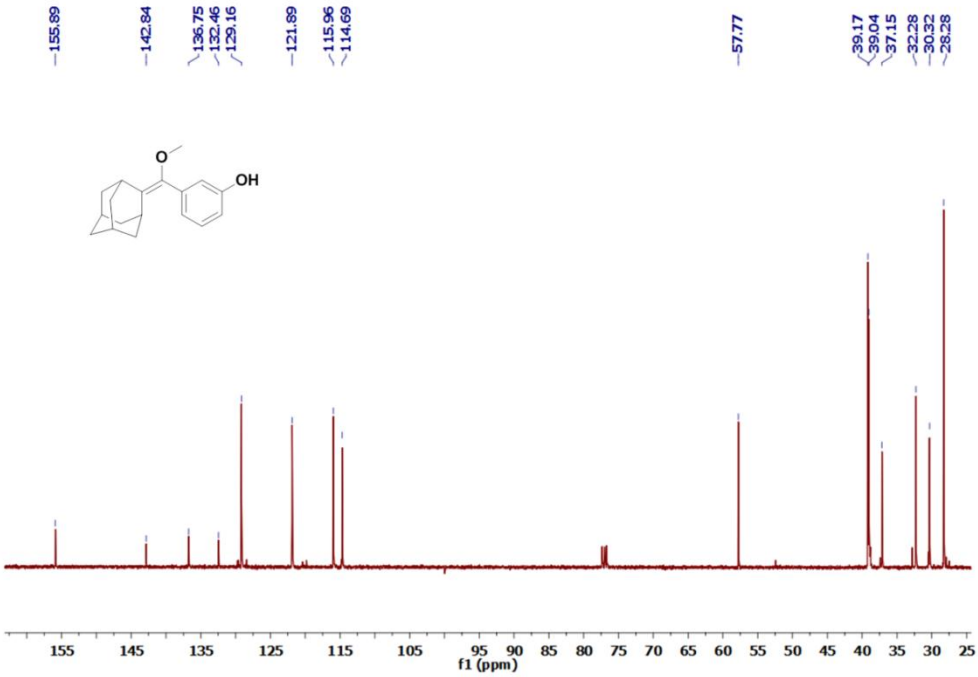

^{13}C-NMR Spectrum of Compound **37**

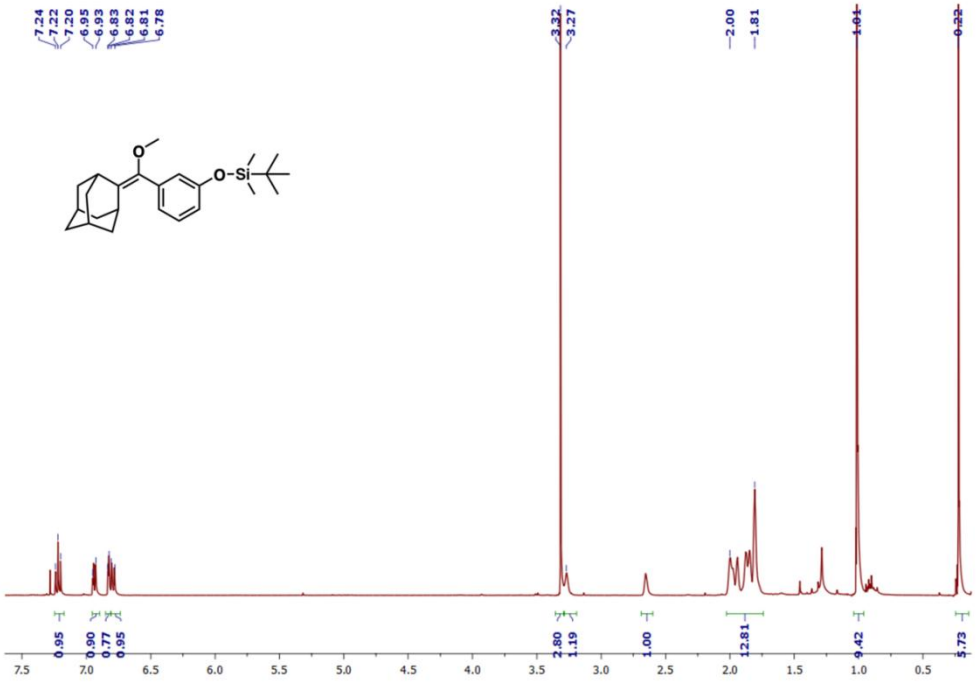

^{1}H-NMR Spectrum of compound **38**

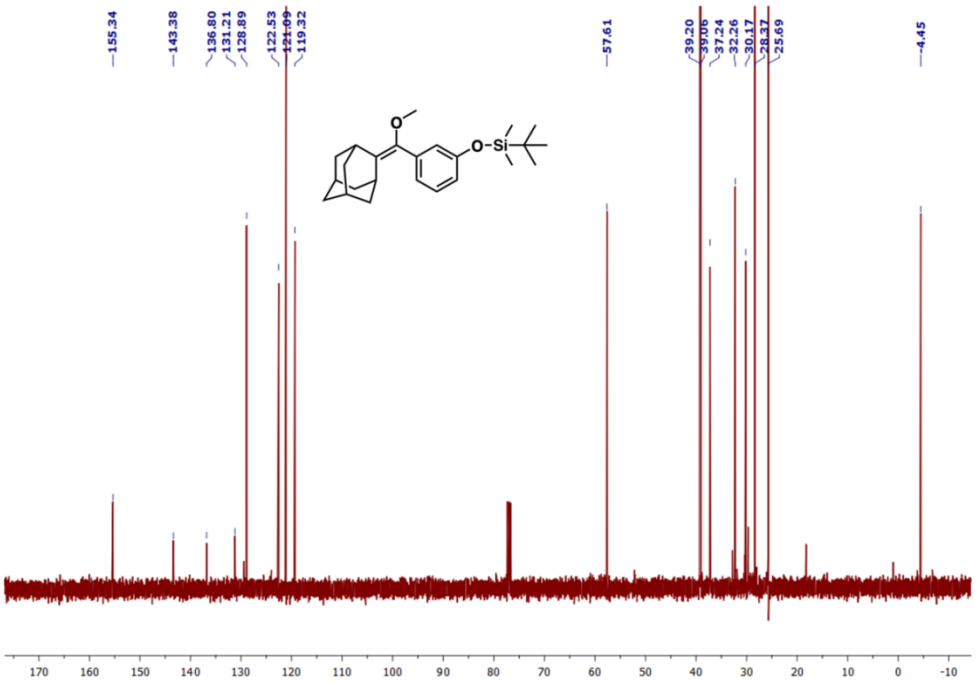

^{13}C-NMR Spectrum of Compound **38**

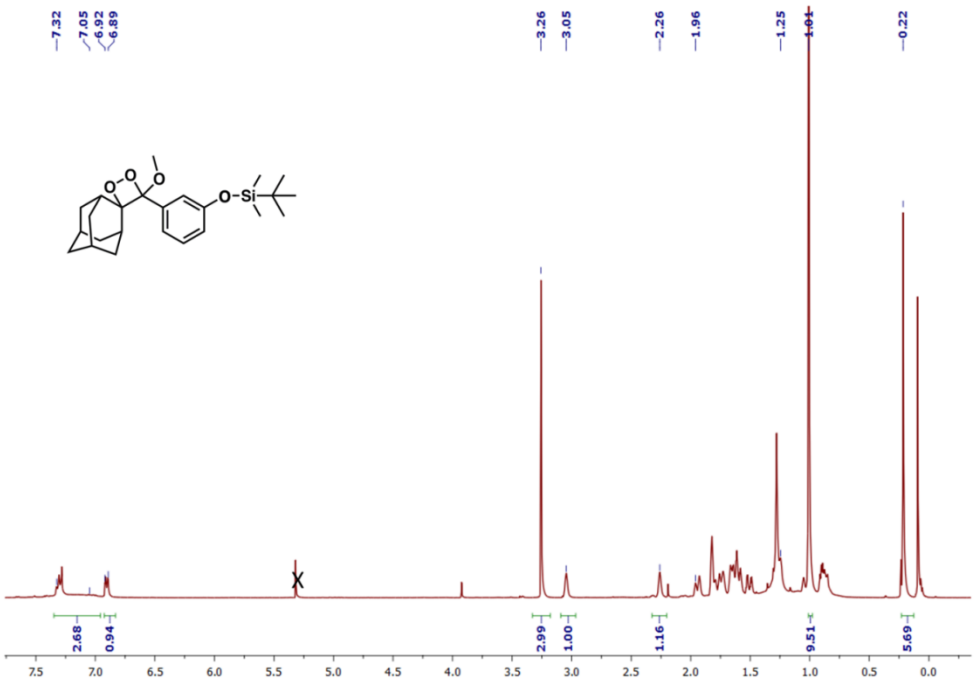

^{1}H-NMR Spectrum of compound **39**

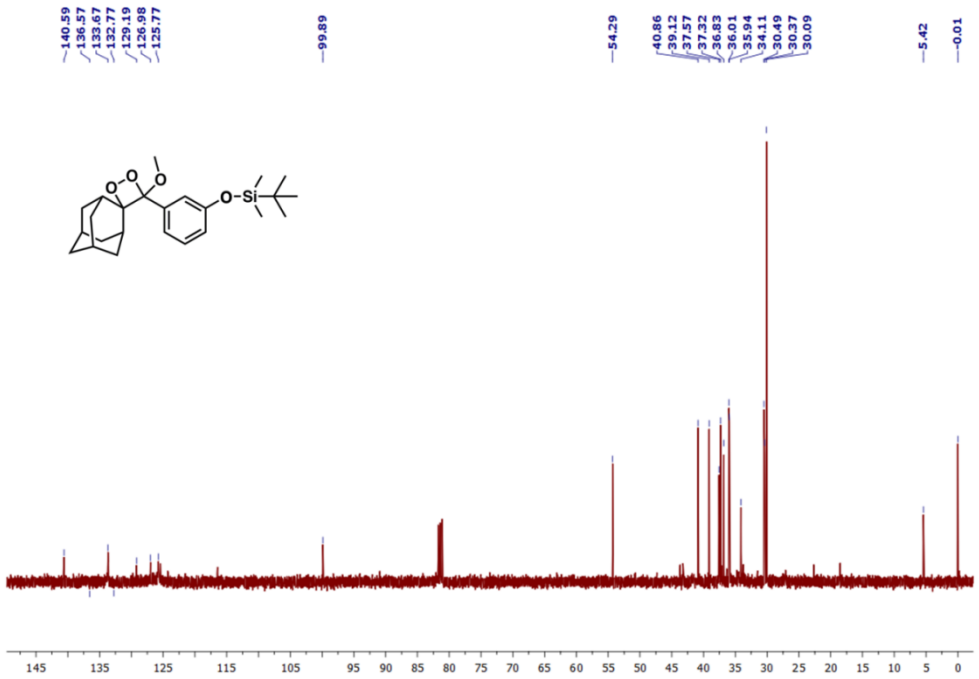

^{13}C-NMR Spectrum of Compound **39**

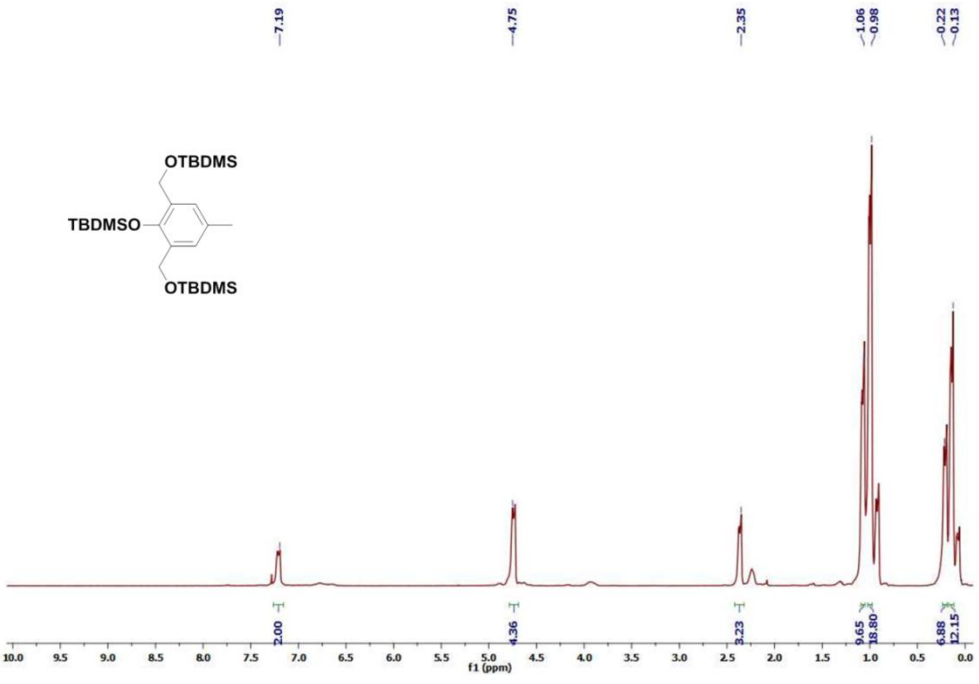

^{1}H-NMR Spectrum of compound **40**

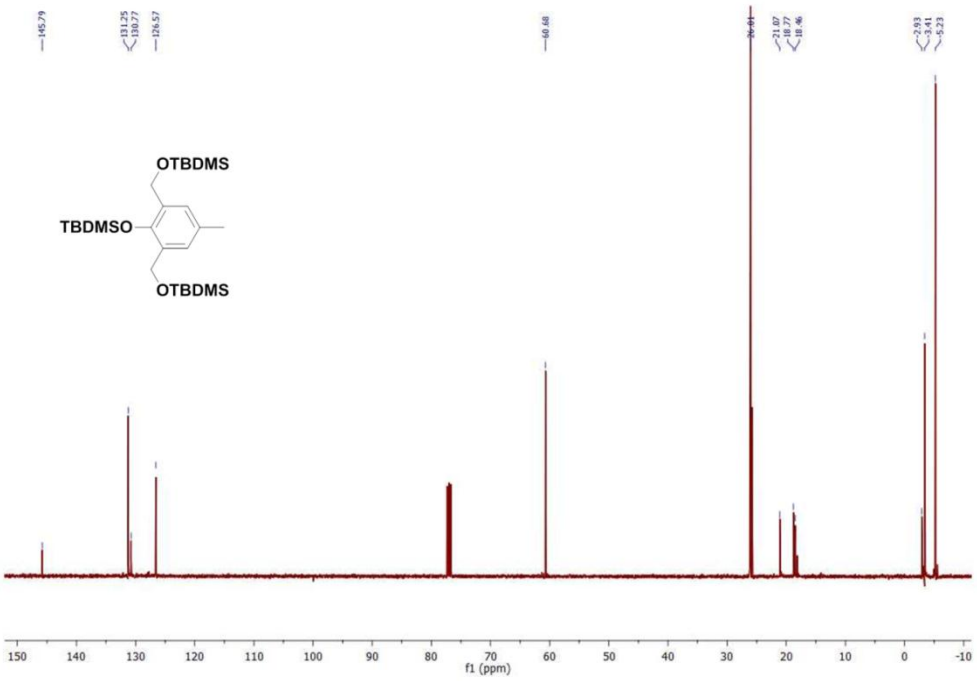

^{13}C-NMR Spectrum of Compound **40**

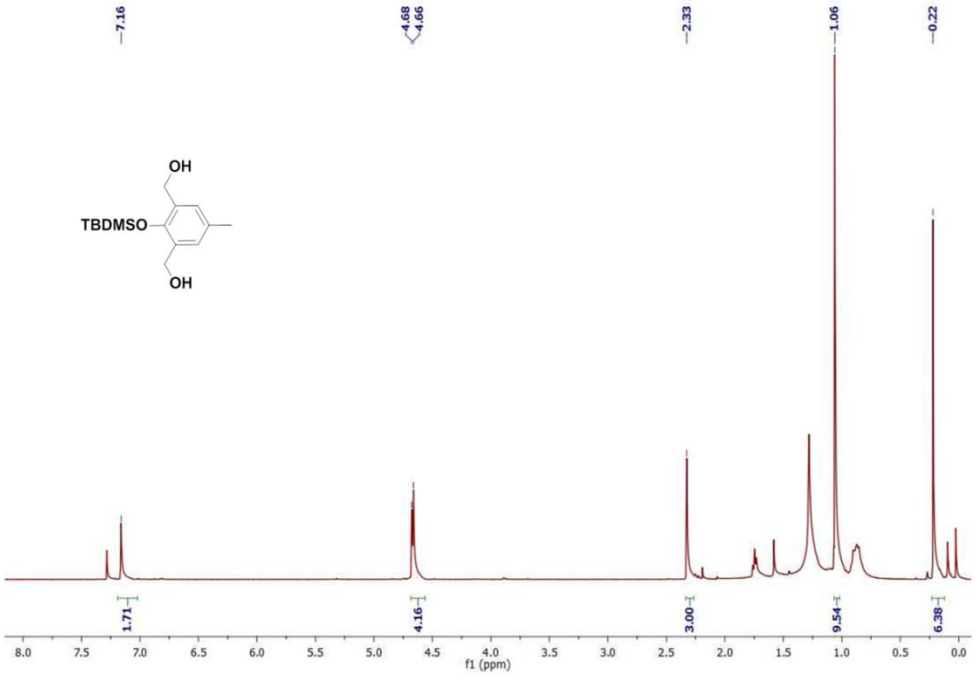

^{1}H-NMR Spectrum of compound **41**

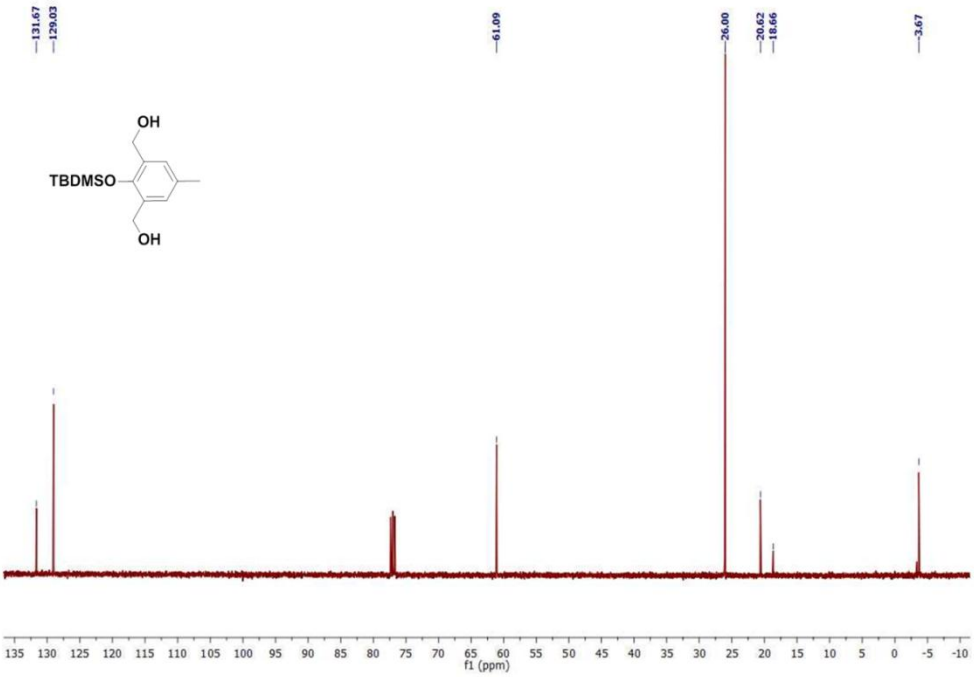

^{13}C-NMR Spectrum of Compound **41**

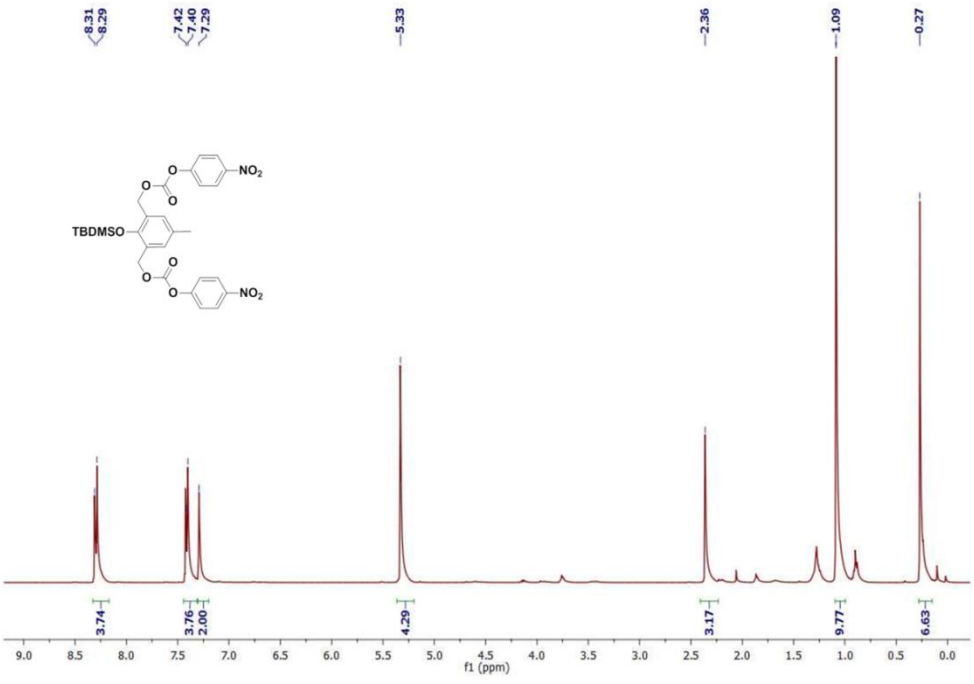

^{1}H-NMR Spectrum of compound **42**

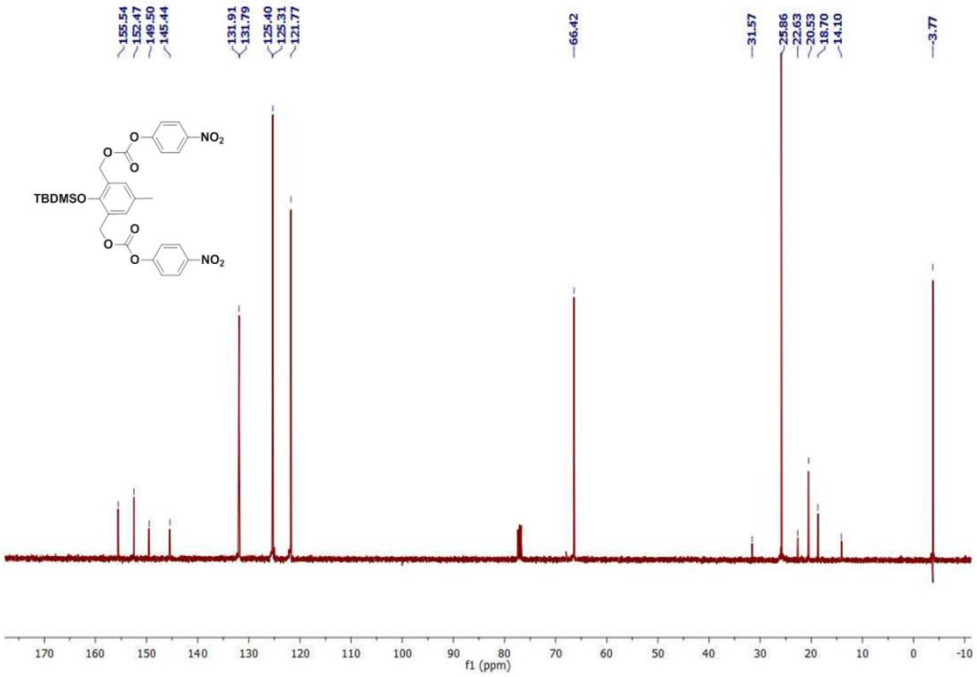

^{13}C-NMR Spectrum of Compound **42**

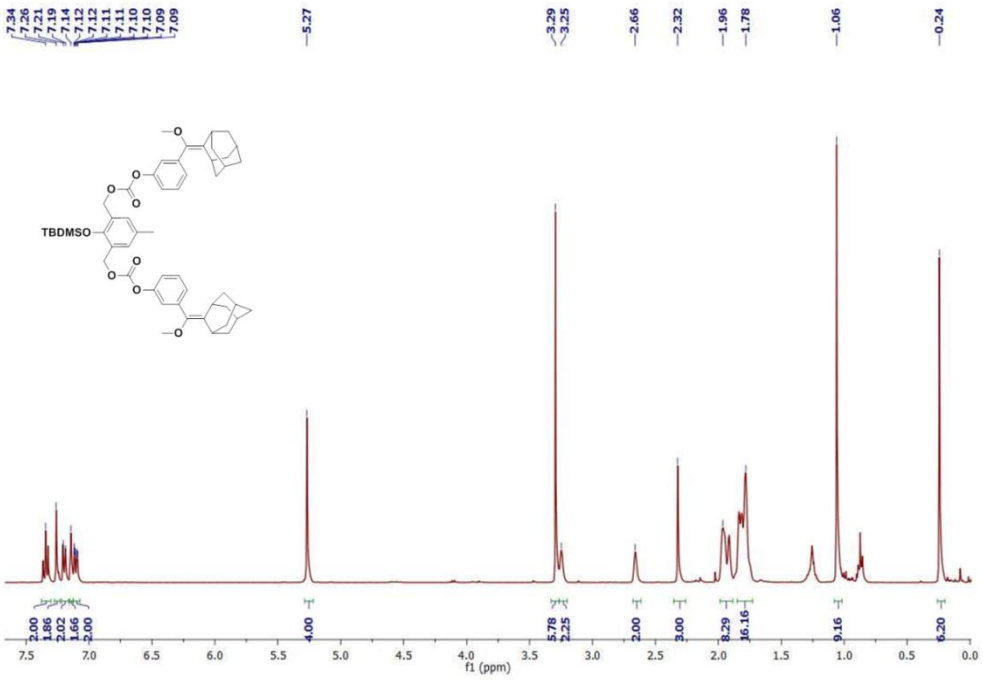

^{1}H-NMR Spectrum of compound **43**

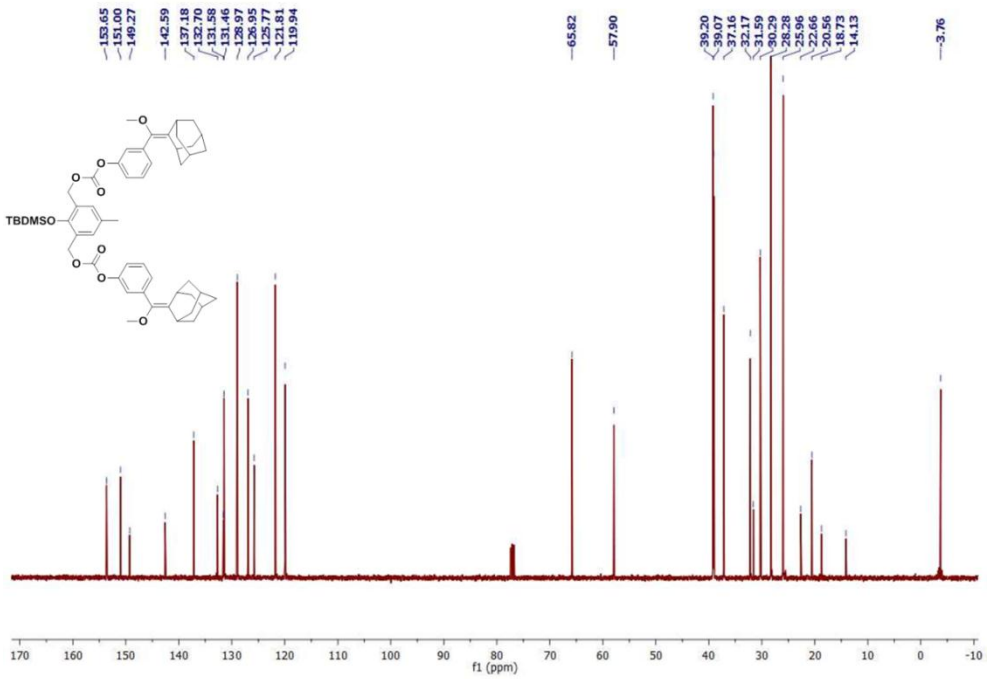

^{13}C-NMR Spectrum of Compound **43**

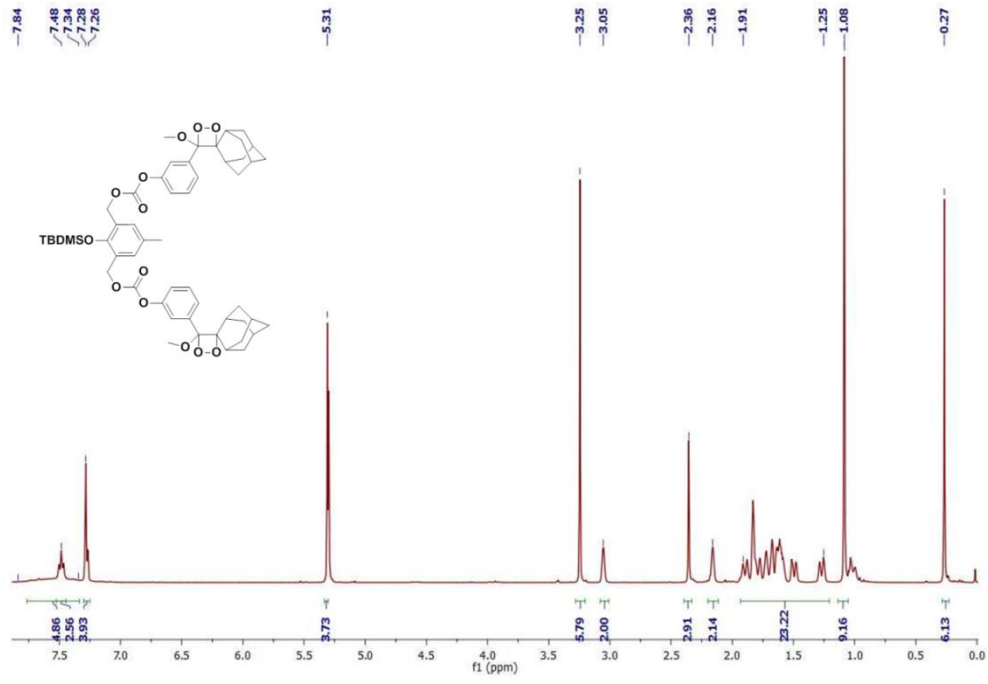

^{1}H-NMR Spectrum of compound **44**

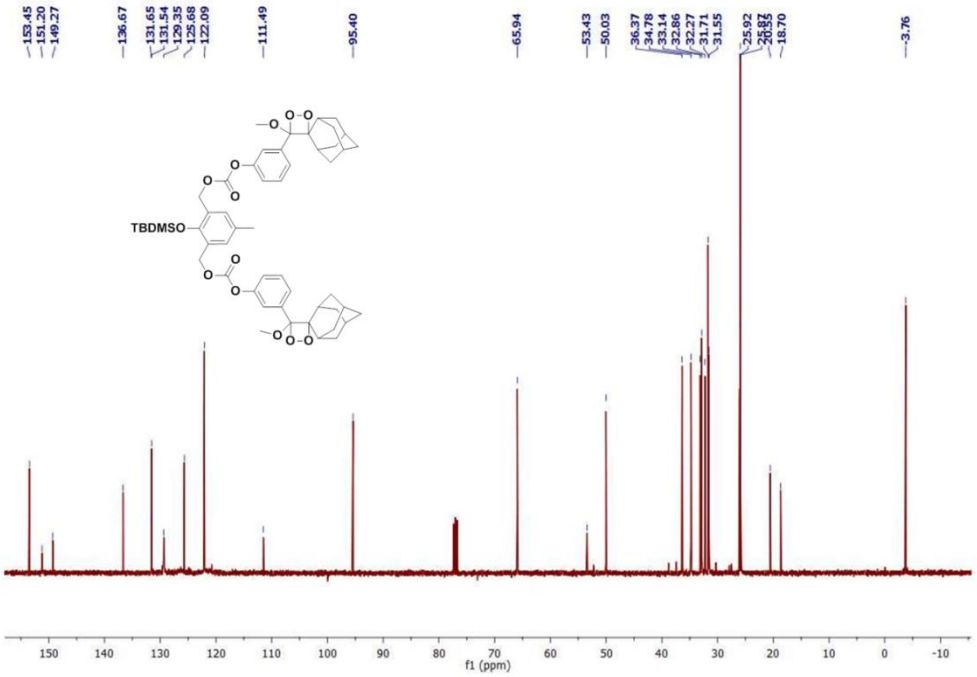

^{13}C-NMR Spectrum of Compound **44**

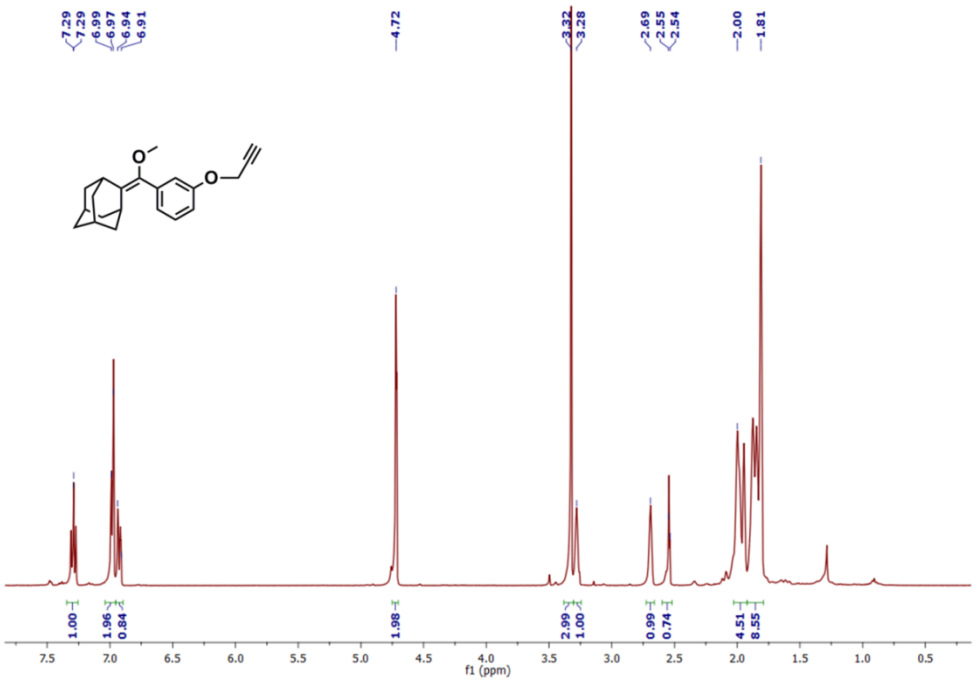

^{1}H-NMR Spectrum of compound **45**

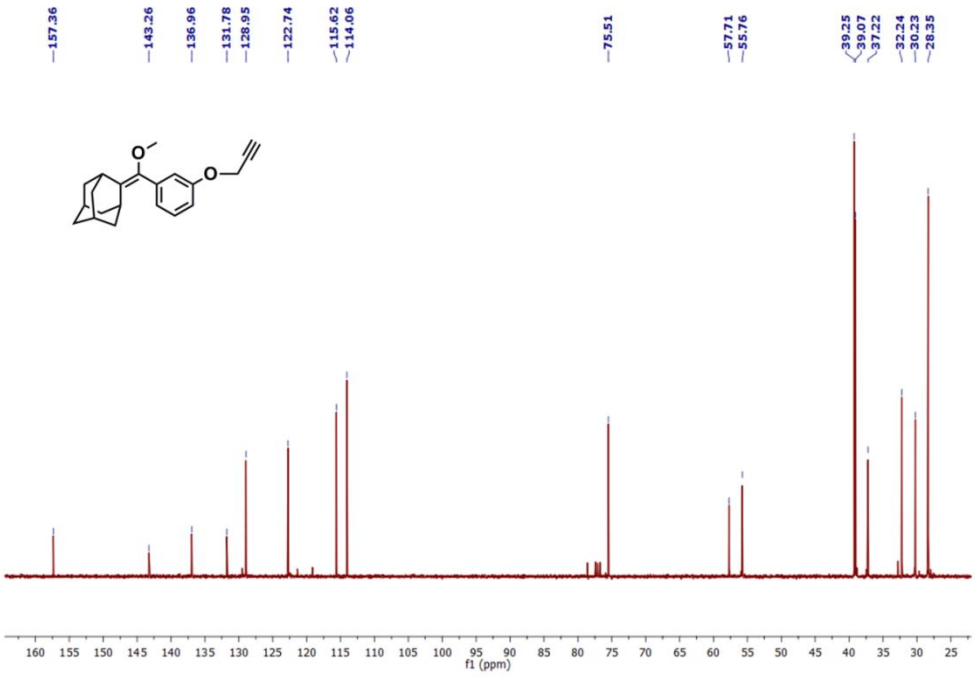

^{13}C-NMR Spectrum of Compound **45**

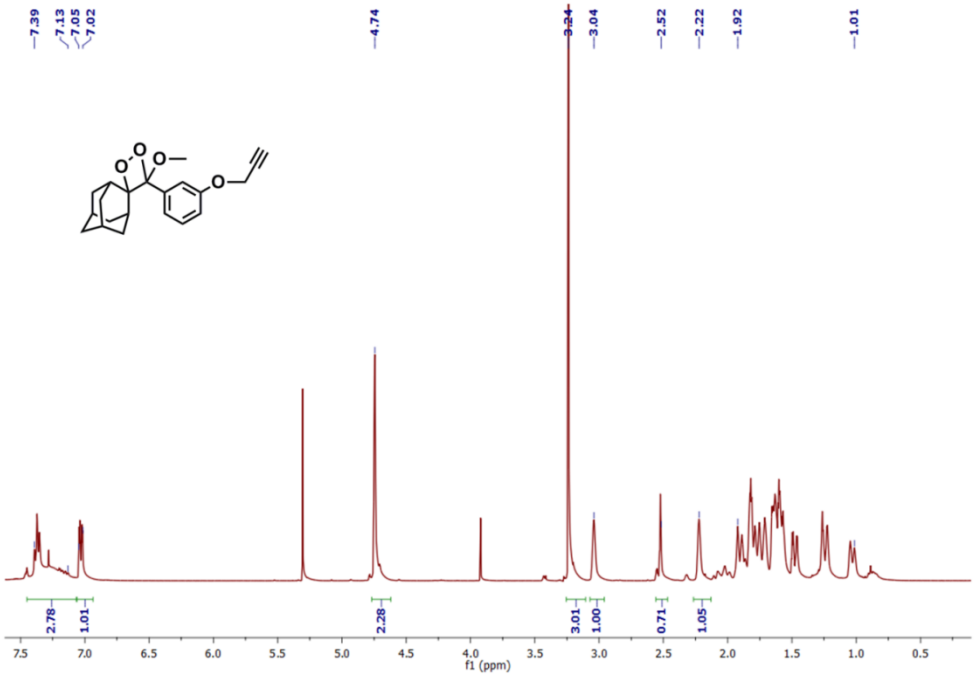

^{1}H-NMR Spectrum of compound **46**

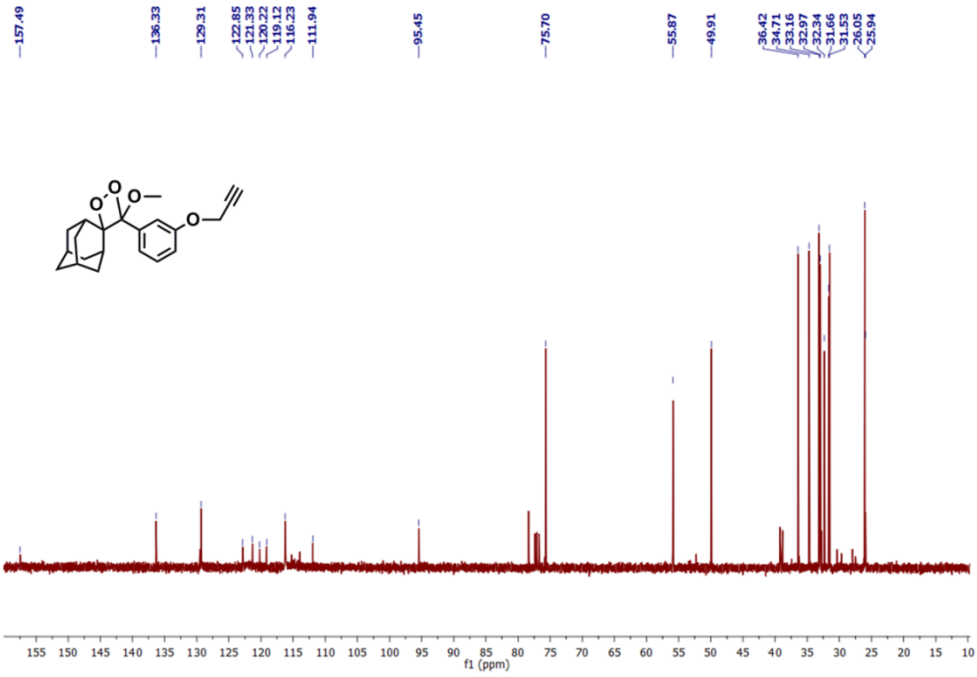

^{13}C-NMR Spectrum of Compound **46**

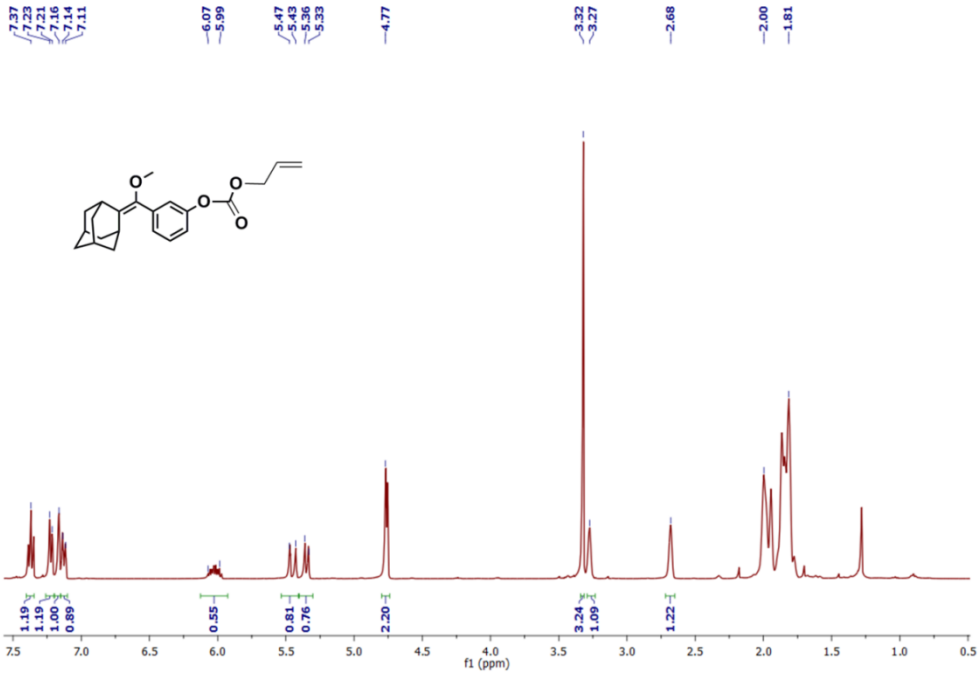

^{1}H-NMR Spectrum of compound **47**

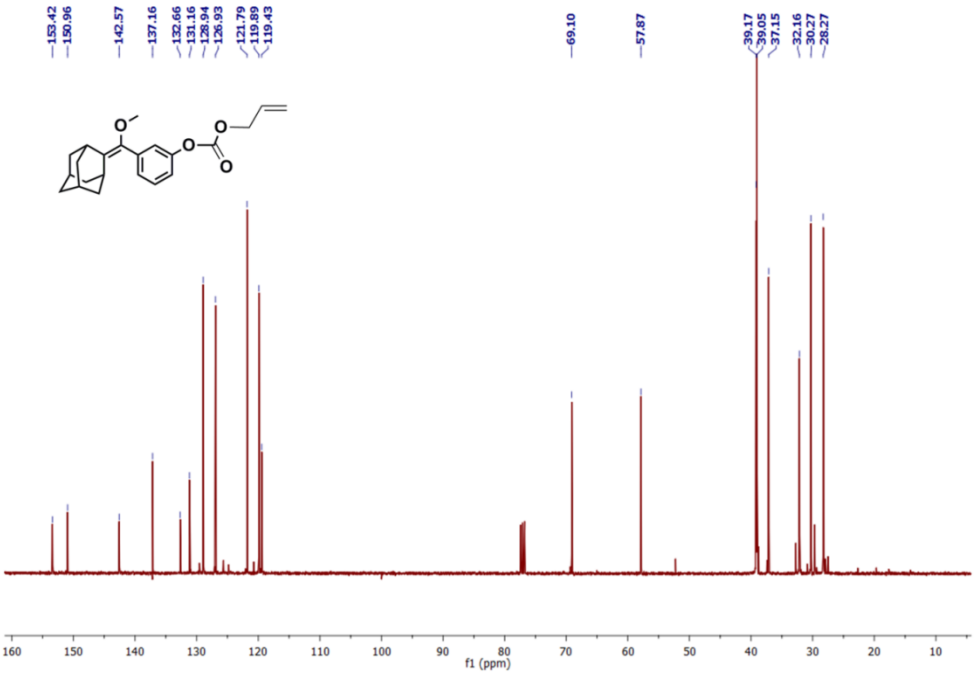

^{13}C-NMR Spectrum of Compound **47**

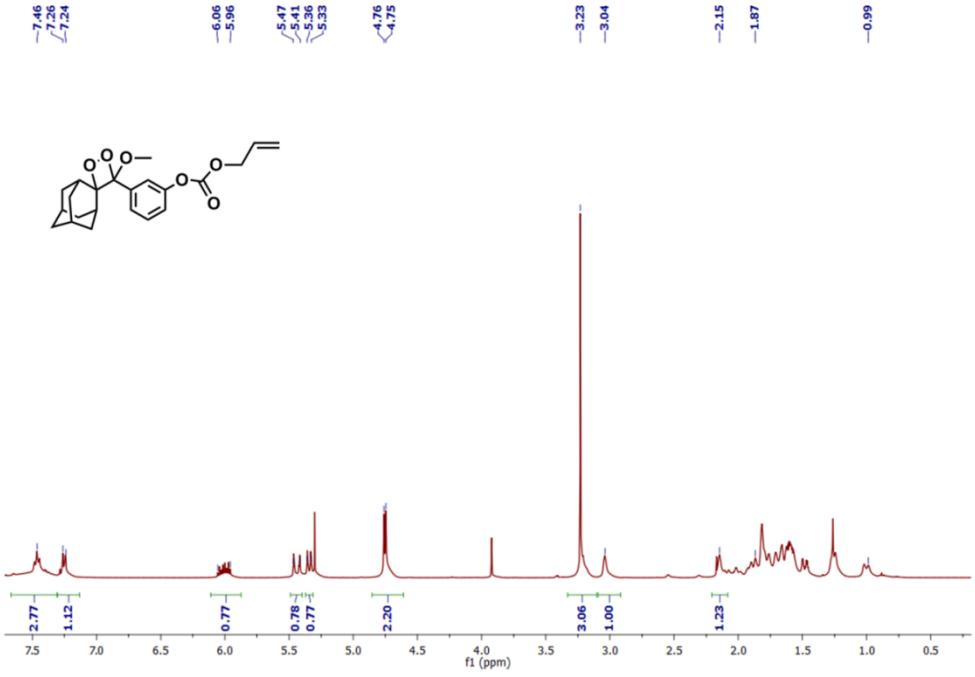

^{1}H-NMR Spectrum of compound **48**

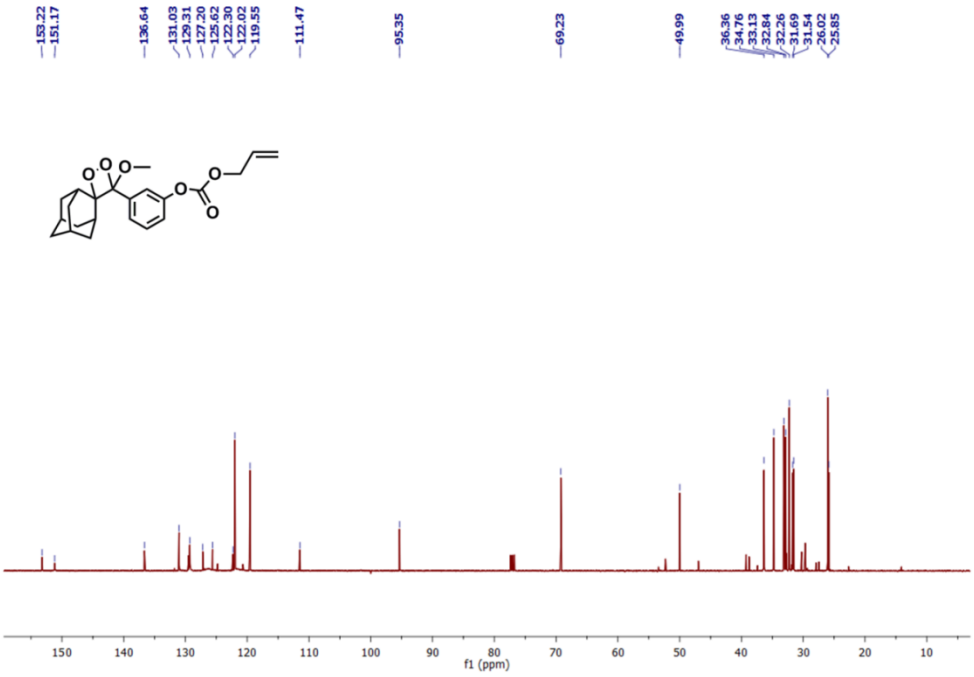

^{13}C-NMR Spectrum of Compound **48**

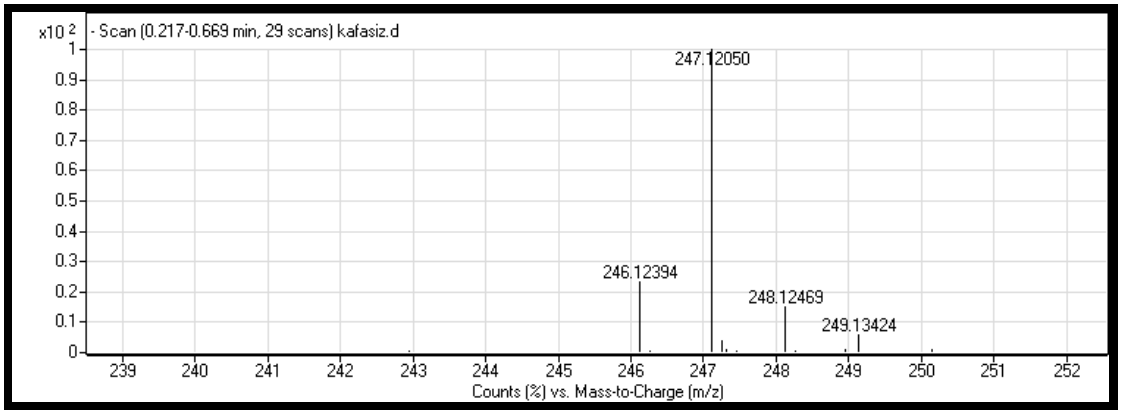

HRMS spectrum of Compound **5**

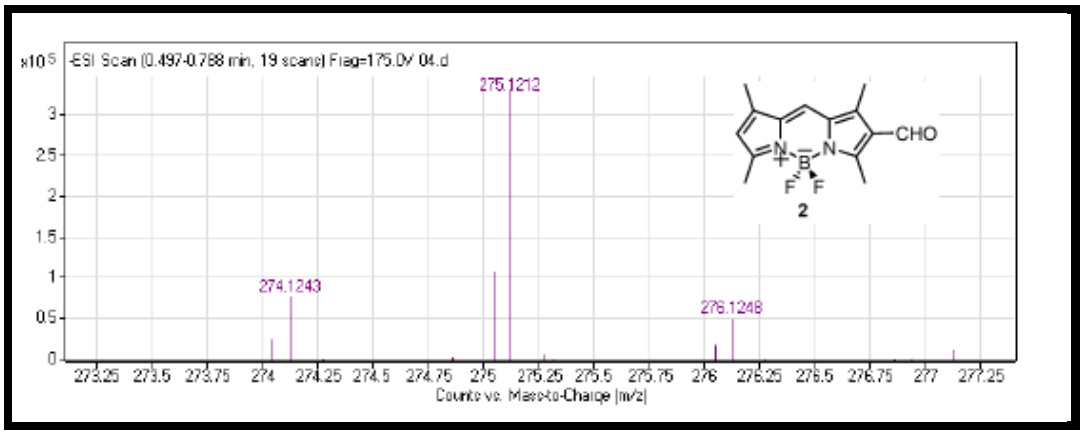

HRMS spectrum of Compound **6**

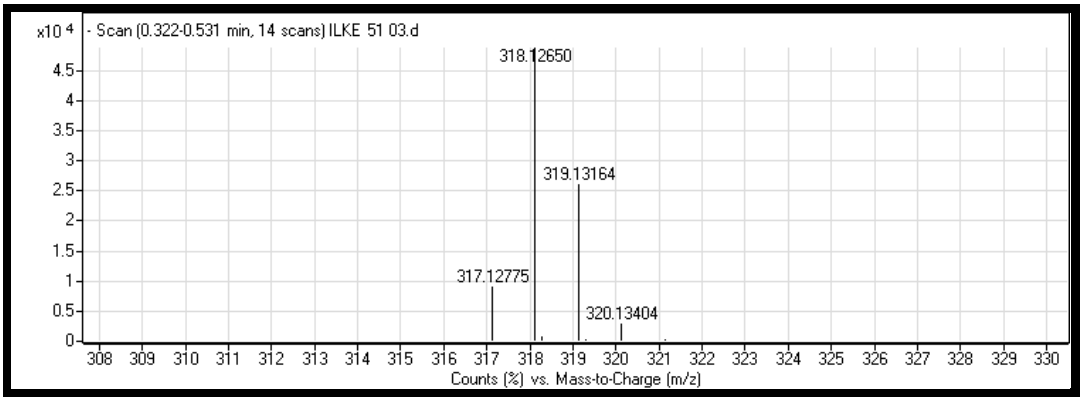

HRMS spectrum of Compound **7**

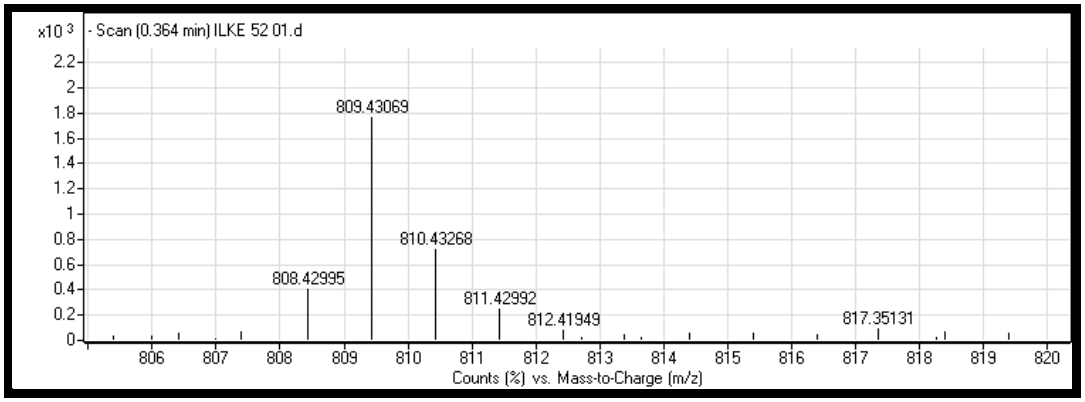

HRMS spectrum of Compound **8**

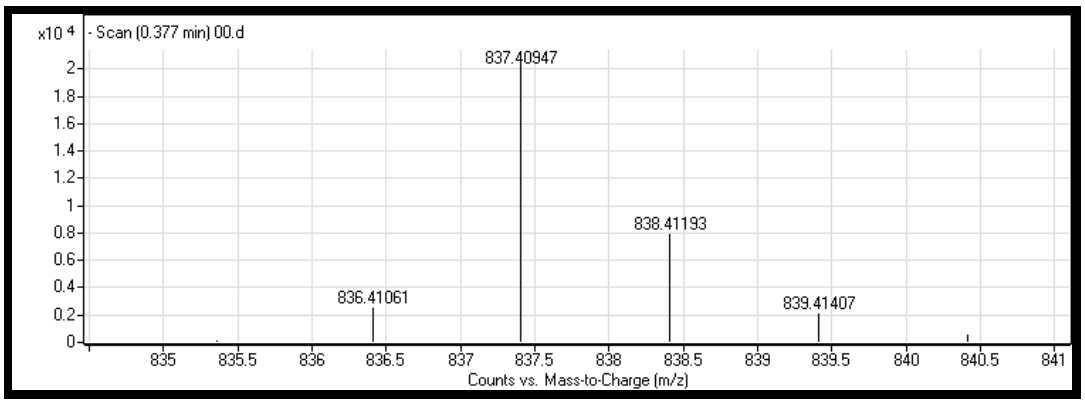

HRMS spectrum of Compound **9**

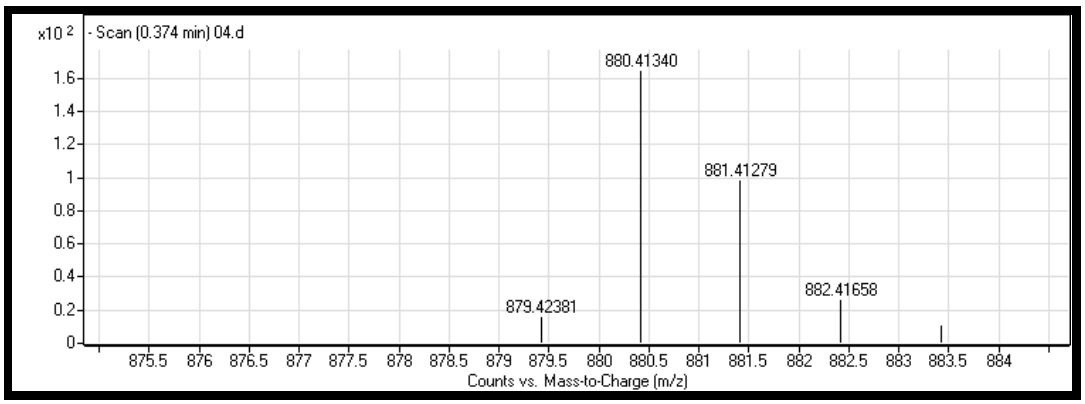

HRMS spectrum of Compound **10**

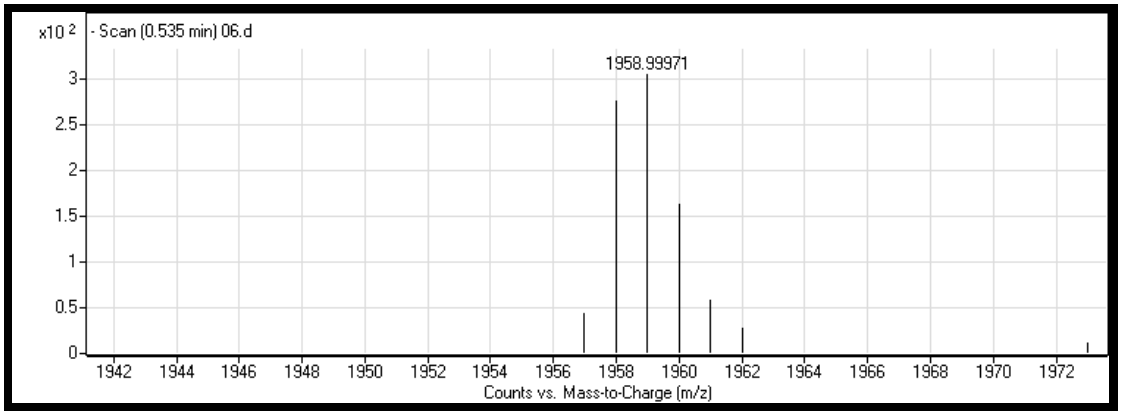

HRMS spectrum of Compound **11**

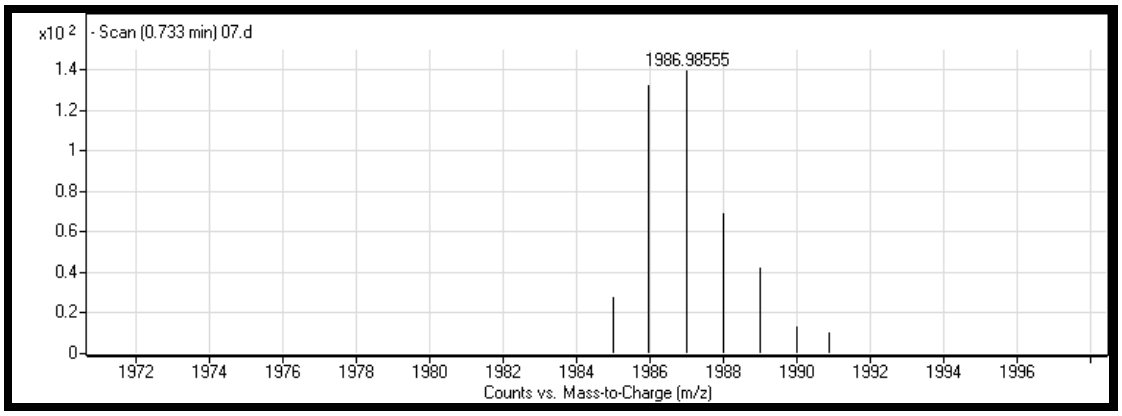

HRMS spectrum of Compound **12**

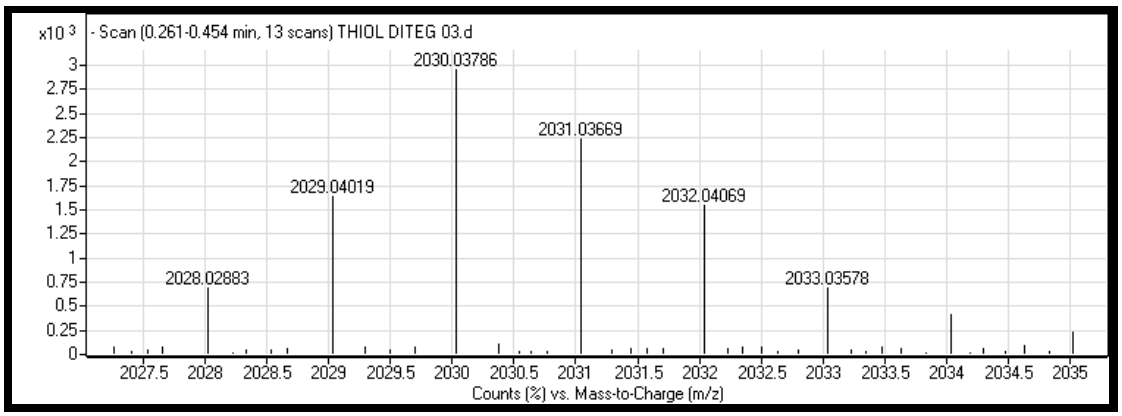

HRMS spectrum of Compound **13**

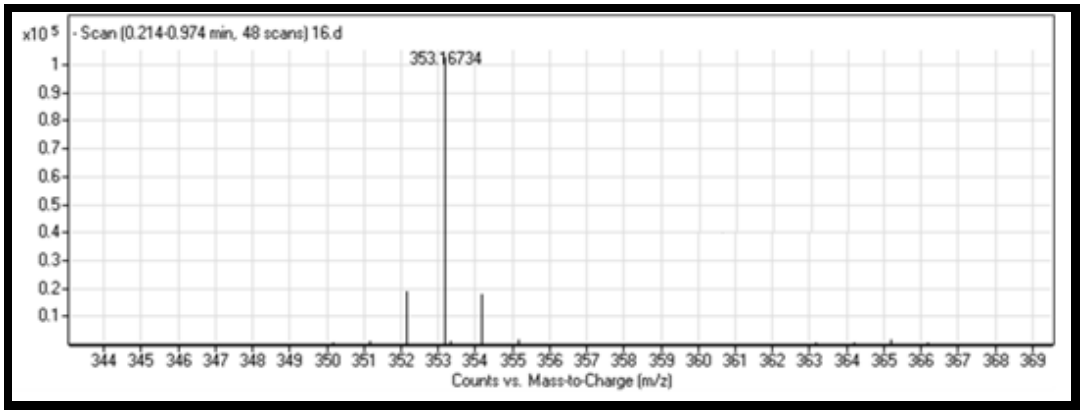

HRMS spectrum of Compound **14**

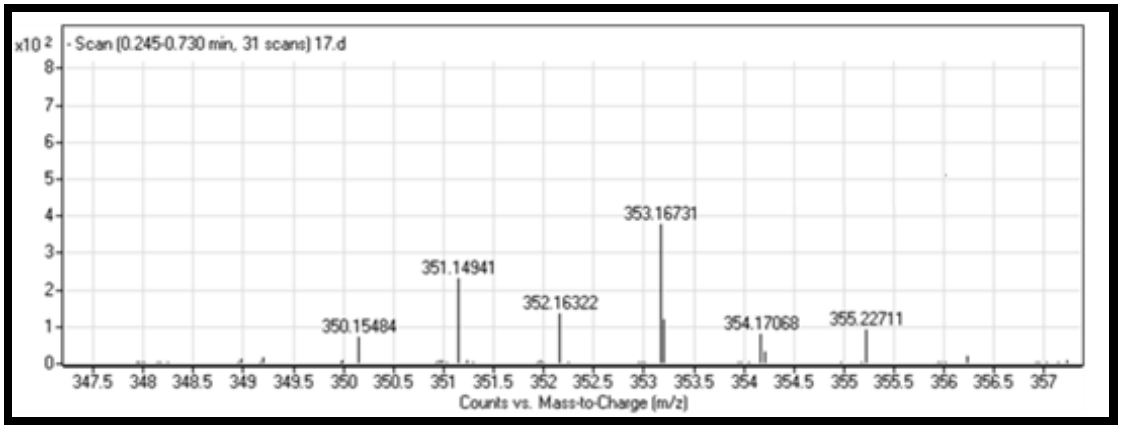

HRMS spectrum of Compound **15**

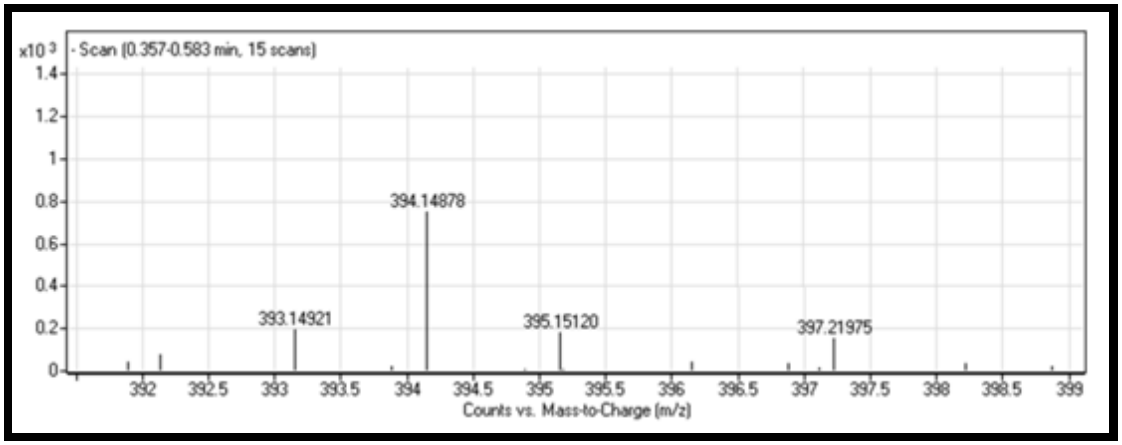

HRMS spectrum of Compound **16**

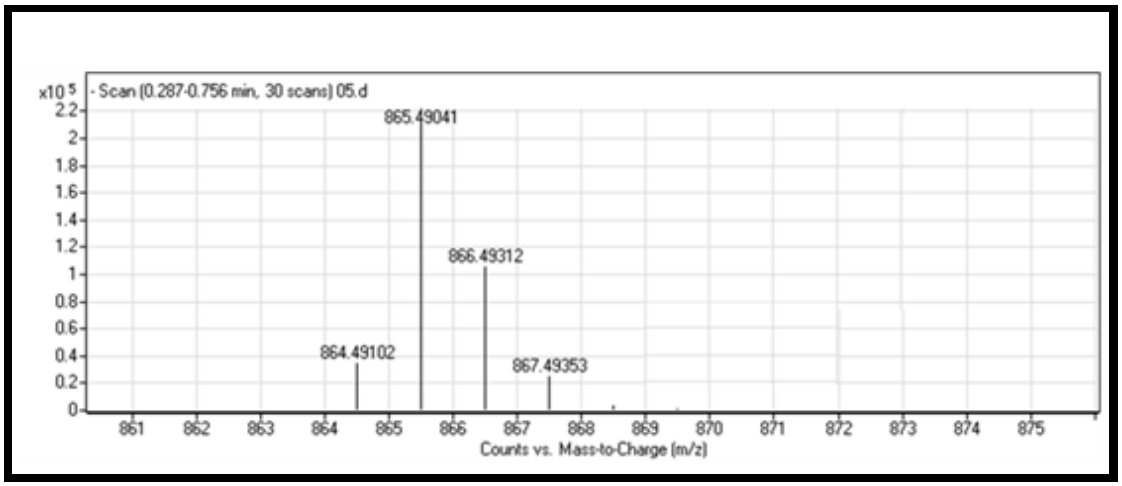

HRMS spectrum of Compound **17**

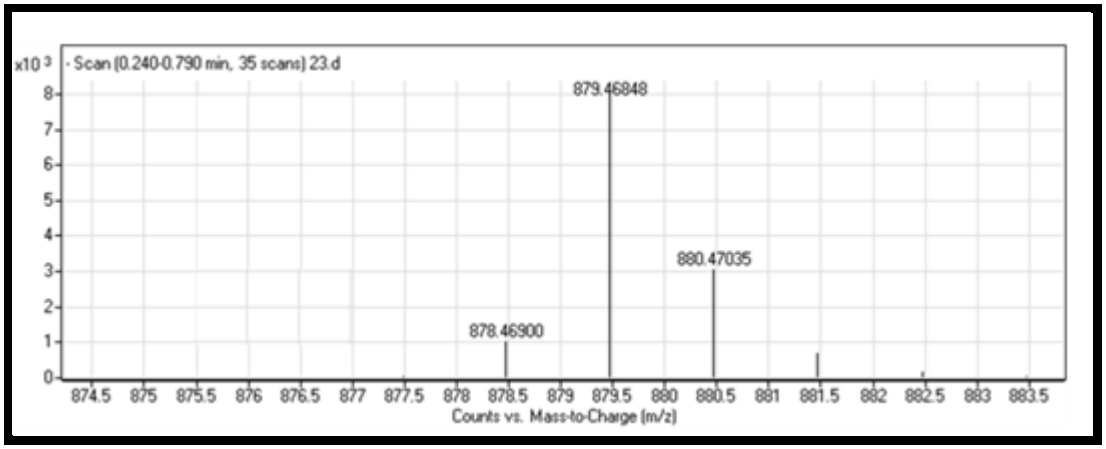

HRMS spectrum of Compound **18**

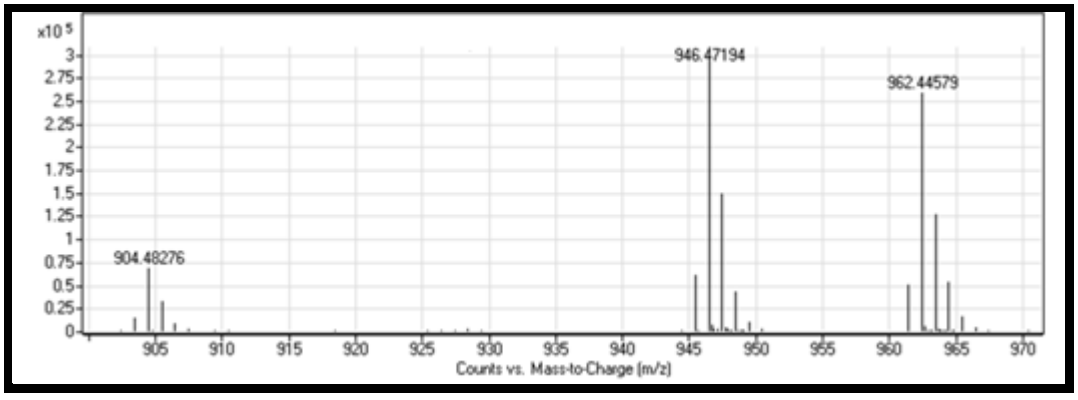

HRMS spectrum of Compound **19**

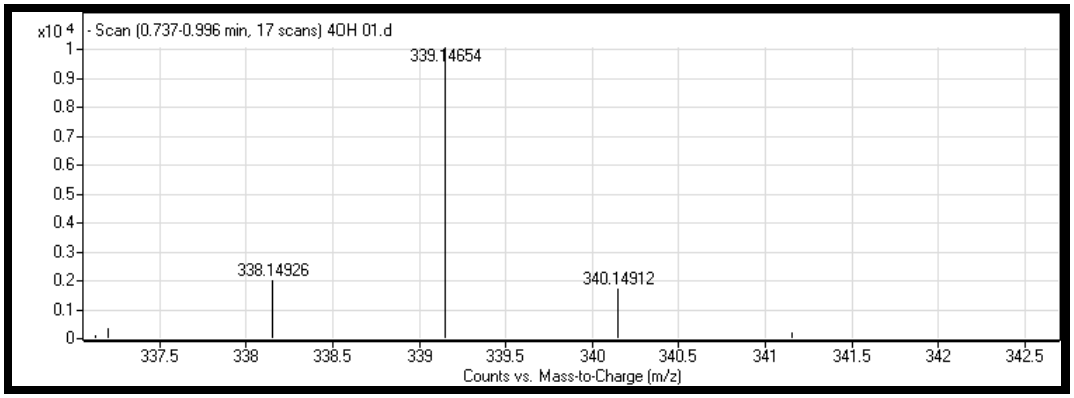

HRMS spectrum of Compound **20**

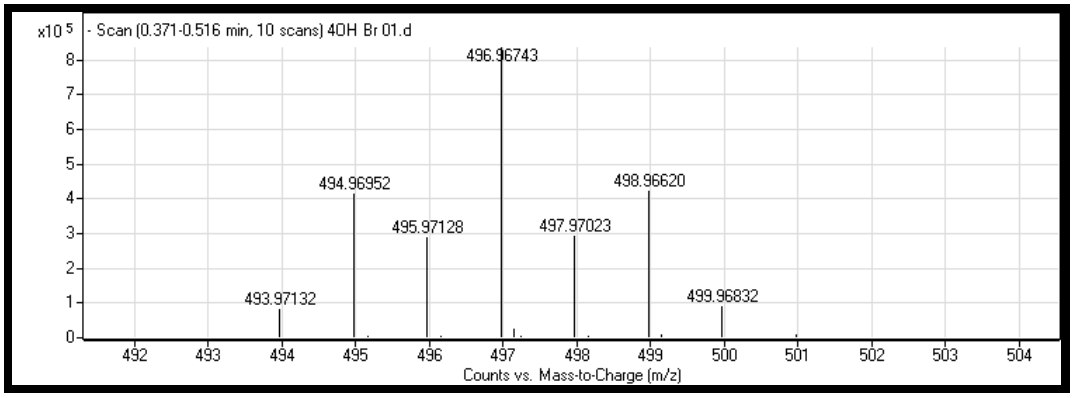

HRMS spectrum of Compound **21**

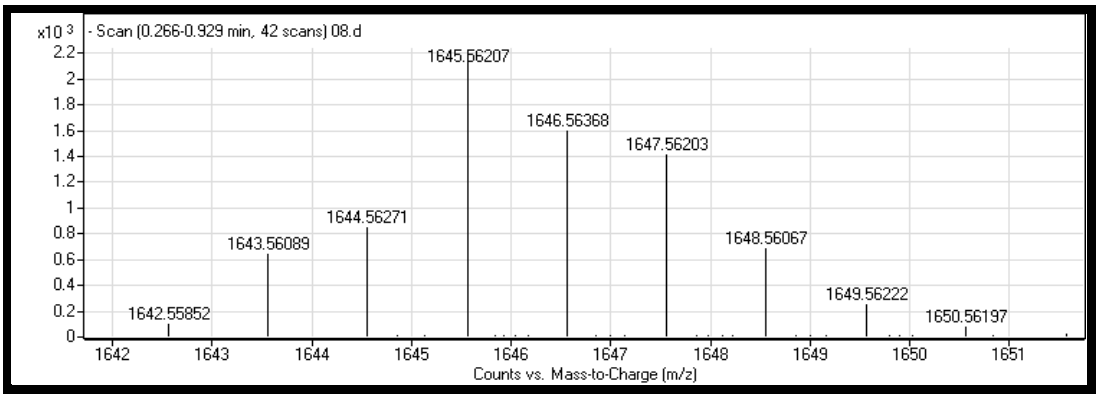

HRMS spectrum of Compound **22**

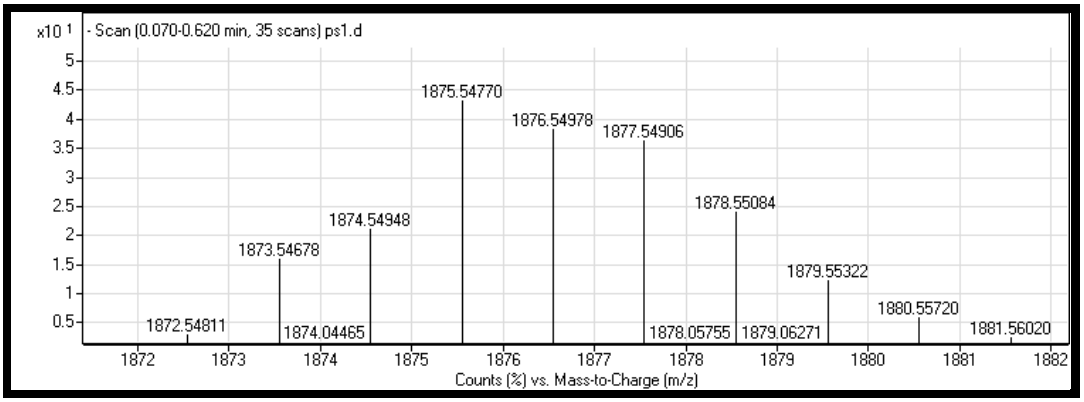

HRMS spectrum of Compound **23**

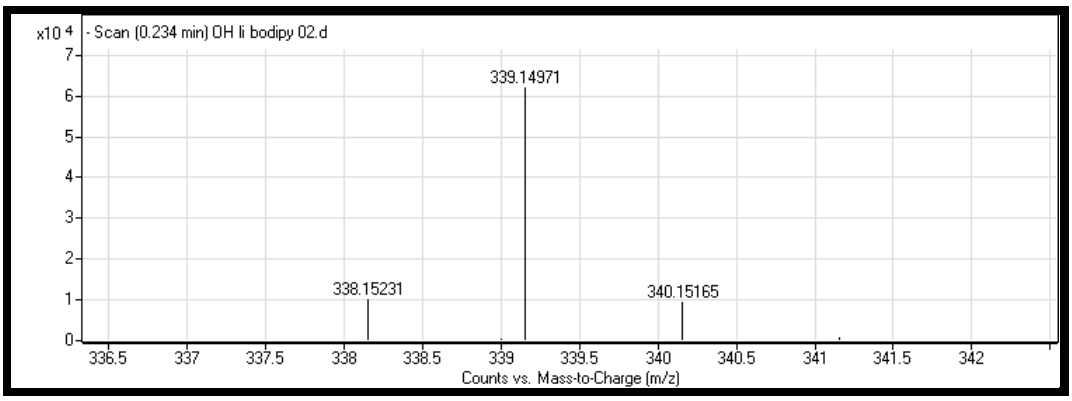

HRMS spectrum of Compound **24**

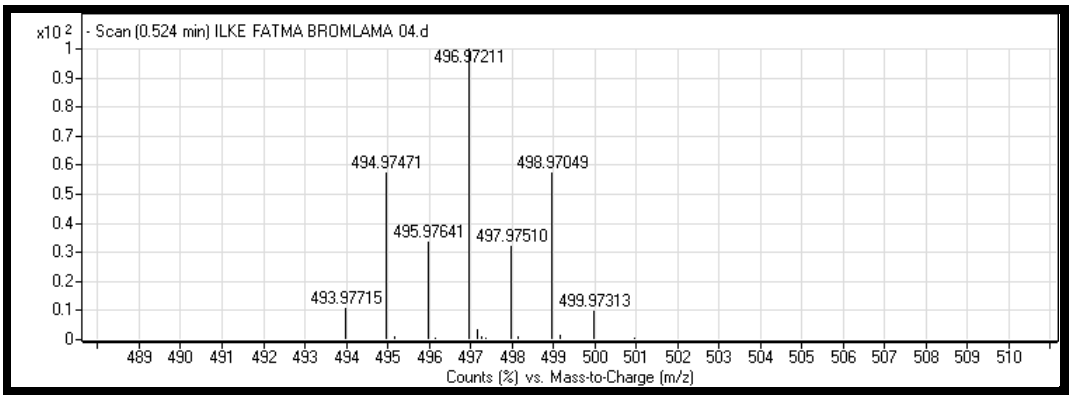

HRMS spectrum of Compound **25**

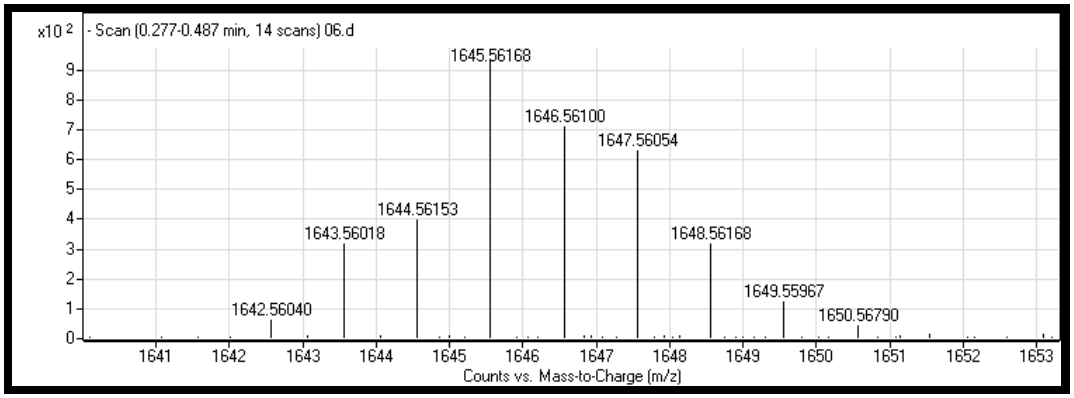

HRMS spectrum of Compound **26**

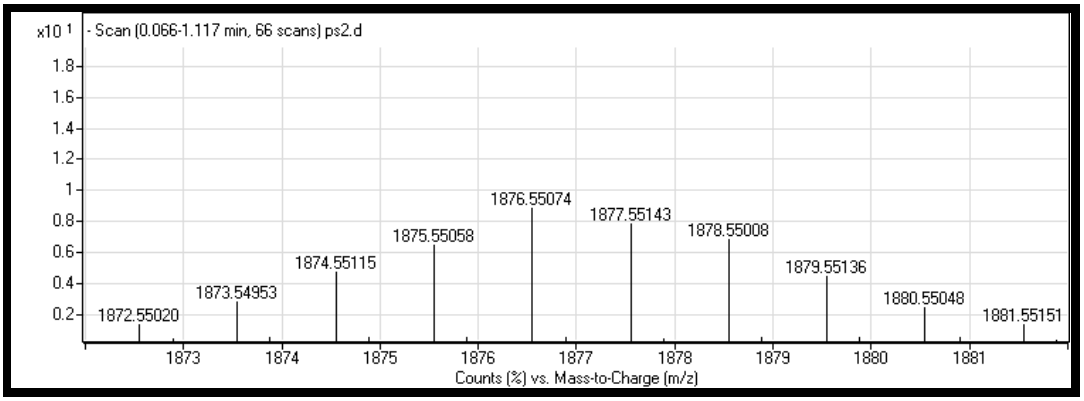

HRMS spectrum of Compound **28**

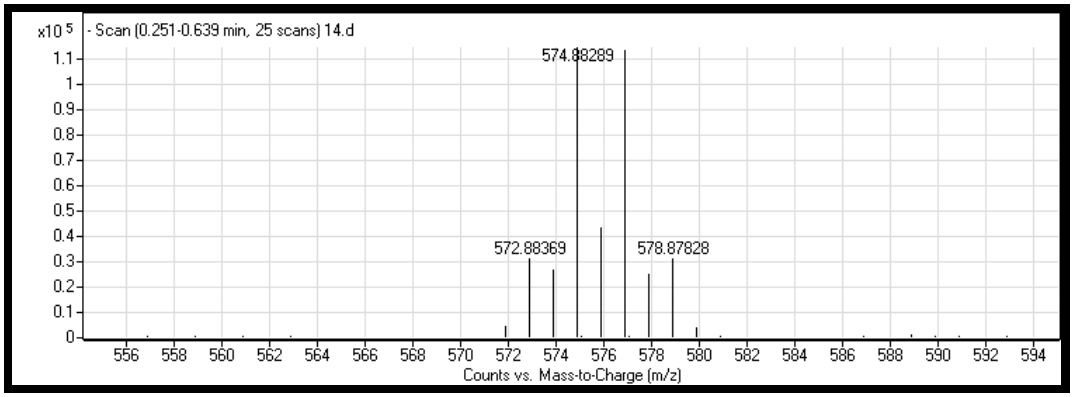

HRMS spectrum of Compound **28**

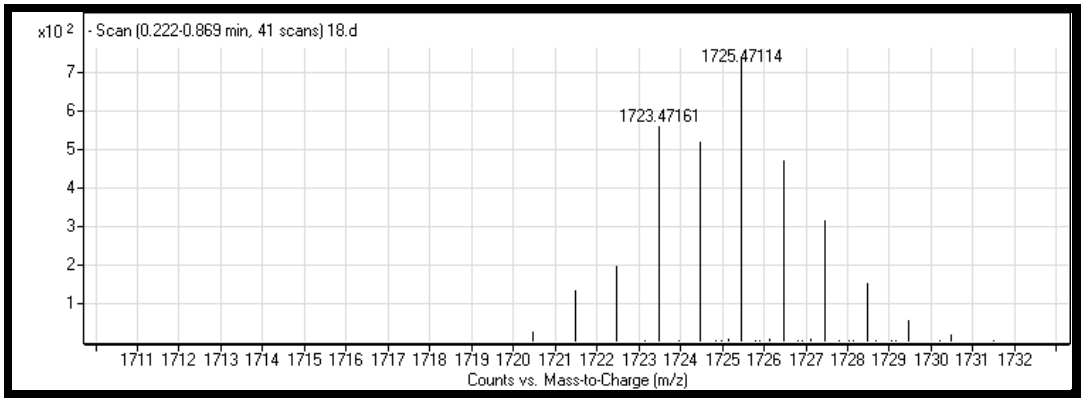

HRMS spectrum of Compound **29**

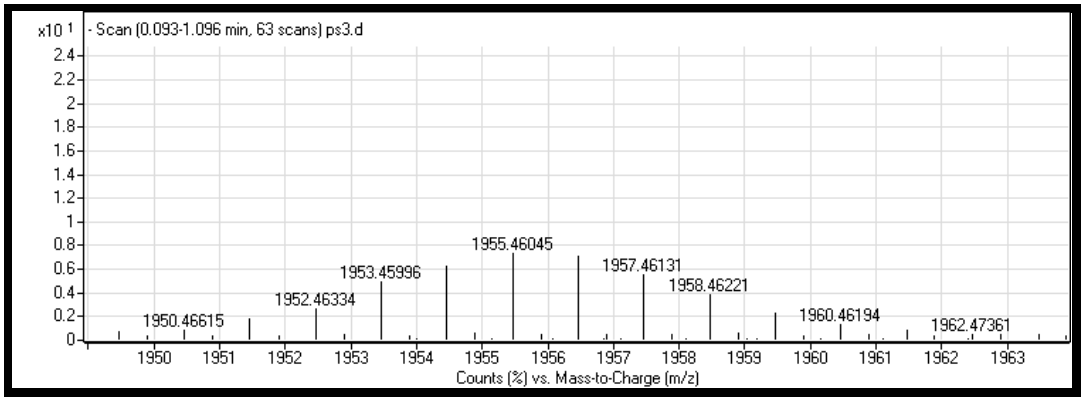

HRMS spectrum of Compound **30**

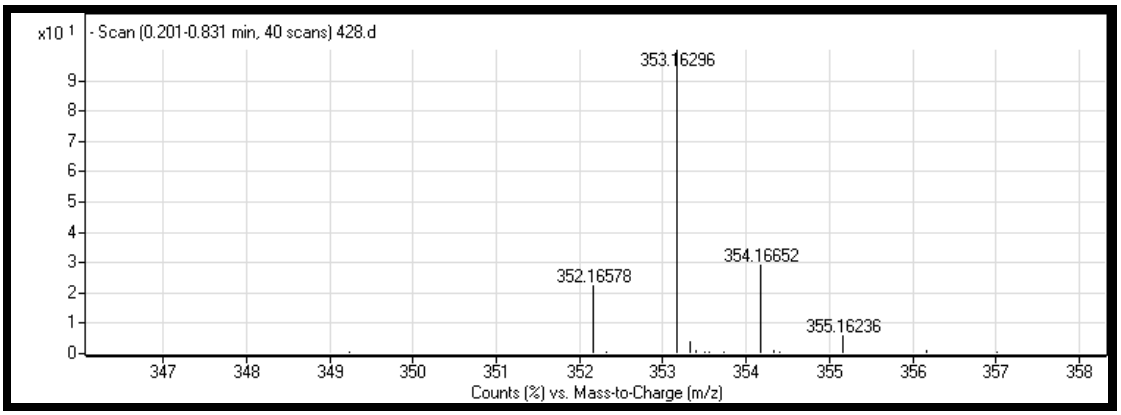

HRMS spectrum of Compound **31**

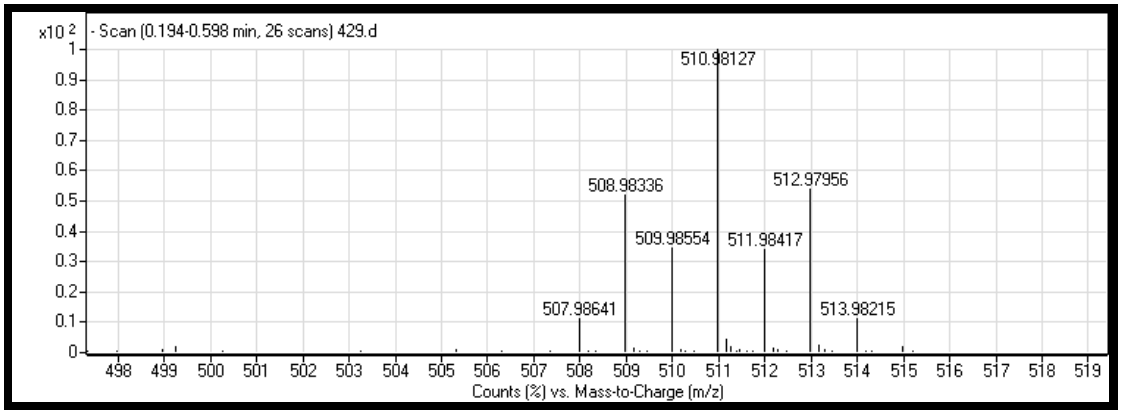

HRMS spectrum of Compound **32**

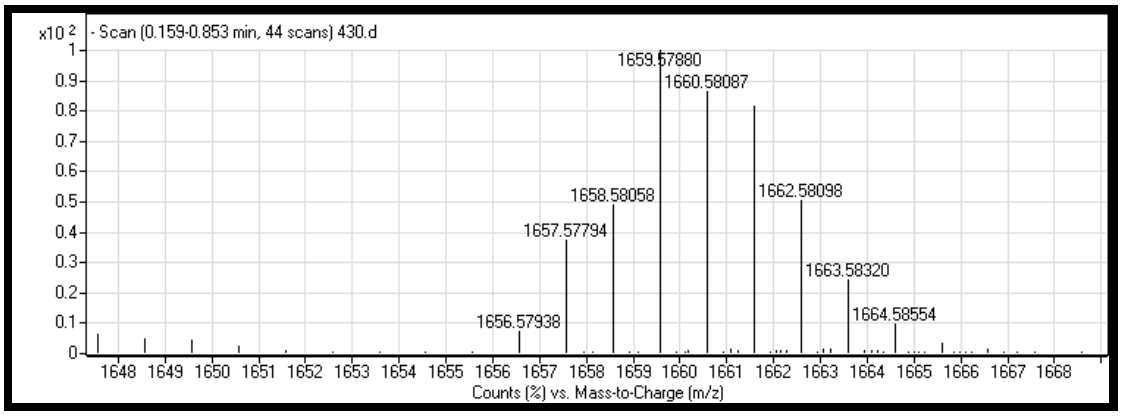

HRMS spectrum of Compound **33**

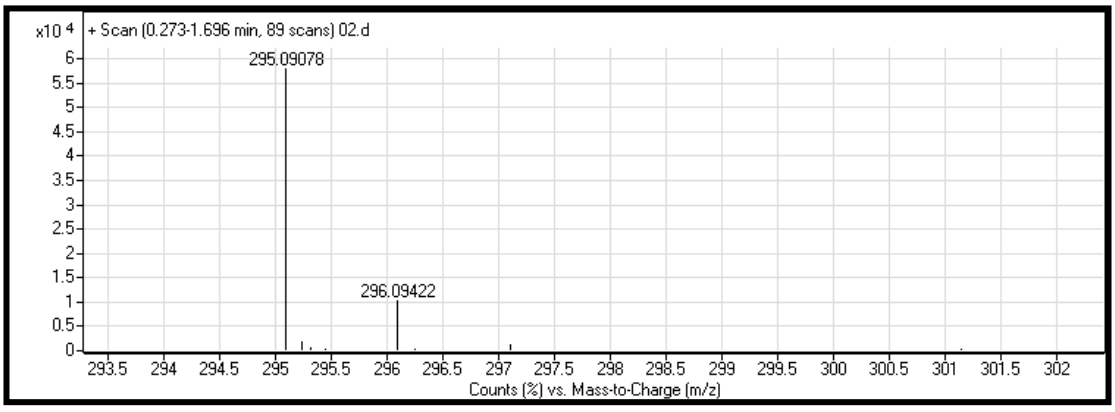

HRMS spectrum of Compound **35**

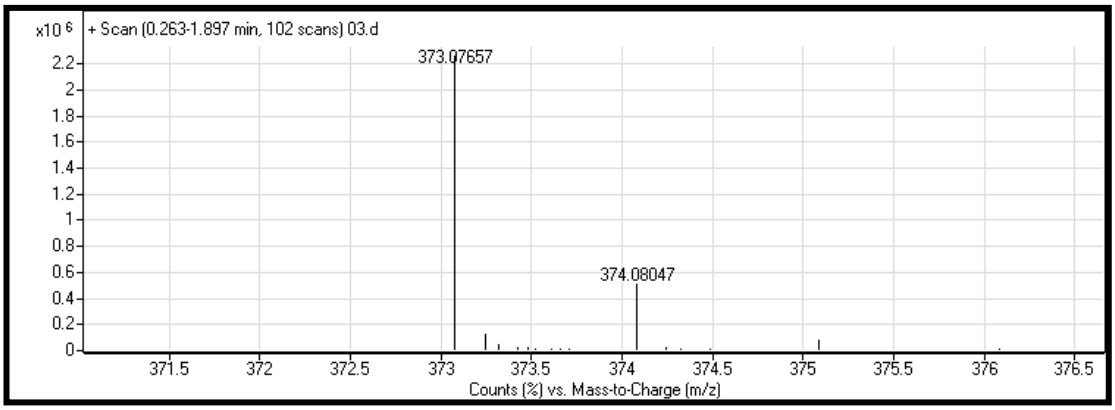

HRMS spectrum of Compound **36**

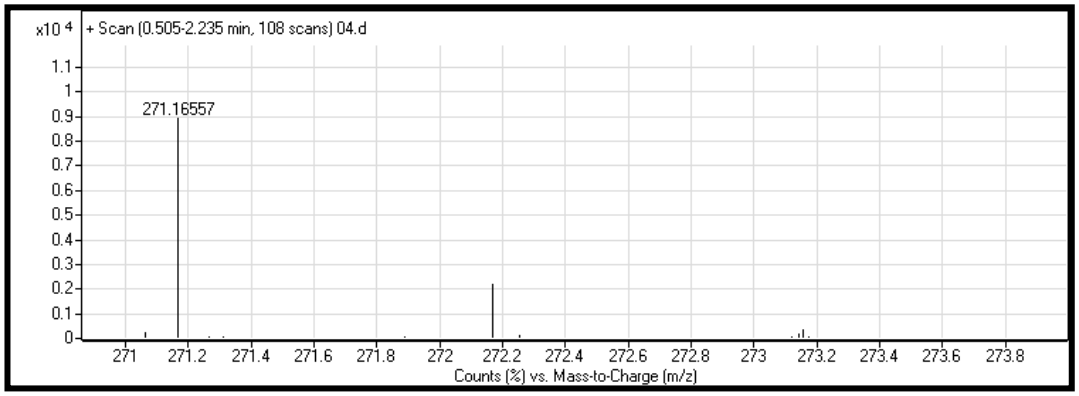

HRMS spectrum of Compound **37**

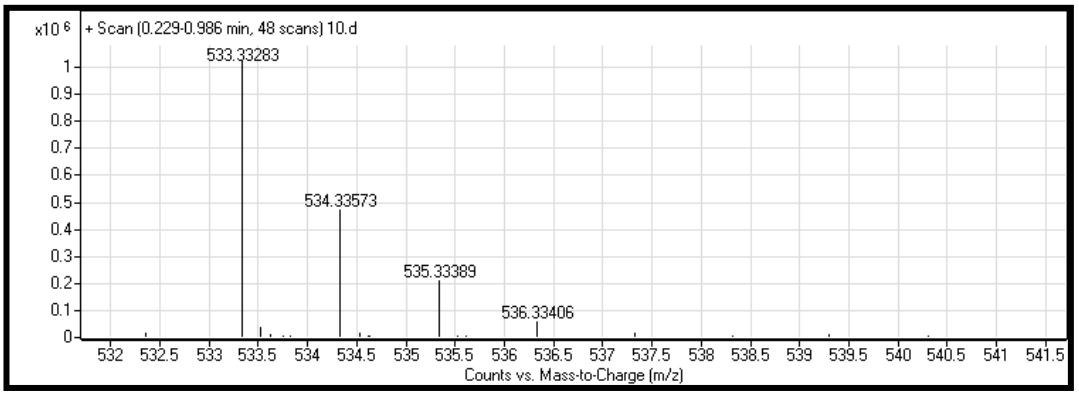

HRMS spectrum of Compound **40**

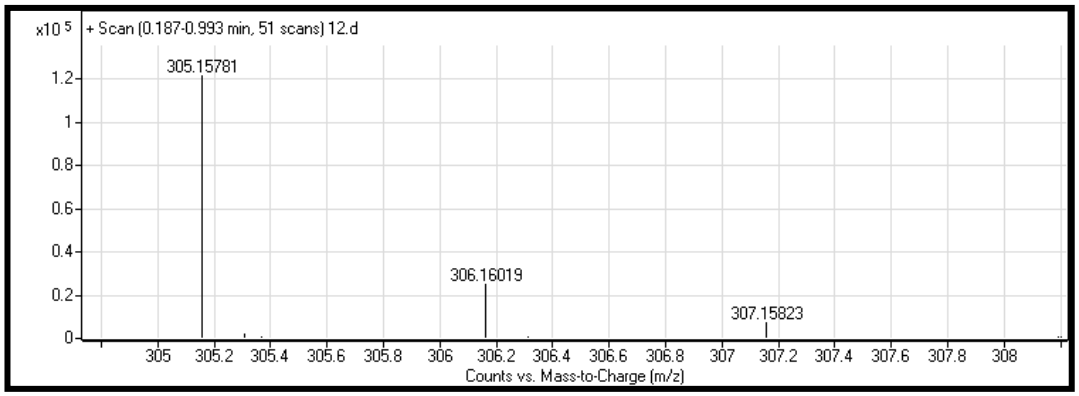

HRMS spectrum of Compound **41**

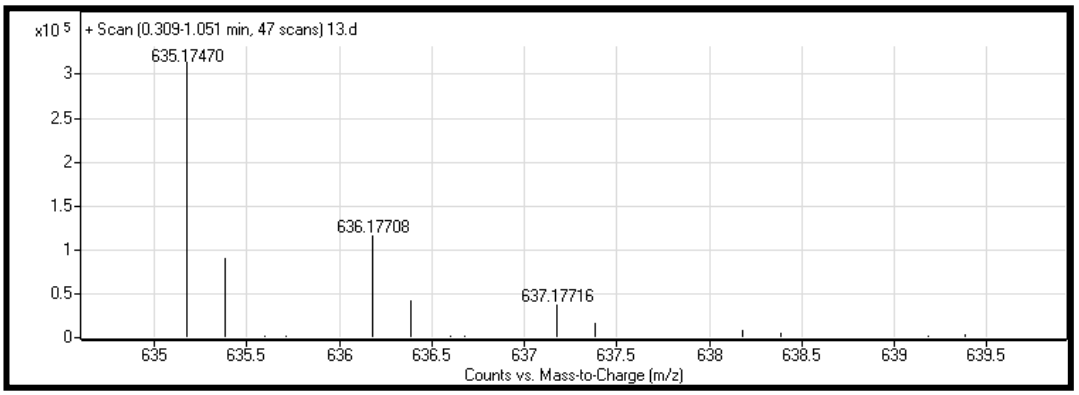

HRMS spectrum of Compound **42**

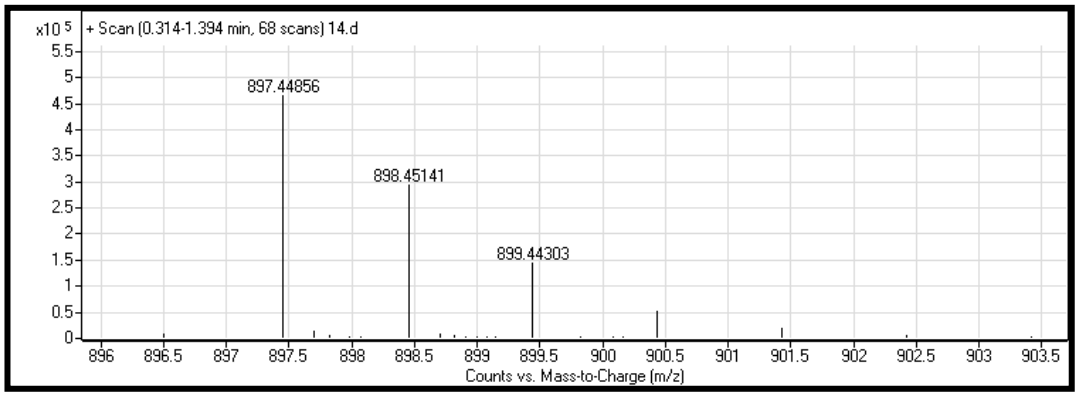

HRMS spectrum of Compound **43**

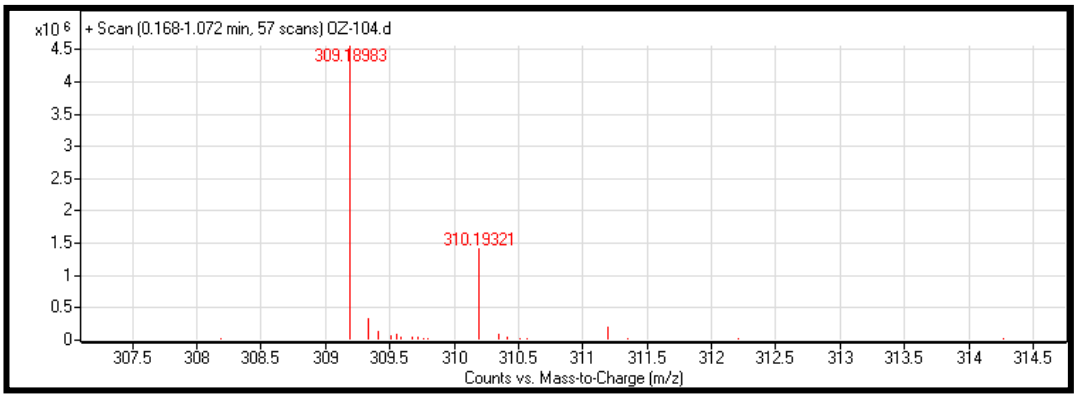

HRMS spectrum of Compound **45**

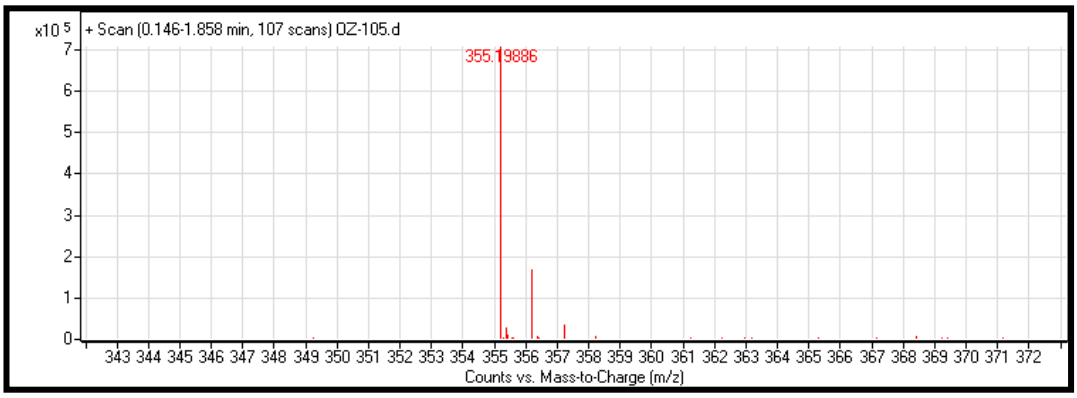

HRMs Spectrum of Compound **47**